Nuclear Science Division

LBL-27840
UC-413

1987-1988
ANNUAL REPORT

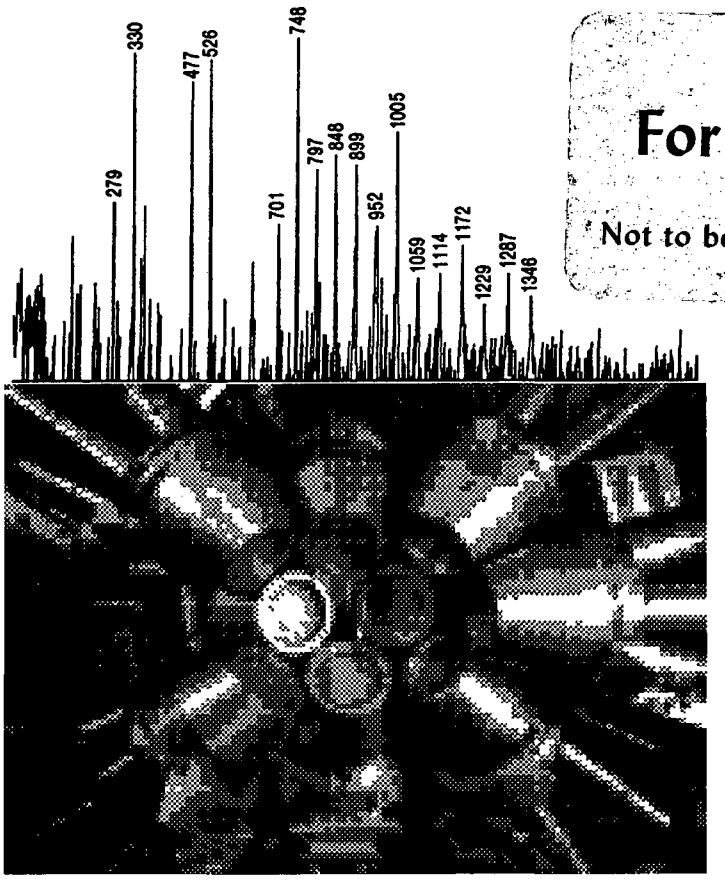

For Reference
Not to be taken from this room

Lawrence Berkeley Laboratory
University of California

October 1989

Prepared for the U.S. Department of Energy under Contract DE-AC03-76SF00098

LBL-27840
Copy 1
Bldg. 50 Library.

DISCLAIMER

This document was prepared as an account of work sponsored by the United States Government. While this document is believed to contain correct information, neither the United States Government nor any agency thereof, nor the Regents of the University of California, nor any of their employees, makes any warranty, express or implied, or assumes any legal responsibility for the accuracy, completeness, or usefulness of any information, apparatus, product, or process disclosed, or represents that its use would not infringe privately owned rights. Reference herein to any specific commercial product, process, or service by its trade name, trademark, manufacturer, or otherwise, does not necessarily constitute or imply its endorsement, recommendation, or favoring by the United States Government or any agency thereof, or the Regents of the University of California. The views and opinions of authors expressed herein do not necessarily state or reflect those of the United States Government or any agency thereof or the Regents of the University of California.

LBL-27840

Nuclear Science Division

Annual Report for the Period

October 1, 1987 – September 30, 1988

Division Director
T.J.M. Symons

Deputy Director
G.J. Wozniak

Assistant Director
J. Dairiki

Editor
Jeannette Mahoney

Editorial Committee
M.A. Deleplanque, W.D. Myers, G. Odyniec

Lawrence Berkeley Laboratory
1 Cyclotron Road
Berkeley, California, 94720, USA

This work was supported by the Director, Office of Energy Research, Office of High Energy and Nuclear Physics, Division of Nuclear Physics and by the Office of Basic Energy Sciences, Division of Nuclear Sciences, of the U.S. Department of Energy under Contract No. DE-AC03-76SF00098

This report summarizes the activities of the Nuclear Science Division during the period October 1, 1987 to September 30, 1988. During this period active research programs continued at our local accelerators as well as a large effort at the CERN SPS.

Highlights of the low energy research program included the identification of new super-deformed bands in gadolinium and palladium isotopes using the HERA array. Other work at the 88-Inch Cyclotron involved studies of the fragmentation of light nuclei, the spectroscopy of nuclear far from stability and interesting new experiments on the properties of the heaviest elements. Two other programs deserve special mention, the new program in Nuclear Astrophysics and the spectroscopic studies being carried out at OASIS. This isotope separator is now in full operation at the SuperHILAC after many years of development.

At the Bevalac, important new results were obtained on the properties of hot dense nuclear matter produced in central collisions of heavy ions. First measurements were made using the di-lepton spectrometer which provide the most direct access to the conditions at the earliest stage of the reaction. New results on pion interferometry have been obtained using the Janus spectrometer and surprises continue to be found in careful analysis of data from the Plastic Ball detector, most recently the identification of a new component of hydrodynamic flow. Also at the Bevalac the intermediate energy program continued to grow, studying the evolution of the reaction mechanism from incomplete fusion to the fireball regime, as did the spectroscopic studies using secondary radioactive beams.

The third major component of the experimental program is the study of ultra-relativistic nuclear collisions using the CERN SPS. This year saw the completion of analysis of the first round of experiments with important results being obtained on general particle production, the space-time evolution of the system and strangeness production.

Research in Nuclear Theory is also a very important part of the division's activities. Of particular note during this period was the beginning of a program in order-to-chaos studies supported by Director's Program Development Funds. This is an interesting new direction for the theory program that is complementary to the ongoing activities in support of the experimental program.

James Symons

PART I: PROGRAMS

Group Descriptions I–XXV

Nuclear Science Division Research 1

PART II: EXPERIMENT

β - Decay Study of ^{27}P Using the RAMA Isotope Separator 13
T.F. Lang, J.D. Robertson, D.M. Moltz, J.E. Reiff and J.C. Cerny

The β^+-p Decay of ^{25}Si 13
J.D. Robertson, J.E. Reiff, T.F. Lang, D.M. Moltz, and J.C. Cerny

The Search for Ground State Proton Decay From Light Proton-Rich Nuclei 15
J.E. Reiff, J.D. Robertson, D.M. Moltz, T.F. Lang, J.C. Batchelder, and J.C. Cerny

Sub-barrier Fusion of ^{16}O + ^{147,149}Sm 16
D.E. DiGregorio, M. diTada, D. Abriola, M. Elgue, A. Etchegoyen, M.C. Etchegoyen, J.O. Fernández Niello, A.M.J. Ferrero, S. Gil, A.O. Macchiavelli, A.J. Pacheco, J.E. Testoni, P.R. Silveira Gomes, V.R. Vanin, R. Liguori Neto, E. Crema, and R.G. Stokstad

Observation of a Constant Average Angular Momentum for Fusion at Subbarrier Energies 17
R.G. Stokstad, D.E. DiGregorio, K.T. Lesko, B.A. Harmon, E.B. Norman, J. Pouliot, and Y.D. Chan

Multiple Dissociation of ^{16}O, ^{14}N and ^{12}C at 32.5 MeV/nucleon 18
R.G. Stokstad, Y.D. Chan, A. Dacal, D.E. DiGregorio, B.A. Harmon, R. Knop, M.E. Ortiz, E. Plagnol, J. Pouliot, C. Moisan, L. Potvin, C. Rioux, and R.Roy

Stripping- and Pickup-Induced Breakup in 11- and 17-MeV/nucleon ^{20}Ne+^{197}Au Reactions 19
S.B. Gazes, H.R. Schmidt, Y. Chan, E. Chavez, R. Kamermans and R.G. Stokstad

Limits on $\bar{\nu}_\mu \rightarrow \bar{\nu}_\epsilon$ Oscillations, Experiment 645 at LAMPF 20
L.S. Durkin, R.W. Harper, T.Y. Ling, J.W. Mitchell, T.A. Romanowski, E.S. Smith, M. Timko, S.J. Freedman, J. Napolitano, B.K. Fujikawa, R. McKeown, K.T. Lesko, W.C. Choi, A. Fazely, R.L. Imlay, W.J. Metcalf, R.D. Carlini, J.B. Donahue, G.T. Garvey, and V.D. Sandberg

Isospin-Forbidden Fermi Decay of ^{56}Ni 21
E.B. Norman, K.T. Lesko, B. Sur, R.M. Larimer, and E. Browne

β^+ Decay of ^{56}Ni 21
K.T. Lesko, E.B. Norman, B. Sur, R.M. Larimer, and E. Browne

β^+ Decay and Cosmic-ray Half-life of ^{54}Mn 21
B. Sur, K.R. Vogel, E.B. Norman, K.T. Lesko, R.M. Larimer, and E. Browne

Level Scheme of ^{148}Pm and the s-Process Neutron Density 22
K.T. Lesko, E.B. Norman, R.-M. Larimer, J.C. Bacelar and E.M. Beck

Search for Motional Narrowing Effects in Nuclear γ-Ray Spectra 23
F.S. Stephens, J.E. Draper, M.A. Deleplanque, R.M. Diamond, and A.O. Macchiavelli

Unusual Rotational Behavior in ^{178}Os 24
J. Burde, A.O. Macchiavelli, M.A. Deleplanque, R.M. Diamond, F.S. Stephens, C.W. Beausang, R.J. McDonald and J.E. Draper

High-Spin Spectroscopy of ^{162}Hf 24
H. Hübel, M. Murzel, E.M. Beck, H. Kluge, A. Kuhnert, K.H. Maier, J.C. Bacelar, M.A. Deleplanque, R.M. Diamond, and F.S. Stephens

Superdeformed Band in ^{148}Gd: a Test of Shell Effects in the Mass 150 Region 26
M.A. Deleplanque, C. Beausang, J. Burde, R.M. Diamond, J.E. Draper, C. Duyar, A.O. Macchiavelli, R.J. McDonald and F.S. Stephens

Superdeformation in ^{104,105}Pd 26
A.O. Macchiavelli, J. Burde, R.M. Diamond, C.W. Beausang, M.A. Deleplanque, R.J. McDonald, F.S. Stephens and J.E. Draper

Identification of ^{145}Er and ^{145}Ho 27
K.S. Vierinen, J.M. Nitschke, P.A. Wilmarth, R.M. Chasteler, A.A. Shihab-Eldin, R.B. Firestone, K.S. Toth, and Y.A. Akovali

High Spin Studies of ^{235}U, ^{234}U, and ^{233}U 28
M.A. Stoyer, J.O. Rasmussen, R.M. Diamond, F.S. Stephens, M.A. Deleplanque, A. Macchiavelli, R. McDonald, D. Cline, A. Kavka, E. Vogt, K. Helmer, C.Y. Wu, W. Kernan, X.T.Liu

Shape Co-Existence in ^{180}Hg and Delineation of the Midshell Minimum 29
G.D. Dracoulis, A.E. Stuchbery, A.O. Macchiavelli, C.W. Beausang, J. Burde, M.A. Deleplanque, R.M. Diamond, and F.S. Stephens

Gamma-Ray Energy Correlations from Nuclei at Very High Spins 30
F.S. Stephens, J.E. Draper, J.C. Bacelar, E.M. Beck, M.A. Deleplanque, and R.M. Diamond

The Decay of ^{141}Tb by Positron Emission and Electron Capture Decay 31
J. Gilat, R.B. Firestone, J.M. Nitschke, K.S. Vierinen, and P.A. Wilmarth

Determination of Q_{EC} Values for Neutron-Deficient Rare Earth Nuclei 32
R.B. Firestone, J. Gilat, J.M. Nitschke, K.S. Vierinen, and P.A. Wilmarth

Nuclear Penetration Effects in ^{233}U 33
E. Browne, B. Sur, E.B. Norman, H.L. Hall, R.A. Henderson, K.T. Lesko, R.M. Larimer, and D.C. Hoffman.

Decay Properties of ^{153}Yb and ^{153}Tm; Excitation Energies of the $s_{1/2}$ and $h_{11/2}$ Proton States in ^{153}Tm 34
M.O. Kortelahti, K.S. Toth, K.S. Vierinen, J.M. Nitschke, P.A. Wilmarth, R.B. Firestone, R.M. Chasteler, and A.A. Shihab-Eldin

Identification of the Neutron-Rich Isotope ^{174}Er 35
R.M. Chasteler, J.M. Nitschke, R.B. Firestone, K.S. Vierinen, P.A. Wilmarth, and A.A. Shihab-Eldin

Single-Particle States in ^{151}Tm and ^{151}Er; Systematics of Neutron States in N=83 Nuclei 35
Y.A. Akovali, K.S. Toth, A.L. Goodman, J.M. Nitschke, P.A. Wilmarth, D.M. Moltz, M.N. Rao, and D.C. Sousa

Beta-Strength Function Studies of Delayed Proton Emission in Heavy, Deformed Nuclei 36
P.A. Wilmarth, J.M. Nitschke, and K.S. Toth

Beta-Decay of ^{154}Lu and ^{154}Yb 37
K.S. Vierinen, A.A. Shihab-Eldin, J.M. Nitschke, P.A. Wilmarth, R.M. Chasteler, R.B. Firestone, and K.S. Toth

Fine structure in ^{153}Tm alpha decay 37
K.S. Toth, P.A. Wilmarth, J.M. Nitschke, R.B. Firestone, K.S. Vierinen, M.O. Kortelahti, and F.T. Avignone III

Beta-Delayed Proton Decay of the N=83 Precursor ^{153}Yb 38
P.A. Wilmarth, J.M. Nitschke, K.S. Vierinen, K.S. Toth, and M.O. Kortelahti

Deep Inelastic Collision Cross Section Calculations 39
R.M. Chasteler

Doorway State Formation and Structure in Beta-Delayed Proton Decay 40
J.M. Nitschke, P.A. Wilmarth, R.B. Firestone P. Möller, K.S. Toth, and J. Gilat

Experimental and Predicted Half-Lives for Neutron- Deficient Lanthanide Isotopes 41
P.A. Wilmarth and J.M. Nitschke

Progress in the Studies of the Hydrolysis and Carbonate Complexation of Dioxoplutonium(V) 41
D.A. Bennett, H. Nitsche, R.J. Silva, D.C. Hoffman

The Synergistic Solvent Extraction of Cf, Am, and Eu by 4-Benzoyl-5-methyl-2-phenyl pyrazol-3-thione (BMPPT) and Tri-n-octyl phosphine oxide (TOPO) 43
Robert B. Chadwick, Barbara F. Smith, Gordon D. Jarvinen, and Darleane C. Hoffman

Search for Lawrencium as a P-Element Using Chromatography Techniques 44
D.T. Jost, H.W. Gäggeler, Ch. Vogel, M. Schädel, E. Jäger, B. Eichler, K.E. Gregorich, and D.C. Hoffman

Chloride Complexation Studies of Element 104 in the H^+, Cl^-/TBP System 45
C.M. Gannett, R.B. Chadwick, K.B. Chen, K.R. Czerwinski, K.E. Gregorich, H.L. Hall, G.R. Haynes, R.A. Henderson, D.M. Lee, J.D. Leyba, M.J. Nurmia and D.C. Hoffman

Alpha Peak Energies and Abundances of ^{257}No 45
C.M. Gannett, R.B. Chadwick, K.B. Chen, K.R. Czerwinski, K.E. Gregorich, H.L. Hall, R.A. Henderson, D.M. Lee, J.D. Leyba, M.J. Nurmia and D.C. Hoffman

A Study of the Decay Properties of the New Isotope, ^{262}No 46
R.W. Lougheed, E.K. Hulet, J.F. Wild, K.J. Moody, R.J. Dougan, C.M. Gannett, R.A. Henderson, D.M. Lee, and D.C. Hoffman

Chemistry of Heavy Ion Reactions 47
D.C. Hoffman

The Heavy Ion Reaction of ^{nat}Ag with 20 MeV/nucleon ^{12}C 47
K.B. Chen, Y.W. Yu, K.E. Gregorich, D.C. Hoffman and G.T. Seaborg

Production Cross Sections for Above and Below Target Elements from the Interactions of ^{44}Ca with ^{248}Cm 48
J.D. Leyba, R.M. Chasteler, R.A. Henderson, D.A. Bennett, C.M. Gannett, H.L. Hall, R.B. Chadwick, K.E. Gregorich, D.M. Lee, M.J. Nurmia, D.C. Hoffman, A. Türler, and H.R. von Gunten

A History and Analysis of the Discovery of Elements 104 and 105 49
E.K. Hyde, D.C. Hoffman, and O.L. Keller, Jr.

Anionic Halide Complexes of Element 105 49
K.E. Gregorich, W. Brüchle, U. Baltensperger, H. Gäggeler, J. Kratz, D.M. Lee, C. Lienert, D. Jost, M.J. Nurmia, Y. Nai-Qi, R.A. Henderson, H.L. Hall, C.M. Gannett, R.B. Chadwick, J.D. Leyba, K.R. Czerwinski, D.C. Hoffman, M. Schädel, U. Scherer, A. Türler, P. Zimmermann,

Absence of Extreme Sub-Barrier Fusion in the Reaction 1.8-MeV p + ^{238}U 50
A. Ghiorso, L.P. Somerville, and S. Yashita

Systematics of Target Fragment Mass Distributions in Intermediate and High Energy Nuclear Collisions 51
W. Loveland, and G.T. Seaborg

Unusual Behavior of Projectile Fragments Produced by the Interactions of Relativistic Ar Ions with Copper 51
K. Aleklett, R. Brandt, G. Dersch, G. Feige, E.M. Friedlander, E. Ganssauge, G. Hasse, D.C. Hoffman, J. Herrmann, B.Judek, W. Loveland, P.L. McGaughey, N.T. Porile, W. Shulz, and G.T. Seaborg

Total Projectile Kinetic Energy Scaling in Energetic Nucleus-Nucleus Collisions 52
W. Loveland, Z. Xu, C. Casey, K. Aleklett, J.D. Liljenzin, D. Lee and G.T. Seaborg

The Role of Compound Nuclei in Intermediate-energy Heavy-ion Reactions 52
L.G. Moretto and G.J. Wozniak

Compound Nuclei, Binary Decay, and Multifragmentation in Intermediate-energy Heavy-ion Reactions 54
L.G. Moretto and G.J. Wozniak

The Role of Compound Nuclei in Complex Fragment Production, Multifragmentation and High Energy Gamma-ray Emission 55
L.G. Moretto, M. Ashworth and G.J. Wozniak

The Role of the Compound Nucleus in Complex Fragment Emission at Low and Intermediate Energies 55
L.G. Moretto and G.J. Wozniak

Complex-Fragment Emission in 12.6 MeV/Nucleon ^{63}Cu Induced Reactions on ^{12}C and ^{27}Al Targets 55
H.Y. Han, K.X. Jing, E. Plagnol, D.R. Bowman, R.J. Charity, L. Vinet, G.J. Wozniak, and L.G. Moretto

Emission of Complex Fragments From Highly Excited Systems Produced in ^{93}Nb + ^{9}Be and ^{27}Al Reactions at E/A = 25.4 and 30.3 MeV 57
R.J. Charity, D.R. Bowman, Z.H. Liu, R.J. McDonald, M.A. McMahan, G.J. Wozniak, L.G. Moretto, S. Bradley, W.L. Kehoe, and A.C. Mignerey

Complex Fragments from Excited Actinide Nuclei: A New Test of the Finite Range Model 58
D.G. Sarantities, D.R. Bowman, G.J. Wozniak, R.J. Charity, Z.H. Liu, R.J. McDonald, M.A. McMahan, and L.G. Moretto

Systematics of Complex Fragment Emission in Niobium Induced Reactions–1 58
G.J. Wozniak, R.J. Charity, and L.G. Moretto

Systematics of Complex Fragment Emission in Niobium-Induced Reactions–2 59
R.J. Charity, M.A. McMahan, G.J. Wozniak, R.J. McDonald, L.G. Moretto, D.G. Sarantites, L.G. Sobotka, G. Guarino, A. Pantaleo, L. Fiore, A. Gobbi, and K.D. Hildenbrand

The Categorical Space of Fission 59
L.G. Moretto and G.J. Wozniak

EC-Delayed Fission Properties of ^{232}Am 61
H.L. Hall, R.A. Henderson, C.M. Gannett, J.D. Leyba, K.R. Czerwinski, K.E. Gregorich, D.M. Lee, M.J. Nurmia, D.C. Hoffman, C.E.A. Palmer, and P.A. Baisden

Hard Photons in Heavy-Ion Collisions: Direct or Statistical? 63
N. Herrmann, R. Bock, P. Braun-Munzinger, H. Emling, R. Freifelder, M. Gnirs, A. Gobbi, E. Grosse, K.D. Hildenbrand, W. Kühn, R. Kulessa, T. Matulewicz, P.R. Maurenzig, V. Metag, R. Novotny, A. Olmi, D. Pelte, R. Rami, R.S. Simon, A.A. Stefanini, H. Stelzer, J. Wessels, and L.G. Moretto

β-Delayed Fission from ^{256m}Es and the Level Scheme of ^{256}Fm 64
H.L. Hall, K. E. Gregorich, R.A. Henderson, D.M. Lee, D.C. Hoffman,

New Mode of Radioactive Decay: Si and Mg Emission from ^{238}Pu 65
Shicheng Wang, D. Snowden-Ifft, K.J. Moody, E.K. Hulet, and P.B. Price

Limits on Contribution of Cosmic Nuclearites to Galactic Dark Matter 65
P.B. Price

Further Analysis of Heavy Fragment Radioactivity of ^{234}U 66
K.J. Moody, E.K. Hulet, Shicheng Wang, and P.B. Price

Where Has All The Fusion Gone...? 66
E. Plagnol, L. Vinet, D.R. Bowman, Y.D. Chan, R.J. Charity, E. Chavez, S.B. Gazes, H. Han, W.L. Kehoe, M.A. McMahan, L.G. Moretto, R.G. Stokstad, G.J. Wozniak, G. Auger

Measurement of Interaction Cross Sections Using Isotope Beams of Be and B and Isospin Dependence of the Nuclear Radii 68
I. Tanihata, T. Kobayashi, O. Yamakawa, S. Shimoura, K. Ekuni, K. Sugimoto, N. Takahashi, T. Shimoda, and H. Sato

Energy Dependence of Fragment Flow in High Energy Nuclear Collisions 70
H.Å. Gustafsson, H.H. Gutbrod, J. Harris, B.V. Jacak, K.H. Kampert, B. Kolb, A.M. Poskanzer, H.G. Ritter, and H.R. Schmidt

A New Component of the Collective Flow in Relativistic Heavy-Ion Collisions 70
H.H.Gutbrod, K.H.Kampert, B.W.Kolb, A.M.Poskanzer, H.G.Ritter, and H.R.Schmidt

Bose-Einstein Correlations of Positive Pions in Collisions of Nb + Nb and Au + Au at 650 MeV/nucleon 71
R. Bock, G. Claesson, K.G.R. Doss, H.Å. Gustafsson, H.H. Gutbrod, K.H. Kampert, B. Kolb, P. Kristiansson, H. Löhner, H.G. Ritter, H.R. Schmidt, T. Siemiarczuk, H. Wieman, and W. Wislicki

Projectile Fragmentation of the Extremely Neutron Rich Nucleus ^{11}Li at 0.79 GeV/nucleon 72
T. Kobayashi, O. Yamakawa, K. Omata, K. Sugimoto, T. Shimoda, N. Takahashi, and I. Tanihata

Search for Free Quarks Produced at 800 GeV/c Using a New Concentration Technique 73
H.S. Matis, R.W. Bland, D.H. Calloway, S. Dickson, A.A. Hahn, C.L. Hodges, D. Joyce, M.A. Lindgren, T.L. Palmer, H.G. Pugh, M.L. Savage, G.L. Shaw, R. Slansky, A.B. Steiner, and R. Tokarek

Di-Leptons at the Bevalac 74
H.S. Matis

Abnormally Large Momentum Loss in Charge Pickup by 900 MeV/N Au Nuclei 74
G. Gerbier, Ren Guoxiao, and P.B. Price

Systematics of Charge-Pickup Reactions by GeV/nucleon Heavy Nuclei 74
Ren Guoxiao, P.B. Price and W.T. Williams

Observation of a Nonspherical Pion Source in Relativistic Heavy-Ion Collisions 75
A.D. Chacon, J.A. Bistirlich, R.R. Bossingham, H.R. Bowman, C.W. Clawson, K.M. Crowe, O. Hashimoto, T.J. Humanic, M.L. Justice, J.M. Kurck, W. McHarris, C.A. Meyer, J.O. Rasmussen, J.P. Sullivan, and W.A. Zajc

Study of the Energy Flow in Oxygen-Nucleus Collisions at 60 and 200 Gev/c per Nucleon 76
A. Bamberger, J. Bartke, H. Bialkowska, R. Bock, R. Brockmann, S.I. Chase, C. De Marzo, M. De Palma, I. Derado, V. Eckardt, C. Favuzzi, D. Ferenc, H. Fessler, P. Freund, M. Gazdzicki, H.J. Gebauer, C. Guerra, J.W. Harris, W. Heck, T. Humanic, K. Kadija, A. Karabarbounis, R. Keidel, M. Kowalski, M. M. Lahanas, S. Margetis, E. Nappi, G. Odyniec, G. Paic, A.D. Panagiotou, A. Petridis, J. Pfennig, F. Posa, K.P. Pretzl, H.G. Pugh, F. Pühlhofer, G. Rai,

A. Ranieri, W. Rauch, R. Renfordt, D. Röhrich, K. Runge, A. Sandoval, N. Schmitz, T. Schouten, L.S. Schroeder, P. Seyboth, J. Seyerlein, E. Skrzypczak, P. Spinelli, R. Stock, H. Ströbele, A. Thomas, M. Tincknell, L. Teitelbaum, S. Tonse, G. Vesztergombi, D. Vranic, and S. Wenig

Strange Particle Production in the NA35 Experiment at CERN 78
A. Bamberger, J. Bartke, H. Bialkowska, R. Bock, R. Brockmann, S.I. Chase, C. De Marzo, M. De Palma, I. Derado, V. Eckardt, C. Favuzzi, D. Ferenc, H. Fessler, P. Freund, M. Gazdzicki, H.J. Gebauer, C. Guerra, J.W. Harris, W. Heck, T. Humanic, K. Kadija, A. Karabarbounis, R. Keidel, M. Kowalski, M. M. Lahanas, S. Margetis, E. Nappi, G. Odyniec, G. Paic, A.D. Panagiotou, A. Petridis, J. Pfennig, F. Posa, K.P. Pretzl, H.G. Pugh, F. Pühlhofer, G. Rai, A. Ranieri, W. Rauch, R. Renfordt, D. Röhrich, K. Runge, A. Sandoval, N. Schmitz, T. Schouten, L.S. Schroeder, P. Seyboth, J. Seyerlein, E. Skrzypczak, P. Spinelli, R. Stock, H. Ströbele, A. Thomas, M. Tincknell, L. Teitelbaum, S. Tonse, G. Vesztergombi, D. Vranic, and S. Wenig

Probing the Space-Time Geometry of Ultra-Relativistic Heavy-Ion Collisions 80
A. Bamberger, J. Bartke, H. Bialkowska, R. Bock, R. Brockmann, S.I. Chase, C. De Marzo, M. De Palma, I. Derado, V. Eckardt, C. Favuzzi, D. Ferenc, H. Fessler, P. Freund, M. Gazdzicki, H.J. Gebauer, C. Guerra, J.W. Harris, W. Heck, T. Humanic, K. Kadija, A. Karabarbounis, R. Keidel, M. Kowalski, M. M. Lahanas, S. Margetis, E. Nappi, G. Odyniec, G. Paic, A.D. Panagiotou, A. Petridis, J. Pfennig, F. Posa, K.P. Pretzl, H.G. Pugh, F. Pühlhofer, G. Rai, A. Ranieri, W. Rauch, R. Renfordt, D. Röhrich, K. Runge, A. Sandoval, N. Schmitz, T. Schouten, L.S. Schroeder, P. Seyboth, J. Seyerlein, E. Skrzypczak, P. Spinelli, R. Stock, H. Ströbele, A. Thomas, M. Tincknell, L. Teitelbaum, S. Tonse, G. Vesztergombi, D. Vranic, and S. Wenig

Charged Particle Multiplicities and Inelastic Cross Sections in High Energy Nuclear Collisions 82
A. Bamberger, J. Bartke, H. Bialkowska, R. Bock, R. Brockmann, S.I. Chase, C. De Marzo, M. De Palma, I. Derado, V. Eckardt, C. Favuzzi, D. Ferenc, H. Fessler, P. Freund, M. Gazdzicki, H.J. Gebauer, C. Guerra, J.W. Harris, W. Heck, T. Humanic, K. Kadija, A. Karabarbounis, R. Keidel, M. Kowalski, M. M. Lahanas, S. Margetis, E. Nappi, G. Odyniec, G. Paic, A.D. Panagiotou, A. Petridis, J. Pfennig, F. Posa, K.P. Pretzl, H.G. Pugh, F. Pühlhofer, G. Rai, A. Ranieri, W. Rauch, R. Renfordt, D. Röhrich, K. Runge, A. Sandoval, N. Schmitz, T. Schouten, L.S. Schroeder, P. Seyboth, J. Seyerlein, E. Skrzypczak, P. Spinelli, R. Stock, H. Ströbele, A. Thomas, M. Tincknell, L. Teitelbaum, S. Tonse, G. Vesztergombi, D. Vranic, and S. Wenig

Negative Particle Production in Nuclear Collisions at 60 and 200 GeV/c per Nucleon 83
A. Bamberger, J. Bartke, H. Bialkowska, R. Bock, R. Brockmann, S.I. Chase, C. De Marzo, M. De Palma, I. Derado, V. Eckardt, C. Favuzzi, D. Ferenc, H. Fessler, P. Freund, M. Gazdzicki, H.J. Gebauer, C. Guerra, J.W. Harris, W. Heck, T. Humanic, K. Kadija, A. Karabarbounis, R. Keidel, M. Kowalski, M. M. Lahanas, S. Margetis, E. Nappi, G. Odyniec, G. Paic, A.D. Panagiotou, A. Petridis, J. Pfennig, F. Posa, K.P. Pretzl, H.G. Pugh, F. Pühlhofer, G. Rai, A. Ranieri, W. Rauch, R. Renfordt, D. Röhrich, K. Runge, A. Sandoval, N. Schmitz, T. Schouten, L.S. Schroeder, P. Seyboth, J. Seyerlein, E. Skrzypczak, P. Spinelli, R. Stock, H. Ströbele, A. Thomas, M. Tincknell, L. Teitelbaum, S. Tonse, G. Vesztergombi, D. Vranic, and S. Wenig

Electromagnetic Spallation of 6.4 TeV ^{32}S Nuclei 85
P.B. Price, Ren Guoxiao, and W.T. Williams

THEORY

Nuclear Dissipation and the Order to Chaos Transition 87
W.J. Swiątecki

Structure Studies of Low-Lying 0^+ States in the Deformed Rare-Earth Region 87
A.A. Shihab-Eldin, M. Stoyer, and J.O. Rasmussen

Classical Simulation of Nuclear Systems 89
C. Dorso and J. Randrup

Deformation and Nilsson Configurations in A≈100 Nuclei 90
K.-L. Kratz, B. Pfeiffer, V. Harms, E. Monnand, H. Gabelmann, and P. Möller

New Features in the Calculation of Heavy-Element Fission Barriers 90
P. Möller, J.R. Nix, and W.J. Świątecki

Astrophysical Implications of β-Strength and Shell Structure Properties far from Stability 92
K.-L. Kratz, V. Harms, A. Wöhr, W. Hillebrandt, W. Ziegert,
F.-K. Thielemann, J. W. Truran, and P. Möller

Comparison of Nuclear Transport Models on 800 AMeV La+La Data 92
J. Aichelin, J. Cugnon, K. Frankel, Z. Fraenkel, C. Gale, M. Gyulassy, D. Keane, C.M. Ko,
J. Randrup, A. Rosenhauer, H. Stöcker, G. Welke, and J.Q. Wu

Implications of Pion Interferometry for O+Au at 200 GeV/nucleon 94
M. Gyulassy and S.S. Padula

The Nuclear Interaction Cross Sections 95
H.S. Chung and W.D. Myers

On the Phase Equilibrium of Nuclear Matter 95
C.-S. Wang and W.D. Myers

The Effective Stiffness of Nuclei Near Magic Numbers 96
W.D. Myers and P. Rozmej

Dense Skyrmion Systems 97
L. Castillejo, P. S.J. Jones, A.D. Jackson, J. J.M. Verbaarschot, and A. Jackson

String-like Solutions in the Skyrme Model 97
A. Jackson

The Decay of the String in the Skyrme Model 98
A. Jackson

An Approach to General Covariance in String-Space of BRST String Field Theory 99
J. Greensite and F.R. Klinkhamer

Hard-Photon Production in the Nucleon-Exchange Transport Model 100
J. Randrup and R. Vandenbosch

Further Studies of the Macroscopic Nuclear Surface Response 100
V.I. Abrosimov and J. Randrup

The Decay of Hot Nuclei 101
L.G. Moretto and G.J. Wozniak

Nuclear Spinodal Decomposition 103
J.A. Lopez and G. Lubeck

Hot Nuclei in a Nucleon Vapor 103
G. Fai and J. Randrup

Hot Gluon Plasma at Large Distances 104
R.F. Alvarez-Estrada and J.A. Lopez

Multifragmentation versus Sequential Fission: Observable Differences? 104
J.A. Lopez and J. Randrup

Nuclear and Astrophysical Evidence on the Equation of State 105
N.K. Glendenning

Skyrme Topological Soliton Coupled to Gravity 105
N.K. Glendenning, T. Kodama, F.R. Klinkhamer,

Quark Matter '87: Concluding Remarks 106
M. Gyulassy

Comment on "Type-II Supernovae from Prompt Explosions" 106
N.K. Glendenning

Pion Interferometry of Ultrarelativistic Nuclear Collisions with Final State Cascading 107
S.S. Padula, M. Gyulassy, and S. Gavin

Heavy Ion Physics Challenges at Bevalac/SIS Energies 108
M. Gyulassy

Vacuum Polarization Effects in the Non-Linear σ, ω-Model 108
Norman K. Glendenning

Vacuum Polarization Effects on Nuclear Matter and Neutron Stars 109
Norman K. Glendenning

METHODS and INSTRUMENTATION

New Developments for OASIS 111
R.M. Chasteler, J.M. Nitschke, L.F. Archambault, A.A. Wydler

Initial Evaluation of a Large NaI(Tl) Spectrometer 112
J.M. Nitschke and K.S. Vierinen

Monte-Carlo Simulation of Gamma-ray Cascades in a Ge Detector 112
K.S. Vierinen, J.L. Feng, P.A. Wilmarth, and J.M. Nitschke

PERALS – Photon-Electron Rejecting Alpha Liquid Scintillation Spectrometer 113
R.B. Chadwick, M.J. Nurmia, D.M. Lee, and D.C. Hoffman

Gas Phase Isothermal Chromatography of Hahnium Bromide Complexes 114
K.E. Gregorich, W. Brüchle, U. Baltensperger, H. Gäggeler, J. Kratz,
D.M. Lee, C. Lienert, D. Jost, M.J. Nurmia, Y. Nai-Qi, R.A. Henderson,
H.L. Hall, C.M. Gannett, R.B. Chadwick, J.D. Leyba, K.R. Czerwinski, D.C. Hoffman,
M. Schadel, U. Scherer, A. Türler, and P. Zimmerman

Development of a Low Energy Proton Detector Array 115
D.M. Moltz, J.D. Robertson, N.W. Madden, D.A. Landis, J.E. Reiff, T.F. Lang, and J.C. Cerny

A Multiple Target Gas-Jet System for Light-Ion Bombardments of Heavy Targets 116
H.L. Hall, M.J. Nurmia, and D.C. Hoffman

Completion of SASSY2 118
A. Ghiorso

Phosphate Glass Detectors with High Sensitivity to Nuclear Particles 118
Shicheng Wang, S.W. Barwick, D.E. Day, D. Snowden-Ifft, P.B. Price, A. Westphal

A Non-aqueous Method for Separating 1+ and 3+ Cations 119

R.A. Henderson, H.L. Hall, C.E.A. Palmer, P.A. Baisden, and D.C. Hoffman

The Response of Scintillators to Heavy Ions - I. Plastics **120**
M.A. McMahan

Comparison of Two Programs for Prediction of Neutron Evaporation Cross Sections for Actinide and Light Projectile Reactions **120**
G.R. Haynes, J.D. Leyba, D.M. Lee, and D.C. Hoffman

A Novel Approach to the Measurement of the Neutron Multiplicity Associated with Reverse Kinematics Heavy Ion Reactions **120**
A. Pantaleo, L. Fiore, G. Guarino, V. Paticchio, G. D'Erasmo, E.M. Fiore, N. Colonna, R.J. Charity, G.J. Wozniak and L.G. Moretto

NMR on β-Emitter ^{37}Ca Produced through Projectile Fragmentation in High-Energy Heavy-Ion Collisions **121**
M. Izumi, A. Kitagawa, K. Takeyama, Y. Nojiri, T. Minamisono, K. Sugimoto, S. Shimoura, K. Ekuni, I. Tanihata, T. Kobayashi, K. Omata, Y. Shida, K. Matsuta, J.R. Alonso, G.F. Krebs, and T.J.M. Symons

Sampling Calorimeters for the Relativistic Heavy-Ion Experiment WA80 at CERN **122**
T.C. Awes, C. Baktash, R.P. Cumby, R.L. Ferguson, A. Franz, T.A. Gabriel, H.A. Gustafsson, H.H. Gutbrod, J.W. Johnson, B.W. Kolb, I.Y. Lee, F.E. Obenshain, A. Oskarsson, I. Otterlund, S. Persson, F. Plasil, A.M. Poskanzer, H.G. Ritter, H.R. Schmidt, S.P. Sorensen, and G.R. Young

Quad Time-to-Amplitude Converter (LBL #21x9191 P-1) **122**
R.J. McDonald, D.A. Landis and G.J. Wozniak

PART I: PROGRAMS

Exotic Nuclei and Decay Modes

Group Leader:
Joseph Cerny

J. Batchelder*
T. F. Lang*
D. M. Moltz
J. E. Reiff*
J. D. Robertson

**Graduate Students*

Studies of nuclei very far from the valley of stability using the 88-Inch Cyclotron provide tests of theoretical models that predict the existence, masses, and shapes of exotic nuclei. In addition, these studies have revealed new modes of radioactive decay as well as spectroscopic information on nuclides with unusually large proton to neutron ratios.

To search for and characterize the decay modes of short lived exotic nuclei (100 $\mu s < t_{1/2} < 10$ ms), we have constructed a fast, variable speed (30–5000 RPM) rotating wheel apparatus. This wheel, with its twelve aluminum catcher foils around the circumference, stops nuclei recoiling from the target and carries them in front of a new low energy proton detector array with gas ΔE and Si E telescopes. Using this method, we have searched for ground state proton decay of ^{65}As and ^{69}Br. In addition, this new detector telescope and the helium jet transport system have been used to characterize the beta-delayed proton decay of ^{25}Si.

Another tool used to study exotic nuclei is the on-line mass separator RAMA (an acronym for recoil atom mass analyzer). RAMA consists of a helium jet which transports recoil nuclei produced in the target chamber to an ion source. The ions are extracted from the source, magnetically analyzed, and collected at a new highly shielded detector station. This low background environment has permitted a study of the $\beta\gamma$ decay of the $T_Z = -3/2$ nuclide ^{27}P.

Nuclear Astrophysics and Fundamental Symmetries

Group Leader:
E.B. Norman

K.T. Lesko
R.M. Larimer
B. Sur

K. Vogel,*
Georgia Institute of Technology

**Undergraduate Student*

We are involved in a number of experiments in two distinct, but not unrelated, areas: 1) nuclear astrophysics and 2) tests of fundamental symmetries. In the area of astrophysics specific studies include:

1. Positions and decay modes of excited states in ^{148}Pm and their relevance for determining the s-process neutron density.
2. Level scheme of ^{180}Ta and the survivability of ^{180}Ta in stars.
3. Level scheme of ^{176}Lu and the age of the s-process elements
4. Searches for the β^- decay of ^{54}Mn and the β^+ decay to ^{56}Ni, and the age of the cosmic rays.

Under the heading of fundamental symmetries, we are involved in several different tests of conservation laws. Specific studies include:

1. Search for the isospin formidden Fermi decay of ^{56}Ni.
2. Searches for massive, long-lived, negatively charged elementary particles.

Nuclear Structure Studies at High Angular Momentum

The group's experiments center on the use of the Berkeley High Energy-Resolution Array, HERA. The 40 bismuth germanate sectors of the small central ball have been placed inside the Ge detectors, and the system gives a sum energy spectrum and a γ-ray fold spectrum. Cuts on these spectra provide cleaner, single-nucleus products.

Studies of superdeformed (SD) bands have continued to be a major emphasis in the program at the 88-Inch Cyclotron during the past year. We have found examples of 2:1 bands in ^{148}Gd and in ^{150}Tb. The latter was the first example of an odd-odd case, but its properties were very similar to those of the doubly even examples. By comparing the moments of inertia of the SD bands of neighboring nuclei wiht calculated values, we could start to learn about the configurations of the bands. And since SD bands appeared at several neighboring mass numbers in Dy, Tb, and Gd nuclei, it appears that both the high-j neutron and proton orbitals are important to the formation of the bands in the mass 150 region. Other regions of the Periodic Table are also under investigation to learn about the systematics of the SD bands.

Group Leaders:
R.M. Diamond
F.S. Stephens

M.A. Deleplanque
C. Beausang
A.O. Macchiavelli

J.E. Draper,
C. Duyar,*
E. Rubel,
U.C. Davis

J. Burde,
Hebrew U.

**Graduate student*

Heavy-ion Reactions at Low and Intermediate Energies

Group Leaders:
R.G. Stokstad
Y.D. Chan

A. Harmon
J. Pouliot

During this past year our group continued its development of plastic scintillator detectors of the phoswich design. These developments were in two directions. The first involved position-sensitive detectors that cover a large solid angle without requiring a corresponding large number of phototubes and electronics. The other direction was to develop arrays of individual phoswich elements that provide high geometrical efficiency through close packing, identification of elements up to Ne, and of course the multi-hit capability that comes with high granularity. Two such arrays have been constructed: one for use at the 88-Inch Cyclotron and the other for an experiment at the Bevalac.

At the 88-Inch Cyclotron we made heavy use of the intense (10 ena on target) and stable beam of fully stripped ^{16}O at 32.5 MeV/nucleon to perform a series of experiments in which nucleon transfer to and from the projectile was studied. At these bombarding energies, nucleon pickup by the projectile produces a highly excited fragment that then decays by particle emission. We were able to show that this process can result in the sequential emission of more than one particle. The stripping of nucleons from the projectile also produces fragments that subsequently decay. It is thus essential to measure coincidences between projectile-like fragments and the accompanying protons and alpha particles if one is to be able to follow the evolution of nucleon transfer reactions as the bombarding energy is raised through the Fermi energy.

Central collisions of projectiles with heavy targets have been investigated by adding a pair of position sensitive parallel-plate avalanche counters to determine the linear momentum transfer associated with the production of fast light particles and other charged fragments observed in the plastic scintillators. It has been possible with this apparatus to determine the spectrum of linear momentum transfer as a function of the multiplicity of the fast, forward-going light particles.

The array of 34 truncated pyramid phoswich detectors was used to study both central and peripheral collisions in a reverse kinematics mode by bombarding targets of Be and C with beams of 32.5 MeV/nucleon ^{12}C, ^{14}N, and ^{16}O. Charged particle multiplicities up to six were observed. In some of the events we expect to be able to account for all of the momentum and energy brought into the collision by the projectile. In particular, the multi-fragmentation of the projectile is of interest.

A forward-angle phoswich hodoscope, also consisting of 34 elements, has been constructed to observe the projectile-like and intermediate mass fragments produced in collisions of 100 MeV/nucleon niobium ions with a gold target. This experiment, which includes an array of nine large solid angle gas-plastic detectors (the "pagoda"), is in collaboration with physicists from LLNL, LASL, and ANL.

The recent installation of two large NaI spectrometers at the 88-Inch Cyclotron has made it possible to study the production of high-energy photons in heavy ion collisions. Our group has decided to pursue the special region of mass and bombarding energy in which nuclear bremsstrahlung, as this process is loosely named, becomes observable. Test experiments with 25 MeV/nucleon ^{4}He on ^{4}He have shown the feasibility of observing energetic photons above the additional background arising from the use of a gas cell target. This opens the possibility for a series of experiments on such

systems as $^{3}He+^{3}He$ and $^{16}O+^{16}O$. These experiments are in collaboration with physicists from TUNL and NBS.

Finally, the measurements of intermediate mass fragments and evaporation residues produced in the reverse kinematics reactions of $^{40}Ar+^{12}C$ (in collaboration with the Moretto/Wozniak group) were completed.

Heavy Element Radiochemistry

Group Leaders:
D.C. Hoffman
G.T. Seaborg

D.A. Bennett*
R.B. Chadwick*
R.M. Chasteler
K.R. Czerwinski*
C.M. Gannett
K.E. Gregorich
H.L. Hall*
G. Haynes
R.A. Henderson*
B. Kadkhydayan*
S.A. Kreek*
D.M. Lee
J.D. Leyba*
M.J. Nurmia

K. Aleklett,
Studsvik Science Research Laboratory

H.R. von Gunten,
A. Türler,*
C. Lienert,*
University of Bern, Switzerland

M. Schädel,
W. Brüchle,
GSI

H. Gäggeler,
D. Jost,
U. Baltensperger,
Y. Nai-Qi,
Paul Scherrer Institut Switzerland

Y.W. Yu,
K.B. Chen,*
National Tsing-Hua University, Taiwan

J. Kratz,
U. Scherer*,
University of Mainz, Germany

W.D. Loveland,
Oregon State Univ.

**Graduate students*

The group uses all three of the LBL accelerators to produce and characterize new elements and isotopes, to perform atom-at-a-time studies of the chemical and nuclear properties of the heavy actinide and transactinide elements, to study nuclear reaction mechanisms, and to educate students in modern nuclear and radiochemistry. Our studies of nuclear and chemical properties are complementary and proceed hand in hand. Current research is focused in the following areas:

1. Synthesis and identification of new actinide and transactinide isotopes.
2. Atom-at-a-time studies of the chemical and nuclear properties of the heavy elements, especially of element 103 which completes the actinide series, and of the transactinide elements 104 and 105.
3. Studies of the spontaneous fission (SF) of the transcalifornium elements where sudden and unpredicted changes in SF half lives and properties have been found to occur. Searches for beta-delayed fission in both neutron-rich and neutron-deficient actinide isotopes have also been initiated.
4. Systematic studies of the production cross sections for actinides from both transfer and compound nucleus reactions using heavy actinide targets and a variety of projectiles including $^{16,18}O$, $^{20,22}Ne$, and $^{40,44,48}Ca$ in order to understand the mechanisms involved and choose the best target-projectile-energy combinations for our studies of nuclear and chemical properties.
5. Characterization of the mechanisms operating in intermediate energy (10-100 MeV/nucleon) and relativistic (≥250 MeV/nucleon) heavy ion reactions through studies of the target fragment yields, energies, angular distributions, etc.

In the past year we have performed experiments with 35-second ^{262}Ha, produced at the 88-Inch Cyclotron via the $^{249}Bk(^{18}O,\alpha,5n)$ reaction, elucidate the chemical properties of element 105. Collaborative studies with sceintists from GSI and the University of Mainz were conducted using automated systems, to obtain more data on the aqueous chemistry, and with the Paul Scherrer Institute and the University of Bern to study the gas phase chemistry of hahnium.

Electron-capture delayed fission has been positively confirmed in ^{232}Am and ^{234}Am using K x-ray-SF coincidence measurements. Development of a multiple target system allows us to increase the yields so that detailed studies of their fission properties could be made for the first time.

Collaborative studies using ^{254}Es targets are continuing and illustrate the feasibility and promise of the proposed Large Einsteinium Activation Program (LEAP). Members of our group have participated in experiments with LLNL in which the new longer-lived isotopes of Lr, 39-minute ^{261}Lr and 216-minute ^{262}Lr were produced by transfer reactions between ^{22}Ne projectiles and ^{254}Es targets. They are produced in sufficient quantity to permit studies of their SF and chemical properties. Their half lives are even longer than originally predicted in the LEAP proposal, confirming the extra stability toward SF of isotopes containing an odd number of protons and/or neutrons. It now seems quite probable that longer-lived isotopes of element 105 should exist and might be produced from ^{254}Es targets.

Radiochemical techniques are also being used to study reaction mechanisms in intermediate energy, relativistic and ultra-relativistic nucleus-nucleus collisions.

New Element and Isotope Synthesis

Group Leaders:
A. Ghiorso
J.M. Nitschke

R.M. Chasteler*
R.B. Firestone
L.P. Somerville
K. Vierinen
P.A. Wilmarth*
S. Yashita

**Graduate Students*

The On-line Apparatus for SuperHILAC Isotope Separation (OASIS) entered a new phase of operation. For the first time heavy nuclear rich beams of ^{132}Xe, ^{170}Er, and ^{176}Yb were used to synthesize new neutron rich isotopes. The heaviest known erbium and holmium isotopes ^{174}Er and ^{171}Ho with half-lives of 3.2 and 0.82 minutes respectively were identified using b and g-ray spectroscopy. In collaboration with the astrophysics group of E. Norman, a preliminary experiment was identified to search for a high-spin, short-lived isomer in ^{180}Lu that could play an important role in the nucleosynthesis of Nature's rarest isotope ^{180}Ta^{m}. The main purpose was to prepare for a later experiment with higher sensitivity using the new Total Absorption Spectrometer (TAS).

A complete computer model for TAS has been developed and Monte Carlo simulations using the EGS4 code have begun. The goal is to calculate the clicker response function from 0 to 15 MeV. This will permit the management of higher strength functions and masses up to the proton drop line, in addition to the study of rare decay branches closer to stability.

On the proton rich side, studies using OASIS were extended across the N=82 closed shell to the A-153, 154, and 154 mass chains. In ^{154}Lu β-decayed α and proton emission were observed and the isomer energy was determined.

The structure in the β-delayed proton spectra of the precursors ^{147}Dy^{g}, ^{149}Er^{g}, and ^{151}Yb^{g} was analyzed within the framework of a doorway-state model. Indications from γ-ray decay studies, β strength-function measurements, and calculations of state densities and Gamow-Teller strength distributions, suggest that some of the observed proton transitions arise from the preequilibrium decay of doorway states populated in β^{+} decay or electron capture.

Following the installation of a stronger quadrupole in SASSY2 a number of experiments were made to determine if we had met our goal of extending the magnetic rigidity range of the separator. This was done by using various beams from the SuperHILAC with known Bρ; we were gratified to find that it was now possible to adequately cover that predicted for element 110, a major accomplishment.

Our next efforts were then directed toward "fine tuning" the electronic equipment and the software needed to extract the data from the 50-detector system. One of the experiments was the bombardment of ^{208}Pb with ^{40}Ar to make the isotope, ^{245}Fm. We succeeded in observing the reaction but also found that there were some problems with the solid state detectors that had to be rectified. It was also apparent that the window problem had not been completely solved because it was possible to break them when the beam was tuned to a fine spot. During the next few months both of these difficulties were overcome.

Our next venture into the very heavy element region was the bombardment of ^{208}Pb with ^{51}V ions to make the isotopes ^{251}Ha and ^{258}Ha. Again, we were successful in obtaining good yields and this time we made use of recoil-alpha-alpha-alpha correlations to prove the assignment of ^{257}Ha by connecting it with its known daughter and granddaughter. It was very gratifying to find that the cross section for this reaction was a good fraction of a nanobarn.

Next on our agenda was to find out whether the SuperHILAC could deliver enough ^{59}Co beam to our target system to make a search for element 110 feasible in a reasonable time. During a dedicated week's running time it was found that indeed it was possible to get as much as a particle microampere with reasonable stripper foil lifetimes if that foil was moved downstream about a meter from the end of the Pre-Stripper tank.

A very important new parameter was added to the separator with the addition of a dE/dx counter between the last dipole magnet and the focal plane detector. this was made possible by the use of a very thin window of polypropylene to isolate its counting gas from the helium of the separator itself. The success of this addition now makes it possible to use this signal together with that from the focal place detector to decide when a recoil has passed through the system that could be due to element 110; when such a candidate is observed the beam is turned off in about a microsecond to reduce backgrounds during the following two or three minutes while waiting for the descendants of element 110 to decay.

Isotopes Project

Group Leaders:
E. Browne
R.B. Firestone

V.S. Shirley
B. Singh

The Isotopes Project is a member of the U.S. Nuclear Data Network (USNDN) with responsibility for evaluating nuclear structure and decay data for mass chains with A=167–194. Evaluations for mass chains with A=167, 184, 185, 189, and 191 were submitted for publication in *Nuclear Data Sheets* in 1988. This represents about 30% of the total number of evaluations submitted by members of the USNDN and the International Network for Nuclear Structure Data Evaluation this year. In addition, the evaluations for mass chains with A=168, 173, 178, 179, 182, and 188, completed last year, were published in *Nuclear Data Sheets*. As of August 1988, sales of books produced by the Isotopes Project totaled 9918 for the *Table of Isotopes*, published in 1978, and 1869 for the *Table of Radioactive Isotopes*, published in 1986.

The Isotopes Project provides access to the LBL/ENSDF database, which contains numerical information from the *Table of Radioactive Isotopes*, from the ENSDF file of nuclear data, and from *The 1983 Atomic Mass Table* of Wapstra *et al.* Computer guest accounts are now available for remote users of the database. These accounts also provide access to the Physics Program Library (PPL) and to the databases of the National Nuclear Data Center at Brookhaven National Laboratory. The PPL program library contains interactive computer codes for calculating commonly used quantities such as log *ft* values and internal conversion coefficients. Computer access can be obtained by telephone or through the HEPnet, MILNET and TYMNET computer networks. In addition, the Isotopes Project performs database searches on request.

The Isotopes Project contributes to the development of methodology for nuclear data evaluation. Topics pursued in 1988 include the normalization of decay scheme intensity data and the adoption of transition energies and branching ratios. Computer codes have been developed to implement our methodology and are being distributed to other evaluation centers.

The Isotopes Project maintains an extensive collection of nuclear physics references and reprints It subscribes to major nuclear physics journals and acts as a specialized library and local resource at LBL.

Complex Fragments and Highly Excited Compound Nuclei

Group Leaders:
L.G. Moretto
G.J. Wozniak

D.R. Bowman*
D.N. Delis*
R.J. Charity
N.Colombo
L. Vinet

G. Guarino,
A. Panteleo,
L. Fiore,
INFN

**Graduate students*

Our recent work has been directed towards elucidating the mechanisms of compound nucleus decay and complex particle emission both at low and high energy.

The recent observation of complex fragment emission in intermediate energy nuclear reactions has been interpreted as evidence for the onset of new reaction mechanisms. At low bombarding energies, virtually the only observed decay modes of excited nuclei are light particle emission, and fission for the heavier elements. This simple and allegedly well understood picture seems to change dramatically as the bombarding energy is raised into the intermediate-energy region (10–100 MeV/nucleon), where previously unobserved decay products with masses between alpha particles and fission fragments are produced in easily detectable amounts.

Preliminary experiments at various energies and projectile-target combinations produced mass distributions apparently following a power law, in general accordance with widely contrasting theoretical predictions such as those based upon cold fragmentation, liquid-vapor equilibrium, and the thermal fragmentation of a participant region. The possibility that these fragments might have their origin in statistical emission by an equilibrated compound nucleus seemed a more likely possibility to us. Since all of the more exotic mechanisms have predicted thresholds somewhere above 10 MeV/nucleon bombarding energy, we decided to search for complex fragment emission from a compound nucleus at very small incident energies, below 50 MeV total center-of-mass energy, using the ^{3}He + Ag reaction. Although the cross sections were very low (sub microbarn), the angular distributions and kinetic energy distributions for fragments from Li to Na were consistent with compound nucleus decay. To certify this as a bona fide compound nucleus process, we have measured the excitation functions associated with individual fragments in the reaction ^{3}He + Ag from just above the barriers up to 130 MeV of total excitation energy. The rapid rise of the excitation functions with energy quantitatively confirms the compound nucleus hypothesis and allows one to obtain the individual conditional-barrier heights. Strong finite-range effects predicted by modern versions of the liquid drop model are verified in detail.

To investigate the mechanism responsible for complex fragment emission at higher energies, we have found it profitable to utilize reverse kinematics reactions with heavy projectiles (^{139}La ,^{93}Nb, ^{63}Cu, ^{40}Ar) and light targets (^{9}Be, ^{12}C, ^{27}Al) at energies ranging from 8 to 50 MeV/nucleon at the SuperHILAC, the 88-Inch Cyclotron, the UNILAC, and the Bevalac. The latter accelerator has allowed us to greatly extend the energy domain over which we could study complex fragment formation. The use of reverse kinematics (projectile much heavier than target) presents many advantages in this kind experiment. The use of light target nuclei limits the range of impact parameters available and hence the number of sources. The kinematic focusing allows for coverage of a very large angular range in the center-of-mass with a small laboratory acceptance angle, thus enhancing greatly the detection efficiency for both singles and coincidences. Furthermore, the large velocity of the center-of-mass allows one to detect and identify the atomic number of the entire range of products. It is important to have access to products with masses between that of the projectile and the target because in this region a much cleaner differentiation of the mass distributions associated with the different mechanisms is expected.

For asymmetric entrance-channel reactions up to 50 MeV/nucleon, we have verified that the binary decay of the equilibrated compound nucleus can account for the major production of complex fragments. At low bombarding energies near the Coulomb barrier, the compound nuclei are produced in complete fusion reactions whereas, at higher energies they are produced in incomplete fusion reactions. In both reactions, highly excited compound nuclei are formed that move forward with high velocity. The two kinematic solutions associated with the isotropic decay in the center of mass with Coulomb-like energies are readily observed and provide a direct measure of the momentum transfer and of the Coulomb splitting. Coincidence measurements verify the binary mechanism and confirm that the sum of the charges is nearly independent of the asymmetry of the decay and close to the Z value of the incomplete fusion product after evaporation is accounted for. These compound nuclei are characterized by a temperature and a mean excitation energy per nucleon approaching the mean nucleon binding energy. It is expected that a great deal can be learned about the stability of nuclei at high excitation energy, in particular about the effect of high temperature on size and surface energy as well as about the modes of decay.

In this series of experiments we have demonstrated the pervasive nature of complex fragment emission from compound nuclei. Clearly, any other novel mechanism of production has to deal with the coexisting compound nucleus mechanism as background. In fact, the expected onset of multifragmentation at even higher excitation energy may very well be dominated by a series of sequential binary decays.

In order to study the onset and the nature of multifragmentation, we are building a detection system consisting of an array of 49 (7×7) telescopes. Each telescope consists of a 0.3 mm Si detector, a 5 mm Li-drifted detector and a 7.5 cm plastic scintillator. The first and second detectors are position sensitive along the x and y directions, respectively. This system has multihit capabilities and should be able to characterize a multifragmentation event completely if the reaction is studied in reverse kinematics. Our immediate goals with this detector system are to follow the binary decay process from 50 MeV/nucleon up to its disappearance and to study the excitation function of multifragmentation events.

As mentioned above sequential binary decay is expected to provide a sizable background to more exotic multifragmentation processes, if they exist. We have called the fragmenting of a system by a compound nuclear sequential binary decay, nuclear comminution. This process can be quantitatively assessed in terms of the complex fragment decay probability. We have shown that this mechanism predicts mass distribution with a characteristic power law dependence in the light mass region. As a consequence such a power law cannot be considered diagnostic of liquid-vapor equilibrium.

Relativistic Nuclear Collisions: Nucleus-Nucleus Collisions

All this group's offices and equipment are located in Birge Hall on the UCB campus, which makes it easy to attract new students but restricts to some extent interaction with Nuclear Science Division staff. Current research falls into the following six principal areas:

1. Systematics of radioactive decay via emission of heavy ions such as ^{14}C, ^{24}Ne, ^{28}Mg, and ^{34}Si (DOE support);

2. Search for highly ionizing particles in e^+e^- annihilation (TRISTAN experiment and LEP [OPAL] experiment, supported by NSF) and in $\bar{p}p$ annihilation (Fermilab experiment, NSF support);

3. Cosmic-ray astrophysics (NASA and NSF support):
   a. Construction of an experiment to detect anti-iron nuclei in cosmic rays at a level 3×10^{-7} of iron (in collaboration with Indiana University and the University of Michigan);

   b. Measurements of the energy spectrum of antiprotons at $E < 1$ GeV with a balloon-borne magnetic spectrometer;

4. Development of new types of glass detectors and an automated measurement system for experiments to resolve isotopes of relativistic nuclei up to lead (NASA support);

5. Ultrarelativistic nucleus-nucleus collisions (DOE support):
   a. 200 GeV/nucleon collisions of ^{16}O and ^{32}S at CERN,

   b. 15 GeV/nucleon collisions of ^{16}O and ^{32}S at Brookhaven,

   c. Detector response as a function of Lorentz factor,

   d. Planning for heavier projectiles.

Group Leader:
P.B. Price

S. Barwick
T. Coan
D. Snowden-Ifft*
D. Lowder*
T. Miller*
M. Solarz
A. Westphal*
W. Williams*

Y-D. He,
G-R. Jing,
Beijing High Energy Physics Institute

**Graduate Students*

Nucleus-Nucleus Collisions: Nucleon Emission and Transfer Studies

Group Leaders:
K.M. Crowe
J.O. Rasmussen

J.A. Bistirlich
H. Bossy
R.R. Bossingham*
A.D. Chacon*
M. Justice*
M.A. Stoyer*

A. Shihab-Eldin,
KISR, Kuwait

Q.Y. Shao,
Fudan University, Shanghai

R. Donangelo,
UFRJ, Rio de Janeiro

P. Kammel,
Austrian Academy of Science, Vienna

H. Radi,
Kuwait University

**Graduate Students*

The Bevalac research of our group has centered on the study of charged pions and correlated pairs of particles produced in relativistic heavy-ion collisions. We have utilized Janus, a large (4 meter flight path) dipole-dipole magnetic spectrometer and combinations of fast scintillators and wire chambers in a series of pion interferometry studies. Pion interferometry experiments allow measurements of size, shape, lifetime, and coherence of the pion emitting source. A two-pion experiment (1.3 GeV/nucleon La on La) was run and is under analysis. Our Bevalac work will shift emphasis to high p_T emission cross sections for p, d, t, ^{3}He and α needed by Equation-of-State theorists.

Our group has also been involved in developing heavy ion one- and two-neutron transfer reactions. $^{235}U(^{206}Pb,^{207}Pb)^{234}U$ at E_{LAB} = 1394 MeV and $^{233}U(^{206}Pb,^{207}Pb)^{232}U$ at E_{LAB} = 1566 MeV reactions were studied in May 1987 at the SuperHILAC. $^{239}Pu(^{90}Zr,^{90}Zr)^{238}Pu$ at E_{LAB} = 500 MeV was studied at the Holifield Heavy Ion Research Facility at ORNL in November, 1988. Such reactions provide a unique tool for work in the actinide region, as they appear to involve mainly "cold" neutron transfer mechanisms, thus minimizing fission competition. Theoretical work is also progressing in understanding these reactions. Recently, in collaboration with Fudan University (Shanghai) and A.A. Shihab-Eldin (Kuwait), a study of 0^+ levels of nuclei, using an exact matrix diagonalization of 9 Nilsson orbitals, was instigated. Level energies, neutron pair transfer probabilities, E0 and E2 matrix elements are all obtained in the calculation. Several rare-earth (Gd, Er, Dy isotopes) and actinide (^{246}Pu and ^{248}Cm) nuclei have been investigated, and most experimental 0^+ energy level spectra can be satisfactorily reproduced with the calculation. In addition, modest agreement is obtained between calculated and experimental (t,p) and (p,t) pair transfer reaction strengths both to ground states and excited states. We are just beginning to correlate E0 and E2 matrix elements with experimental data.

Our research group has constructed and taken to CERN a Jet Drift Chamber (JDC) to be used in the Crystal Barrel experiment at CERN's Low Energy Antiproton Ring (LEAR). The JDC is a 20-inch diameter, 18-inch long cylinder with 30 pie-shaped sectors comprised of multi-layers of precision-positioned sense, guard and field wires, strung axially. The charge deposited on the sense wire (by passage of a charged particle in a gas medium and 1kV/cm electric field) will be processed by a differential amplifier based on the Fujitsu-MB43468 chip. We have successfully tested our JDC prototype and two types of prototype amplifiers at SIN using pions and protons to give us a good understanding of the background noise, dynamic range and compatibility with flash-type analog to digital converters.

The main issue of the proposed experiment, PS 197, is the search for the phenomena related to Quantum Chromodynamics (QCD). A striking prediction of this theory is the existence of new boson resonances with constituent gluons: glueballs and hybrids. Experimental detection of these hadronic states would be a milestone in the understanding of low energy QCD.

Relativistic Nuclear Collisions: HISS

The HISS facility consists of a large solid angle magnetic spectrometer designed to measure multi-particle final states produced in relativistic heavy ion collisions. The heart of the facility is a 7 Tm, superconducting magnet surrounded by a variety of detectors which can be arranged in different ways to suit the needs of specific experiments. In addition to the local group listed here, users from RIKEN, KEK, Osaka, Michigan State University, Kent State University, U.C. Riverside and GSI-Darmstadt are active at the facility.

During the period under review, three major experiments ran at the HISS facility. The RIKEN-KEK-OSAKA-LBL collaboration took data on the fragmentation of secondary beams such as ^{11}Li and ^{8}He. These experiments follow on from earlier experiments studying interaction cross sections and interesting results have already been obtained regarding the momentum distributions of nucleons in these nuclei. The second experiment was to measure complex fragment emission at midrapidity. This is of great interest as a means of measuring the entropy of the final state. Finally, a new experiment was done measuring pion-correlation in Ar and X induced reactions. Both of these latter experiments used the new 2 time 1.5 m drift chamber to measure multiparticle completions.

During the year, considerable progress was made on the development of the MUSIC II detector which measures the change and position of highly charged ions. Initial tests of the detector have been successful and an electronic readout system is now being developed for the detector. Finally, initial design was done for a new time-of-flight array that will augment the system presently available at the HISS facility.

Technical Director:
H. Wieman

F.S. Bieser
E. Chang
P. Davis
J. Engelage
D.L. Olson
J. Rubeor
T.J.M. Symons
J. Wolf

H.J. Crawford,
L. Greiner,
UCSSL

W. Christie,*
C. Tull,*
U.C. Davis

I. Flores,
AF&RD

**Graduate students*

Relativistic Nuclear Collisions: The Plastic Ball

Group Leaders:
A.M. Poskanzer
H.G. Ritter

K.G.R. Doss
A. Franz
P. Jacobs
R. Romeiser*
R. Schicker

**Graduate Student*

The work of the group centers on the use of the Plastic Ball and other detectors to study central collisions of nuclei at bombarding energies ranging from 200 MeV/nucleon to 200 GeV/nucleon, with the aim of learning about nuclear matter at high temperature and density. In the past two years a major experiment was performed at the CERN Laboratory's Super Proton Synchrotron (SPS) using 60 and 200 GeV/nucleon ^{16}O, and 200 GeV/nucleon ^{32}S beams. This is a collaboration involving GSI, the University of Münster, Lund University and Oak Ridge National Laboratory. The experiment, called WA80, consists of five detector systems: The Plastic Ball, Multiplicity Arrays, a Lead Glass Spectrometer, a Mid-Rapidity Calorimeter, and a Zero-Degree Calorimeter. The goal is to study the systematics in this energy range and to search for signatures of the quark-gluon plasma. Excellent data were obtained with both the ^{16}O and ^{32}S beams, and several papers have been published based on the ^{16}O results.

The Bevalac Plastic Ball data are still being analyzed. An important event in the last year was the discovery of a new component of the collective flow, called Squeeze-out, and a detailed study of this effect is in process. Another goal of the analysis is to learn about multifragmentation or the liquid-gas phase change. This latter work is in collaboration with the Harris group and a group from LANL.

Relativistic Nuclear Collisions: DLS

Group Leaders:
G. Roche
L.S. Schroeder

E. Lallier
A. Letessier-Selvon
H.S. Matis
C. Naudet
P. Seidl
Z.F. Wang
A. Yegneswaran

G. Krebs,
AF&RD

The construction of the Dilepton Spectrometer (DLS) was completed and the whole system successfully tested with an Ne beam in November 1986. The DLS is a large aperture two-arm magnetic detector constructed and operated by a consortium involving the Lawrence Berkeley Laboratory, Johns Hopkins University, Louisiana State University, Northwestern University, UCLA and Clermont-Ferrand. It is instrumented with segmented gas Cerenkov arrays in front and back of the magnets to discriminate $e^{\pm}$'s from $\pi^{\pm}$'s and protons, scintillation hodoscopes (front and back) for fast charged particle triggering, and drift chambers in front and back for tracking. A multiplicity detector will be constructed in 1988. The system is installed in the BEVALAC beam-30 cave.

The goal of DLS collaboration is to measure the e^+e^- mass spectrum between 100-800 MeV and p_T distribution up to 700 MeV/c. The program includes both proton-nucleus and nucleus-nucleus collisions. In proton-nucleus interactions, it aims to establish the existence of direct lepton (electron) pairs at BEVALAC energies and help clarifying the mechanism(s) of their production. In nucleus-nucleus collisions, dileptons are excellent probes of the hot, compressed phase of the nuclear medium and should tell us a great deal about the fundamental processes going on at this stage of the collision and provide another means for obtaining additional information on the nuclear equation of state.

In December 1986, data were taken in p + Be at 4.9 GeV and the existence of a direct electron pair signal established by mid-February of 1987. The strength of the signal, expresses as usual in terms of e/π ratio, is estimated in between 5×10^{-5} and 5×10^{-4}, which is consistent with the high energy typical number of a few 10^{-4}. A second of the DLS was done in May 1987. Two reactions were studied: p + Be at 2.1 GeV and Ca + Ca at 1.95 GeV/nucleon. Here again direct electron pairs were observed at about the same rate. The analysis of these data is in progress.

Relativistic Nuclear Collisions: Radioactive Beam Study and Light Particle Emission Study

Group Leaders:
L.S. Schroeder
K. Matsuta

J.R. Alonso
G.F. Krebs
K. Sugimoto,
T.J.M. Symons

O. Hashimoto,
Y. Shida,
INS, University of Tokyo, Japan

M. Izumi,
T. Minamisono,
Y. Nojiri,
N. Takahashi
K. Takeyama,
Laboratory of Nuclear Studies, Osaka University, Japan

I. Tanihata,
RIKEN Wako, Saitama, Japan

S. Shimoura,
E. Ekuni,
Kyoto University Kyoto, Japan

Our group has been studying high-energy heavy-ion reactions at the Bevalac in a collaboration between the Institute for Nuclear Study (INS), the University of Tokyo, Osaka University, and LBL. The experimental program of the group emphasizes two types of measurements, one measures the interaction cross section (E690H and E852H) and magnetic moments (E732H) using beams of radioactive nuclei, and the other measures light particle emissions ($\pi^{\pm}$, p, d) from heavy-ion collisions (E593H,E733H).

In experiment E852H interaction cross sections between two nuclei were measured using beams of secondary nuclei at 790 MeV/nucleon and at 400 MeV/nucleon. In addition to ^{6,7,8,9,11}Li, which was reported last year, ^{14}Be and ^{15}B show remarkably large radii. A momentum spectrum of ^{9}Li, which is emitted from the fragmentation of ^{11}Li at 790 MeV/nucleon, has been measured. This is the first measurement of the fragmentation of radioactive nuclei. The momentum spectrun shows two components in momentum fluctuation of nucleons inside ^{11}Li which in turn indicates an existence of a long tail (giant neutron halo) in the density distribution. The same behavior was observed for ^{14}Be fragmentation. The coulomb dissociation cross sections of neutron rich nuclei have also been measured. The analysis of the data is now in progress.

A new experiment E732H was undertaken to determine nuclear moments of unstable nuclei in the $f_{7/2}$ shell. For this purpose an NMR method was applied to short-lived β emitting nuclei produced through projectile fragmentation. Test runs have been made in Bevalac beam line B-44 to confirm the separability of isotopes and polarization production using a tilted foil technique. In the test run, ^{20}F, ^{21}F, ^{37}Ca and ^{39}Ca nuclei were successfully collected and the nuclear lifetimes were obtained by detecting β rays. NMR on ^{39}Ca was detected to show a significant amount of polarization in the beam. The technique will be applied for determination of magnetic moments of ^{37}Ca and ^{43}Ti.

Experiment E593H measured pion spectra at 0° in coincidence with heavy fragments emitted at the same angle for studying Coulomb distortion effects on pion spectra. The experiment was performed at HISS using a La beam of 800 MeV/nucleon, and the data analysis is in progress. A prominent peak has been observed in the π^- spectrum at around the projectile velocity. The peak position shifts to lower momentum for smaller impact parameter, and this shift is thought to be due to larger friction in collisions of smaller impact parameter. The distribution of the projectile fragment sum charge has been measured in the La + C reaction. The results indicate that a transverse growth of the cascade has a large effect in the reaction.

The projectile- and target-mass dependence of light particle production in heavy ion collisions has been studied by measurements of pions and light nuclear fragments (p, d, t, ^{3}He, and ^{4}He) in La + La collisions at 800 MeV/nucleon (E733H). A magnetic spectrometer was used for detection of these particles and a set of 120 multiplicity counters was used for event selection. We have measured (a) energy spectra, (b) angular distributions, (c) the pion to nucleon yield ratio, and (d) the coalescence relation for

the formation of composite fragments in both low- and high-multiplicity events. By comparing these results with the previous data for lighter mass collisions, we have found that both pion yield and pion kinetic energy are greatly influenced by final state interactions.

Streamer Chamber Experiments

Group Leaders:
J.W. Harris
H.G. Pugh
L.S. Schroeder

J.P. Brannigan
S.I. Chase*
G. Odyniec
G. Rai
W. Rauch
S. Tonse
L. Teitelbaum*
L.M. Tinay
J.-M. Walker

**Graduate student*

The Streamer Chamber allows the study of charged particles as well as K^0 and Λ^0 over most of the 4π solid angle in high energy heavy ion collisions. Using it, and a forward angle 384-element scintillator array, we have made measurements of π^- multiplicities and spectrum shapes as a function of beam energy and of participant number (i.e., impact parameter). We have studied Λ^0 production in near-central collisions, and we have reconstructed and measured all the tracks in a large sample of events, to extract such quantities as flow and transverse momentum distributions. Our results indicate that the nuclear matter equation of state is stiffer than had been supposed.

Several improvements to the Streamer Chamber facility are underway to extend these studies to the heaviest projectiles (which is desirable to minimize surface effects and to emphasize bulk properties of the "fireball"); to provide enhanced particle identification (and hence more complete evaluation of individual events); and to permit greater efficiency in data analysis.

High-gain image intensifiers and CCD cameras have been installed, together with a fully digitized data acquisition and analysis system, developed and tested on the NA35 experiment at CERN. A test run was completed at the Bevalac in Spring of 1987. The Streamer Chamber was successfully operated at lower pulse voltages near the avalanche mode with complete elimination of "flares," improved track definition, and linearity of response (which is important for particle identification by dE/dx measurement). On-line monitoring of the chamber performance and on-line studies of event topologies (with, for example, on-line availability of track multiplicities) were performed. The complete digitization of the data acquisition and analysis system will permit rapid automatic scanning and preselection of events, and a major enhancement in the speed of (operator-assisted) total event reconstruction.

The CCD camera system uses three cameras, each with 1024×1024 pixels. The information in the pixels is digitized to 9 bits and transferred in parallel to an on-line image processing system based on a VAXstation II computer (Micro VAX II). Attached to this is a 10 million-instruction-per-second integer coprocessor, the Mercury Computer System 3216, and peripherals. Data are stored on a high density digital VHS cassette tape recording system.

Nuclear Theory

The nuclear theory program covers a broad range of topics in nuclear physics as decribed below.

Group Leaders:
N.K. Glendenning
M. Gyulassy
W.D. Myers
J. Randrup*
W.J. Świątecki

S. Gavin
A. Jackson
F.R. Klinkhamer
J.A. Lopez
S.S. Paduila
M. Redlich
K.E. Tang

G. Fái,
Kent State Univ.

P. Möller,
Lund Univ.

L. Wilets,
Univ. of Washington

**Scientific Director*

Ultra-Relativistic Nuclear Collisions

A major component of the theory program focuses on problems associated with ultra-relativistic nuclear collisions and the search for the quark-gluon phase of nuclear matter. This topic is addressed on both the phenomenological level in close contact with local experimental groups and on the formal theoretical level of developing QCD and hadronic transport theories. The phenomenological work in the past year concentrated on two of the most controversial and provocative sets of data to emerge from the first CERN/SPS experiments with 200A GeV ions: (1) the increased suppression of J/ψ production with increasing transverse energy and (2) the anomalous pion source space-time parameters deduced by pion interferometry. Both results have been interpreted by others as evidence for the sought plasma transition. Our work was aimed at exploring the uniqueness of those interpretations, using as a basis the Lund string model that was developed here into an independent Monte Carlo program (ATTILA) and compared to extensive multiplicity and transverse energy data in the past two years. In these new applications the Lund model is used to relate global observables (such as the transverse energy) to local ones (such as rapidity density) and to geometrical aspects. For the J/ψ problem, we found that a continuous and quantitative explanation of the data from p+p to p+A to O+A could be achieved by taking into account initial state gluon interactions and final state J/ψ dissociation in the comoving hadronic resonance gas. Remarkably, the same resonance gas source computed by the Lund model was found to reproduce quantitatively all the features of the pion interferometry data as well. Therefore, our present conclusions are that the reported data are in fact consistent with a purely hadronic resonance dynamical model. In the future we intend to pursue the problem of determining which observables are most sensitive to purely plasma effects and are less influenced by complex hadronic effects. Presently we are investigating baryon stopping power by comparing the Dual Parton and Lund versions of string models to predictions based on Landau hydrodynamic models.

We have recently begun a new series of investigations of deep-inelastic e+A scattering from the point of view of string models. The goal here is to test whether such reactions could provide independent information on the space-time development of hadronization through the A dependence of final-state cascading particles. Models for the space-time development have been recently developed here and merged with the Lund model, which is formally a momentum-space model. In addition to applications to e+A scattering, that model will be used to compute the evolution of the baryon and energy density in ultra-relativistic nuclear collisions. Preliminary results indicate that the maximum energy density in CERN reactions may be as low as 1 GeV/fm^3, which provides a possible explanation as to why hadronic models are still so successful in accounting for the new data.

On the formal level we have started work on interacting and dynamical string models using effective field theories such as the Landau-Ginzberg and Higgs models to

predict possible consequences of high density string formation. The long-range goal with such models is to develop a QCD transport theory taking non-perturbative dynamical vaccuum effects into account. Transport phenomena in superconductors are being studied as a possible analog to the situation encountered in high-energy hadronic processes. For example, as the string density increases, what is the time scale for the quenching of the color electric superconducting vacuum? Up to now no attempt has been made to address such dynamical questions in proposed QCD transport theories.

Nuclear Physics at Bevalac Energies

In the past year, intensified efforts were made on topics of relevance to the Bevalac. Thanks to a special grant from the LBL Exploratory Research and Development Fund for Institutional Projects it was possible to support a postdoc for the local core effort and to organize a strong visitor program, involving over thirty active theorists in the field; there was also considerable interaction with experimentalists. This program was so successful that we are requesting additional funds, beginning in FY90, to sustain such an effort (see last section). Particular progress was made in the areas of reaction dynamics and dilepton production. For example, cascade, fluid dynamic, and statistical models were employed and compared with data, in order to ascertain their reliability. Below is described only the progress in this area made by members of the Theory Group at LBL.

The possibility for determining the nuclear equation of state from inclusive data has been examined in dynamical simulation models and a new method for determining the azimuthal orientation of the reaction plane has been proposed. Constraints on the nuclear equation of state have been established from a wide range of nuclear and astrophysical phenomena. In order to determine the equation of state of hot subsaturation matter, which is of interest in both astrophysics and heavy-ion physics, the problem of very hot nuclei imbedded in a nucleon vapor was addressed.

The possibility for exploiting the kinematical differences to distinguish between sequential-binary breakup and simultaneous (true) multifragmentation has been studied and the methods developed have already been employed by several experimental groups in their data analysis. Work is well underway to develop a formal theory of nuclear multifragmentation processes based on the transition-state approximation. This theory connects the Bohr-Wheeler description of (sequential) binary fission at low energy with statistical descriptions of multifragmentation at high energy and thus provides a good basis for studying the evolution of the disassembly process as the excitation of the nuclear system is raised. A special advantage is that the freeze-out volume is determined within the theory and need not be prescribed separately, contrary to existing models.

A self-consistent momentum-dependent Vlasov equation has been derived from quantum hadrodynamics for application to Bevalac energies. Moreover, the formulation of one-body dynamical simulation models is being extended to encompass the evolution of fluctuations in the one-body phase-space density. Pre-equilibrium emission of neutrons and photons was studied within the Nucleon Exchange Transport model, yielding a good overall understanding of a variety of data.

Field Theory Studies

Non-perturbative aspects of field theories are becoming increasingly relevant to nuclear physics. The areas of research include the structure of the Interactions in superstring theory, the quark-confinement mechanism, and topological solutions to effective meson field theories.

Studies of the Skyrmion model for the nucleon have led to the discovery of novel solutions, including one with string-like properties. The stability and decay properties of this object are being further investigated. Using relativistic hadronic field theory, the existence of phase transitions, abnormal matter and hyperons in neutrons stars have been studied. Current studies include pion production in a hot nuclear fireball model and vacuum renormalization effects in neutron stars.

Nuclear Properties

Nuclear masses and deformations have been calculated in a microscopic-macroscopic model for 8979 nuclei for a region extending from the proton to the neutron drip lines. Fission properties of elements from Z=94 to Z=110 have been studied and fission half-lives have been calculated in a model that takes into account paths leading both to compact and to elongated scission shapes. A computer code for calculating Gamow-Teller β-strength functions has been further developed. The computer code is based on a model of the quasi-particle RPA type and has been extended to employ folded-Yukawa single-particle wave functions. Other extensions are that either a BCS or a Lipkin-Nogami pairing model may be used and that decay from a certain class of excited states can now be considered. A code for β-decay half-lives also has been developed.

The predictive power of the Droplet Model is being steadily improved. Recent advances include a finite-range correction term and the surface contributions to nuclear moments. In order to further extend the description of macroscopic nuclear properties a computationally intensive program is underway for the calculation of nuclear masses, radii, fission barriers, etc. The statistical model approach previously employed for studies of nuclear matter phase equilibrium, nuclear density distributions, surface properties, thermal properties and certain questions concerning supernova explosions is being used to calculate nuclear masses with special emphasis on the limits of stability. The same approach is also being applied to the calculation of fission barriers for rapidly rotating nuclei and to the calculation of interaction radii for exotic nuclear species being produced at the Bevalac.

Transition from Order to Chaos in Nuclei

In many different fields of science work is now underway to understand the behavior of dynamical systems in the intermediate regime between relatively simple, explicitly soluble (integrable) situations and the fully chaotic regime that one treats by statistical mechanics and thermodynamics. One of the recent fundamental discoveries in dynamics, ranking in importance with the advances made by Hamilton and Boltzmann, is the realization that this intermediate regime between order and chaos has an incredibly rich structure, implying unsuspected potentialities for pure and applied science.

Within our theory group a special initiative has been mounted for the application of these new developments to problems of interest in nuclear physics. The two main points of contact that are being studied are, first, the statistics of nuclear level spacings and, second, the very close connection between the nature of the dynamics of nuclear shape evolutions (in Fission or nucleus-nucleus collisions) and the ordered or chaotic nature of the nucleonic motions in the nuclear mean field. (In the regime of ordered motions the nucleus should behave as an elastic solid, in the regime of chaotic motions as a fluid with an exotic viscosity, and in the intermediate regime as a viscoelastic substance.) We are engaged in a series of studies illustrating the relation between the order-to-chaos transition in nucleonic motions and the solid-to-fluid transition of an idealized nucleus undergoing shape oscillations of various multipolarities. Specific problems being considered concern the fluctuations in eigenvalue distributions (level densities) in irregularly shaped (chaotic) potential wells, (of importance in the interpretation of nuclear masses and deformations), and the dissipation associated with Landau-Zener transitions in time-dependent quantal systems, such as nuclei.

An allocation from the LBL Exploratory Research and Development Fund for Innovative Science Projects has permitted us to add a postdoc with expertise in this area and to initiate a program of visiting speakers, workshops and study groups. Relationships have been established with workers in France, the United Kingdom and Poland, and several joint undertakings have been initiated. A number of students have also begun to participate in the program and a weekly workshop with participants from the UC Berkeley campus has contributed to the rapid growth in the size of the program.

Nuclear Theory Visitor Program

The Nuclear Theory Program at LBL has a long-standing tradition for playing a coordinating and catalyzing role in the development of specific areas at the forefront of our field, primarily by means of a vigorous and dedicated visitor program in conjunction with a sustained local core effort involving both senior staff and postdoctoral fellows. As referred to above, we are requesting additional funds to allow this valuable activity to continue in the coming years, as we are facing the important programmatic needs presented by the major new experimental facilities underway.

Most recently (in FY88) the Theory Group organized an intensified program focused on nuclear physics amenable to study with medium-energy heavy-ion facilities, such as the Bevalac at LBL or the SIS-18 now nearing completion at GSI in Germany. This program was made possible by a special grant from the LBL Exploratory Research and Development Fund. (In recent years the general cost escalation has seriously eroded our bugetary situation to such a degree that our base funding will only permit a very modest visitor program, and does not make room for even a single postdoctoral fellow.)

The main motivation for undertaking the program was that the Nuclear Theory Group at LBL has been an international focal point for the development of the field of high-energy nuclear collisions, including especially the intermediate-energy regime characteristic of the Bevalac. Improvements in the capability of the Bevalac would make it possible to carry out much more quantitative and detailed experimental investigations of phenomena occurring in nuclear collisions at intermediate energies. In order to

provide a basis for planning the experimental program, further theoretical developments are necessary.

The Exploratory Research and Development funds permitted us to support a postdoctoral fellow for the local core effort, as well as support a more senior sabbatical visitor working in the area. In addition, a substantial number (over thirty) of internationally reknown theorists active in the area took part in the visitor program. A large part of these participants are based in Europe, where the intermediate-energy heavy-ion field is both strong and growing.

The program was succesful in a variety of ways. Most importantly, it demonstrated the strong theoretical interest in the physics of medium-energy heavy-ion collisions and has helped to broaden the scientific basis for this venture. Several specific advances were made on the topics in focus. For example, the major current dynamical theories were compared and examined critically and confrontation with data was made; intense work was also carried out on the use of dileptons as probes in Bevalac collisions. The program activity has already been of direct benefit to the experimental program at the Bevalac and is expected to become even more useful as the follow-up efforts bear fruit.

The above description of last year's successful visitor program serves to illustrate the important role such intensified efforts can play in the advancement of our field. One of the important aspects of such programs is that they are especially well-suited to involve individual researchers who are situated in relative isolation and who might otherwise not be able to contribute. Another important aspect, which is essential for such efforts to have an impact on the field, is the involvement of experimentalists in the program.

In the coming years, it is particularly important to address the physics of nuclear collisions at ultrarelativistic energies. Large experimental programs are being established at the AGS and some experiments have been made at CERN at higher energies. As these programs expand and RHIC moves closer to realization, it is essential to mount a strong effort in theory, to help direct and interpret the experiments. Our experience through two decades has shown that dedicated programs of the type described above can play a crucial role in shaping the field. (In fact, the present quest for exploring the quark-gluon plasma via ultra-relativistic nuclear collisions, including the proposal to build RHIC, has grown out of several years of dedicated visitor programs at LBL, including several widely attended summer studies.) For such programs to succeed, two components are necessary:

(1) a vigorous visitor program seeking to involve as many leading physicists as possible, and

(2) a healthy core program to maintain the momentum of the effort; this latter component requires that a number of good postdoctoral fellows be associated with the program.

NUCLEAR SCIENCE DIVISION RESEARCH

Bevalac Research Program

The Bevalac at the Lawrence Berkeley Laboratory is a world-class heavy-ion facility capable of delivering all ions (protons to uranium) from energies of 30 MeV per nucleon up to relativistic energies of 1–2 GeV/nucleon. With these beams a wide-ranging basic research program in nuclear science, atomic and cosmic-ray physics, as well as biology and medicine, is carried out. Utilizing unique experimental facilities, the planned Bevalac scientific program will both complement and actively compete with the research to be carried out at SIS 18 at GSI during the early 1990s.

The Bevalac's research community is drawn from universities and laboratories throughout the world and provides an excellent training ground for research students over a broad spectrum of disciplines. A recent survey shows that 250–300 scientists are engaged in nuclear science research at the Bevalac. During the last five years scientists representing over 40 U.S. and 40 foreign institutions have pursued research at the Bevalac. To date, approximately 80 graduates have received their PhDs from Bevalac-related work. Currently, 40–50 graduate students are taking part in Bevalac experiments.

The central focus of the nuclear physics program at the Bevalac is the production and study of extreme conditions in nuclear matter where baryon and meson degrees of freedom are excited. Early studies with the Plastic Ball and Streamer Chamber have shown that nuclear systems at high temperatures (50–100 MeV) and densities (2–4 times normal) are produced in the central collision of two nuclei and have provided the first evidence for "collective flow"in nuclear matter. From such studies, thermodynamic and transport properties(hence an equation of state (EOS)) of nuclear matter can be deduced. This is of fundamental importance in nuclear physics and is of particular relevance to our understanding of the extreme conditions which can exist in the interior of neutron stars.

Other critical probes of extreme conditions involve the detection of dileptons (electron-positron pairs). Due to their relatively weak interaction with matter, leptons can be used to probe the hot, dense, early stage of the collision process. Recent measurements with the Dilepton Spectrometer (DLS) indicate that pion annihilation in the nuclear medium may be a major contributor to the observed dilepton spectrum and provide us with a new tool for studying the role of pions in hot nuclear matter. Finally, coupled with the recent record beam currents (e.g., over 1010 Si/pulse) provided by the Bevalac, subthreshold kaon and antiproton measure-

ments (a recent experiment has obtained about 100 antiproton events) are playing an increasingly important role in our understanding of cooperative phenomena in nuclei.

With the availability of heavy beams (typically A>100) at energies of 30–150 MeV/nucleon, studies of nuclear matter at intermediate temperatures, but at below-normal densities (near the liquid-gas phase transition), have taken on increased importance at the Bevalac. The studies focus on the question of how much energy can be contained in the nuclear system before it disassembles. Understanding the transition from binary statistical decay to multifragmentation as temperature rises is central to this effort.

Distant or grazing collisions between nuclei at the Bevalac provide unique opportunities for creating nuclear fragments containing extreme ratios of neutrons and protons, allowing the study of nuclear matter out to the proton and neutron driplines. A pioneering research program is being carried out at the Bevalac, by several Japanese groups, involving production of radioactive beams to study the fundamental properties of ground-state nuclear matter far from the line of stability. Recent accomplishments have included studies with beams of ^{11}Li and the observation that this nucleus has a "neutron halo," consisting of a pair of weakly bound neutrons.

A variety of experiments in other scientific areas continue to flourish at the Bevalac. Cosmic-ray scientists from around the world continue to use Bevalac beams to calibrate their detectors for later flights on high altitude balloons or satellites and to measure fragmentation cross sections crucial to our understanding of cosmic ray propagation. The Bevalac is the only facility in the world at present which can deliver the complete periodic table from low to intermediate t relativistic energies. Virtually all of the heavy-ion detectors which have flown on satellites over the last 10 years have been calibrated at the Bevalac.

A growing number of atomic physicists study the extreme conditions of 1- and 2-electron uranium atoms at the Bevalac to push the limits of our understanding of quantum electro-dynamics. Atomic physics cross section measurements (e.g., stripping measurements) continue to be carried out at the Bevalac; these are of practical importance to other accelerators such as the AGS Booster at BNL and to RHIC. A recent result that may open up new avenues in both atomic and nuclear physics research is the first observation of channeling of uranium ions through silicon crystals.

Low Energy Research Program

The NSD low energy research program makes use of beams from the SuperHILAC and the 88-Inch Cyclotron, which is operated by the division. Currently the cyclotron has a maximum energy of 55 MeV for protons, 32 MeV/nucleon for other elements up to oxygen, thereafter falling gradually to 5 MeV/nucleon (about the Coulomb barrier) at mass 150. The ECR source produces beams of all elements except the few most refractory. In addition, a polarized proton and deuteron source is available. The cyclotron has one of the leading ECR development programs in the U.S., and will put into operation an advanced ECR source (14.5 GHz) about a year from now (initial testing will begin in a few months). This will extend the range of usable (3 2pnA) beams above the Coulomb barrier to about mass 210. Furthermore, a conceptual design for a gyrotron-driven ECR source has been developed, which, if funded, would result in usable beams of uranium above the Coulomb barrier. These ECR sources will be valuable in many other applications. Coupled to the cyclotron, they make an extremely versatile and reliable heavy-ion facility.

One of the recent major additions to research equipment at the cyclotron has been the HERA array of 21 Compton-suppressed Ge γ-ray detectors. This array has been quite successful in discovering and studying superdeformed nuclei, in characterizing the rotational damping process, in identifying rotational band terminations, and in measuring deformations (i.e., E2 lifetimes) using the Doppler-shift-attenuation method, among other things. It is heavily used by local groups (in addition to the nuclear-structure group that built it), by other U.S. groups, and by several foreign groups. An approximately 4π central ball of 40 BGO elements has just been added to HERA in order to measure the total gamma-ray energy and multiplicity, which are closely related to the excitation energy and spin of the nucleus prior to the gamma-ray cascade. A Livermore group is developing a strong nuclear-structure program (involving half a dozen people) using HERA and plans to construct a recoil-distance lifetime apparatus to use with the array and, in addition, to participate with a UC Davis group to add a mini-orange electron spectrometer. Several groups have used particle and neutron detectors in conjunction with HERA, and there is interest in adding a detector for residual nuclei. There is no doubt that this array will be extensively exploited over the next five years. At the same time, we will be planning for future GAMMASPHERE experiments.

The 88-Inch Cyclotron has a strong heavy-element program involving both a local group and a Livermore group. These groups have made pioneering chemical investigations of elements 102–105, studied the spontaneous fission properties of the heaviest elements including the transition from asymmetric to symmetric mass division and bimodal fission, and produced a direct proof of electron-capture

delayed fission, as well as studying many other aspects of the heaviest elements. They have a unique combination of the ability to prepare, handle, and irradiate rare and radioactive targets (like 249Bk or 248Cm), access to microampere beams of neutron-rich ions like 18O or 22Ne, and an efficient helium jet system. Over the next five years they plan to develop and use extremely fast automated systems to radiochemically separate elements 105 and 106 for studies of spontaneous fission and chemical properties, implement the Large Einsteinium Activation Program (LEAP) at the cyclotron, develop a gas-detector system for measuring Z and A of short-lived fissioning species, and design and build a modified Stern-Gerlach apparatus for determining the atomic ground-state configurations of transfermium elements.

Nuclear reaction programs at the cyclotron have shown a limiting l-value in subbarrier fusion, searched for subbarrier (Coulomb-induced) fission, measured projectile excitation and breakup, demonstrated the emission of complex fragments from compound nuclei and studied the formation and decay of hot nuclei produced in heavy-ion reactions. Another group studies the decay of exotic nuclei at, or near, the proton drip line using the on-line mass separator RAMA. Recently this group has been involved in searches for ground-state proton and two-proton emitters and has developed detectors for especially low-energy protons. An astrophysics group has been involved in experiments related to the effects of astronomical environments on nuclear decay rates. The group used HERA to study the level schemes of selected nuclei in order to determine their effective half-lives at stellar temperatures, and is searching for positron branches in several electron-capture nuclei which are of interest in cosmic-ray physics. For the latter "off-line" studies this group has built a low-background laboratory with a variety of gamma-ray, X-ray, and electron detectors. A group from Duke University has used polarized proton beams to identify the iso-vector giant quadrupole resonance, and polarized deuteron beams to study D-state effects in light nuclei. This group is developing a detector system involving two large shielded NaI detectors. In addition to the programs mentioned, there are a number of other smaller ones, all contributing to the diversity and vitality of the facility. Several other factors contribute to the strength of the 88-Inch Cyclotron Facility. There is strong outside-user participation and involvement; in FY 1988, 70 outside users from about 25 institutions ran at the cyclotron using about 30% of the research time. Many, if not most, of these provide specialized equipment, as well as ideas and enthusiasm to the facility. On average, there are about 20 students working at the cyclotron every year, about half of whom are from UC Berkeley. The facility benefits greatly from its proximity and close ties to UCB. The cyclotron also contributes to the broader scientific community by making available, at cost, a significant amount of time to space and medical sciences. Finally, we would like to note that a new, modern computer system is being implemented at the cyclotron.

Ultrarelativistic Research Program

The heavy ion program at the Super Proton Synchrotron (SPS) at CERN was initiated by a collaboration between GSI and LBL in 1983. The LBL Nucalear Science Division has constructed and delivered the RFQ pre-accelerator and has been an active collaborator in three major experiments. Thetotal CERN heavy ion program has now expanded to over 600 scientists. In the first round of experiments, oxygen and sulfur beams at energies up to 200 GeV/nucleon have been used. This is a factor of 100 increase in beam energy over the Bevalac, opening up a whole new world of physics. The purpose of the SPS experiments is to raise the density and temperature of nuclear matter sufficiently to achieve a phase transition to the theoretically expected baryon-rich quark-gluon plasma.The experiments in which LBL is involved are NA35, NA36, WA80, the free quark search NA39, and the emulsion experiments EMU01 and EMU02. NA35 is based on a streamer chamber with supplemental calorimetry. A TPC for tracking in the near 0° dense cone of particles will be added next year for the second round of experiments. NA36 is a TPC experiment to measure multi-strange particle production. WA80 is a non-magnetic experiment using the Plastic Ball, hadron and photon calorimeters, and multiplicity detectors. A new BGO photon calorimeter will be added next year. The results of the CERN program so far indicate a surprising amount of stopping even at the full energy of the SPS. It also appears that the energy densities achieved are sufficient for the transition to the baryon-rich quark-gluon plasma, and a number of effects consistent with its formation have been observed. However, the theoretical interpretations are not unambiguous. These experiments will continue with sulfur beams in 1990 and 1991.At the same time, LBL has also sought to take advantage of the high energy beams available at the AGS. A dilepton experiment has been explored, and, more recently, a collaborative experiment to investigate the feasibility of detecting light antinuclei using the 802 beam line has been approved.It is very probable that a new injection system for the SPS will be built so that beams up to lead can be accelerated by 1993. This will give a significant increase in the size and lifetime of the hot dense interaction region. In order to consolidate the LBL effort, the NA35 and WA80 collaborations have submitted a joint letter of intent for a lead beam experiment which would include a large TPC, RICH detectors, and an enlarged BGO photon calorimeter. These activities complement the expected RHIC facility program, and prepare for it with physics understanding and state-of-the-art detector development. In addition, LBL is engaged in a program of detector R&D for RHIC, hosted a RHIC detector workshop, and organized the Quark Matter '86 Conference.

Nuclear Theory Program

The theory program covers a broad range of topics in nuclear physics, partly reflecting but also extending beyond the already rather broad range of the experimental program. In addition to the (five) senior theorists, the group has several (currently eight) researchers at the postdoctoral level, funded from a variety of sources, and a vigorous visitor program with a few dozen short- and long-term visitors annually, including some senior sabbatical visitors. The program is illustrated by the following highlights of recent research.

A wide range of equations of state have been used to delimit the possible observables associated with the chromodynamic phase transition. The influence of hadronic cascade on plasma signatures, such as the J/Y suppression and the K+/9+ enhancement, has been investigated. Refined pion interferometry, including resonance decay and the evolution of the source, has been used to analyze recent CERN data. A QCD transport theory is being developed and refined to address the data, and high-energy pp phenomenology is being extended to nuclear collisions for the calculation of specific observables. Rapidity fluctuations and correlations are also studied.

Constraints on the nuclear equation of state have been established from a wide range of nuclear and astrophysical phenomena. The possibility for determining the nuclear equation of state from inclusive data has been examined in dynamical simulation models. Pion production has been studied in a nuclear field theory description of expanding hot dense matter. A transition-state theory is being developed for the disassembly of very excited nuclei into arbitrary multifragment channels; it is being used to study the gradual transition from sequential-binary breakup to simultaneous (true) multifragmentation. Pre-equilibrium production of nucleons, photons, and mesons at intermediate energies is also being investigated. Further improvements are being made in our description of general nuclear properties, such as fission barriers and b-strength functions.

A new thrust focusing on ``Order, Chaos, and the Atomic Nucleus" has been initiated and a vigorous visitor program has resulted in several productive cross-disciplinary contacts. Extensive numerical studies have been carried out, illustrating how ordered nucleonic motions result in a solid-like behavior of the nucleus, whereas nucleonic chaos produces a fluid-like nucleus.

Over the next several years, the theory program will have a strong emphasis on the forefront area of ultrarelativistic nuclear collisions, while the long-standing effort at intermediate energies will be maintained. The activities in the areas of chaos in nuclei and dense matter astrophysics are expected to develop further. New areas of research will be taken up as our field continues to develop.

Nuclear Data Evaluation

The Isotopes Project compiles, evaluates, and disseminates nuclear structure and radioactive-decay data for basic and applied research, and for diverse technical applications. Since 1979, the project has coordinated its efforts with the national and international nuclear data networks, and is responsible for the evaluation of properties of nuclei with mass numbers A=167 to 194. This responsibility includes preparing data in computerized form for entry into the Evaluated Nuclear Structure Data File (ENSDF).

Comprehensive evaluations, produced from ENSDF, are subsequently published in the journal Nuclear Data Sheets. On-line access to the databases is also provided to the scientific community. Concurrent with evaluation of data, the Isotopes Project develops methods and computer codes for data analysis.

The Isotopes Project produced seven editions of the Table of Isotopes from 1940 to 1978; the group is now responsible for the production of the Table of Radioactive Isotopes, first published in 1986. This book provides a concise source of recommended data derived from ENSDF, and is tailored to the needs of applied users in industry, biology, medicine, and other fields. A new publication containing nuclear structure information is being considered to address the needs of the basic research community. In addition, new ways of handling and accessing large amounts of nuclear structure data (as expected with GAMMA-SPHERE) are being explored.

Summary

Over the years the course of nuclear physics has been significantly shaped by the contributions from LBL scientists. We expect this to continue. The planned forefront research program will carry LBL firmly into the 1990s. Building on this program and the unique facilities and resources of a multiprogram national laboratory, we look forward to the challenges of new opportunities and facilities. We are committed to maintaining LBL as a leading nuclear physics center.

88-INCH CYCLOTRON OPERATIONS

F.S. Stephens
D.J. Clark
L.F. Chlosta
R.M. Larimer
G.L. Low, Jr.
C.M. Lyneis
P.F. McWalters
J.W.Roberts

The Nuclear Science Division operates, maintains and improves the 88-Inch Cyclotron, beam transport facilities and experimental areas. It also maintains the building and shop facilities, and coordinates the use of the cyclotron by scientists and graduate students from institutions throughout the world. In FY89 the cyclotron will operate 14.5 shifts for research and one shift per week for routine maintenance until the middle of February and then operate 17.5 shifts per week for the remainder of the year.

Accelerator Use

The cyclotron operating efficiency continued to benefit from the ECR source. There are long periods of steady operation, and only one operator per shift is required. The range of ions available from the ECR source has continued to expand. Cyclotron reliability was very high, with less than 1% of the operating time being lost to unscheduled maintenance.

Ions and Energies

The experimental program calls for an enormous range of beam masses, energies and intensities. Heavy element radiochemistry experiments need several emA beams of ^{12}C, ^{18}O, ^{20}Ne, ^{22}Ne, ^{40}Ar and ^{44}Ca at 6–8 MeV/nucleon. The study of β-delayed proton emission and of light proton-rich nuclei require a few emA of ^{3}He at 40–110 MeV, and ^{12}C, ^{28}Si, ^{32}S and ^{40}Ca at 6–7 MeV/nucleon. The nuclear astrophysics group typically use beams of protons, deuterons, ^{3}He and ^{4}He at energies of 8–25 MeV/nucleon. The study of high spin states requires beams of ^{22}Ne, ^{26}Mg, ^{28}Si, ^{30}Si, ^{31}P, ^{37}Cl, ^{45}Sc and ^{48}Ti at 4-6 MeV/nucleon and intensities of 20 enA. Groups studying heavy ion reaction mechanisms and complex fragmentation of highly excited nuclei use about 10 enA of beams such as ^{15}N and ^{16}O at 30 MeV/nucleon, ^{20}Ne at 26 MeV/nucleon, ^{28}Si at 22 MeV/nucleon and ^{40}Ar and ^{63}Cu at 13 MeV/nucleon. Beams of 20–50 MeV polarized deuterons were used to study the D state of ^{4}He. For the testing of electronic chips low intensities of beams of 4 MeV/nucleon are used. A charge/mass ratio of 1/5 was chosen for these beams, so that

the ion species can be switched in a few minutes between ions such as ^{15}N, ^{20}Ne, ^{40}Ar, ^{65}Cu, ^{80}Kr and ^{126}Xe. Table I shows the range of ion species, beam intensity and energy per nucleon available from the cyclotron. Many new beams from the ECR ovens have been produced, as described below.

ECR Ion Source Development

Two ovens are used for the feed of vapor from solid materials in the LBL ECR source. They are located outside the plasma, so their vapor feed rates depend only on their temperatures. This is an advantage over wire or rod feed.

At the 1 emA level at the source, the charge states from the oven beams are similar to those from gases in the same mass range, indicating that the oven feed systems have been well optimized. In the low temperature oven, operating up to 700 deg. C, beams of lithium and phosphorus have been added to the previous beams of magnesium, potassium, calcium, titanium and bismuth. The new high temperature oven is now in full operation. It has a resistance-heated tantalum crucible, operating up to 2000 deg. C. It has been used for scandium, iron, nickel, copper, silver, lanthanum and terbium beams from the ECR source. The long term stability is excellent. During a 3-day run beams of Cu19+, Cu17+ and Cu15+ required very little source adjustment. A 3-day run of Sc10+ was also very successful. The acceleration of lanthanum and terbium has demonstrated that the cyclotron can produce beams of at least 5 MeV/nucleon up to mass 150.

Stabilization of the ECR power supplies was completed by installing new firing circuits into the unmodified supplies. This reduces the sensitivity of the ECR source to line voltage fluctuations.

Accelerator Improvements

The improvements made on the cyclotron are focused on improving its stability to take full advantage of the high stability beams produced by the ECR source. To improve the stability and tuning of the cyclotron, new valley coil power supplies have been installed. These replace the old unregulated power supplies and improve the long term stability of the cyclotron. New controls for the valley coil supplies are under fabrication and will be installed in the next few months. This will give the cyclotron operators better control of the valley coil settings and improve beam transmission through the cyclotron. Installation of a new rf screen supply for the final amplifier has reduced the ripple of the Dee voltage. Installation of a new control system for the trimmer capacitor has improved the frequency tracking of the rf system.

The key element in developing new capabilities at the 88-Inch Cyclotron will be the construction of a new Advanced Electron Cyclotron Resonance (AECR) source. Phase I of this project to construct and test the AECR source began early in FY89. The AECR operating at 14.5 GHz will produce beams of greater intensity and higher charge states than are now available using the LBL ECR. Phase II of the project in FY90 will couple the AECR to the Cyclotron Injection line. Since the maximum energy from the Cyclotron for heavy ions increases as the square of the charge state, the higher charge ions produced by the AECR will boost the Cyclotron energies. The enhanced performance of this source both in terms of intensity and maximum charge state will allow a significant improvement in the performance of the cyclotron.

Design of Advanced ECR (AECR) Source

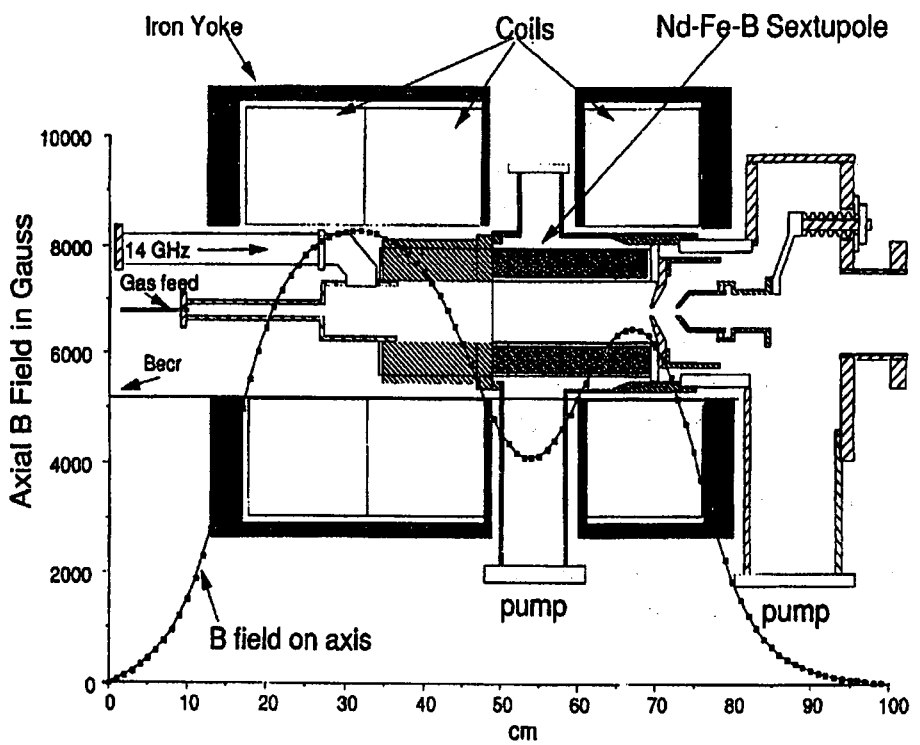

Future Plans

In FY90 the cyclotron will operate at 17.5 shifts per week for the full fiscal year. This will increase time available for nuclear physics compared to FY88 by almost 1000 hours/year. The AECR source will begin supplying higher charge state and more intense ion beams for the cyclotron toward the end of the year. In FY91 the cyclotron will again operate at 17.5 shifts per week for the full fiscal year. Physics research again with beams produced using either the LBL ECR or the AECR with the cyclotron will continue. The AECR will be optimized so that beams with mass up to 200 can be accelerated to the Coulomb barrier.

Table I 88-Inch Cyclotron Beam List

Ion	Charge State	External Beam (emA)	E/A Ion Range or Max (MeV/u)
p	1	100-10	.2-55
p(pol.)	1	.7-.4	6-50
d	1	100-10	.3-32
d(pol)	1	.7-.4	5-32
^{3}He	2	100-10	1-47
^{4}He	2	100-10	1-32
^{12}C	4	2.0	16
	5	0.06	24
	6	0.001	32
^{14}N	5	3.0	18
	6	0.15	26
	7	0.005	32
^{16}O	6	3.0	20
	7	0.1	27
	8	0.03	32
^{19}F	7	0.6	20
^{20}Ne	6	3.0	13
	7	0.4	17
	8	0.1	22
	9	0.015	28
^{24}Mg	6	2.0	9
	7	0.4	12
	8	0.2	16
	9	0.1	20
	10	0.03	24
^{28}Si	6	2.0	6
	7	1.0	9
	8	0.6	11
	9	0.1	14
	10	0.04	18
	11	0.007	22
^{31}P	8	0.5	5
	10	0.1	9

Ion	Charge State	External Beam (emA)	E/A Max MeV/u)
^{32}S	7	3.5	7
	8	2.0	9
	9	1.0	11
	10	0.4	14
	11	0.1	17
	12	0.02	20
	13	0.003	23
^{35}Cl	9	0.4	9
	10	0.1	11
	11	0.02	14
	12	0.005	16
^{39}K	9	4.0	7
	10	2.0	9
	11	1.0	11
	12	0.02	13
^{40}Ar	9	3.0	7
	10	1.5	9
	11	0.6	11
	12	0.4	13
	13	0.09	15
	14	0.015	17
^{40}Ca	9	1.5	7
	10	1.0	9
	11	0.8	11
	12	0.4	13
	13	0.06	15
	14	0.006	17
^{44}Ca	12	0.6	8.9
^{48}Ca	13	0.05	8.6
^{63}Cu	15	0.1	8
	19	0.03	12
^{84}Kr	17	0.2	6
	19	0.08	7
	20	0.04	8
^{129}Xe	23	0.01	4
	27	0.01	6

The listed currents are based on natural isotropic source feed, except for 3He,44Ca, and 48Ca. Beam intensity on target will vary according to beam line optics, collimation, and energy resolution requirements. Other ions include Li, Sc, Ti, Fe, Ni, Ag, I, La, Tb, and Bi, for which charge states are similar to those in the table in the same mass range.

PART II: EXPERIMENT

β - Decay Study of ^{27}P Using the RAMA Isotope Separator

T.F. Lang, J.D. Robertson, D.M. Moltz, J.E. Reiff and J.C. Cerny

We have used the RAMA isotope separator in a β-γ and γ-γ coincidence study of the $T_z = -3/2$, A = 4n + 3 nucleus ^{27}P, produced via the ^{28}Si(p,2n)^{27}P reaction at E_p = 45 MeV. ^{27}P was originally discovered via its weak beta-delayed proton branch;[1] the β-p data was used to probe the predicted clustering of Gamow-Teller (GT) strength above the isobaric analog state (IAS) in ^{27}Si. We have attempted to extend this measurement to states below the IAS by employing on-line isotope separation to remove background from copiously produced competing β-γ emitters and by utilizing a newly completed shielded detector station to reduce neutron-induced background. Although we were able to assign six gamma rays to the decay of ^{27}P, a combination of a low cross section ($\sim$ 50μB) and a still significant neutron-induced background coincidence rate ($\sim$1 coincidence/second), prevented measurement of the GT strength distribution. In order to successfully measure complete GT strength distributions for ^{27}P and other exotic light nuclei, we must improve the efficiency of the RAMA system by at least a factor of ten. To this effect, we plan to implement major changes to the ion source region. In the near term, this means increasing the pumping rate at the ion source, permitting us to improve transmission by decreasing the He-jet ion source distance. In the long term, this involves moving the ion source to our target area, thus significantly reducing attenuation of short-lived nuclei due to transit time through the He-jet capillary.

Footnotes and References

1. J. Äystö, X.J. Xu, D.M. Moltz, J.E. Reiff, J. Cerny and B.H. Wildenthal Phys. Rev. **C32**, 1700 (1985)

The β^+-p Decay of ^{25}Si

J.D. Robertson, J.E. Reiff, T.F. Lang, D.M. Moltz, and J.C. Cerny

The experimental study of Gamow-Teller (GT) beta decay is important to a fundamental understanding of nuclear structure. Because the GT operator is simple and restrictive in its action, the value of its matrix elements can provide particularly sensitive tests of nuclear wave functions. Specifically, when Q values provide access to a significant range of excitation energies, the distribution of the GT matrix element values as a function of energy provides information about the global response of the parent wave function to spin-isospin excitation.

We have recently measured the β^+-p decay of the T_z=-3/2 nuclide ^{25}Si in order to compare the observed GT strength distribution to the predicted distribution from the full space $d_{5/2}$-$s_{1/2}$-$d_{3/2}$ shell model calculations of Wildenthal.[1] Typical allowed beta decays occur near the valley of stability with small Q values. As a result, only the lowest few levels in the daughter system are sampled in the beta decay. The beta decay of ^{25}Si with a Q value of 12.74 MeV, on the other hand, offers a chance to observe the allowed beta decay to a large fraction of the levels in the daughter system. Moreover, although phase space factors favor beta decay to lower-lying states in ^{25}Al, the calculations of Wildenthal[1] predict that a significant fraction of the allowed decays will occur to states in ^{25}Al that lie above the proton separation energy. Specifically, over 95% of the GT strength in the decay of ^{25}Si is predicted to occur to levels above 2.3 MeV.

Silicon-25 was produced via the ^{24}Mg(^{3}He,2n)^{25}Si reaction by bombarding a 1.6-mg/cm^2-thick natural magnesium target with a 40 MeV ^{3}He beam from the 88-Inch Cyclotron. The reaction products were collected and transported to a low-background counting station using a He-jet transport system. In order to minimize the loss of short-lived ^{25}Si and reduce the longer-lived β^+ activities, the transported activity

was deposited directly in front of the detector telescope on a rotating wheel. The detector telescope used in this experiment was the low-energy charged particle detector telescope which we have recently developed.[2] This new telescope provided us with the advantage in that it was able to identify protons with energies as low as 150 keV. In the previous, most extensive investigation of ^{25}Si decay, the lower energy cutoff for protons was 700 keV.[3]

A total of 32 proton groups have been assigned to the β^+-p decay of ^{25}Si. Thirty of these groups have been assigned to specific transitions based upon energy sum relationships to known levels in ^{25}Al.[4] A comparison between the predicted and observed GT strength distribution for ^{25}Si β^+-p decay is shown in Fig. 1.

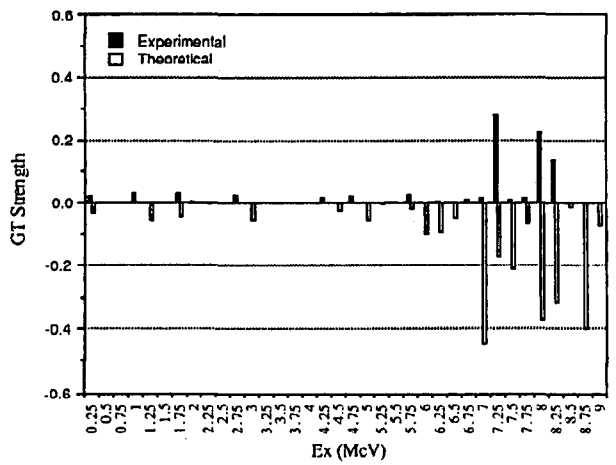

Fig. 1. A comparison of the predicted and observed GT strength distribution from ^{25}Si decay. The predicted values are from the full space sd calculations of Wildenthal.[1]

For the levels below the proton separation energy, the beta intensity was calculated by a comparison to the mirror ^{25}Na beta decay.[4] If we set a cutoff at 5.5 MeV excitation energy, the total strength observed is less than that which is predicted by a factor of 0.59, a result which is in good consistency with the global sd-shell result of 0.58.[5] On the other hand, the ratio of observed to predicted strength in the region between 5.5 MeV and 8.5 MeV is 0.40 rather than 0.58. This discrepancy would suggest that either the model predictions for this particular range of higher excited states in the mass 25 region deviate from the norm of lower excited state predictions or that the experiment has failed to identify some of the strength in the higher energy range.

Footnotes and References

1. B.H. Wildenthal, private communication (1988).

2. J.D. Robertson *et al.*, LBL Report No. LBL-25295, p. 137, 1987 (unpublished).

3. P.L. Reeder *et al.*, Phys. Rev. 147, 781 (1966).

4. P.M. Endt and C. Van Der Leun, Nucl. Phys. **A310**, 127 (1978).

5. B.A. Brown and B.H. Wildenthal, Nucl. Data Tables **33**, 348 (1985).

The Search for Ground State Proton Decay From Light Proton-Rich Nuclei

J.E. Reiff, J.D. Robertson, D.M. Moltz, T.F. Lang, J.C. Batchelder, and J.C. Cerny

Ground state (g.s.) proton decay, first discovered in 1982, has been observed from the decays of only four nuclides: ^{151}Lu ($t_{1/2}$ = 85±10 ms), ^{147}Tm ($t_{1/2}$ = 560±40 ms), ^{113}Cs ($t_{1/2}$ = 33±7 μs), and ^{109}I ($t_{1/2}$ = 109±17 μs).[1] This decay mode requires that the available proton decay energy and the associated Coulomb and angular momentum barriers combine in such a way that the nucleus lives long enough to be observed but decays quickly enough to compete with beta decay.

For the two proton emitting nuclei near A = 150, the half-lives are relatively long and beta decay is a competitive decay mode. The ratio of the experimentally observed proton partial half-life to the value predicted by the WKB approximation is quite good: 1.3 for ^{151}Lu and 0.90 for ^{147}Tm.[1] In sharp contrast, however, the corresponding ratios for the two nuclei near A = 110 are 47 for ^{113}Cs and 8.4 for ^{109}I. These discrepancies are the result of a reduction in the proton reduced width with respect to the theoretical calculations. The differences are most likely due to a change in the nuclear configuration between the parent and the daughter which are not taken into account in the calculations.

Recently, we have begun searching for g.s. proton emission in the A = 70 region in order to determine whether or not this discrepancy persists in lighter mass systems. The lightest $T_z = -1/2$ nuclei which are predicted to decay by g.s. proton emission are ^{65}As and ^{69}Br. Their proton separation energies have been calculated to be −570±200 keV and −810±300 keV, respectively, using the Coulomb displacement energy formulae of Antony, *et al.*[2] with updated masses.[3] From these separation energies we calculate that the half-life of ^{65}Ar should fall between 100 ps and 1 ms and the half-life of ^{69}Br should be in the range of 1 ps to 1 μs. These calculations assume that the emitted protons have an angular momentum of $\ell = 3$; this expectation is based on the proposed spin and parity of 5/2− for the parents.

In order to search for these exotic decays, we used our rapidly rotating recoil catcher wheel[4] and our newly developed gas - silicon telescopes[5] which we have incorporated into two six-telescope arrays. Together, these enable us to identify low energy protons (down to 150 keV) which may be emitted from nuclei with half-lives as short as 100 μs. Although the half-lives predicted above are at the lower limit of what we can observe, if the proton reduced width continues to remain significantly smaller than that which is predicted, these nuclei may have half-lives up to 100 times longer than what is calculated and lie well within our experimental range. The search for ^{65}As was conducted using the reaction ^{40}Ca (^{28}Si, p2n) and the cross bombardment reaction ^{40}Ca (^{32}S, αp2n); to search for ^{69}Br we employed the ^{40}Ca (^{32}S, p2n) reaction. The 175 MeV ^{28}Si and 200 MeV ^{32}S beams were produced by the 88-Inch Cyclotron.

Although we did not detect any low energy protons from these reactions, we were able to assign an upper limit for the half-life and hence the proton energy expected from the decay of ^{69}Br. Based on the production cross section predicted by the statistical model fusion-evaporation code ALICE,[6] the beam intensity, the running time, and the detector efficiencies, we concluded that the half-life for ^{69}Br cannot exceed 100 μs. This would indicate that ^{69}Br is unbound by at least 450 keV (assuming no reduction in the reduced width). Because we did not observe a low energy proton group, we cannot determine whether the trend of a decreased reduced width relative to theoretical predictions continues in this lighter mass nucleus.

On the other hand, the absence of a proton group from ^{65}As is most likely due to the fact that it is more bound than previously thought rather than its half-life being too short for us to see. It has been found that the Kelson-Garvey mass relation often under-

predicts the binding energy of a nucleus, sometimes by up to 200 keV. Thus, if the proton separation energy for ^{65}As is as small as –370±200 keV, its proton partial half-life can, in principle, range from 100 ns to 2.8 h and beta decay could then be a competetive decay mode at the upper end of this range. Believing that this is the case, we intend to search once again for a partial proton branch of ^{65}As, this time changing our experimental parameters such that we are sensitive to half-lives in the range of 10 ms to 100 ms.

Footnotes and References

1. S. Hofmann, "Proton Radioactivity" in Particle Emission From Nuclei, ed. by M. Ivascu and D.N. Poenaru, CRC Press, Boca Raton, Florida, 33431, p. 1(1988).

2. M.S. Antony, et.al., At. Data Nucl. Data Tables 34, 279 (1986).

3. G. Audi and A. Wapstra, The 1986 Audi-Wapstra Mid-Stream Mass Evaluation, distributed by P. Haustein, Brookhaven National Laboratory, Upton, New York 11973, U.S.A., May, 1986.

4. J.E. Reiff, *et al.*, Nucl. Instr. and Methods, **A276**, 228–232 (1989).

5. J.D. Robertson, et.al., LBL-25295, p. 137 (1988).

6. M. Blann and J. Bisplinghoff, Lawrence Livermore National Laboratory Report Number UCID-19614 (1982).

Sub-barrier Fusion of ^{16}O + ^{147,149}Sm

D.E. DiGregorio,† M. diTada,† D. Abriola,† M. Elgue,† A. Etchegoyen,† M.C. Etchegoyen,† J.O. Fernández Niello,† A.M.J. Ferrero,† S. Gil,† A.O. Macchiavelli,† A.J. Pacheco,† J.E. Testoni,† P.R. Silveira Gomes,§ V.R. Vanin,‡ R. Liguori Neto,‡ E. Crema,‡ and R.G. Stokstad

Fusion cross sections have been measured for ^{16}O + ^{147,149}Sm at bombarding energies in the range 61 MeV $\leq$ E_{lab} (^{16}O) $\leq$ 75 MeV by off-line observation of x-rays emitted in the radioactive decay of Yb isotopes and their daughters. These measurements complete our experimental study of the influence of nuclear deformation in the fusion of ^{16}O with all stable samarium isotopes. The fusion excitation functions are similar to those of the adjacent even Sm isotopes. It appears therefore, that the odd valence neutrons do not have any unusual influence on the subbarrier enhancement of σ_{fus} in these systems. An analysis based on a one dimensional barrier-penetration model that includes the effect of nuclear deformation shows that the behavior of the values of β_2 deduced from σ_{fus} follows the systematics established by the even-even isotopes, i.e., the quadrupole deformation parameters obtained for the odd isotopes fit well with the trend of values determined for the even isotopes. This trend shows that the onset of strong collectivity occurs rapidly as nucleons are added to ^{144}Sm.

Footnotes and References

*Condensed from LBL-25676 and Phys. Rev. C, (in press), (1988).

†Departamento de Fisica-TANDAR, Comisión Nacional de Energia Atómica, Buenos Aires, Argentina

§Instituto de Fisica da Universidade Federal Fluminense, Niteroi, Brazil

‡Instituto de Fisica da Universidade de Sao Paulo, Sao Paulo, Brazil

Observation of a Constant Average Angular Momentum for Fusion at Subbarrier Energies*

R.G. Stokstad, D.E. DiGregorio,† K.T. Lesko, B.A. Harmon, E.B. Norman, J. Pouliot, and Y.D. Chan

The measurement of high spin isomer ratio is a sensitive technique for probing the average angular momentum in the entrance channel that leads to fusion. The cross sections for populating the ground ($J^{\pi} = 3/2^{+}$, $t_{1/2} = 9.0$ h) and isomeric ($11/2^{-}$, 34.4 h) states in ^{137}Ce (in the fusion reaction ^{128}Te(^{12}C,3n)^{137}Ce) were measured from E_{cm} = 34.5 to 50 MeV (See Fig. 1a) by observing the resulting x-ray and gamma-ray activities off-line. The isomer ratio, R, decreases rapidly from a value of $\simeq$34 at 47 MeV to an essentially constant value of $\simeq$1.5 below 38 MeV (See Fig. 1b). The nearly constant value for R at low energies confirms the prediction that the centroid of the angular momentum distribution leading to fusion, λ, will reach an approximately constant value at energies sufficiently far below the fusion barrier [1]. By using a statistical model to relate the angular momentum distribution in the entrance channel to the isomer ratio (and to calculate the relative yields of the 2n, 3n, and 4n channels) we found that the energy dependence below the barrier for both σ(E) and R could be well reproduced by a barrier penetration calculation (See curves in Fig. 1). Thus, in this energy region, the observed cross sections and the deduced average angular momenta are self-consistent.

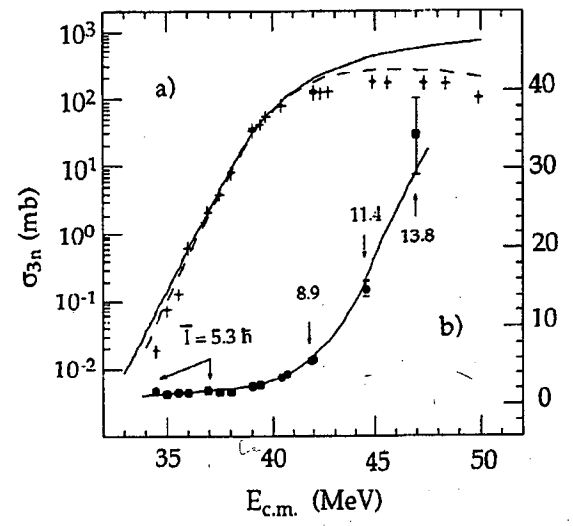

Fig. 1. a) Experimental cross sections for the reaction ^{128}Te(^{12}C,3n)^{137}Ce. The vertical error bars include both statistical and systematic errors. The horizontal bars represent the difference in the beam energy at the entrance and exit of the target combined with an estimate of the variation in beam energy due to straggling. The full curve is a calculation of the total fusion cross section as described in the text. The dashed line shows the prediction for the 3n cross section, obtained using the predicted x-n distributions. b) The experimental isomer ratio. The vertical error bars are standard deviations. The full curve is a prediction based on the angular momentum distribution calculated from the code CCFUS and a statistical decay calculation made with the code PACE. The predicted average angular momentum is indicated for selected bombarding energies.

Footnotes and References

*Condensed from LBL-25865 and Phys. Rev. Lett. (in press).

†On leave from Departamento de Fisica-TANDAR, Comisión Nacional de Energía Atómica, 1429 Buenos Aires, Argentina.

1. C.H. Dasso and S. Landowne, Phys. Rev. **C32**, 1094 (1985).

Multiple Dissociation of ^{16}O, ^{14}N and ^{12}C at 32.5 MeV/nucleon*

*R.G. Stokstad, Y.D. Chan, A. Dacal,† D.E. DiGregorio,‡ B.A. Harmon, R. Knop, M.E. Ortiz,† E. Plagnol,S J. Pouliot, C. Moisan, L. Potvin,** C. Rioux,** and R.Roy***

The probability for the projectile to break up into more than two components, i.e., multiple dissociation, increases rapidly with energy in the intermediate energy region (20-100 MeV/nucleon). Exclusive measurements of the breakup process resulting in as many as five charged particles have been performed to determine the extent of multiple dissociation. Such information is important in understanding the dynamics responsible for projectile excitation in a peripheral collision, as well as addressing the question of prompt or sequential decay mechanisms.

Beams of fully-stripped ^{16}O, ^{14}N, and ^{12}C ions were produced in the LBL Electron Cyclotron Resonance ion source and accelerated by the 88-Inch Cyclotron to a bombarding energy of 32.5 MeV per nucleon. The charged reaction products were detected by a 34-element plastic scintillator phoswich array centered about the beam axis in a 5×7 (horizontal × vertical) configuration. Each element viewed the target directly and subtended an angle of 5°. Events resulting from the breakup of the primary projectile-like nucleus were selected by requiring that the sum of the identified charges be equal to the charge of the projectile. This, coupled with the energy threshold for particle identification implied by the 1mm thick fast plastic, effectively eliminated the contribution of low energy particles evaporated by an excited target-like nucleus. The peripheral nature of the reaction was further tested by checking that the relative yields of the fragments are nearly independent of the target and that the reconstructed center of mass velocity of the detected particles approximates the projectile velocity.

The absolute cross sections of the different observed channels for ^{16}O on Au target are plotted in Fig. 1(a) as a function of the separation energy (Q_0) for that channel (Table I). Experimental uncertainties on the cross-sections are estimated at 25%. Because mass identification was limited to the hydrogen isotopes, the channels are distinguished only by the combination of atomic numbers. One observes that the yields of the different channels correlate approximately with the exponential of Q_0 for channels varying in intensity over a range of 3 to 4 orders of magnitude. More quantitatively, the yields could be characterized by an approximate slope parameter, TQ_0, which has values of 6.4, 5.5 and 6.0 MeV (10.3) for ^{16}O, ^{14}N and ^{12}C beams respectively. To have a better understanding of the projectile multi-breakup mechanism, the excitation energy spectrum of the projectile prior to its decay has been reconstructed using the positions and energies of each of the detected particles is a given event. The total relative kinetic energies (K_{tot}) of the fragments in this coordinate system is given by $K_{tot} = \sigma_i \frac{1}{2} m_i (V_i - V_{pp})^2$ where m_i and V_i are the mass and the lab. velocity of a fragment respectively and Vpp the velocity of the center of mass of the primary projectile-like nucleus. The excitation energy E^* of the primary projectile-like nucleus is then reconstructed by $E^* = K_{tot} - Q_0$, where Q_0 is the appropriate Q-value for the individual channels. In this case, a correction is made for the different isotopic compositions of a given channel. This is done by estimating the yields of the individual isotopic combinations using the above slope parameter and a weighting factor $\exp(Q_0/T)$. An appropriate number of events are then off-set by the more negative Q_0-value associated with that isotopic combination. Fig.1(b) shows the primary excitation spectrum for ^{16}O that results from this procedure. This spectrum shows that, although most of the decomposition proceeds through excitation energies within 20 MeV of the lower particle-decay thresholds, excitation energies extending up to 80 MeV can be produced in the primary stage of the reaction. We have also calculated the yields of the different chan-

nels by assuming a series of binary splits, governed by the density of states at the saddle point. Our calculation[1] is similar to one described by Auger, *et al.*.[2] with the exception that we use ground state masses throughout and neglect rotational energy. An added feature of the present calculation is that, in any binary split, both of the two fragments may undergo further decay. The results are shown as cross marks in Fig. 1(a). It can be seen that the calculations give a reasonable description of the relative yields of the channels having Q_0-values up to −30 MeV, but underestimate the relative yields of the least abundant channels.

Table I

Observed breakup channels resulting from ^{16}O included in Fig. 1.

^{16}O-Channels	Q-Values
C-He	-7.2
N-H	-12.1
He-He-He-He	-14.4
C-H-H	-22.3
B-He-H	-23.1
B-Li	-30.9
Li-He-He-H	-31.8
He-He-He-H-H	-34.3
Li-Li-He	-35.3
B-H-H-H	-42.9
Li-Li-H-H	-49.1
Li-He-H-H-H	-51.6

Footnotes and References

*Condensed from LBL-25810.

†Instituto De Fisica, UNAM, México D.F. 01000, México.

‡On leave from Dep. de Física-TANDAR, CNEA, 1429 Buenos Aires, Argentina.

§GANIL BP 5027 F-14021 Caen CEDEX France.

**Foster Rad. Lab., Université McGill, Montréal, Québec, H3A 2B2.

††Laboratoire de Physique Nucléaire, Université Laval, Québec, G1K 7P4, Canada

1. See LBL-26439, "Brandex: a Fortran/Pascal code for the multiple binary decay of a nucleus."

2. F. Auger *et al.*, Phys. Rev. **C35**, 190 (1987).

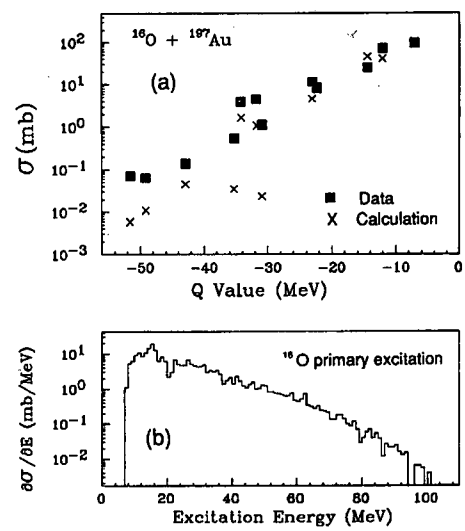

Fig. 1. (a) Yields for individual breakup channels observed in 16O+^{197}Au (the square symbols). The cross symbols are model calculations (see text). (b) Reconstructed primary excitation spectrum for ^{16}O.

Stripping- and Pickup-Induced Breakup in 11- and 17-MeV/nucleon ^{20}Ne+^{197}Au Reactions*

S.B. Gazes, H.R. Schmidt, Y. Chan, E. Chavez, R. Kamermans and R.G. Stokstad

Breakup processes in 220 and 341-MeV ^{20}Ne + ^{197}Au reactions were studied by performing coincidence measurements of the secondary fragments. Projectile-like fragments and light particles corresponding to primary stripping, pickup, and inelastic channels were examined. The projectile-like fragments were detected near the classical grazing angle. Kinematic reconstructions of the three-body

final state were used to deduce the excitations in the primary projectile-like and target-like fragments. At both bombarding energies, the stripping channels produced relatively cold ejectiles, with the excitation residing mostly in the target recoil. However, the pickup channels tended to leave the target cold, while populating higher excitations in the ejectile. The data are consistent with nucleon transfer as the dominant mode for generating higher excitation, with the partition of excitation energy between the fragments governed by the direction of the transfer. An extended version of the optimum-Q-value model of Siemens *et al.*[1] prediects target-like excitations in good agreement with data at 11 Mev/nucleon, but with deviations occurring at 17 MeV/nucleon.

Footnotes and References

*Condensed from Phy. Rev. C **38**, 712 (1988)

1. P.J. Siemens *et al.*, Phys. Lett. **36B**, 24 (1971).

Limits on $\bar{\nu}_\mu \rightarrow \bar{\nu}_e$ Oscillations, Experiment 645 at LAMPF*

*L.S. Durkin,† R.W. Harper,† T.Y. Ling,† J.W. Mitchell,† T.A. Romanowski,† E.S. Smith,† M. Timko,† S.J. Freedman,‡ J. Napolitano,‡ B.K. Fujikawa,§ R. McKeown,§ K.T. Lesko, W.C. Choi,** A. Fazely,** R.L. Imlay,** W.J. Metcalf,** R.D. Carlini,†† J.B. Donahue,†† G.T. Garvey,†† and V.D. Sandberg††*

We have continued our search for the phenomenon of neutrino oscillations this year. The experiment was carried out at LAMPF, experiment No. 645. The neutrino source consists of an equal admixture of $\bar{\nu}_\mu$, ν_μ, *and* ν_e arising from decays of stopping π^+ and μ^+ produced by 780 MeV protons in a beam stop. We sought for $\bar{\nu}_e$ arising from $\bar{\nu}_\mu \rightarrow \bar{\nu}_e$ using the inverse β-decay reaction. The segmented 20 metric ton detector was located 26.8 m from the beam stop. It consists of 40 liquid scintillator planes and 41 x-y pairs of proportional-drift-tube planes. The detector was shielded by 2000g/cm^2 overburden and a 4π active shield. The electronics kept a 53ms past history and 107ms future history for each trigger. Events which were tagged by the neutron capture on Gd were recorded in the future history, while past history was used to reject cosmic ray muons. At the completion of the last run cycle we have collected data for 5100 C of protons on the beam stop, yielding 3.14×10^{13} n/cm^2 at the detector. 1.27×10^6 triggers were recorded, of which a majority resulted from cosmic ray events.

Analysis of these triggers results in a beam excess signal of 12.3±4.7 events. These excess events can be ascribed to conventional backgrounds from the dominate neutrinos, charged-current interactions on various nuclei in the detector (^{12}C, ^{13}C, ^{27}Al, ^{16}O) and there is no evidence for neutrino oscillations through the mode $\bar{\nu}_\mu \rightarrow \bar{\nu}_e$.

We have performed a binned maximum likelihood analysis on the data and have obtained limits on δm^2 and $\sin^2(2\theta)$. At 90% confidence level we obtained, $\delta m^2 < 0.11 eV^2$ for maximal mixing
$\sin^2(2\theta) < 0.014$ for large δm^2.

Footnotes and References

*Condensed from Phys. Rev. Lett. 61, 1811 (1988)

‡Argonne National Laboratory, Argonne, Illinois 60439

§California Institute of Technology, Pasadena California 91125

**Lousiana State University, Baton Rouge Louisiana 70803

†† Los Alamos National Laboratory, Los Alamos New Mexico 87545

Isospin-Forbidden Fermi Decay of ^{56}Ni

E.B. Norman, K.T. Lesko, B. Sur, R.M. Larimer, and E. Browne

If isospin were a good quantum number, then $0^+ \rightarrow 0^+$ ($\Delta T \neq 0$) β transitions would be forbidden. Thus the observation of such decays provides information on the isospin purity of the nuclear states involved. We used two independent techniques to search for the isospin-forbidden electron-capture Fermi decay of the doubly magic nucleus ^{56}Ni to the $J^\pi = 0^+$ level at 1451 keV in ^{56}Co. In the first experiment, the gamma-ray intensity into and out of this level was accurately determined. The second method relied on measuring the number of 1451-keV (158+812+481) events in coincidence and in anticoincidence with the 269-keV gamma ray that populates the 1451-keV level in the allowed Gamow-Teller decay of ^{56}Ni. Both methods yielded results consistent with zero and upper limits on the branching ratio of 1×10^{-3}. From this limit we derived a Coulomb matrix element of <58 keV.

β^+ Decay of ^{56}Ni

K.T. Lesko, E.B. Norman, B. Sur, R.M. Larimer, and E. Browne

A major product of nucleosynthesis in stars is the doubly magic nucleus ^{56}Ni. Soon after the supernova that produces the ^{56}Ni takes place, temperatures are low enough that neutral atoms can exist. Thus ^{56}Ni would electron-capture decay with its laboratory half life of 6.1 days. However, supernovae may be sites of cosmic-ray production and acceleration. If ^{56}Ni produced in such explosions were accelerated to high energies, it would be stripped of its electrons. Thus, the cosmic ray half life of ^{56}Ni would be determined by its β^+ decay rate. Future observations of ^{56}Ni in the cosmic rays could be used to determine the time interval between nucleosynthesis and cosmic-ray acceleration if this half life were known.[1] We are attempting to measure the β^+ decay partial half life of ^{56}Ni using a fourfold coincidence technique. No positive effect has been observed, and an upper limit of 7×10^{-7} has been established on the branching ratio for this decay. This establishes a lower limit of 2.4×10^4 years for the cosmic-ray half life of ^{56}Ni .

Footnotes and References

1. M. Casseé, 13th Int. Conf. Cosmic Rays, Vol. **1**, 546 (1973).

β^+ Decay and Cosmic-ray Half-life of ^{54}Mn*

B. Sur, K.R. Vogel, E.B. Norman, K.T. Lesko, R.M. Larimer, and E. Browne

^{54}Mn is an odd-odd nucleus which decays in the laboratory with a half-life of 312 days via an allowed electron capture transition to the 835 keV level in ^{54}Cr. In the cosmic rays, ^{54}Mn is believed to be produced through spallation of primary iron nuclei by interstellar hydrogen. As a high-energy cosmic ray, ^{54}Mn would be stripped of all its atomic electrons, thus preventing its decay by electron capture. However it is energetically possible for it to decay via second forbidden unique transitions to the ground states of ^{54}Cr and ^{54}Fe by positron or negatron emission, respectively. From studies of the decays of ^{10}Be, ^{22}Na and ^{26}Al, the log *ft* values for such transitions have been found to be between 13.9 and 15.7 yielding estimates of the partial half-lives for these decay modes in ^{54}Mn of $8.4 \times 10^7 y < t_{1/2}(\beta^+) < 6.0 \times 10^9 y$ and $9.2 \times 10^5 y < t_{1/2}(\beta^-) < 6.5 \times 10^7 y$. Because of these long β^+ and β^- half-lives, ^{54}Mn has been proposed as a cosmic-ray chronometer and a probe of models of the interstellar medium and cosmic-ray

propagation.[1] More recently, the presence of a long-lived radioactive isotope of manganese in the cosmic rays has been experimentally confirmed,[2] with a half-life estimated to be (1 to 2) $\times 10^6$ years in order to explain the measured abundance as a function of cosmic-ray energy.[3] While the dominant decay mode for fully ionized ^{54}Mn is expected to be β^- decay, it is extremely hard to experimentally isolate this small branch in the laboratory from the de-excitation g rays from the; 100% EC decay branch. Instead, we have searched for the even smaller, but easier to detect, β^+ decay branch by measuring its energy spectrum with a silicon particle detector telescope in coincidence with the back-to-back 511-keV positron annihilation g-rays detected in a large annular NaI detector. In a total running time of 360.4 hours over a period of 21 days, with a 7.3 μCi ^{54}Mn source, we observed no positrons in excess of those due to background with a 1σ upper limit of 15.5. Using our experimentally determined efficiency of 0.10% for detecting positrons, this results in an upper limit of 4.4×10^{-8} for the β^+ decay branching ratio of ^{54}Mn, which corresponds to a lower limit of 2.0×10^7 years for the partial half-life of this decay channel. This result clearly rules out the possibility that β^+ is the dominant decay mode for the ^{54}Mn nuclei found in cosmic rays. Using the accepted value of 1377 keV for the mass difference between ^{54}Mn and ^{54}Cr, we obtain a lower limit of 13.3 for the log *ft* value of this transition. Using this log *ft* value for the β^- decay branch with 697 keV of available energy, we obtain a lower limit of 4×10^4 years for the partial half-life of this decay mode. This value is $\approx$25 times shorter than the estimated half-life of ^{54}Mn in cosmic rays and thus consistent with β^- as the dominant channel for this decay. Experiments to measure the β^- decay rate of ^{54}Mn are now in progress.

Footnotes and References

*Condensed from Phys. Rev. C **39**, 1511 (1989)

1. M. Cassé, Astrophys. J. **180**, 623 (1973).

2. G. Tarlé, S.P. Ahlen and B.G. Cartwright, Astrophys. J. **230**, 607 (1979).

3. L. Koch *et al.*, Astron. and Astrophys. **102**, L9 (1981).

Level Scheme of ^{148}Pm and the s-Process Neutron Density*

K.T. Lesko, E.B. Norman, R.-M. Larimer, J.C. Bacelar and E.M. Beck

We have finalized our studies of the level scheme of ^{148}Pm in order to exploit the s-process branching which occurs at this nucleus in order to determine the s-process neutron density. We have deduced level scheme of ^{148}Pm up to 800 keV of excitation energy using gamma-ray coincidence data and published particle transfer data. We collected gamma ray coincidence data using the ^{148}Nd(p,n)^{148}Pm reaction with HERA, the 21 Ge detector array. The 88-Inch Cyclotron provided an 8 MeV proton beam. Approximately 106 gamma-ray transitions have been placed between 36 levels under 800 keV. We have identified three levels below 500 keV in excitation (six levels in all under 800 keV) which decay to both the ground state ($J^\pi=1^-$, $t_{1/2}$=5.37 d) and to the isomeric level at 137 keV ($J^\pi=6^-$, $t_{1/2}$=41.3 d). The presence of these levels guarantees that ^{148}Pm^{g,m} are in thermal equilibrium during the s process. The s-process neutron density inferred from the branch point at ^{148}Pm is deduced to be $3\times10^8/\mathrm{cm}^3$.

Footnotes and References

*Condensed from Phys. Rev C **39**, 619 (1989).

Search for Motional Narrowing Effects in Nuclear γ-Ray Spectra*

F.S. Stephens, J.E. Draper, M.A. Deleplanque, R.M. Diamond, and A.O. Macchiavelli

At moderate temperatures in nuclei (~0.5 MeV) there is evidence for damping effects[1] in the rotational behavior.[2,3] Instead of normal rotational bands, each state can emit any one of a distribution of γ-ray energies. Fig. 1 shows some of the evidence for this, where the "dips" (absence of counts) at the gate energy in coincidence spectra are much smaller in area than is expected for good rotational behavior. In fact, at gate energies of ~1.4 MeV there is no longer any evidence at all for a dip; whereas, for a good rotor the dip would extend nearly all the way to the base line. The damping explanation involves a mixing of the rotational bands at the high level densities involved at moderate temperatures. On the other hand at still higher temperatures, there are expected to be motional narrowing effects,[4] where the damping widths decrease with further increases in temperature. In fact, Fig. 1 shows that the dips monotonically decrease in area with increasing gate energy (very likely associated with increasing temperature), suggesting no decrease in the damping width. This is confirmed by detailed comparisons of the data with simulation codes that include the expected motional narrowing effects. The absence of the expected motional narrowing effects raises some interesting questions about how well rotational damping is understood at these temperatures

Footnotes and References

*Condensed from: Phys. Rev. Lett. **60**, 2129 (1988).

1. B. Lauritzen *et al.*, Nucl. Phys. **A457**, 61 (1986).
2. J.E. Draper *et al.*, Phys. Rev. Lett. **56**, 309 (1986).
3. J.C. Bacelar *et al.*, Phys. Rev. Lett. **55**, 1958 (1985).
4. R.A. Broglia *et al.*, Phys. Rev. Lett. **58**, 326 (1987).

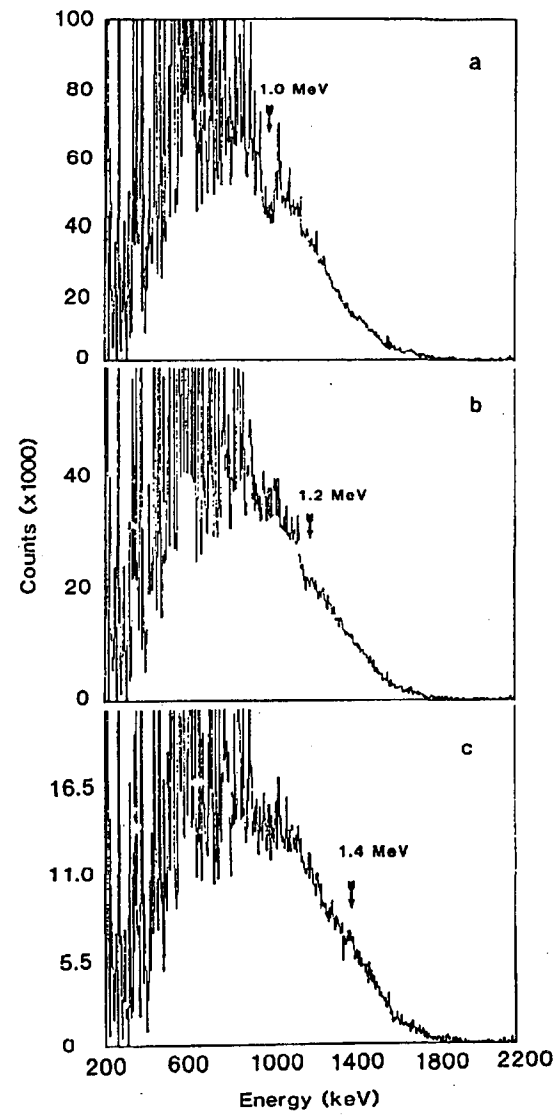

Fig. 1. Gamma-ray spectra following the reaction, ^{40}Ar (180 MeV) + ^{124}Sn, where 20-keV wide gates were set at: (a) 1.0 MeV; (b) 1.2 MeV; (c) 1.4 MeV.

Unusual Rotational Behavior in ^{178}Os*

J. Burde,† A.O. Macchiavelli,‡ M.A. Deleplanque, R.M. Diamond, F.S. Stephens, C.W. Beausang, R.J. McDonald and J.E. Draper§

A very unusual rotational band has been found in ^{178}Os. It consists of seven regularly spaced transitions about 36 keV apart, which corresponds closely to the separation in the superdeformed band in ^{152}Dy after an $A^{5/3}$ normalization. This band populates the yrast band directly, thus permitting, after multipolarity determinations, rather reliable spin assignments. Based on these, the moments of inertia $J^{(1)}$ are found to be much smaller than the $J^{(2)}$ derived from the γ-ray spacings described above, and, in fact, do not even reach the rigid-sphere value, shown in Fig. 1. To our knowledge, such a large disparity in moment of inertia values has not been seen before, and probably arises from a well-deformed band that is undergoing systematic increases in deformation and/or decreases in pairing. An increase in alignment throughout the region of high, constant values of $J^{(2)}$ also is possible, but should lead to a decrease at still higher frequency. Further work is needed to answer this interesting problem.

Footnotes and References

*Condensed from Phys. Rev. C **38**, 2470 (1988).

†Racah Institute of Physics, The Hebrew University, 91904 Jerusalem, Israel

‡Comision Nacional de Energía Atómica, 1429 Buenos Aires, Argentina

§Physics Department, University of California, Davis, CA 95611

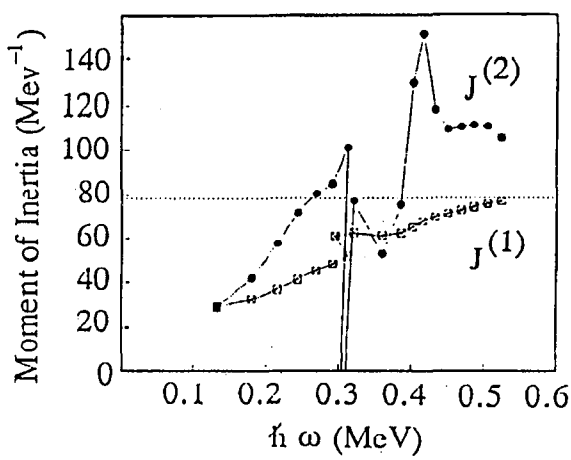

Fig. 1. Moments of inertia, $J^{(1)}/\hbar^2$ and $J^{(2)}/\hbar^2$, vs $\hbar\omega$. The dotted horizontal line gives the rigid-sphere value.

High-Spin Spectroscopy of ^{162}Hf*

H. Hübel,† M. Murzel,† E.M. Beck,† H. Kluge,‡ A. Kuhnert,‡ K.H. Maier,‡ J.C. Bacelar, M.A. Deleplanque, R.M. Diamond, and F.S. Stephens

Excited states in ^{162}Hf were investigated up to spin I $\sim$ 38 using the 21 Compton-suppressed Ge array, HERA. In addition, information was obtained on ^{161}Hf. The analysis of triple coincidences was crucial for the construction of the level schemes, Fig. 1. The results are interpreted within the framework of the cranked shell model and are compared to neighboring isotopes and isotones, showing Fermi level and deformation effects. The systematic behavior of the band crossings in the Hf isotopes and the N=90 isotones is discussed.

Footnotes and References

*Condensed from Z. Phys. **A329**, 289 (1988).

†Institut für Strahlen-und Kernphysik, Bonn University, D-5300 Bonn 1 Fed. Rep. of Germany

‡Hahn-Meitner-Institut, 1000 Berlin 39, Fed. Rep. of Germany

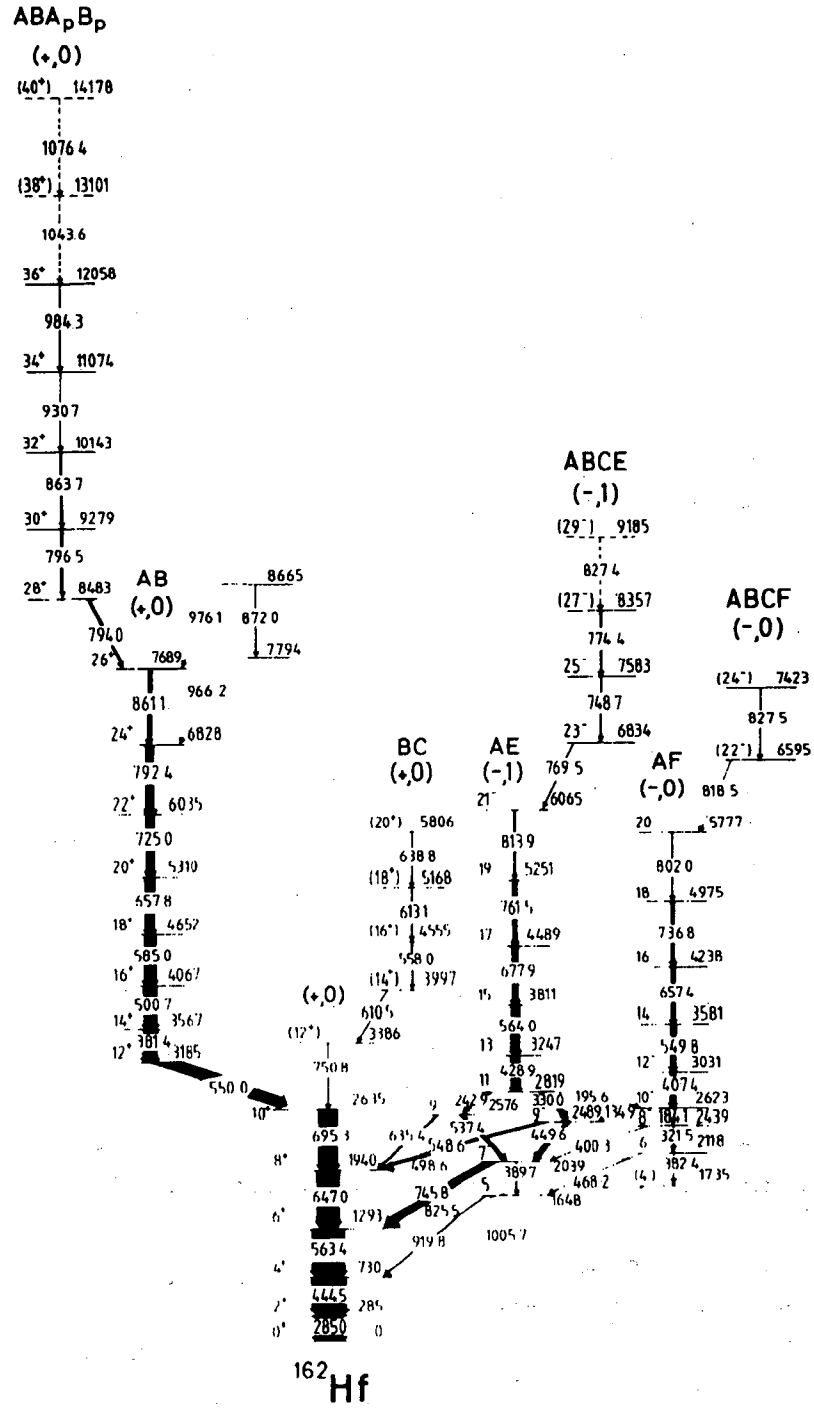

Fig. 1. Level scheme of ^{162}Hf.

Superdeformed Band in ^{148}Gd: a Test of Shell Effects in the Mass 150 Region

M.A. Deleplanque, C. Beausang, J. Burde, R.M. Diamond, J.E. Draper, C. Duyar, A.O. Macchiavelli, R.J. McDonald and F.S. Stephens

A discrete superdeformed (SD) band was found in the nucleus ^{148}Gd produced in both reactions: ^{48}Ca+^{104}Ru $\rightarrow$ ^{148}Gd+4n at 215 MeV and 200 MeV, and ^{29}Si +^{124} Sn $\rightarrow$ ^{148}Gd+5n at 157 MeV and 150 MeV. Since the energies of several SD lines coincide with those of strong known lines in ^{148}Gd, triple coincidence were used (where all double-gate combinations of SD lines were summed) to confirm the existence of a SD band. This was the third discrete SD band found in the mass 150 region. Of the three SD bands known in this mass region, it is the weakest, has the fewest transitions, and is the least regular. This suggests that the SD bands become less "perfect" as one moves away from the nucleus ^{152}Dy which is thought to be a superdeformed "magic" nucleus. The properties of the SD bands observed in ^{148}Gd and ^{149}Gd are consistent with that idea, but a study of SD bands in other neighboring nuclei would be needed to confirm the magicity of ^{152}Dy.

Footnotes and References

*Condensed from Phys. Rev. Lett. **60**, 1626 (1988).

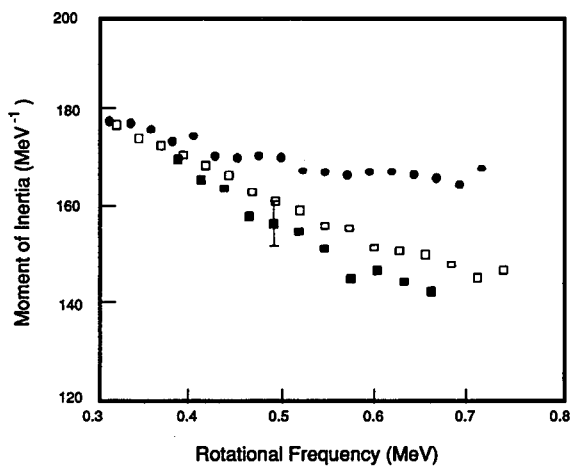

Fig. 1. Dynamic moment of inertia $\Im^{(2)}$ band, normalized to mass 152 for the nuclei ^{152}Dy (full circle), ^{149}Gd (open square) and ^{148}Gd (full square). A representative error bar is given for ^{148}Gd.

Superdeformation in ^{104,105}Pd*

A.O. Macchiavelli,† J. Burde,‡ R.M. Diamond, C.W. Beausang, M.A. Deleplanque, R.J. McDonald, F.S. Stephens and J.E. Draper§

A rotational band has been observed in ^{105}Pd, and possibly in ^{104}Pd, that can be interpreted as arising from a superdeformed shape in the generalized sense that the strongly deformed bands in the Ce-Nd region are superdeformed. That is, the moments of inertia, $J^{(1)}$ and $J^{(2)}$, of these bands are similar to those measured in the Ce-Nd region, once the $A^{5/3}$ mass dependence is removed (Fig. 1). In addition, the bands end suddenly with no observable connections to the ground bands, as is also observed in the mass-130 region. The moments of inertia imply a deformation of $\epsilon = 0.35$–0.4. If quadrupole moment determinations by lifetime measurements confirm such values, this is a third mass region where such strongly deformed bands have been found at high spin.

Footnotes and References

*Condensed from Phys. Rev. C **38**, 1088 (1988).

†Comision Nacional de Energia Atomica, 1429 Buenos Aires, Argentina

‡Racah Institute of Physics, The Hebrew University, 91904 Jerusalem, Israel

§Physics Department, University of California, Davis, CA 95611

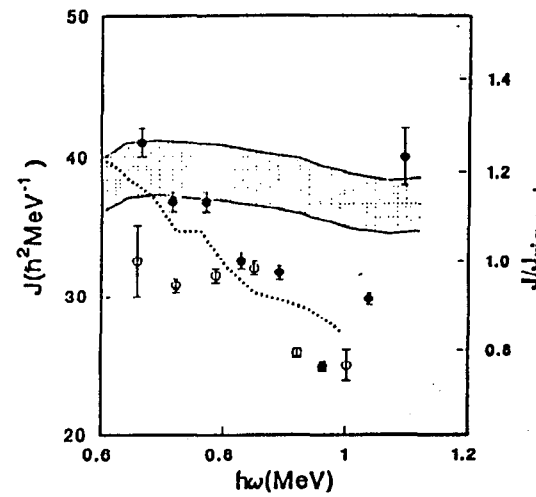

Fig. 1. Moments of inertia for the observed rotational bands. The dotted areas represent $J^{(1)}$ for ^{105}Pd with an uncertainty of $\pm$ 2 in the spin assignement. Open circles are $J^{(2)}$ for ^{104}Pd and filled circles are for ^{105}Pd. For comparison, the dynamic moment of inertia (scaled by $A^{5/3}$) in the SD band in ^{132}Ce is shown by the dotted line. The right-hand scale is in units of the rigid sphere.

Identification of ^{145}Er and ^{145}Ho

K.S. Vierinen, J.M. Nitschke, P.A. Wilmarth, R.M. Chasteler, A.A. Shihab-Eldin, R.B. Firestone, K.S. Toth,† and Y.A. Akovali†

On-line mass separation and K x-ray coincidences at the SuperHILAC's OASIS facility[1] were used to identify the β decays of ^{145}Er and ^{145}Ho. Only β-delayed proton emission was observed for ^{145}Er ($T_{1/2}$=0.9±0.3 s), and a total of 16 γ rays were assigned to the β decay of ^{145}Ho ($T_{1/2}$=2.4±0.1 s). A ^{145}Ho decay scheme was constructed which incorporates 13 γ-ray transitions and 10 excited levels in ^{145}Dy and establishes the $\nu h_{11/2}$ isomeric level at E_x=118.2 keV (see Fig. 1). The low-lying neutron-hole structure in ^{145}Dy was compared to level systematics in even-Z nuclei with N=77, 79 and 81.

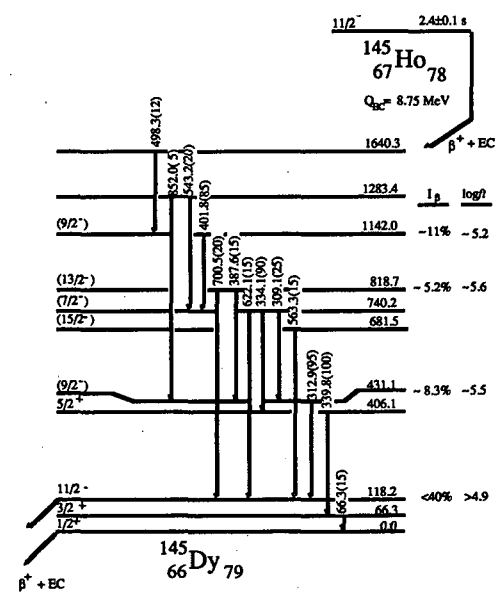

Fig. 1. Partial decay scheme of ^{145}Ho. Intensities are relative to a value of 100 for the 339.8-keV γ ray. Excitation and γ-ray energies are given in keV.

Footnotes and References

*Condensed from: LBL-**26481**.

†Oak Ridge National Laboratory, Oak Ridge, TN **37831**.

1. J.M. Nitschke, Nucl. Instrum. and Methods **206**, 341 (1983).

High Spin Studies of ^{235}U, ^{234}U, and ^{233}U*

M.A. Stoyer, J.O. Rasmussen, R.M. Diamond, F.S. Stephens,
M.A. Deleplanque, A. Macchiavelli, R. McDonald, D. Cline,†
A. Kavka,† *E. Vogt,*† *K. Helmer,*† *C.Y. Wu,*† *W. Kernan,*† *X.T.Liu*‡

Heavy ion neutron transfer reactions and Coulomb excitation were used to study the rotational level schemes of ^{235}U, ^{234}U, and ^{233}U. Several experiments were performed at the LBL SuperHILAC using ^{206}Pb projectiles, and at the University of Rochester Nuclear Structure Research Laboratory tandem accelerator using ^{58}Ni. Gamma-ray energy spectra were obtained using a particle-particle-γ coincidence technique, Doppler corrections were made using particle angle information, and specific transitions were isolated using lower known γ-transitions and γ-γ coincidence techniques. Spin states as high as $\frac{47}{2}^-$ in ^{235}U, 28^+ in ^{234}U, and $\frac{49}{2}^+$ in ^{233}U were observed. Results for ^{233}U are shown in Fig. 1 and Table I. There was no observational evidence for backbending in any of the nuclei studied. Experimental g-factors and $\frac{M1}{E2}$ mixing ratios were extracted for ^{233}U.

Footnotes and References

*Condensed from a paper presented at the October, 1988 American Physical Society Meeting in Sante Fe, NM.

†Nuclear Structure Research Laboratory, University of Rochester, Rochester, NY 14627, USA

‡Department of Physics and Astronomy, University of Tennessee, Knoxville, TN 37996-1200, USA

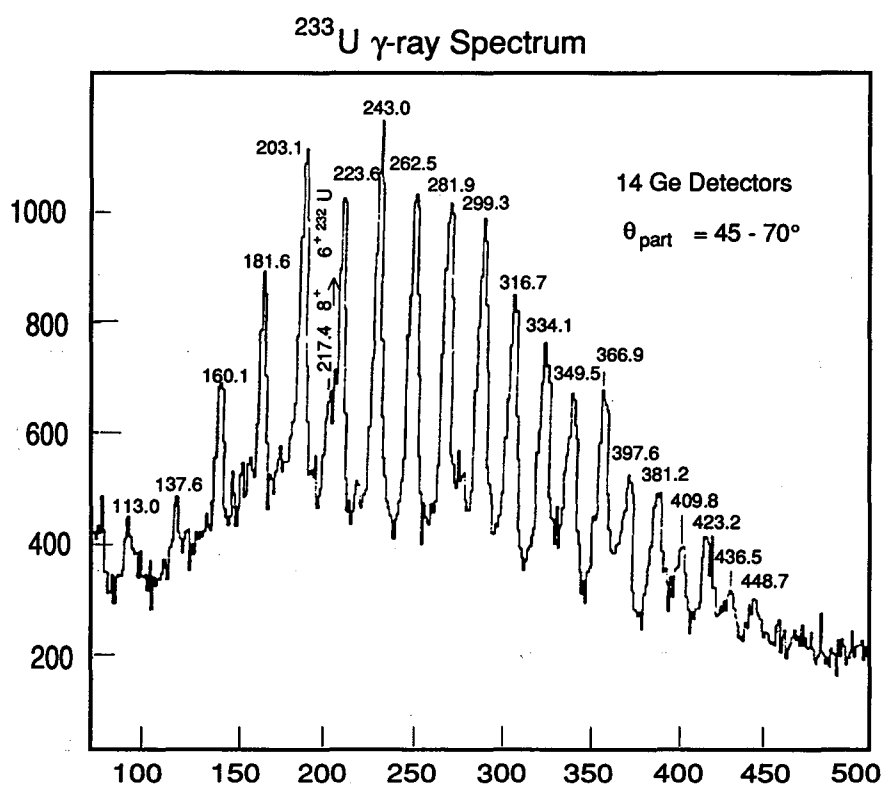

Fig. 1. See text.

Table I Observed Transitions in ^{233}U

Transition	Energy (keV)	Transition	Energy (keV)
$\frac{11}{2}^+ \rightarrow \frac{7}{2}^+$	113.0(2)	$\frac{13}{2}^+ \rightarrow \frac{9}{2}^+$	137.6(2)
$\frac{15}{2}^+ \rightarrow \frac{11}{2}^+$	160.1(2)	$\frac{17}{2}^+ \rightarrow \frac{13}{2}^+$	181.6(2)
$\frac{19}{2}^+ \rightarrow \frac{15}{2}^+$	203.1(2)	$\frac{21}{2}^+ \rightarrow \frac{17}{2}^+$	223.6(2)
$\frac{23}{2}^+ \rightarrow \frac{19}{2}^+$	243.0(2)	$\frac{25}{2}^+ \rightarrow \frac{21}{2}^+$	262.5(2)
$\frac{27}{2}^+ \rightarrow \frac{23}{2}^+$	281.9(2)	$\frac{29}{2}^+ \rightarrow \frac{25}{2}^+$	299.3(2)
$\frac{31}{2}^+ \rightarrow \frac{27}{2}^+$	316.7(2)	$\frac{33}{2}^+ \rightarrow \frac{29}{2}^+$	334.1(4)
$\frac{35}{2}^+ \rightarrow \frac{31}{2}^+$	349.5(4)	$\frac{37}{2}^+ \rightarrow \frac{33}{2}^+$	366.9(4)
$\frac{39}{2}^+ \rightarrow \frac{35}{2}^+$	381.2(4)	$\frac{41}{2}^+ \rightarrow \frac{37}{2}^+$	397.6(4)
$\frac{43}{2}^+ \rightarrow \frac{39}{2}^+$	409.8(4)	$\frac{45}{2}^+ \rightarrow \frac{41}{2}^+$	423.2(4)
$\frac{47}{2}^+ \rightarrow \frac{43}{2}^+$	436.5(4)	$\frac{49}{2}^+ \rightarrow \frac{45}{2}^+$	448.7(4)

Shape Co-Existence in ^{180}Hg and Delineation of the Midshell Minimum*

G.D. Dracoulis,† A.E. Stuchbery,† A.O. Macchiavelli,‡ C.W. Beausang, J. Burde,§ M.A. Deleplanque, R.M. Diamond, and F.S. Stephens

Excited states in the very neutron-deficient ^{180}Hg, produced in the reaction ^{144}Sm(^{39}K,p2n), have been identified up to spin 16^+. The decay pattern observed is indicative of a shape co-existence similar to that in the heavier Hg isotopes. The prolate deformed band is higher in energy, relative to the oblate ground band, than in ^{182}Hg. This result when added to the Hg sequence shown in Fig. 1 establishes a clear minimum in the prolate-oblate energy difference near N=103, mid shell for the $i_{13/2}$ neutrons.

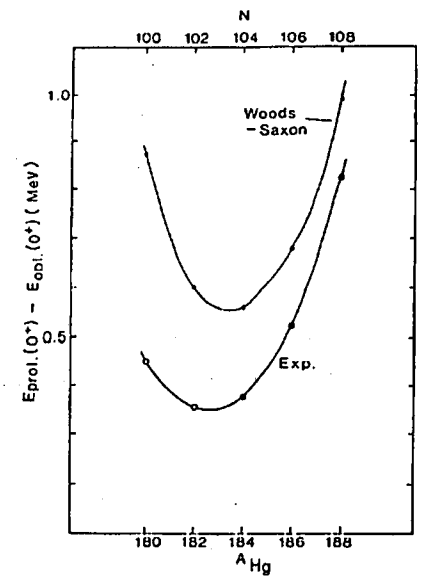

Fig. 1. Comparison between the calculated and experimental prolate-oblate energy differences for the light Hg isotopes. The closed experimental points are observed, excited, 0^+ state energies. The open circles are the results of the present extrapolations. Their perturbed energies will be about 15 keV higher.

Footnotes and References

*Condensed from Phys. Lett. **B208**, 365 (1988).

†Department of Nuclear Physics, Australian National University, P.O.Box 4, Canberra, A.C.T. 2600, Australia

‡Comisión Nacional de Energía Atómica, 1429 Buenos Aires, Argentina

§Racah Institute of Physics, The Hebrew University, 91904 Jeusalem, Israel

Gamma-Ray Energy Correlations from Nuclei at Very High Spins*

F.S. Stephens, J.E. Draper, J.C. Bacelar, E.M. Beck, M.A. Deleplanque, and R.M. Diamond

We have studied the correlations between (unresolved) γ-ray energies emitted by nuclei at very high spins. This correlation manifests itself (in part) as a reduced probability of finding two γ rays of the same energy,[1,2] and we have measured the detailed shape of this reduced probability distribution. This shape is shown in Fig. 1 for three gate-energy regions in data from the reaction, ^{40}Ar + ^{100}Mo $\rightarrow$ ^{136}Nd + (plus some other products). These (and other) data can be explained by a superposition of γ rays coming from a high-temperature region where the rotational motion is heavily damped and a low-temperature region where there is little or no damping.

Footnotes and References

*Condensed from: Phys. Rev. C37, 2927 (1988).

1. J.E. Draper *et al.*, Phys. Rev. Lett. **56**, 309 (1986).

2. J.C. Bacelar *et al.*, Phys. Rev. Lett. **55**, 1858 (1985).

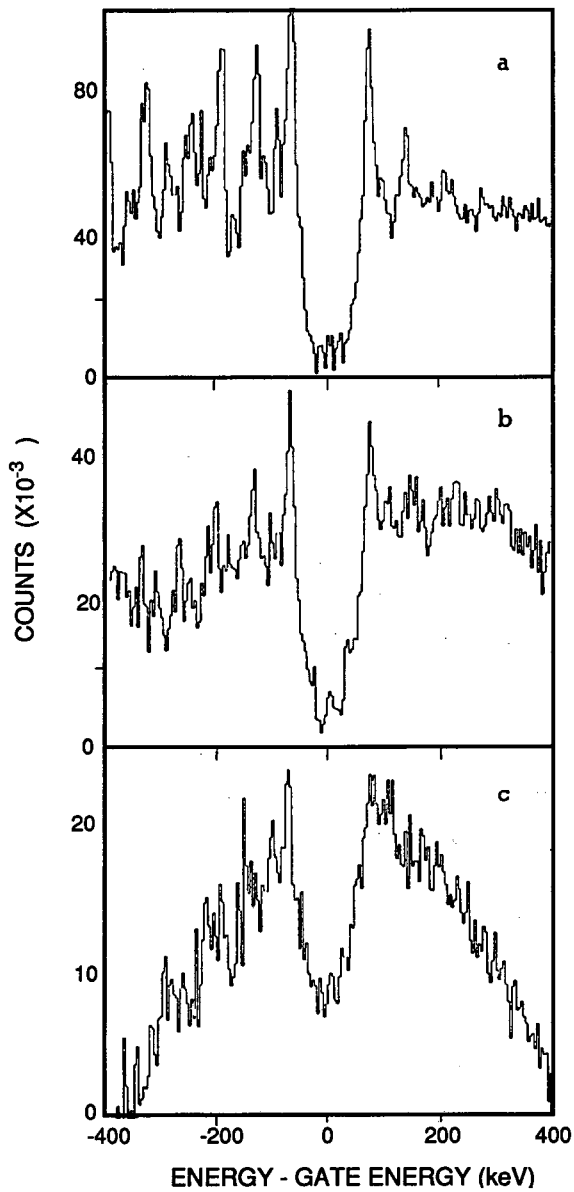

Fig. 1. Partial γ-ray spectra from the 136Nd data, treated in a special way (see the original text). Fifty spectra, each with a gate 4-keV wide, have been shifted (to align the gates) and added, covering the following energy ranges: (a) 1.0-1.2 MeV; (b) 1.2-1.4 MeV; (c) 1.4-1.6 MeV. The γ-ray energies are given on the abscissa as distances from the gate energy, and, whereas the vertical height is arbitrary, the vertical expansions are given on the ordinate scale.

The Decay of ^{141}Tb by Positron Emission and Electron Capture Decay

J. Gilat, R.B. Firestone, J.M. Nitschke, K.S. Vierinen, and P.A. Wilmarth

The decay of ^{141}Tb has been investigated with at the SuperHILAC with the OASIS on-line mass separator facility. 34 γ rays were placed in a decay scheme on the basis of $\gamma\gamma$- and xγ-coincidence information and half-life. The decay scheme in Fig. 1 was constructed assuming no β-feeding to the 377.7-keV $11/2^-$ level. From our analysis of 511-keV and Gd x-ray intensities, we have determined that >80% of the decay intensity has been observed in transitions feeding the 0.0- and 377.7-keV states. The spins of the first five levels have been assigned on the basis of the systematics. The other level spins have been assigned on the basis of interconnecting γ-ray transitions and allowed β-decay feeding to the indicated levels from a $5/2^-$ parent. Other consistent parent spins are $7/2^-$ and $9/2^+$, however neither is consistent with available Nilsson orbitals. For ϵ_2=0.17-0.28, the $\pi h_{11/2} 5/2^-[532]$ level is predicted to be the ground state for nuclei near N=76,[1] and ϵ_2=0.18 is predicted by the Grodzins' phenomenological estimate for ^{141}Tb. The establishment of $5/2^-$ spin for ^{141}Tb breaks the systematics of $11/2^-$ and $1/2^+$ isomer pairs for heavier odd-A Tb isotopes and clearly establishes a significant deformation at N=76 near the Z=64 semi-magic shell.

Footnotes and References

1. J.A. Cizewski and E. Gulmez, Phys. Lett. **B175**, 11 (1986).

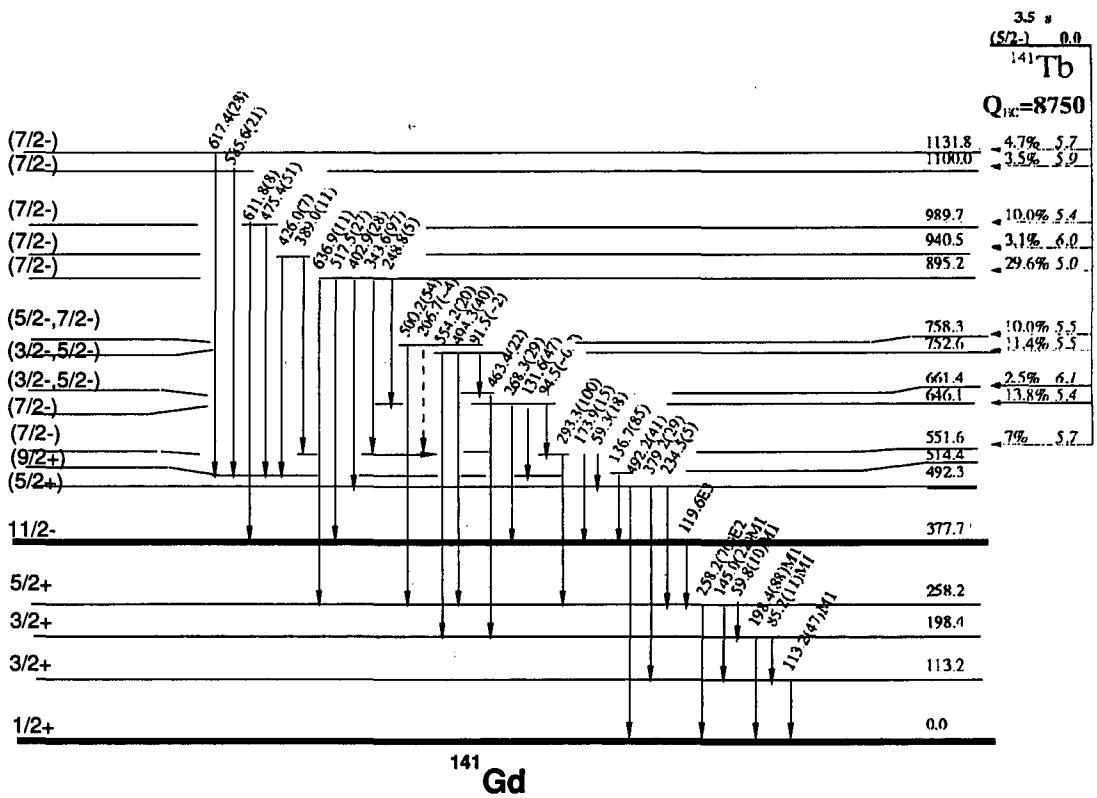

Fig. 1. Decay scheme for ^{141}Tb

Determination of Q_{EC} Values for Neutron-Deficient Rare Earth Nuclei

R.B. Firestone, J. Gilat, J.M. Nitschke, K.S. Vierinen, and P.A. Wilmarth

Decay schemes of neutron-deficient rare-earth nuclei near the proton drip line have been investigated at the SuperHILAC with the OASIS on-line mass separator facility. Absolute electron capture and β^+ branching intensities have been determined for many of these decays from K x-ray intensities and 511-keV annihilation radiation intensities. Q_{EC} values for these decays can be determined from these branching intensities and the decay schemes. A limitation to determining Q_{EC} values by this method is that the decay schemes must be complete. Otherwise, unobserved statistical decay to high-lying daughter levels will lead to systematically low Q_{EC} values. For A=140 and A=142 nuclei studied with OASIS, a favorable situation for determining Q_{EC} exists because the decay schemes are strongly dominated by ground-state transitions. These high-energy, low log*ft* β-decays dominate statistical feeding and greatly reduce the uncertainty in the derived Q_{EC} value. A comparison of the experimental Q_{EC} values with the evaluated and systematic values of Wapstra *et al*[1] and the calculated values of Liran and Zeldes[2] are shown in Table I. Excellent agreement has been obtained in all cases confirming the utility of this method for these nuclei.

Footnotes and References

1. A.H. Wapstra, G. Audi, and R. Hoekstra, At. Data Nucl. Data Tables **39**, 281 (1988).

2. S. Liran and N. Zeldes, At. Data Nucl. Data Tables **17**, 431 (1976).

Table I
Comparison of experimental and theoretical Q_{EC} values

		Q_{EC}		
Isotope	$t_{1/2}$	Experiment	Wapstra *et al*	Liran and Zeldes
$^{140}Eu^g$	1.51(2) s	8.6(4)	8.4(5)	8.3
^{140}Gd	15.8(4) s	4.8(4)	4.5(7)	5.5
^{140}Tb	2.4(2) s	>11.3	10.7(11)	10.9
^{142}Pm	40.5(5) s	4.88(16)	4.87(4)	5.1
^{142}Sm	72.49(5) min	<2.1	2.10(5)	2.2
^{142}Eu	2.34(12) s	7.0(3)	7.40(10)	7.5
^{142}Gd	70.2(6) s	4.1(2)	4.2(4)	4.6
^{142}Tb	597(17) ms	10.2(4)	10.0(7)	9.9
^{142}Dy	2.3(3) s	7.00(10)	6.4(11)	7.1

Nuclear Penetration Effects in ^{233}U

E. Browne, B. Sur, E.B. Norman, H.L. Hall, R.A. Henderson, K.T. Lesko, R.M. Larimer, and D.C. Hoffman.

The decay scheme of ^{233}Pa, as shown in Fig. 1, consists of three measured β^- transitions, populating the 5/2(633), 3/2(631), and 1/2(631) rotational bands in ^{233}U, respectively, and about fifteen γ-ray transitions between levels in these bands. Gehrke *et al.*[1] noted that their precisely measured value for the emission probability of the 312-keV γ ray (=38.6±0.5%) was inconsistent with the decay-scheme transition intensity balance, in that it allowed no β^- intensity to the ground-state rotational band. They noted an additional inconsistency, this one originating from the total K x-ray intensity measured in the decay of ^{233}Pa. This intensity was about 18% smaller than that expected from the γ-ray data and theoretical conversion coefficients.[2]

Both of these inconsistencies suggested smaller conversion coefficients than those predicted by theory,[2] leading to the decision to make precise measurements of these quantities for the 300, 312, and 340 keV γ rays. The conversion coefficients were determined by measuring each transition's γ-ray and conversion-electron intensities simultaneously, with a high-purity coaxial Ge detector and a lithium-drifted silicon detector, respectively. The resulting values, which are about 18% smaller than those predicted by theory,[2] were interpreted in terms of nuclear penetration effects in the conversion process. The total K x-ray intensity and the combined β^- intensity to the ground plus 40-keV levels (=6±2%), deduced from the γ-ray data and new conversion coefficients, are now consistent with the experimental data.

An independent measurement of the combined β^- intensity to the ground plus 40-keV levels (=8.8±1.4%) was made with a Au(Si) surface barrier detector shielded by a large NaI annular detector operated in anticoincidence. It is also consistent with the value deduced from the decay-scheme intensity balance. Finally, the emission probability for the 312-keV γ ray (=38.6±2.6%) was remeasured, using a ^{237}Np source with its daughter ^{233}Pa in equilibrium. This value agrees with that from Gehrke *et al.*[1]

Footnotes and References

1. R.J. Gehrke, R.G. Helmer, and C.W. Reich, Nucl. Sci. and Eng.**70**, 298 (1979).

2. F. Rosel, H.J. Fries, K. Alder, and H.C. Pauli, At. Data and Nucl. Data Tables **21**, 291 (1978).

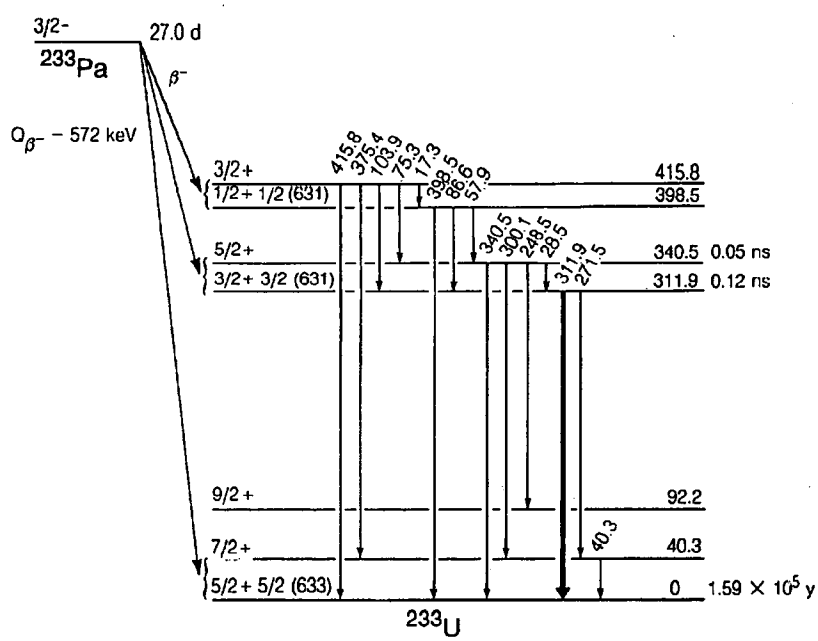

Fig. 1. See text.

Decay Properties of ^{153}Yb and ^{153}Tm; Excitation Energies of the $s_{1/2}$ and $h_{11/2}$ Proton States in ^{153}Tm*

M.O. Kortelahti,† K.S. Toth,‡ K.S. Vierinen, J.M. Nitschke, P.A. Wilmarth, R.B. Firestone, R.M. Chasteler, and A.A. Shihab-Eldin

The decay properties of ^{153}Yb and ^{153}Tm, produced in ^{64}Zn bombardments of ^{92}Mo at the SuperHILAC, were investigated following on-line mass separation at the OASIS facility.[1] A decay scheme, incorporating 34 transitions and 25 levels in ^{153}Tm, was constructed for ^{153}Yb. It establishes the $s_{1/2}$ proton level in ^{153}Tm to be isomeric at an excitation energy of 43.2 keV (see the level systematics in Fig. 1). The α decay branch of the $h_{11/2}$ ^{153}Tm ground state was determined to be 91±3%. In addition, a partial decay scheme was put together for the 9% β^+ branch. About 66% of this β^+ decay proceeds to the $h_{9/2}$ state located at 299.3 keV in ^{153}Er. Only one transition, 266.5 keV, could be assigned to the β^+ decay of the ^{153}Tm $s_{1/2}$ isomer; it is suggested that this γ ray deexcites the $p_{3/2}$ neutron level to the $f_{7/2}$ ^{153}Er ground state. Based on the intensity of the 266.5-keV γ ray the α branch of the low-spin isomer was estimated to be ~93%.

Footnotes and References

*Condensed from: M.O. Kortelahti *et al.*, to be published in Phys. Rev. C.

†University of Jyväskylä, SF-40100 Jyväskylä, Finland.

‡Oak Ridge National Laboratory, Oak Ridge, TN 37831.

1. J.M. Nitschke, Nucl. Instr. and Methods **206**, 341 (1983).

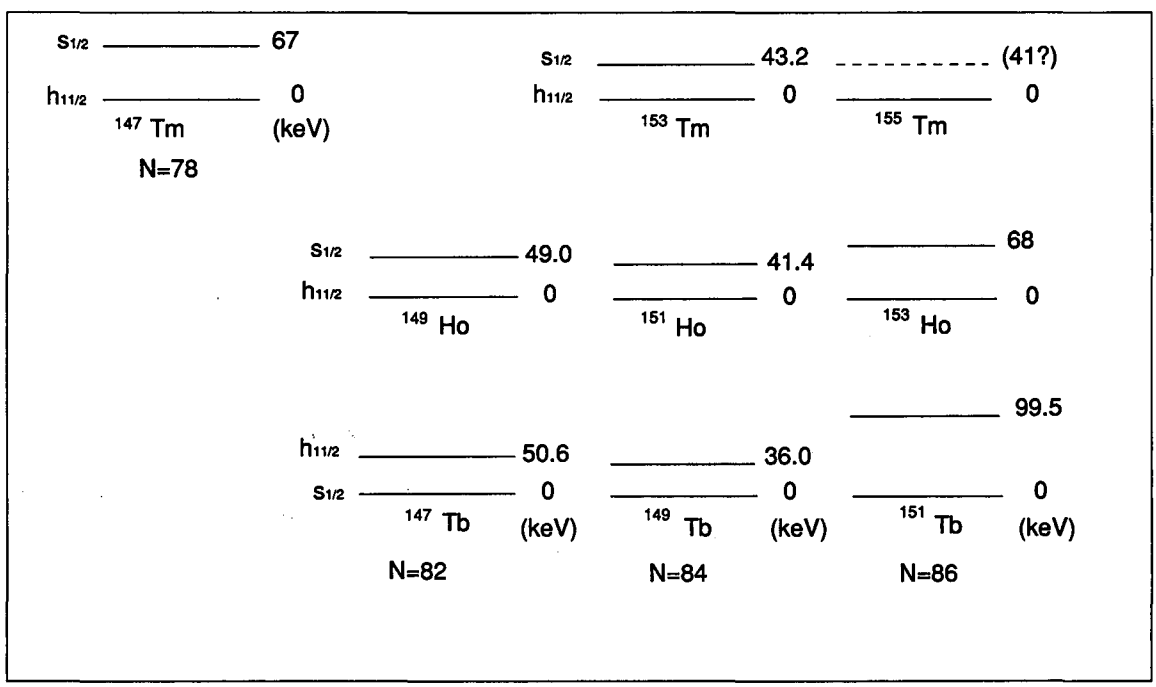

Fig. 1. Excitation energies of $h_{11/2}$ and $s_{1/2}$ proton states in ^{147,149,151}Tb (Z=65), ^{149,151,153}Ho (Z=67), and ^{147,153,155}Tm (Z=69).

Identification of the Neutron-Rich Isotope ^{174}Er*

R.M. Chasteler, J.M. Nitschke, R.B. Firestone, K.S. Vierinen, P.A. Wilmarth, and A.A. Shihab-Eldin

The heaviest known erbium isotope, 3.3(2) min. ^{174}Er, has been identified using the OASIS mass-separation facility and by β and γ-ray spectroscopy. It was produced using deep inelastic collisions of 8.5 MeV/nucleon ^{176}Yb ions, from the SuperHILAC, with ^{nat}W targets. Twelve γ rays were placed in a preliminary decay scheme consisting of six levels shown in Fig. 1. The mass of the new isotope was established by the separator and the Z was deduced from Tm K x ray coincident β and γ rays. In addition, the heaviest known isotope of holmium ^{171}Ho was observed with a half-life of 49(5) s confirming a previous observation of this activity[1].

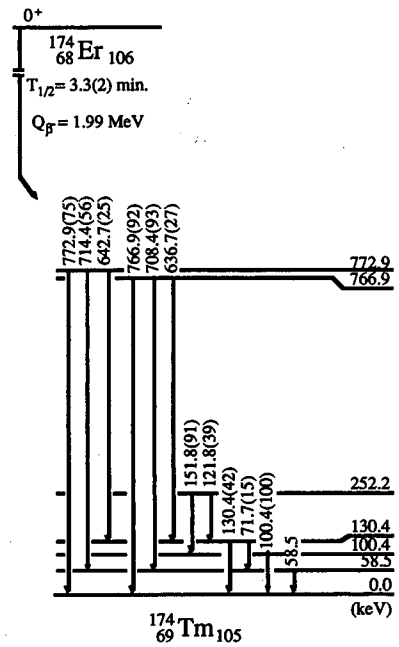

Fig. 1. Proposed partial decay scheme for ^{174}Er. Intensities are relative to the 100.4-keV γ ray.

Footnotes and References

*Condensed from Z. Phys. A **332**, 239 (1989).

1. K. Rykaczewski, *et al.*, GSI Scientific Report 1987, p. 30.

Single-Particle States in ^{151}Tm and ^{151}Er; Systematics of Neutron States in N=83 Nuclei

Y.A. Akovali, K.S. Toth,* A.L. Goodman,† J.M. Nitschke, P.A. Wilmarth, D.M. Moltz, M.N. Rao,‡ and D.C. Sousa§*

With the use of mass-separated sources produced at the LBL SuperHILAC's OASIS facility, the β-decay properties of ^{151}Yb and ^{151}Tm were investigated. Based on these radioactivity measurements, the $h_{11/2}$, $s_{1/2}$, $d_{3/2}$, $d_{5/2}$, and $g_{7/2}$ single-proton states in ^{151}Tm and the $f_{7/2}$, $h_{9/2}$, $p_{3/2}$, $i_{13/2}$, and probably the $p_{1/2}$ single-neutron states in ^{151}Er were identified. Systematics of neutron states in even-Z N=83 isotones are compared with the predictions of spherical Hartree-Fock-Bogoliubov calculations. It is found that if a proper effective interaction is used, the calculated energy levels agree with the experimental excitation energies.

Footnotes and References

*Oak Ridge National Laboratory, Oak Ridge, TN 37831

†Tulane University, New Orleans, LA 70118

‡Universidade de Sao Paulo, C.P. 20516, Sao Paulo, Brazil 01498

§Eastern Kentucky University, Richmond, KY 40475

Beta-Strength Function Studies of Delayed Proton Emission in Heavy, Deformed Nuclei

*P.A. Wilmarth, J.M. Nitschke, and K.S. Toth**

From a systematic study of the β-delayed proton emission process in neutron-deficient lanthanide precursors[1] at the SuperHILAC's OASIS facility (where spectral shapes, branching ratios, and final state feeding were measured), statistical model calculations[2] using quasiparticle random phase approximation (QRPA)[3] β-strength functions were found to give better agreement with the experiment than were calculations based on constant or gross theory[4] β-strength functions. Standard prescriptions (described in more detail in ref. 1) for the various input parameters to the statistical model were used and the spectral shapes could be well reproduced as shown in Figs. 1(a) and 1(b) for both odd-odd and even-odd precursors, respectively. This was expected since most of the assumptions of the statistical model, such as high level densities, would be valid for heavy, deformed nuclei. However, in the vicinity of the N=82 closed shell, the statistical model calculations could not match the shape of the experimental spectrum regardless of choice of strength function, which can be seen in Figs. 1(c) or 1(d) for odd-odd or even-odd precursors, respectively. The rather simple assumptions of the statistical model appear to breakdown near closed shells where nuclear structure effects and low level densities are expected to be of significance.

Footnotes and References

*Oak Ridge National Laboratory, Oak Ridge, Tennessee 37831.

1. P.A. Wilmarth, Ph.D. Thesis, **LBL-26101** (1988).

2. P. Hornshoj, *et al.*, Nucl. Phys. **A187**, 609 (1972).

3. J. Krumlinde and P. Möller, Nucl. Phys. **A417**, 419 (1984).

4. K. Takahashi, M. Yamada and T. Kondoh, At. Data Nucl. Data Tables **12**, 101 (1973).

5. J.M. Nitschke, *et al.*, in *Proceedings of the Fifth International Conference on Nuclei Far From Stability, Rosseau Lake, Ontario, Canada, 1987*, edited by I.S. Towner (AIP Conference Preceedings, New York, 1988) p. 697.

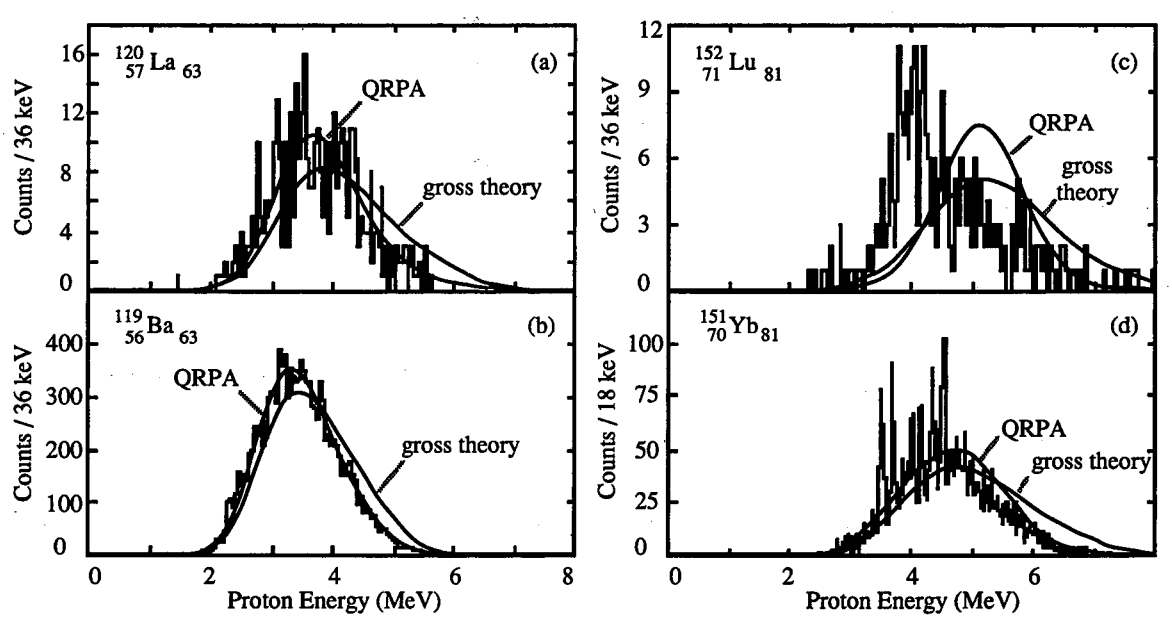

Fig. 1. Comparison between experimental delayed proton spectra (the histograms) and statistical model calculations (the smooth curves) based on gross theory or QPRA β-strength functions.

Beta-Decay of ^{154}Lu and ^{154}Yb*

K.S. Vierinen, A.A. Shihab-Eldin, J.M. Nitschke, P.A. Wilmarth, R.M. Chasteler, R.B. Firestone, and K.S. Toth†

Using mass-separated sources produced at the OASIS facility on-line at the SuperHILAC, the β-decay properties of ^{154}Lu and ^{154}Yb were investigated (see Fig. 1). Beta-decay feedings from ^{154}Lu to the first 8^+ and 6^+ levels in ^{154}Yb suggest a 7^+ spin for the odd-odd parent; also delayed proton emission and an indication of delayed α-particle emission were observed to follow the β decay of ^{154}Lu. The β-decay branch of the α-emitting nucleus ^{154}Yb was identified for the first time by the observation of one intense 133.2-keV γ ray. This transition deexcites a 1^+ 133.2-keV level in ^{154}Tm which is fed by an allowed $0^+ \rightarrow 1^+$ β transition with a logft value of 3.6±0.3. The decay of ^{154}Lu to ^{154}Yb has been studied previously by Rathke[1] and by Habenicht *et al.*;[2] Rathke[1] has also performed in-beam γ-ray measurements in an investigation of ^{154}Yb levels. The isotope ^{154}Lu was also produced in a previous study of ^{154}Yb α-particle emission.[3]

Footnotes and References

*Condensed from: K.S. Vierinen *et al.*, Phys. Rev. C **38**, 1509 (1988).

†Oak Ridge National Laboratory, Oak Ridge, TN **37831**.

1. G.E. Rathke, in *Proceedings of International Winter Meeting on Nuclear Physics, Bormio, Italy, 1984*, p. 53.

2. W. Habenicht *et al.*, in Proceedings of 7th International Conference of Atomic Masses and Fundamental Constants (AMCO7), Darmstadt, FRG, 1984, edited by O. Klepper, p. 244.

3. S. Hofmann *et al.*, Z. Phys. A **291**, 53 (1979).

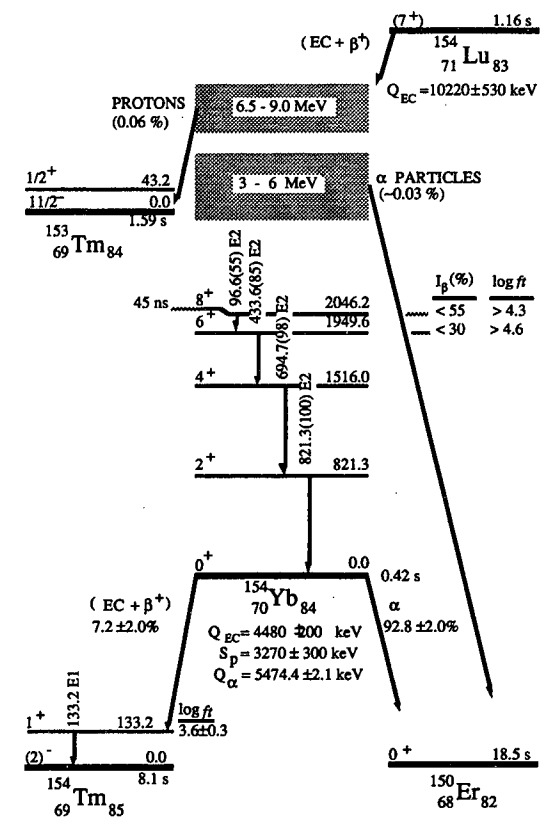

Fig. 1. Decay schemes of ^{154}Lu and ^{154}Yb. All energies are expressed in keV.

Fine structure in ^{153}Tm alpha decay*

K.S. Toth,† *P.A. Wilmarth, J.M. Nitschke, R.B. Firestone, K.S. Vierinen, M.O. Kortelahti,*‡ *and F.T. Avignone III*§

In an investigation of A=153 isotopes at the OASIS facility at the SuperHILAC, α/γ coincident counting was used to observe weak fine structure in ^{153}Tm α decay. In addition to the previously known α transitions that feed the ^{149}Ho $h_{11/2}$ ground state and $s_{1/2}$ (49.0 keV) isomer, the two, very much weaker, α groups shown in Fig. 1 were found to populate the $d_{3/2}$ (220.4 keV) and $d_{5/2}$ (564.4 keV) states in ^{149}Ho. Based on the ^{149}Ho level scheme and on the Q_α values for the two main ^{153}Tm α transitions,

it was determined that the $h_{11/2}$ level in ^{153}Tm is the ground state and that the $s_{1/2}$ state lies 43±7 keV above it. These isomer energies are consistent with systematics for the $s_{1/2}$ and $h_{11/2}$ proton states in even-N odd-Z nuclei near N=82.

Footnotes and References

*Condensed from: K.S. Toth *et al.*, Phys. Rev. C **38**, 1932 (1988).

†Oak Ridge National Laboratory, Oak Ridge, Tennessee 37831.

‡Lousiana State University, Baton Rouge, Louisiana 70803 and University of Jyväskylä, SF-40100 Jyväskylä, Finland.

Fig. 1. Part (a) shows the singles α-particle spectrum at A=153, while parts (b) and (c) show α groups observed in prompt coincidence with the 171.4- and 344.0 keV γ rays in ^{149}Ho, respectively. The largest peak in part (a) is an unresolved doublet consisting of the 5096-keV $s_{1/2} \rightarrow s_{1/2}$ and 5103 keV $h_{11/2} \rightarrow h_{11/2}$ α transitions in ^{153}Tm decay.

§University of South Carolina, Columbia, South Carolina 29208.

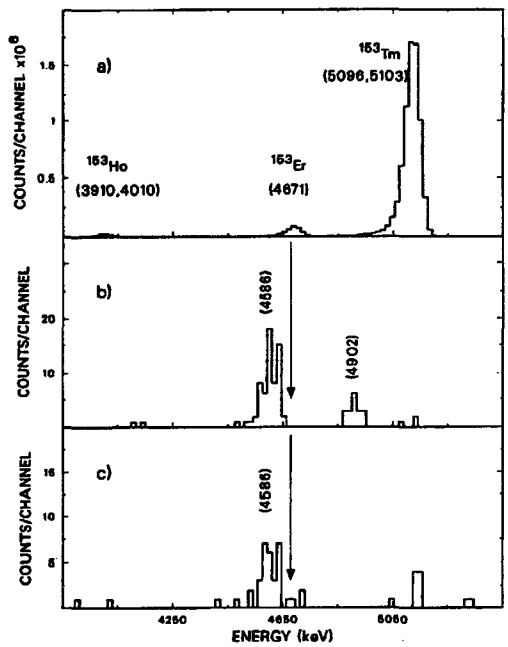

Beta-Delayed Proton Decay of the N=83 Precursor ^{153}Yb*

P.A. Wilmarth, J.M. Nitschke, K.S. Vierinen, K.S. Toth†, and M.O. Kortelahti‡

An investigation of β and particle decays of A=153 isobars was performed at the OASIS mass separation facility[1] on-line at the LBL SuperHILAC. A β-delayed proton branch was observed for the N=83 precursor ^{153}Yb extending the known region of delayed proton emission in the lanthanides across the N=82 shell for the first time. The delayed protons were assigned to ^{153}Yb on the basis of mass separation, coincident Tm K x rays, and coincident γ-ray transitions in the daughter nucleus ^{152}Er. The 4.0±0.5 s delayed proton half-life is in agreement with the previous value from α-decay studies[2] and with the 3.9±0.1 s half-life derived from the strongest γ rays following ^{153}Yb β decay.[3] Proton final state branching ratios deduced from proton- coincident γ-ray intensities are consistent with a $7/2^-$ precursor spin expected from systematics; and the proton branching ratio is $(8\pm2) \times 10^{-5}$. The delayed proton energy spectrum was essentially structureless and statistical model calculations using standard parameter sets were in good agreement with the experiment. The decay of ^{153}Yb is schematically shown in Fig. 1.

Footnotes and References

*Condensed from LBL-24653 and Z. Phys. A **329**, 503 (1988).

†Oak Ridge National Laboratory, Oak Ridge, TN 37831, USA

‡Louisiana State University, Baton Rouge, LA 70803, USA and University of Jyväskylä, SF-40100 Jyväskylä, Finland

1. J.M. Nitschke, Nucl. Instr. Meth. **206**, 341(1983).

2. E. Hagberg, *et al.*, Nucl. Phys. **A293**, 1(1977).

3. M. Kortelahti, *et al.*, Phys. Rev. C (to be published).

4. A.H. Wapstra and G. Audi, Nucl. Phys **A432**, 1(1985).

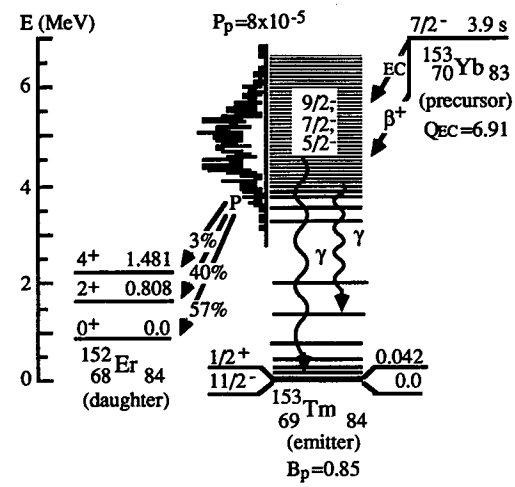

Fig. 1. Energetics and branching ratios for ^{153}Yb delayed proton decay. The values for Q_{EC} and B_p were taken from ref. 4. All energies are in MeV. The ground state and isomer energies in ^{153}Tm are from ref. 3.

Deep Inelastic Collision Cross Section Calculations

R.M. Chasteler

With the push for the search of new neutron-rich rare-earth isotopes at the LBL SuperHILAC's OASIS mass-separation facility,[1] a code for calculating the cross-sections for these transfer reactions was needed. A modeling code[2] for determining cross-section distribution for heavy-ion bombardmensts of actinide targets served as a starting point. It assumes a binary reaction mechanism and calculates a triple differential cross-section distribution, $\partial^3\sigma/\partial Z\partial N\partial E^*$ (E^* is the excitation energy of the product). The original code had this distribution deexcite by neutron emission or fission. Since the fission barriers are large in the rare-earth region, the fission channel was removed. Also more recent mass formulae[3] were used that predict more accurate masses in this region. This modified code is used predominantly as a tool to predict the best reaction to produce the desired product. Fig. 1 shows some sample cross-section calculations for ^{176}Yb + ^{186}W.

Footnotes and References

1. J.M. Nitschke, Nucl. Instr. & Meth. **206**, 341 (1983).

2. K.E. Gregorich, Ph.D. Thesis, LBL-20192, 1985.

3. P.E. Haustein, At. Data Nucl. Data Tables **39**, 185 (1988).

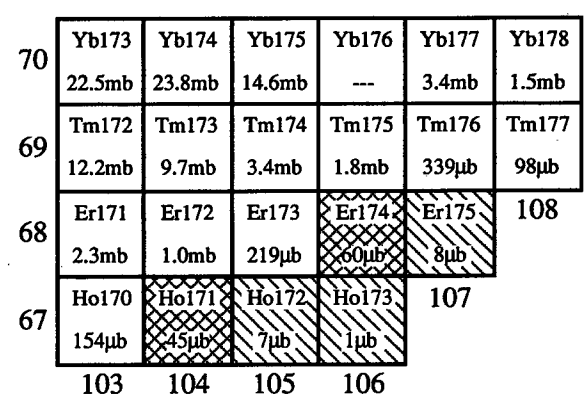

Fig. 1. Sample cross-section calculations for ^{176}Yb + ^{186}W. The bombarding energy is 20% above the Coulomb Barrier in the center of mass system. Shaded isotopes were unkown at the start of this work, and ^{174}Er and ^{171}Ho were identified in a preliminary experiment.

Doorway State Formation and Structure in Beta-Delayed Proton Decay

J.M. Nitschke, P.A. Wilmarth, R.B. Firestone P. Möller, K.S. Toth,† and J. Gilat‡

The structure in the β-delayed proton spectra of the precursors $^{147}_{66}Dy^g$, $^{149}_{68}Er^g$, and $^{151}_{70}Yb^g$ is analyzed within the framework of a doorway state model. Indications from γ-ray decay studies, β-strength function measurements, and calculations of state densities (Fig. 1) and Gamow-Teller strength distributions, lead us to suggest that some of the observed proton transitions arise from the preequilibrium decay of doorway states populated in β^+/EC decay. This is contrary to the statistical model assumption that the deexcitation proceeds *via* states of increasing complexity to the equilibrated compound nucleus state which subsequently decays through the two competing processes of charged particle and γ-ray emission, as described by an evaporation model, and where the structure in the proton spectra is interpreted as a fluctuation phenomenon.

In Fig. 1, the complexity of states increases from (b) (2 particle-1 hole) to (f) (4 particle-3 hole). The particle (n,p) hole (n^{-1},p^{-1}) structure of the states is indicated on the left using the notation ($nn^{-1}pp^{-1}$). The β-delayed proton spectrum of the $^{147}_{66}Dy$ precursor is shown in (a). Competing p and γ decay has been observed for region I in (a). States in region II are populated *via* β decay of $^{147}_{66}Dy^g$ but cannot deexcite *via* γ-ray decay to the states in region III due to the large differences in their nuclear structure; and states in region V can only be reached with small probability by two step processes. The strong suppression of the γ-decay channel enables the proton decay to dominate the deexcitation process, as observed in the experiment (a).

Footnotes and References

*Condensed from LBL-24750

†Oak Ridge National Laboratory, Oak Ridge, TN 37831

‡Soreq Nuclear Research Center, Yavne 70600, Israel

1. M. Herman and G. Reffo, Phys. Rev. C **36**, 1546 (1987).

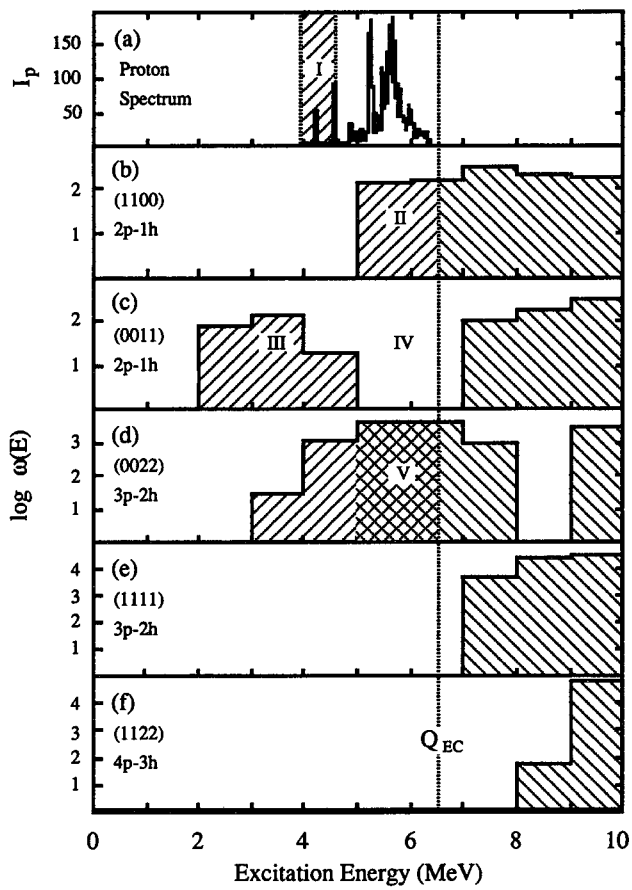

Fig. 1. State densities ω(E) for $^{147}_{65}Tb$ estimated from combinatorial calculations.[1]

Experimental and Predicted Half-Lives for Neutron- Deficient Lanthanide Isotopes

P.A. Wilmarth and J.M. Nitschke

While comparing gross theory[1] and quasiparticle random phase approximation (QRPA)[2] β-strength functions and their effects on statistical model calculations of the β-delayed proton emission process in neutron-deficient lanthanide isotopes, the question of predicting precursor half-lives with the two different β- strength function models arises. For about forty neutron-deficient lanthanide isotopes studied at the OASIS facility,[3] the ratios of predicted half-lives to measured half-lives are plotted in Fig. 1. The QRPA β-strength functions result in slightly better half-life predictions than the gross theory which consistently predicts longer half-lifes than the experimental values. However, both models show generally good agreement with the experimental values and, surprisingly, the two models usually predict similar values. The Q_{EC} values[4] were the same in both calculations and, since two very different models show similar deviations from the measured values, it was suspected that errors in the Q-value predictions are the source of these deviations. For the gross theory calculations, changing the Q_{EC}'s by $\pm 5\%$ resulted in half-lives that were $\sim$1.5 times longer for the lower Q_{EC}'s and $\sim$0.7 times shorter for the larger Q_{EC}'s. This strongly suggests that the accurate prediction of masses far from stability is perhaps more important in half-life predictions than the exact form of S_β.

Footnotes and References

1. K. Takahashi, M. Yamada and T. Kondoh, At. Data Nucl. Data Tables **12**, 101 (1973).

2. J. Krumlinde and P. Möller, Nucl. Phys. **A417**, 419 (1984).

3. P.A. Wilmarth, Ph.D. Thesis, LBL-26101 (1988).

4. S. Liran and N. Zeldes, At. Data Nucl. Data Tables **17**, 431 (1976).

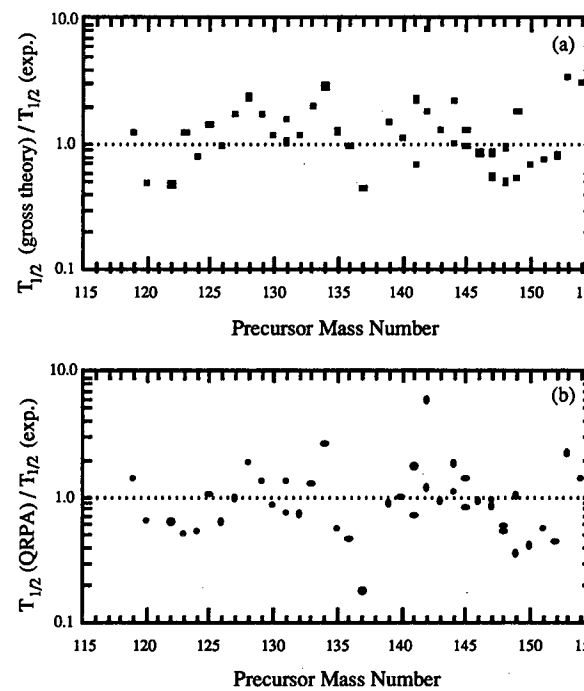

Fig. 1. Comparison between the experimental and predicted half-lives from (a) the gross theory of β-decay and (b) from QRPA β-strength function calculations for the delayed proton precursors reported in ref. 3.

Progress in the Studies of the Hydrolysis and Carbonate Complexation of Dioxoplutonium(V)

D.A. Bennett, H. Nitsche, R.J. Silva, D.C. Hoffman*

Solubility studies have shown that Pu(V) is a dominant soluble species in near neutral solutions.[1-4] These results indicate that Pu(V) may play a major role in the possible migration of plutonium from nuclear waste repositories through interaction with natural waters. At Yucca Mountain, the natural waters

are carbonate rich and have an oxidizing potential of 700 mv.[5] Therefore, the hydrolysis (Q) and carbonate complexation (β_{11}) constants of Pu(V) are important parameters for the thermodynamic database for the geochemical modeling for safe nuclear waste disposal. Equation 1 illustrates a potential migration mechanism at Yucca Mountain.

$$\mathrm{PuO_{2(s)}} + 4\mathrm{H^+} \rightleftharpoons \mathrm{Pu^{4+}} + 2\mathrm{H_2O}$$

$$\downarrow\uparrow \mathrm{Eh} = 700\mathrm{mV}$$

$$PuO_2^+ + OH^- \ or \ CO_3{}^2 \qquad (1)$$

$$\downarrow\uparrow \mathrm{Q\ or}\ \beta_{11}$$

$$\mathrm{PuO_2(OH)\ or\ PuO_2(CO_3)^-}$$

Last year, we reported a preliminary value log of $\beta_{11} = 4.7 \pm 0.5$ for the first carbonate complexation constant of Pu(V). This value was considered preliminary because the ionic strength was not controlled. This year, numerous experiments were attempted with a background electrolyte to maintain constant ionic strength. However, precipitation interfered with the measurements. The resulting solid was characterized by Fourier Transform Infrared Spectroscopy and x-ray powder diffraction and identified to be $\mathrm{NaPuO_2CO_3}$.

The solubility problems necessitated a new method of measurement. Laser Induced Photoacoustic Spectroscopy (LIPAS) is one promising technique. LIPAS is inherently more sensitive than conventional spectrophotometry because it relies on the direct measurement of absorbed photon energy, rather than the difference between incident and transmitted radiation as measured conventionally. In LIPAS, some of the absorbed photon energy from a pulsed laser is converted via non-radiative decay to an acoustic wave. This process is illustrated in Fig. 1. Because the sensitivity of LIPAS is 100-1000 times that of conventional spectrophotometry [6,7], the hydrolysis and carbonate complexation experiments can be conducted at lower concentrations to avoid solubility problems.

A LIPAS system was recently assembled in R.J. Silva's laboratory at Lawrence Livermore National Laboratory. We have just completed the measurement of Beer's Law plots for Pu(IV), Pu(V), and Pu(VI). As shown in Table I, the LIPAS system offers increased sensitivity. The next step will be to repeat the hydrolysis and carbonate complexation experiments at lower concentrations using LIPAS.

Table I
Comparison of the Approximate Detection Limits of Conventional Spectrophotometry versus LIPAS

Species	Conventional Spectrophotometry	LIPAS
Pu^{4+}	$1\times10^{-4}\underline{M}$	$1\times10^{-6}\underline{M}$
PuO_2^+	$4\times10^{-4}\underline{M}$	$4\times10^{-6}\underline{M}$
PuO_2^{2+}	$1\times10^{-5}\underline{M}$	$7\times10^{-7}\underline{M}$

Footnotes and References

*Permanent address: Lawrence Livermore National Laboratory, Livermore, CA 94550

1. H. Nitsche, *Inorg. Chim. Acta,* 126, No. **2**, **207** (1987)

2. H. Nitsche and N.M. Edelstein, *Radiochim. Acta,* 39, **23** (1985)

3. E.A. Bondietti and S.A. Reynolds, Field and Laboratory Observations of Plutonium Oxidation States, L.L. Ames (Ed.), Proc. Actinide-sediment Reactions Working Meeting, Battella Northwest lab., USDOE Rep BNWL-2117, pp. 505-537 (1976)

4. D. Nelson, statement at Workshop on Environmental Chemistry of Plutonium, Savannah River, April 1-2 (1980)

5. A.E. Ogard and J.F. Kerrisk, Groundwater Chemistry Along the Flow Path between a Proposed Repository Site and the Accessible Environment, Los Alamos National Laboratory report UR LA-10188 MS, New Mexico (1984)

6. F.T. Ewart, M. Liezers, J.W. McMillan, P.M. Pollard, and H.P. Thomason, The Development of a Laser Induced Photoacoustic Facility for Actinide Speciation, AERE-R 12875 Harwell Laboratory (1988).

7. R.E. Russo, R.J. Silva, J.J. Bucher, N.M. Edelstein, Measurements of Actinide Speciation at Ultralow Solution concentrations Using Photoacoustic Spectroscopy, Lawrence Livermore Laboratory Annual Report (1986)

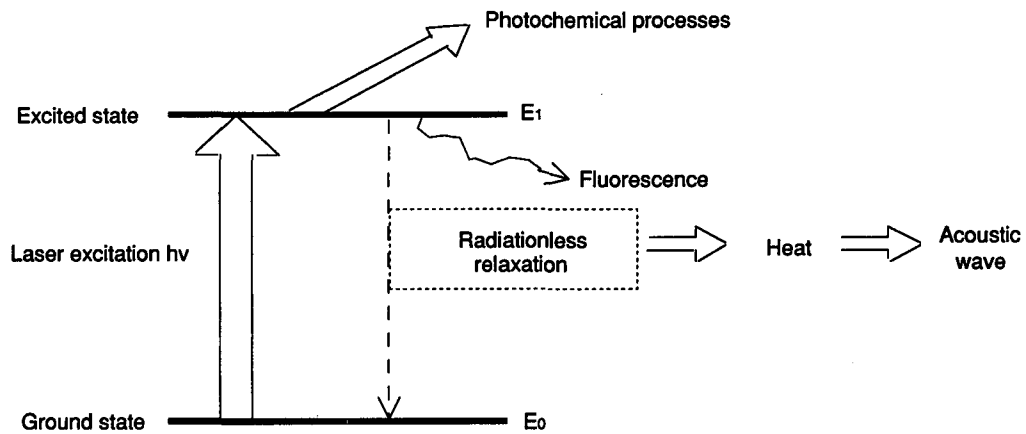

Fig. 1. The photo-acoustic process.

The Synergistic Solvent Extraction of Cf, Am, and Eu by 4-Benzoyl-5-methyl-2-phenyl pyrazol-3-thione (BMPPT) and Tri-n-octyl phosphine oxide (TOPO)

Robert B. Chadwick, Barbara F. Smith, Gordon D. Jarvinen, and Darleane C. Hoffman

Our group is interested in the production and chemical and nuclear properties of the heaviest elements, which we produce at the 88-Inch Cyclotron. The heavy actinides (Am to Lr) and still heavier elements (Rf and above) are all radioactive and in their synthesis copious quantities of fission products, including radioactive lanthanides, are produced. In the lanthanides and actinides the 4f and 5f electron shells are being filled, respectively. This causes the lanthanides and actinides to have similar chemical properties and leads to difficulty in their separation. To study the chemical and nuclear properties of an element it must first be in a pure state, so our group requires fast and simple methods of separating these elements.

One of the simplest separation methods is solvent extraction, where an aqueous phase containing a mixture of metal ions is equilibrated with an immiscible organic phase in which an organophilic chelating agent is dissolved. With the proper chelating agent, the selective extraction of the metal ion of interest is possible. One chelating agent that has been found to quantitatively extract Am, Cm, Bk and Eu (but not separate them from each other) is 1-phenyl-3-methyl-4-benzoylpyrazolone-5 (PMBP).[1] However, several sulfur containing extractants have shown interesting selectivity in the separation of the actinides and lanthanides.[2,3] This has led colleagues at Los Alamos National Laboratory to investigate the extraction properties of the mono-thio deriva-

tive of PMBP, 4-benzoyl-5-methyl-2-phenyl pyrazol-3-thione (BMPPT). Their work has shown that BMPPT in synergistic combination with tri-n-octyl phosphine oxide (TOPO) will selectively extract Am over Eu (Am/Eu = 68, pH 3.0, 0.30 M BMPPT, 0.01 M TOPO).[4] In a collaborative effort with LANL our group is investigating the extractant properties of BMPPT for the heavy actinides.

Separation between Cf, Am and Eu has been found to be possible (Cf/Am = 7, pH 2.0, 0.10 M BMPPT, 0.05 M TOPO). Also, through the technique of slope analysis of logarithmic plots of distribution coefficient vs. concentration, the most probable stoichiometric reactions have been determined. For the perchlorate aqueous system the slope of the acid dependency was found to be 1.8 ± 0.15 for Cf, 2.7 ± 0.1 for Am, and 1.6 ± 0.1 for Eu. The slope of the BMPPT dependency was found to be 2.5 ± 0.1, 2.8 ± 0.1, and 2.7 ± 0.1 for Cf, Am, and Eu, respectively. The slope of the TOPO dependency was found to be 2.1 ± 0.1, 2.1 ± 0.1, and 2.2 ± 0.1 for Cf, Am, and Eu, respectively. This indicates that the most probable product species are $Cf(BMPPT)_2(HBMPPT)(TOPO)_2(ClO_4)$, $Am(BMPPT)_3(TOPO)_2$, and $Eu(BMPPT)_2(HBMPPT)(TOPO)_2(ClO_4)$. The selectivity found is unusual in that Eu and Am have analogous ground state electronic structures ([Xenon core] $4f^7\ 6s^2$ for Eu vs. [Radon core] $5f^7\ 7s^2$ for Am), while Cf and Eu have essentially the same ionic radii (0.95 angstroms). This suggests that a delicate balance of steric and electronic effects is responsible for the selectivity observed. However, more data is needed to further elucidate the reasons for this selectivity and extraction studies on other actinide and lanthanide elements are in progress.

Footnotes and References

1. B.F. Myasoedov, M.K. Chmutova, I.A. Lebedev, Proceedings International Solvent Extraction Conference, Volume 1, 815-19, (1971).

2. W.H. Hardwick and M. Moreton-Smith, Analyst 83, 9 (1958).

3. C. Musikas, Proceedings of the International Symposium on Actinide-Lanthanide Separations, G.R. Choppin, J.D. Navratil and W.W. Schulz, Eds. World Scientific, Philadelphia, 1984, pp. 19-30.

4. B.F. Smith, G.D. Jarvinen, G.G. Miller, R.R. Ryan, and E.J. Peterson, Solvent Extraction and Ion Exchange **5**, 895 (1987).

Search for Lawrencium as a P-Element Using Chromatography Techniques*

D.T. Jost, H.W. Gäggeler, Ch. Vogel, M. Schädel, E. Jäger, B. Eichler, K.E. Gregorich, and D.C. Hoffman

Multidimensional relativistic Dirac-Fock calculations predict that the last member of the actinides series, Lr, might behave like a p-element with a $[Rn]5f^{14}7s^27p_{1/2}$ ground state electronic configuration, rather than the traditionally expected $[Rn]5f^{14}6d7s^2$ configuration. On-line gas chromatography was applied to search for Lr as a volatile p-element. These investigations were preformed with ^{260}Lr ($T_{1/2}$ = 3 min), produced in the $^{249}Bk(^{18}O, \alpha 3n)$ reaction. Quartz and Pt chromatography columns were used. No evidence for Lr as a volatile element was found under reducing conditions at temperature of about 1000°C. Our results give a lower limit for the adsorption enthalpy $\Delta = H_a$ for Lr on quartz and Pt surfaces of 290 kJ/mol. This value is significantly higher than the estimated values for Lr(p).

Footnotes and References

*Condensed from Inorganica Chimica Acta **146**, 255-259 (1988).

Chloride Complexation Studies of Element 104 in the H^+, Cl^-/TBP System

C.M. Gannett, R.B. Chadwick, K.B. Chen, K.R. Czerwinski, K.E. Gregorich, H.L. Hall, G.R. Haynes, R.A. Henderson, D.M. Lee, J.D. Leyba, M.J. Nurmia and D.C. Hoffman

The 65-second isotope $^{261}104$, produced by bombarding a ^{248}Cm target with 96-MeV $^{18}O^{5+}$ ions (cross section = 5 nb) at the 88-Inch Cyclotron, was used in studies of the chloride complexation behavior of element 104. This study utilizes a liquid-liquid extraction system consisting of HCl and LiCl in the aqueous phase and 0.25 M tributyl phosphate in benzene as the organic phase. Two studies have been accomplished. In the first, the concentration of HCl without LiCl was varied from 2 M to 12 M yielding an unusually steep positive slope of log K_d vs log[HCl] from about 7 M to 10 M HCl (Fig. 1). In the second, the hydrogen ion concentration was kept constant at 7 M while the amount of chloride ion was varied by the addition of LiCl. A plot of log K_d vs log[Cl^-] gave a slightly negative slope (Fig. 2) indicating a weak [Cl^-] dependence. Data which have been obtained for hafnium under the same experimental conditions indicate that the complexation of element 104 is stronger than that of its chemical homolog hafnium (Fig. 1).

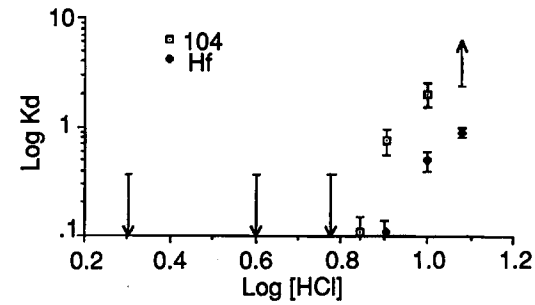

Fig. 1. See text.

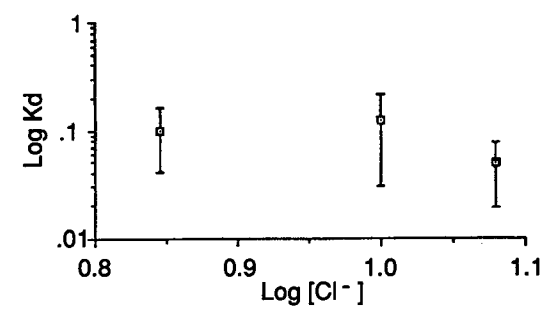

Fig. 2. See text.

Alpha Peak Energies and Abundances of ^{257}No

C.M. Gannett, R.B. Chadwick, K.B. Chen, K.R. Czerwinski, K.E. Gregorich, H.L. Hall, R.A. Henderson, D.M. Lee, J.D. Leyba, M.J. Nurmia and D.C. Hoffman

The 26-second isotope ^{257}No was produced by bombarding a ^{248}Cm target with 70-MeV $^{13}C^{4+}$ at LBL's 88-Inch Cyclotron in order to verify its alpha peak energies and abundances. Previous work[1] had found alpha peaks and abundances to be 8.22 MeV (55 ± 3%), 8.27 MeV (26 ± 2%), and 8.32 Mev (19 ± 2%). In that study the authors indicated that the abundances for the two latter peaks may have been too high due to conversion electrons summing with the lower energy peak. In the present work in order to avoid this potential problem, the ^{257}No source was measured with a silicon surface barrier detector subtending a geometry of 5% of 4π.

The reaction products were carried from the target chamber through a capillary tube via a helium jet, deposited on a nickel foil, flamed, then counted for alpha activity. A total of 114 alpha events were attributed to ^{257}No. Under the conditions of this experiment there appeared to be an unresolved multiplet centered at 8.224 MeV including a strong indication of a peak at 8.246 MeV. The abundance of this group is 76 ± 11%. Additional peaks were cen-

tered at 8.299 MeV (11 ± 3% and 8.336 MeV (13 ± 3%). As suspected in the previous work,[1] the two higher energy peaks do indeed show a lower abundance when the effects of conversion electron summing are removed.

Footnotes and References

1. P. Eskola, K. Eskola, M. Nurmia and A. Ghiorso, Phys. Rev. C **2**, 1058 (1970).

A Study of the Decay Properties of the New Isotope, ^{262}No

R.W. Lougheed, E.K. Hulet,* J.F. Wild,* K.J. Moody,* R.J. Dougan,* C.M. Gannett, R.A. Henderson, D.M. Lee, and D.C. Hoffman*

^{262}Lr was reported earlier[1] to have a 216-m half life, appearing to decay by spontaneous fission. However, from considerations of odd-particle fission hindrance and an estimated Q_{EC} of 2 MeV, ^{262}Lr is expected to decay by electron capture to ^{262}No, which has been predicted[2–6] to have a very short half-life and fission via a symmetric mass division. To look for this possibility, we performed an X-ray fission coincidence experiment at the 88-Inch Cyclotron. An ^{254}Es target was bombarded with 127-MeV ^{22}Ne ions to produce the ^{262}Lr via a ^{8}Be transfer reaction. The recoiling product atoms were stopped in a molybdenum catcher foil, which at the end of bombardment was dissolved and the Lr atoms chemically separated from other elements produced in the reaction. The Lr atoms were electrodeposited on a thin gold layer that had previously been deposited on a thin polyimide foil. The resulting foil was placed in a specially built high-geometry counting chamber[7] for measuring X-ray and fission singles and coincidences. After analysis of the X-ray fission coincidence data, we found that ^{262}Lr was decaying by electron capture to ^{262}No, which then fissioned with a 5-ms half-life. As predicted, ^{262}No is found to fission with a symmetric mass distribution. The total kinetic energy distribution is asymmetric with peaks at 237 MeV and 200 MeV. This distribution is similar to that of other nuclides in which a bimodal fission decay process has been observed. The fraction of ^{262}No decaying via high-energy symmetric fission is greater than was observed in ^{258}No. This observation is consistent with measurements of the fission properties of fermium and mendelevium isotopes, which show an increasing high-energy fission component with increasing neutron number. The SF half-life of the ^{262}Lr, however, is some 100 times longer than had been predicted. These data will be extremely useful in the further advancement of the theory of the fission process.

Footnotes and References

*Lawrence Livermore National Laboratory, Livermore, Ca

1. D.C. Hoffman, D.M. Lee, C.M. Gannett, R.A. Henderson, R.W. Lougheed, E.K. Hulet, J.F. Wild, K.J. Moody, and R.J. Dougan, LBL 25295, 62 (1988)

2. P. Möller, J.R. Nix, and W.J. Świątecki, Nucl. Phys. **A469**, 1 (1987)

3. U. Brosa, S. Grossmann, and A. Müller, Z. für Phys. A **325**, 241 (1986)

4. V.V. Pashkevich, Nucl. Phys. **A477**, 1 (1988)

5. E.K. Hulet, J.F. Wild, R.J. Dougan, R.W. Lougheed, J.H. Landrum, A.D. Dougan, M. Schädel, R.L. Hahn, P.A. Baisden, C.M. Henderson, R.J. Dupzyk, K. Sümmerer, and G.R. Bethune, Phys. Rev. Lett. **56**, 313 (1986)

6. P. Möller, private communication

7. E.K. Hulet, R.W. Lougheed, J.F. Wild, R.J. Dougan, K.J. Moody, R.L. Hahn, C.M. Henderson, R.J. Dupzyk, and G.R. Bethune, Phys. Rev. C **34**, 1394 (1986)

Chemistry of Heavy Ion Reactions*

D.C. Hoffman

The use of heavy ions to induce nuclear reactions was reported as early as 1950. Since that time it has been one of the most active areas of nuclear research. Intense beams of ions as heavy as uranium with energies high enough to overcome the Coulomb barriers of even the heaviest elements are available. The wide variety of possible reactions gives rise to a multitude of products which have been studied by many ingenious chemical and physical techniques. Chemical techniques have been of special value for the plethora of other nuclides present. Heavy ion reactions have been essential for the production of the trans-Md elements and a host of new isotopes. The systematics of compound nucleus reactions, transfer reactions, and deeply inelastic reactions have been elucidated using chemical techniques. A review of the variety of chemical procedures and techniques which have been developed for the study of heavy ion reactions and their products is given. Determination of the chemical properties of the trans-Md elements, which are very short-lived and can only be produced an "atom-at-a-time" via heavy ion reactions, is discussed.

Footnotes and References

*Abstract of Invited Paper presented at the Second International Conference on Nuclear and Radiochemistry, Brighton, England, July 11-15, 1988, submitted to **The Analyst.**

The Heavy Ion Reaction of ^{nat}Ag with 20 MeV/nucleon ^{12}C

K.B. Chen, Y.W. Yu,* K.E. Gregorich, D.C. Hoffman and G.T. Seaborg*

We are interested in symmetric fission induced by intermediate energy heavy-ion reactions. The bombardment of two ^{nat}Ag targets with 245 MeV ^{12}C was performed at the LBL 88-Inch Cyclotron. One target was surrounded by mylar catcher foils, the other target was surrounded by aluminum catcher foils. The Ag, Sc, Fe, Co and Ni were radiochemically separated from the aluminum catcher foils the ^{nat}Ag target. The isolated fractions were then counted for gamma activities. We have observed ^{43}K, ^{48}Sc, ^{48}V, ^{52}Mn, ^{52}Fe, ^{55}Co and ^{57}Ni. So far, only cumulative yields have been determined. We hope to identify symmetric fission from the forward to backward ratio of the products and the mass-yield distributions. The heavy products ^{95}Tc, ^{97}Ru, ^{99m}Rh, ^{101}Pd,..., ^{108m}In, and ^{113g}Sn also have been observed. We will determine if these nuclides are produced by deexcitation of the compound nucleus by sequential particle emission before low energy fission. To identify the product radioactivities in the target and catcher foils or in the separated chemical fractions derived from the target and catcher foils, a microcomputer analysis program has been developed based on a two megabyte γ-ray table stored in an IBM-PC AT. This system is based upon three existing FORTRAN codes TAU1, TAU2,[1] and EXFIT.[2] TAU1 constructs decay curves for all observed γ-ray transitions, TAU2 matches known γ-ray energies and half-lives to each measured decay curve and EXFIT fits the decay curves by an error-weighted non-linear least squares analysis.

Footnotes and References

*Tsing Hua University, Taiwan R.O.C.

1. D.J. Morrissey *et al.*, Nucl. Instr. and Meth. **158**, 499 (1979).

2. K.E. Gregorich, (Ph.D. Thesis), LBL-20192.

Production Cross Sections for Above and Below Target Elements from the Interactions of ^{44}Ca with ^{248}Cm

J.D. Leyba, R.M. Chasteler, R.A. Henderson, D.A. Bennett, C.M. Gannett, H.L. Hall, R.B. Chadwick, K.E. Gregorich, D.M. Lee, M.J. Nurmia, D.C. Hoffman, A. Türler, and H.R. von Gunten*,†*

Production cross sections for isotopes of Th, U, Np, Pu, Am, Cm, Bk, Cf, Es, and Fm were measured from bombardments of ^{248}Cm with ^{44}Ca ions at the LBL 88-Inch Cyclotron for five energies ranging from just below the Coulomb barrier to about 1.4 times the Coulomb barrier. The excitation functions for this system are all similar in shape and decrease slowly with increasing projectile energy. The shapes of the excitation functions are consistent with the calculated reaction energies for the specific nuclides based upon ground state Q values and the differences between incoming and outgoing Coulomb barriers assuming touching spherical nuclei. The excitation functions from the ^{44}Ca-^{248}Cm system are similar to excitation functions with comparable reaction energies from the ^{40}Ca-^{248}Cm and ^{48}Ca-^{248}Cm systems.[1] Typical excitation functions for two Es isotopes are shown in Fig. 1 for ^{40}Ca, ^{44}Ca, and ^{48}Ca interactions with ^{248}Cm. For the ^{48}Ca-^{248}Cm system it was shown that the maxima of the isotopic distributions for isotopes of Bk, Cf, Es, and Fm were shifted two to three mass units higher relative to the maxima from the ^{40}Ca- ^{248}Cm system. The maxima of the isotopic distributions from the ^{44}Ca-^{248}Cm system occur zero to two mass units higher than the corresponding maxima from the ^{40}Ca-^{248}Cm system. Generally speaking, for these three systems the largest cross sections occur for transfers involving the fewest number of nucleons and decrease rapidly as the number of nucleons transferred increases. The shapes of the isotopic distributions from the ^{44}Ca-^{248}Cm system (Fig. 2) are very comparable to those from systems observed previously including ^{16}O,^{18}O, ^{20}Ne, ^{22}Ne, ^{40}Ca, and ^{48}Ca with ^{248}Cm.[1,2] These similarities are indicative of the fact that the final isotopic distributions are somewhat independent of the projectile. With the help of the data from these systems we hope to gain a better understanding of the division of energy in these reactions so that theoretical models can be developed for transfer reactions.

Footnotes and References

*Universität Bern, Switzerland

†Eidg. Institut für Reaktorforschung, Würenlingen, Switzerland

1. D.C. Hoffman, *et al*, Phys. Rev. **C31**, 1763 (1985).

2. D. Lee *et al*, Phys. Rev. **C25**, 286 (1982).

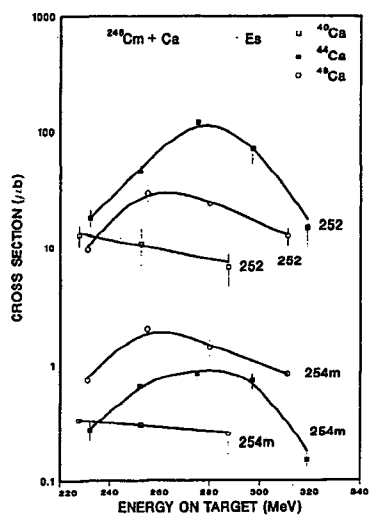

Fig. 1. See text.

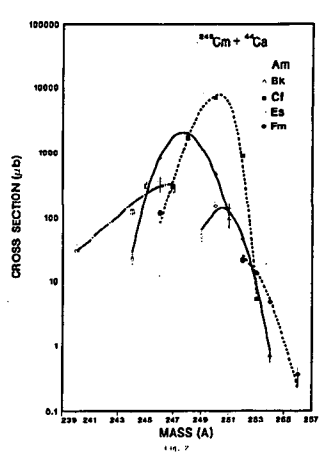

Fig. 2. See text.

A History and Analysis of the Discovery of Elements 104 and 105*

E.K. Hyde, D.C. Hoffman, and O.L. Keller, Jr.†

Although the scientific literature now includes information on ten isotopes of element 104 and six isotopes of element 105, no official ruling has been made by any international body concerning their names nor the assignment of credit for discovery. A controversy has developed between research teams at the Joint Institute for Nuclear Research, Dubna, USSR, and research teams at LBL concerning the right to be recognized as the discoverers of elements 104 and 105. This paper reviews the experimental studies carried out at both laboratories during the period from 1960 to 1977 and makes a critical assessment of the physical and chemical evidence relating to the synthesis of these elements and the claims based upon that evidence. Work done at other institutions is also cited when it is pertinent to these claims. (Eight-six references are included.) It is concluded that the information on element 104 published in 1969 by Ghiorso *et al.*[1] was correct and that their information meets the criteria for discovery of new elements stated by Harvey *et al.*[2] and by Flerov and Zvara.[3] It is further concluded that the evidence for element 105 presented by Ghiorso *et al.*[4,5] also meets these criteria. We recommend that they should be credited with both discoveries and their choices of the name rutherfordium (Rf) for element 104 and hahnium (Ha) for element 105 be adopted.

Footnotes and References

*Condensed from LBL-17093; Radiochim. Acta **42**, 57 (1987).

†Chemistry Division, Oak Ridge National Laboratory, Oak Ridge, TN

1. A. Ghiorso, M. Nurmia, J. Harris, K. Eskola and P. Eskola, Phys. Rev. Lett. **22**, 1317 (1969).

2. B.G. Harvey, G. Herrmann, R.W. Hoff, D.C. Hoffman, E.K. Hyde, J.J. Katz, O.L. Keller, Jr., M. Lefort, G.T. Seaborg, Science **193**, 1271 (1976).

3. G.N. Flerov and I. Zvara, Joint Institute of Nuclear Research, Dubna, USSR, Report D7-6013, August 1971.

4. A. Ghiorso, M. Nurmia, K. Eskola, J. Harris, P. Eskola, Phys. Rev. Lett. **24**, 1498 (1970).

5. A. Ghiorso, M. Nurmia, K. Eskola, and P. Eskola, Phys. Rev. C **4**, 1850 (1971).

Anionic Halide Complexes of Element 105

K.E. Gregorich, W. Brüchle, U. Baltensperger,† H. Gäggeler,† J. Kratz,‡ D.M. Lee, C. Lienert,§ D. Jost,† M.J. Nurmia, Y. Nai-Qi,† R.A. Henderson, H.L. Hall, C.M. Gannett, R.B. Chadwick, J.D. Leyba, K.R. Czerwinski, D.C. Hoffman, M. Schädel,* U. Scherer,‡ A. Türler,§ P. Zimmermann,‡*

In 1986, we performed a series of experiments which showed that hahnium (element 105) behaves chemically like the other members of group 5 of the periodic table, but its fluoride complexation is significantly different from that for tantalum.

In September and October of 1988, we hosted a collaboration to study the chemical properties of hahnium in more detail. One major focus of this collaboration was to study the stabilities of anionic halide complexes of hahnium and compare them with the stabilities of halide complexes of other group 5 elements. The 34-s isotope, ^{262}Ha, was formed at the 88-Inch Cyclotron via the ^{249}Bk(^{18}O, 5n) reaction and this activity was transported to the chemical separation apparatus on KCl aerosol particles with the He-jet technique. Because of the short half-life and the low production rate (enough for the detection of a few atoms per hour) of this activity, rapid chemical

separation techniques which could be repeated on a one-minute time scale had to be devised. A miniaturized, computer-controlled liquid chromatography apparatus (Mini-ARCA) was built for these separations. With this Mini-ARCA, we performed anion exchange separations from mixed HCl / HF solutions, using chromatography columns incorporating the anion exchanger triisooctyl amine (TIOA) on an inert column support material. The ^{262}Ha was detected by measuring the fission and 8.45- and 8.66-MeV alpha activities associated with its decay. Its alpha decay daughter, 4.2-s ^{258}Lr, also decays by alpha emission, so the detection of parent and daughter alpha particles from the same nucleus provides a unique identification of the presence of ^{262}Ha. In a first series of experiments, the Ha was adsorbed onto the column material from a 12 M HCl / 0.02 M HF solution. The TIOA, along with the activity was stripped from the column with 0.02 M HF in acetone. This acetone strip fraction was dried and counted and was found to contain the ^{262}Ha activity, demonstrating that anionic complexes are formed.

In a second series of experiments, the activity was adsorbed on the TIOA column as before. A Nb-Pa fraction was removed from the column with 4 M HCl / 0.02 M HF, and a Ta fraction was removed with 6 M HNO_3 / 0.015 M HF. The ^{262}Ha activity was found in the Nb-Pa fraction, showing that the anionic halide complexes are not as strong as for Ta, and are more like those for Nb or Pa.

A third series of experiments was performed in which the activities were adsorbed on the TIOA column from 10 M HCl. A Pa fraction was removed with 10 M HCl / 0.025 M HF, and a Nb fraction was removed with 6 M HCl / 0.015 M HF. The ^{262}Ha was found to be equally divided between the Pa and Nb fractions, indicating that its halide complexing strength is between that for these two elements.

Footnotes and References

*Gesellschaft für Schwerionenforschung, Darmstadt, West Germany

‡Universität Mainz, FRG

†Paul Scherrer Institute, Würenlingen, Switzerland

§Universität Bern, Switzerland

Absence of Extreme Sub-Barrier Fusion in the Reaction 1.8-MeV p + ^{238}U

A. Ghiorso, L.P. Somerville, and S. Yashita

Ajitanand *et al.*[1] reported cross sections for the fusion of 1- to 2-MeV protons with ^{235}U and ^{238}U which were orders of magnitude larger than the predictions using the optical model. Using mica track detectors we established a cross-section upper limit of 5 picobarns for fission events or fusion in the reaction 1.8±0.2-MeV p + ^{238}U. This result is about two orders of magnitude lower than the measurement by Ajitanand *et al.* Our upper limit is, however, consistent with the optical model and with other fusion data, since it is above both the optical model calculation[1] and an extrapolation of the fusion cross sections at higher proton energies.[2,3]

Footnotes and References

1. N.N. Ajitanand, K.N. Iyengar, R.P. Anand, D.M. Nadkarni, and A.K. Mohanty, Phys. Rev. Lett. **58**, 1520 (1987).

2. V.N. Kononov, E.D. Poletaev, and P. P. D'yachenko, Yad. Fiz. **27**, 298 (1978) [Sov. J. Nucl. Phys. **27**, 162 (1978)].

3. J.R. Boyce, T.D. Howard, R. Bass, H.W. Newson, E.G. Bilpuch, F.O. Purser, and H.W. Schmitt, Phys. Rev. C **10**, 231 (1974).

Systematics of Target Fragment Mass Distributions in Intermediate and High Energy Nuclear Collisions*

W. Loveland,[†] *and G.T. Seaborg*

A summary of all data on target fragment mass distributions from the interaction of 8.5-14,5000 MeV/nucleon lighter heavy ions (C-Ne) with target nuclei ranging from Cu to U is presented. A universal scaling law for mass distributions[1] was shown to have limited validity due to the fundamentally different shapes of the isobaric yield distributions for medium A and high A target nuclei. The measured distributions at relativitistic projectile energies are in good agreement with the predictions of the intranuclear cascade (INC) model.[2] The measured distributions at intermediate energies are described adequately by a Boltzmann equation similar to that used in the INC calculation but with the specific inclusion of Pauli blocking.

Footnotes and References

*Condensed from Revue Romaine de Physique, **33**, 721 (1988).

†Department of Chemistry, Oregon State University, Corvallis, OR 97331

1. X. Campi, J. Desbois and E. Lipparini, Phys. Lett. **138B**, 353 (1984).

2. Y. Yariv and Z. Fraenkel, Phys. Rev. **C20**, 2227 (1979).

Unusual Behavior of Projectile Fragments Produced by the Interactions of Relativistic Ar Ions with Copper*

K. Aleklett,[†] *R. Brandt,*[‡] *G. Dersch,*[‡] *G. Feige,*[‡] *E.M. Friedlander, E. Ganssauge,*[§] *G. Hasse,*[‡] *D.C. Hoffman, J. Herrmann,*[**] *B.Judek,*[††] *W. Loveland,*[‡‡] *P.L. McGaughey,*[§§] *N.T. Porile,*[**] *W. Shulz,*[§] *and G.T. Seaborg*

Radiochemical activation techniques were used to study the behavior of projectile fragments formed in the interaction of 0.9 A and 1.8 GeV/nucleon ^{40}Ar ions within thick Cu-targets. Two identical 1 cm Cu-disks were irradiated with separations between the disks of 0, 10, and 20 cm, respectively. We observed an unusual behavior of the energetic secondaries produced in the interaction of 1.8 GeV/nucleon ^{40}Ar with copper but none in the experiment at the lower (0.9 GeV/nucleon) energy. Two effects were observed: a large value of the ratio of light target residue activity in the second disk relative to the first disk in the contact configuration, R_o, and a decrease in the activity ratio with increasing distance between the disks. Our calculations which were based on conventional physics and the available high-energy data fail to explain either effect. There are at least two possible explanations (or combinations thereof) based on new phenomena.

First, it is possible that energetic secondaries are abundantly emitted at wide angles, i.e., with very large transverse mommentum components. However, such secondaries were not seen in appreciable numbers in a related emulsion (though not entirely comparable) experiment and hence our calculations, if based on this experiment alone, fail to explain our observations.

Second, some unstable secondaries possess unusually large interaction cross sections (or at least large partial cross sections for the production of the light nuclear residues investigated here); then they "decay" in flight (i.e., revert to 1"normal" cross sections).

Experiments are in progress to determine whether the first interpretation is the correct one.

Footnotes and References

*Condensed from Phys. Rev. C **38**, 1658 (1988).

†The Studsvik Science Research Laboratory, S-61182 Nyköping, Sweden

‡Kernchemie, Philipps-Universität, D-3550 Marburg, Federal Republic of Germany

§Fachbereich Physik, Philipps-Universität, D-3550 Marburg, Federal Republic of Germany

**Department of Chemistry, Purdue University, West Lafayette, IN 47907

††High Energy Physics Section, National Research Council, Ottawa K1A0R6 Canada

‡‡Department of Chemistry, Oregon State University, Corvallis, OR 97331

§§Los Alamos National Laboratory, Los Alamos, NM 87545

Total Projectile Kinetic Energy Scaling in Energetic Nucleus-Nucleus Collisions*

W. Loveland,† Z. Xu,† C. Casey,† K. Aleklett,‡ J.D. Liljenzin,§ D. Lee and G.T. Seaborg

The target fragment production cross sections have been measured for the reaction of 150 Mev per nucleon ^{139}La with ^{197}Au. From these cross sections, the fragment isobaric yields were deduced. The resulting isobaric yield distribution is similar to that observed for ^{197}Au fragmentation induced by projectiles of the same total kinetic energy and unlike ^{197}Au fragmentation induced by roughly equivalent velocity ions. This apparent validity of total kinetic energy (TKE) scaling is the most dramatic demonstration of this idea to date.

To help understand these results, we did a series of numerical simulations of the reactions using the Yariv-Fraenkel intranuclear cascade (INC). The INC model reproduced the observed distributions satisfactorily. Further simulations showed the apparent validity of TKE scaling for the reactions studied to be due to a combination of two approximately cancelling effects. For collisions of two different projectiles of the same TKE with a given target nucleus at a given impact parameter, the collision of the larger projectile with the target nucleus leads to (a) more projectile nucleons being transferred (due to greater overlap) and (b) a lower excitation energy per transferred nucleon (due to the lower energy/nucleon of the larger projectile). Predictions were made that show TKE scaling is not generally valid for all collisions.

Footnotes and References

*Condensed from Phys. Rev. C **38**, 2094 (1988).

† Department of Chemistry, Oregon State University, Corvallis, OR 97331

‡ Studsvik Neutron Research Laboratory, S61182 Nyköping, Sweden

§ Department of Chemistry, University of Oslo, 0315 Oslo 3, Norway

The Role of Compound Nuclei in Intermediate-energy Heavy-ion Reactions*

L.G. Moretto and G.J. Wozniak

Intermediate-energy heavy-ion reactions have confronted us with a wealth of phenomena unmatched in the lower energy regime. The tidy picture of low-energy nuclear physics is framed by a few basic mechanisms. At one extreme we have direct reactions, involving a narrow subset of nuclear modes, typically single particle degrees of freedom. In between we have quasi-elastic and deep-inelastic reactions involving a much larger number of modes, both single particle and collective, and associated with a much more profound degree of relaxation. At the other extreme we have compound nucleus (CN) processes, in

which there is full relaxation of all the modes, and which are characterized by a complete decoupling between entrance and exit channels.

At intermediate energies this simple picture seems to disappear, drowned by a florid overgrowth of exit channels. To the untrained eye, such complexity can create irresistible images of new and exotic processes. For example, the variety and abundance of complex fragments produced in these reactions suggested mechanisms like the shattering of glass-like nuclei,[1] or the condensation of droplets out of a saturated nuclear vapor,[2] or the somewhat equivalent picture of a nuclear soup curdling simultaneously into many fragments.[3,4] Such images were, and perhaps still are, so powerful that they thrived on themselves rather than on experiment. The word "multifragmentation" became very popular despite the perplexing lack of evidence for truly multi-fragment exit channels. This exuberance, initially a welcome indicator of the vitality of our field, should be tempered by a more sober interpretation of the data.

Complexity is not synonymous with novelty! Caution should be used by assuring oneself that the complexity of the reactions under study is not due to the proliferation and overlapping of conventional processes made possible by the large available energy. More than ever, it is necessary to assess the "background" of conventional processes before a new theory is declared proven or a new mechanism prematurely discovered! In particular, one would be well advised to check how large is the CN contribution to the production of complex fragments, gamma rays and even pions. This is the main topic of this paper and we shall dwell on it at length.

At this juncture it may be useful to remark on a now widespread tendency to compare data directly with more or less "ab initio" calculations, like mean field theories with collision terms, etc. In our opinion this is at best not useful, and is at worst quite dangerous. If we had the "exact" theory describing heavy ion reactions on the basis of the nucleon-nucleon interaction, we would be able, by definition, to fit the data perfectly. In fact, a calculation on a computer would be equivalent to the corresponding experiment performed at an accelerator. However, if we do not understand the experiment, it is truly of little consequence to know that our calculation reproduces it correctly. What we would have proved is that the nucleon-nucleon interaction used in our calculation is adequate.

This underscores the need for empirical macroscopic categories which are solidly based upon experimental observations and which allow for a simple classification and quantitative assessment of the data over a broad range of experimental environments. The CN is one of such empirical categories that has proven its usefulness at low energies and, in our belief, is still an extremely useful concept at intermediate energies. An "ab initio" calculation could very well go through a "compound nucleus" stage unbeknownst to us and to itself. And yet the empirical verification of whether a CN is involved or not is most relevant to our understanding.

As a final remark, in the complex and confusing experimental environment characteristic of intermediate energies, it is profitable and often necessary to choose the reactions judiciously. A little ingenuity in such a choice may emphasize the process one intends to study and minimize the disturbing noise arising from "irrelevant" features of the reactions. For instance, efforts to limit the number of sources of complex fragments or to make their identification easier may be quite beneficial.

Footnotes and References

*Condensed from LBL-25322.

1. J. Aichelin and J. Hüfner, Phys. Lett. 136B, 15 (1984)

2. J.E. Finn *et al.*, Phys. Rev. Lett. **49**, 1321 (1982)

3. D.H.E. Gross *et al.*, Z. Phys. **A309**, 41 (1982)

4. J.P. Bondorf *et al.*, Nucl. Phys. **A443**, 321 (1985)

Compound Nuclei, Binary Decay, and Multifragmentation in Intermediate-energy Heavy-ion Reactions*

L.G. Moretto and G.J. Wozniak

In recent experiments, we have been able to follow the evolution of complex fragment emission up to 100 MeV/nucleon in the reactions ^{139}La + ^{12}C, ^{27}Al. Coincidence data confirm the binary nature of the decay. The Z_1 - Z_2 scatter plots show the diagonal band characteristic of binary decay. The Z_1 - Z_2 correlation diagrams at 18, 50, 80, 100 MeV/nucleon are shown in Figs. 1 and 2. In the case of the ^{139}La + ^{12}C system, the correlation diagrams show the characteristic band of approximately constant $Z_1 + Z_2$ up to 100 MeV/nucleon. This band is very narrow at 18 MeV/nucleon and becomes progressively broader with increasing bombarding energy, but remains still quite distinct at 100 MeV/nucleon. The corresponding sum spectra show a peak that is progressively shifted downward from charge values near that of complete fusion and is correspondingly broadened. Presumably the downshift and the associated broadening arise from both incomplete fusion and sequential evaporation.

In the case of the ^{139}La + ^{27}Al system, the correlation diagrams show a distinct binary band up to 50 MeV/nucleon. At 80 and 100 MeV/nucleon, one observes a progressive filling of the low Z_1, Z_2 area, indicating that the binary correlation is progressively spoiled. The corresponding sum spectra show a reasonably sharp peak up to 50 MeV/nucleon, which broadens and extends towards the low charge region at the highest energies.

The general impression is that a progressively larger amount of excitation energy is brought into the systems with increasing bombarding energy, and that the energy deposited at the same bombarding energy is larger for the heavier target. At the lower energies, binary decay dominates and is progressively substituted by multifragment decay at the higher energies.

The evidence presented above is but a small sample of the evidence available for CN emission of complex fragments at bombarding energies up to 100 MeV/nucleon. We have seen that binary decay dominates the picture at the lower energies, while multifragmentation seems to set in at higher energies. Does that mean, automatically, that the role of the CN is over? Most likely not!

Footnotes and References

*Condensed from LBL-25631.

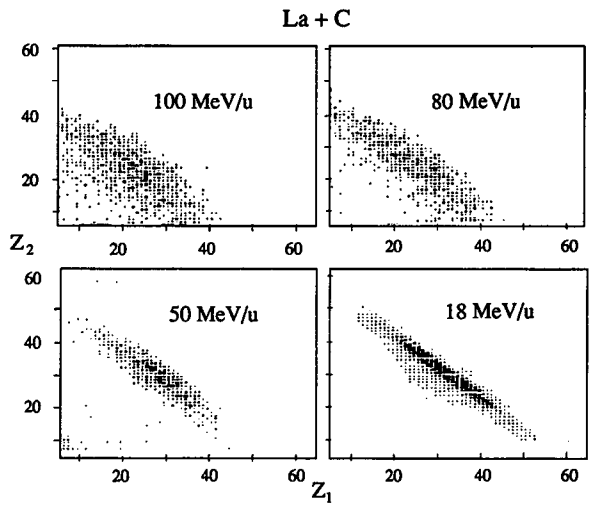

Fig. 1. $Z_1 - Z_2$ correlation diagrams for the reaction ^{139}La + ^{12}C from 18 to 100 MeV/nucleon.

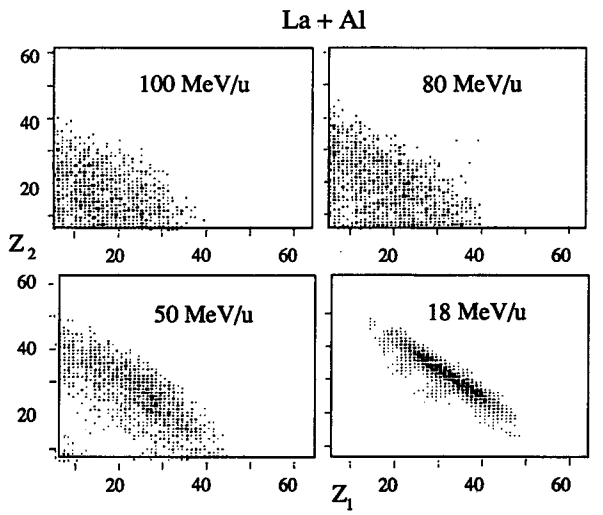

Fig. 2. Same as for Fig. 1 for the reaction ^{139}La + ^{27}Al.

The Role of Compound Nuclei in Complex Fragment Production, Multifragmentation and High Energy Gamma-ray Emission*

L.G. Moretto, M. Ashworth and G.J. Wozniak

The presence of compound nuclei in the exit channels of many intermediate energy reactions is reviewed. The statistical decay of such compound nuclei may be responsible for many of the observed features. The role of compound nuclei in complex fragment production, multifragmentation and high energy gamma-ray emission is illustrated.

Footnotes and References

*Condensed from LBL-24722

The Role of the Compound Nucleus in Complex Fragment Emission at Low and Intermediate Energies*

L.G. Moretto and G.J. Wozniak

The origin of complex fragments produced at low and intermediate energies is discussed and the leading theories as well as the experimental evidence are reviewed. Particular attention is focused on the compound nucleus formed in either complete or incomplete fusion as a possible source of complex fragments. Theoretical aspects of compound nucleus emission are reviewed in detail. The experimental demonstration of the existence of compound nucleus emission at extremely low energy is given and the process is followed by means of a series of reactions up to 50 MeV/nucleon.

These results allow one to conclude that, in the general class of reactions under investigation, complex fragments come either from statistical compound nucleus emission, or they are target and/or projectile-like fragments formed in quasi and deep inelastic reactions, or in incomplete fusion as spectators.

The multifragmentation process is discussed in terms of novel theories like liquid-vapor equilibrium, nuclear shattering, nuclear disassembly, etc. as well as in terms of established physics like the process of comminution resulting from the sequential emission of many fragments from an extremely excited compound nucleus. The origin of fragments at higher energies is also briefly considered.

Footnotes and References

*Condensed from Prog. in Part. and Nucl. Phys. **21**, 401 (1988).

Complex-Fragment Emission in 12.6 MeV/Nucleon ^{63}Cu Induced Reactions on ^{12}C and ^{27}Al Targets*

*H.Y. Han,† K.X. Jing,† E. Plagnol,‡ D.R. Bowman, R.J. Charity,§ L. Vinet,** G.J. Wozniak, and L.G. Moretto*

Complex fragments from the 12.6 MeV/nucleon ^{63}Cu + ^{12}C, ^{27}Al reactions were investigated. For both systems a projectile-like and/or a target-like component was observed along with an isotropic component. The isotropic component can be seen for many fragment Z-values in both reactions. Therefore, one can attempt to separate the isotropic from the anisotropic component in the angular distributions and obtain the angle-integrated cross section of both components. When the angular distributions are not isotropic, one can take a constant equal to the minimum value of $d\sigma/d\theta$ as an upper limit for the compound nucleus cross sections. These angle-integrated charge distributions are displayed in

Figs. 1 and 2.

The isotropic component from the $^{63}Cu + ^{12}C$ reaction shows the characteristic U-shaped pattern which we have now learned to associate with the decay of compound systems below the Businaro-Gallone point. For the $^{63}Cu + ^{27}Al$ system, the Z-distribution is much flatter. This flattening of the shape of the charge distribution is due to the larger excitation energy and angular momentum associated with the latter system. The yields of the isotropic component for the $^{63}Cu + ^{27}Al$ system are generally more than an order of magnitude larger than those for the $^{63}Cu + ^{12}C$ system. This large increase in yield is due both to the larger excitation energy and larger angular momentum available in the compound system formed in the $^{63}Cu + ^{27}Al$ reaction.

The predicted compound nucleus cross sections, of course, depend strongly on the energy dependent branching ratios between complex fragment emission and light particle emission. Consequently, the experimental absolute cross sections contain the strongest information regarding the mechanism of complex fragment emission. In order to verify the compound nucleus hypothesis we have fitted the data with the Monte Carlo code Gemini,[1] which, beside treating light fragment evaporation in a conventional way, specifically allows compound nuclei to decay by complex fragment emission. Every fragment produced in the decay is followed until all of the available excitation energy is exhausted.

Crucial ingredients of these calculations are the angular-momentum-dependent conditional barriers as a function of mass asymmetry. These barriers have been calculated with the finite range model developed by Sierk.[2] For the system $^{63}Cu + ^{12}C$, a maximum angular momentum of $\ell \cong 40\hbar$ is expected from the Bass model.[3,4] Consequently, the resulting charge distribution should be U-shaped, namely with a minimum at symmetry where the barriers are higher.

For the system $^{63}Cu + ^{27}Al$, the calculated[3] maximum angular momentum is $\ell \cong 71\hbar$, well above the Businaro-Gallone value. Therefore, a rather flat dis-

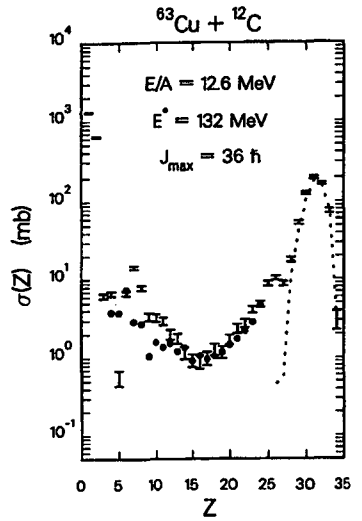

Fig. 1. Comparison of experimental and calculated charge distributions for the $^{63}Cu + ^{12}C$ reaction. The experimental data are indicated by the dots and the calculated values are shown by the error bars. The dashed line corresponds to the calculated yield of classical evaporation residues, which have not emitted a particle heavier than an alpha particle.

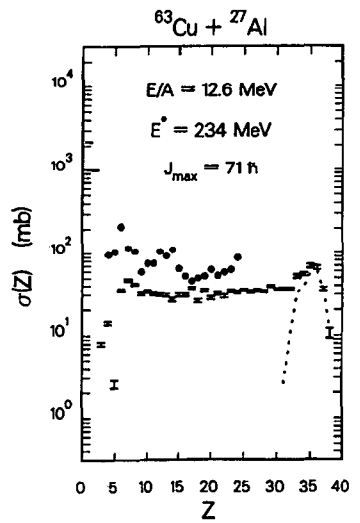

Fig. 2. Comparison of experimental and calculated charge distributions for the $^{63}Cu + ^{27}Al$ reaction (see Fig. 1).

tribution should be expected with the possibility of a weak minimum or peaking at symmetry depending on the relative contributions from the low and high partial waves to the cross section.

The only parameter used in fitting the data was the maximum angular momentum. The fit to the charge distribution for ^{63}Cu + ^{12}C system is shown in Fig. 1. The quality of the fit is acceptable, except for fluctuations in the lighter element cross sections partly due to poor Monte Carlo statistics, partly due to difficulties in handling sequential decay by the code. The extracted maximum angular momentum should correspond to the fusion cross section. The Bass model[3,4] predicts $\ell_{max} \cong 40\hbar$, while we obtain $\ell_{max} \cong 36\hbar$ from the fit to the data in good agreement with the prediction.

In the case of the ^{63}Cu + ^{27}Al reaction, one finds quite a different picture. It was possible to reproduce the shape but not the magnitude of the experimental data with $J_{max} < J_{crit}$. The calculations shown in Fig. 2 were obtained with $\ell_{max} \cong 71\hbar$ and significantly underestimate the experimental data. The Bass model[3,4] predicts $\ell_{max} \cong 71\hbar$. This implies, for the Cu + Al system, that most of the complex fragments are being produced in reactions with ℓ-waves of angular momentum greater than J_{crit}.

One should note that GEMINI predicts that the evaporation residues (dashed lines in Figs. 1 and 2) are the dominant fusion products in the ^{63}Cu + ^{12}C system, whereas the binary decay products are dominant fusion products for the ^{63}Cu + ^{27}Al system. As the compound nucleus is produced with larger excitation energy and angular momentum, the fusion yield appears as binary decay products.[5] At even larger energies and angular momentum, one might expect 3- and 4-body sequential decay products to be abundantly produced from compound nuclei.

Footnotes and References

*Condensed from Nucl. Phys. **A492**, 138 (1989)

†Institute of Atomic Energy, Beijing, China.

‡GANIL, B.P. 5027 - 14021 Caen Cedex, France.

§Gesellschaft für Schwerionenforschung, 6100 Darmstadt, West Germany

**CERN, Division EP, Ch-1211, Geneva 23, Switzerland.

1. R.J. Charity *et al.*, Nucl. Phys. **A483**, 371 (1988).
2. A.J. Sierk, Phys. Rev. **C33**, 2039 (1986).
3. R. Bass, Nucl. Phys. **A231**, 45 (1974).
4. R. Bass, Phys. Rev. Lett. **39**, 265 (1977).
5. E. Plagnol *et al.*, LBL-25742.

Emission of Complex Fragments From Highly Excited Systems Produced in ^{93}Nb + ^{9}Be and ^{27}Al Reactions at E/A = 25.4 and 30.3 MeV*

R.J. Charity, D.R. Bowman, Z.H. Liu,† R.J. McDonald, M.A. McMahan, G.J. Wozniak, L.G. Moretto, S. Bradley,‡ W.L. Kehoe,§ and A.C. Mignerey§

Complex fragments with atomic numbers intermediate between those of the target and projectile have been detected in the reverse-kinematics reactions of ^{93}Nb plus ^{9}Be and ^{27}Al at bombarding energies of E/A = 25.4 and 30.3 MeV. Experimental results from inclusive and coincidence measurements are presented and are used to characterize these fragments as the statistical, binary-decay products of highly excited compound nuclei formed in fusion-like reactions.

Footnotes and References

*Condensed from Nucl. Phys. **A476**, 516 (1988).

†Institute of Atomic Energy, Beijing, China

‡Kaman Sciences, 2560 Huntington Ave., Alexandria, VA 22303.

§Department of Chemistry, University of Maryland, College Park, Maryland, 20742.

Complex Fragments from Excited Actinide Nuclei: A New Test of the Finite Range Model*

D.G. Sarantities,† D.R. Bowman, G.J. Wozniak, R.J. Charity, Z.H. Liu,‡ R.J. McDonald, M.A. McMahan, and L.G. Moretto

Complex fragments ranging in charge from $7 \leq Z \leq 45$ have been detected in binary coincidence following the reaction of 8.4 MeV/nucleon ^{232}Th + ^{12}C, and are shown to arise from the binary decay of a ^{244}Cm compound nucleus. This work confirms earlier radiochemical observations of very light fragments in the fission fragment mass distribution, establishes their origin in a binary decay rather than in a ternary process as previously suggested, and interprets their yield in terms of finite range potential energy barriers.

Footnotes and References

*Condensed from Phys. Letters B **218**, 427 (1989).

†Department of Chemistry, Washington University, St. Louis, Missouri, 63130

‡Institute of Atomic Energy, Beijing, China.

Systematics of Complex Fragment Emission in Niobium Induced Reactions–1*

G.J. Wozniak, R.J. Charity, and L.G. Moretto

At low bombarding energies (<10 MeV/nucleon), the formation of compound nuclei (CN) in fusion reactions and their sequential statistical decay have been extensively studied. Two commonly observed decay modes of the CN are the evaporation of light particles and fission. These modes are just two extremes of a more general binary decay mode[1] involving the entire range of mass asymmetry. Compound nucleus decay at intermediate asymmetries has been shown to give rise to complex fragments, though at low bombarding energies such binary decays are exceedingly rare.[2–4]

In general, the decay chain of a CN is associated with a number of sequential binary decays. The most common example of this is the formation of an evaporation residue by sequential emission of light particles. In the case of fission decay, the fission fragments themselves in turn may emit light fragments such as neutrons. Typically, in the latter case, the decay chain is associated with one near symmetric and a number of very asymmetric binary decays.

More recently, the concept of CN decay has been successfully applied to the intermediate energy regime (10–100 MeV/nucleon).[5–6] CN produced in fusion reactions, and at the higher bombarding energies in incomplete fusion reactions, are formed with very large temperatures and angular momenta. As a consequence, the intermediate asymmetry decay modes which are rare at the low bombarding energies, become of increasing importance. Recent studies have found that CN decay is an important mechanism for the production of complex fragments at bombarding energies up to at least E/A = 50 MeV.[6] These fragments were shown to be produced in a fission-like decay where only one binary division in the decay chain is not a light particle evaporation.

For these reasons, complex fragment emission from the reactions Nb + Be, C, and Al at bombarding energies of E/A = 11.4, 14.7, and 18.0 MeV have been investigated. These experiments, in conjunction with previous studies of the same reactions at higher (E/A= 25.4 and 30.3 MeV) and lower (E/A = 8.4 MeV) bombarding energies, allow one to observe the evolution of complex fragment emission from the low to the intermediate energy regime.

Footnotes and References

*Condensed from LBL-24737, Proceedings of the

Texas A&M University Symposium on Hot Nuclei, College Station, TX, Dec. 7-10, 1987.

1. Moretto, L.G., Nucl. Phys. **A247**, 211 (1975)

2. Sobotka, L.G., *et al.*, Phys. Rev. Lett. **51**, 2187 (1983)

3. Sobotka, L.G., *et al.*, Phys. Rev. Lett. **53**, 2004 (1984)

4. McMahan, M.A., *et al.*, Phys. Rev. Lett. **54**, 1995 (1985)

5. Charity, R.J., *et al.*, Nucl. Phys. **A476**, 516 (1988)

6. Bowman, D.R., *et al.*, Phys. Lett. **B189**, 282 (1987)

Systematics of Complex Fragment Emission in Niobium-Induced Reactions–2*

R.J. Charity,† M.A. McMahan, G.J. Wozniak, R.J. McDonald, L.G. Moretto, D.G. Sarantites,‡ L.G. Sobotka,‡ G. Guarino,§ A. Pantaleo,§ L. Fiore,§ A. Gobbi,† and K.D. Hildenbrand†

Complex fragments of $3 < Z < 35$ have been detected in the reverse-kinematics reactions of ^{93}Nb plus ^{9}Be, ^{12}C and ^{27}Al at bombarding energies of E/A = 11.4, 14.7 and 18.0 MeV. Velocity spectra and angular distributions show the presence of projectile and target-like components along with a component isotropic in the reaction plane. This latter component appears as a Coulomb ring in the invariant cross section plots indicating the presence of a binary decay which is confirmed by the coincidence data. Statistical model calculations indicate that for the Nb + Be and C reactions, the isotropic component is associated with the binary decay of compound nuclei formed in complete fusion reactions. The charge distributions for these two systems are consistent with the conditional barriers predicted with the Rotating Finite Range Model. For the Nb + Al reactions, there is an additional isotropic component besides compound nucleus decay, which may arise from fast fission.

Footnotes and References

*Condensed from Nucl. Phys. **A483**, 371 (1988).

†Gesellschaft für Schwerionenforschung, 6100 Darmstadt, West Germany.

‡Chemistry Department, Washington University, St. Louis, MO, 63110 USA.

§Istituto Nazionale di Fisica Nucleare INFN, Sezione di Bari, Italy.

The Categorical Space of Fission*

L.G. Moretto and G.J. Wozniak

Early history and traditional views

To the deceptively simple question "What is fission?" the uncautious interviewer will obtain more of an answer than he bargained for. This is because fission has many shifting facets and corners and its definition changes with the space and time cross section of the scientists to whom the question is addressed.

Before 1939, fission was still in imaginary space. It emerged into an altogether too real world by virtue of two chemists who dared thinking the unthinkable. It was much more obvious to assume, as did Fermi, that the activities produced by neutrons on uranium were due to transuranium elements! So we can well imagine his surprise and mixed feelings when he realized he had been working with fission all along, much like Molière's character who discovers with perplexity and a touch of awe that he has been speaking prose all of his life.

Even today a good number of our physics colleagues think of fission as a peculiar reaction occurring somewhere around uranium, a somewhat em-

barassing process that gave and still gives us a bad reputation; then with nuclear bombs, now with nuclear energy.

Even among "experts," fission is somehow associated with heavy elements. If its presence is acknowledged, as far down as the lead region and even lower, its existence becomes progressively more evanescent as one moves farther down the periodic table and its cross section becomes lost in the abyss of nanobarns.

Most emphatically, fission is believed to be a unique kind of compound nucleus reaction when compared with the more commonplace decays, like those involving the emission of protons, alphas and other "particles." A fission fragment is no "particle." It has nothing elementary about it, and its emission suggests the involvement of collective degrees of freedom not associated with neutron decay. Furthermore, its high kinetic energy and its mass, both so far removed from those of an evaporated light particle seem to underscore the uniqueness of this process. Fission appeared so different from the other modes of compound nucleus decay that a separate theory was devised to calculate its decay width. As a result, we now have one theory for "evaporation" and another for fission.

Yet, a typical mass distribution of fission fragments while peaked, at times sharply, at masses near the symmetric splitting, is nonetheless a continuous distribution for which there are no firm boundaries other than those set by the total mass of the system. In all fairness, the search for ever lighter (and heavier) fission products was actively pursued by radiochemists, who were eventually stopped only by the abysmally small cross sections. So the belief was consolidated that fission fragments were confined to a rather narrow range of masses, despite the occasional disturbing detection of intermediate mass fragments like Na, Si, etc. in higher energy reactions. With a curious twist of insight, these lighter fragments were at times attributed to ternary fission, rather than to a more obvious, highly asymmetric binary fission. But why should the fission mass distribution not extend all the way to alpha particles and protons?

The turbulent history of complex fragments

The advent of low energy heavy ions familiarized the nuclear community with products of deep inelastic reactions ranging throughout the periodic table. While, in many ways, deep inelastic reactions do remind us of fission, the obvious genetic relationship of these products with either target or projectile keeps these processes more or less within the categorical boundaries of "direct reactions."

Complex fragments made their grand entrance with intermediate-energy heavy ion reactions. In these processes, the elegant simplicity of quasi and deep inelastic processes is substituted by a glorious mess of products that seem to bear no relationship to either of the entrance channel partners. Their glaringly abundant production, together with the turbid experimental environment prevailing in early studies, prompted a tumultuous development of theories, claims and counterclaims about their origin and manner of production.

To the still untrained eye, such a complexity created irresistible images of new and exotic processes. For instance, the broad mass range and abundance of these fragments suggested mechanisms like the shattering of glass-like nuclei or the condensation of droplets out of a saturated nuclear vapor, or the somewhat equivalent picture of a nuclear soup curding simultaneously into many fragments. Such images were, and perhaps still are, so powerful that they thrived on themselves rather than on experiment.

Fortunately, in spite of the confusion, it did not escape some perceptive members of our community that most, if not all of the complex fragments were associated with essentially binary processes. Furthermore, after an allowance was made for target and projectile-like fragments, the remaining fragments appeared to originate from the binary decay of an isotropic source. Finally, the excitation functions of these fragments appeared to behave in accordance with compound nucleus branching ratios. The inescapable conclusion was that compound nucleus decay was responsible for the production of these frag-

ments by a mechanism able to feed all the possible asymmetries. The name that comes to mind as the most appropriate for this process is, of course, fission.

Fission, fission everywhere.....

This evidence, which continues to grow by the day, demonstrates the very pervasive presence of statistical complex fragment emission throughout the periodic table, at low and high excitation energies, covering the entire range of asymmetries, though not with equal intensity. In fact, the observed modulation of the mass distribution is a most revealing signature of the underlying potential energy as a function of mass asymmetry and underscores the essential unity of these processes.

Here one has the key for the unification of all compound nucleus decays into a single process. The natural connection between all these modes of decay is the mass asymmetry coordinate. Typical light particle evaporation (n, p, alpha, etc.) corresponds to very asymmetric decays, while "fission" of heavy systems corresponds to a very symmetric decay. The lack of emission at intermediate asymmetries is only apparent. Such an emission does in fact occur, albeit very rarely at low energies. The rarity of this occurrence is due to the important but accidental fact of the high potential barriers associated with the emission. A suitable increase of the excitation energy, or the lowering of the barriers by an increase in the angular momentum readily increases the cross section of these intermediate mass fragments to an easy level of detection.

Similarly the apparent lack of "fission" in lighter systems suggested by the absence of a symmetric fission peak in the mass distribution is another manifestation of the underlying potential energy that forces the mass distribution to assume a characteristic U shape. Consequently, in spite of the variety of mass distributions brought about by the different dependence of the potential energy on the mass asymmetry, we are confronted with a single process responsible for the production of the whole range of masses from the decay of compound nuclei throughout the periodic table (with the notable exception of gamma ray and meson emission). This process, with a minimal generalization of the term might well be called "fission."

In this way we have reached a very remarkable conclusion. Fission, rather than being a peculiar process relegated to the upper reaches of the periodic table and to a remote area of nuclear physics cultivated by oddball scientists, surprisingly turns out to be the most general, all-pervasive reaction in compound nucleus physics. If anything, it is the standard evaporation that should be regarded as a peculiar limiting case of very asymmetric fission... Like the ghost of Hamlet's father, fission is *hic et ubique* – here, there and everywhere.

Footnotes and References

*Condensed from LBL-25744.

EC-Delayed Fission Properties of ^{232}Am

H.L. Hall, R.A. Henderson, C.M. Gannett, J.D. Leyba, K.R. Czerwinski, K.E. Gregorich, D.M. Lee, M.J. Nurmia, D.C. Hoffman, C.E.A. Palmer, and P.A. Baisden**

The study of the neutron deficient actinide isotopes is of interest for several reasons. Delayed fission processes, which are important to astrophysical models of the r–process,[1] should become an observable decay mode as one moves away from the line of β–stability. EC–delayed fission also provides a method for indirectly investigating the shape of the fission barrier in this region.[2] Such data are needed to refine theoretical predictions of the fission characteristics of heavier nuclei and to further our understanding of shell-stabilized fission barriers.

However, delayed fission processes have been reported in only a few systems. Beta–delayed fission has been reported to occur in ^{236}Pa and ^{238}Pa,[3] al-

though a recent investigation using chemical separations failed to confirm the result for ^{238}Pa[4] and hence casts doubt on the result for ^{236}Pa as well. We have observed β-delayed fission in the decay of ^{256m}Es to ^{256}Fm.[5] EC-delayed fission has been reported in the light Am and Np isotopes,[6,7] and ^{232}Am has been reported by Habs *et al.*[8] to to have a delayed fission branch of 1.3% of total decay.

Since the delayed fission probability of ^{232}Am was measured by ref. 8 be quite large, we undertook to produce this isotope so that we could study its fission decay properties. ^{232}Am was produced at the LBL 88-Inch Cyclotron via the ^{237}Np(α,9n)^{232}Am reaction channel, using 103-MeV α particles. The α beam passed through a vacuum window into our recoil chamber where it impinged on a stack of 10 ^{237}Np targets. These foils were held in the LIM target system[9] which allowed KCl–laden helium to sweep out the recoiling reaction products. These recoils were transported about five meters via capillary to our MG-RAGS system. The reaction products, attached to KCl aerosols, were collected on thin (~40 μg/cm^2) polypropylene foils on the periphery of an 80 position wheel. The samples were stepped sequentially between six pairs of silicon surface-barrier detectors. Alpha particles and fission events were pulse-height analyzed and this data was stored in event-by-event mode on magnetic tape for later analysis.

2201 coincident fission pairs were observed in the course of the experiment. From these events, the fission total kinetic energy (TKE) and mass-yield distribution were determined. This is the first measurement of these properties for any delayed-fissile nucleus. The TKE was found to be symmetric and centered at ~175 MeV with a full-width at half-maximum of roughly 40 MeV. The mass-yield distribution was highly asymmetric, peaking at ~100 MeV and ~130 MeV with a peak-to-valley ratio of ~2.3. These results are shown in Fig. 1.

We were also able to determine the half life more precisely than either the experiment by ref. 8 or the discovery experiment,[6] respectively. The value we obtained is (78.6±2.4) seconds, much closer to Kuznetsov's discovery experiment than that of Habs. The decay curve is shown in Fig. 2.

Footnotes and References

*LLNL Nuclear Chemistry Division, Inorganic Chemistry Group

1. H.V. Klapdor, T. Oda, J. Metzinger, W. Hillebrandt, and F.K. Thielmann, Z. Physik A **299**, 213–229 (1981).

2. H.V. Klapdor, C.-O. Wene, I.N. Isosimov, and Yu.W. Naumow, Z. Physik A **292**, 249–255 (1979).

3. Yu. P. Gangrskii, G.M. Marinescu, M.B. Miller, V.N. Samosyuk, and I.F. Kharisov, Sov. J. Nucl. Phys. **27(4)**, 475–478 (1978).

4. A. Baas–May, J.V. Kratz, and N. Trautmann, Z. Physik A **322**, 457–462 (1985).

5. H.L. Hall, R.A. Henderson, K.E. Gregorich, D.M. Lee, D.C. Hoffman, M.E. Bunker, M.M. Fowler, P. Lysaght, J.W. Starner, and J.B. Wilhelmy, Phys. Rev. C **39**, 1866 (1989).

6. V.I. Kuznetsov, N.K. Skobelev, and G.N. Flerov, Sov. J. Nucl. Phys. **5**, 191 (1967).

7. N.K. Skobelev, Sov. J. Nucl. Phys. **15**, 249 (1972).

8. D. Habs, H. Klewe-Nebenius, V. Metag, B. Neumann and H.J. Sprecht, Z. Physik A **285**, 53–57 (1978).

9. H.L. Hall, M.J. Nurmia, and D.C. Hoffman, Nucl. Inst. Meth. A **276**, 649 (1989).

Am-232 Delayed Fission

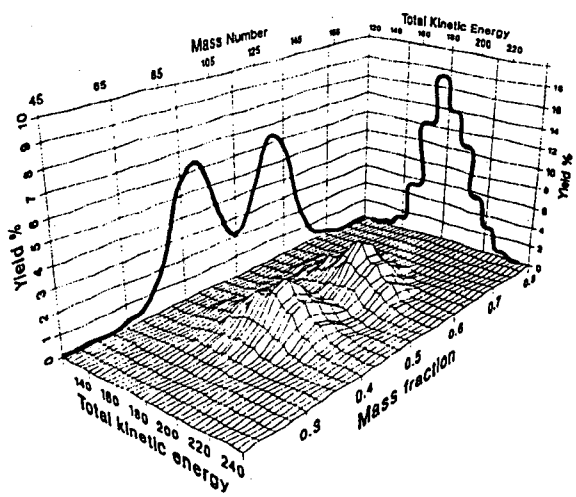

Fig. 1. See text.

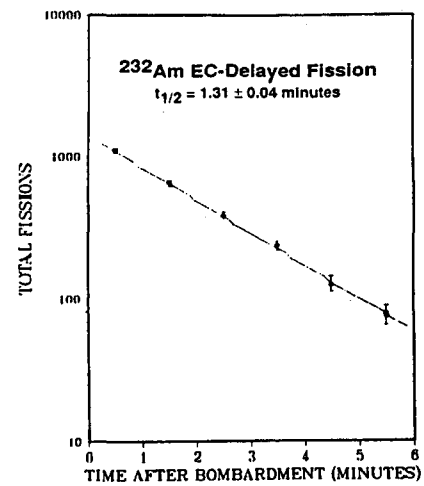

Fig. 2. See text.

Hard Photons in Heavy-Ion Collisions: Direct or Statistical?*

*N. Herrmann,† R. Bock,† P. Braun-Munzinger,†† H. Emling,† R. Freifelder,† M. Gnirs,** A. Gobbi,† E. Grosse,† K.D. Hildenbrand,† W. Kühn,§ R. Kulessa,† T. Matulewicz,† P.R. Maurenzig,‡ V. Metag,§ R. Novotny,§ A. Olmi,‡ D. Pelte,** R. Rami,† R.S. Simon,† A.A. Stefanini,‡ H. Stelzer,† J. Wessels,† and L.G. Moretto*

Photons with energies from 2 to 60 MeV have been measured in coincidence with binary fragments in the reaction ^{92}Mo + ^{92}Mo at an incident energy of 19.5 A MeV. The rapid change of the γ-ray spectrum and multiplicity with the fragment total kinetic energy in the exit channel indicates that the γ rays are emitted statistically by the highly excited fragments. Temperatures as high as 6 MeV are inferred.

Footnotes and References

*Condensed from Phys. Rev. Letters 60, 1630 (1988).

†Gesellschaft für Schwerionenforschung, Darmstadt, West Germany.

‡Università di Firenze and Instituto Nazionale di Fisica Nucleare, Florence, Italy.

§Physikalisches Institut, Universität Giessen, Giessen, West Germany.

**Physikalisches Institut, Universität Heidelberg, Heidelberg, West Germany.

††Department of Physics, State University of New York at Stony Brook, New York, 11794.

β-Delayed Fission from ^{256m}Es and the Level Scheme of ^{256}Fm*

H.L. Hall, K. E. Gregorich, R.A. Henderson, D.M. Lee, D.C. Hoffman,
M.E. Bunker,† M.M. Fowler,† P. Lysaght,† J.W. Starner,† J.B. Wilhelmy†

The 7.6-h isotope ^{256m}Es was produced from a 2.5-μg/cm^{2}target of ^{254}Es by the (t,p) reaction. The reaction products were separated radiochemically, and the decay properties of ^{256m}Es were determined via β-γ, γ-γ, and β-fission correlation techniques. From these measurements we were able to assign 57 γ-rays to 26 levels in the daughter ^{256}Fm. An isomeric level was observed at 1425 keV and assigned a spin and parity of 7^-. This level has a $t_{1/2}$ of (70 ± 5) ns and we observed two β-delayed fissions with delay times in the proper time range to be associated with fission from this level. This gives a β–delayed fission probability of 2×10^{-5} for this level and a partial fission half-life of $0.8^{+8.8}_{-0.7}$ ms at the 95% confidence level. The level scheme is shown in Fig. 1.

Footnotes and References

*Condensed from Phys. Rev. C **39**, 1866 (1989)

†Isotope and Nuclear Chemistry Division, Los Alamos National Laboratory

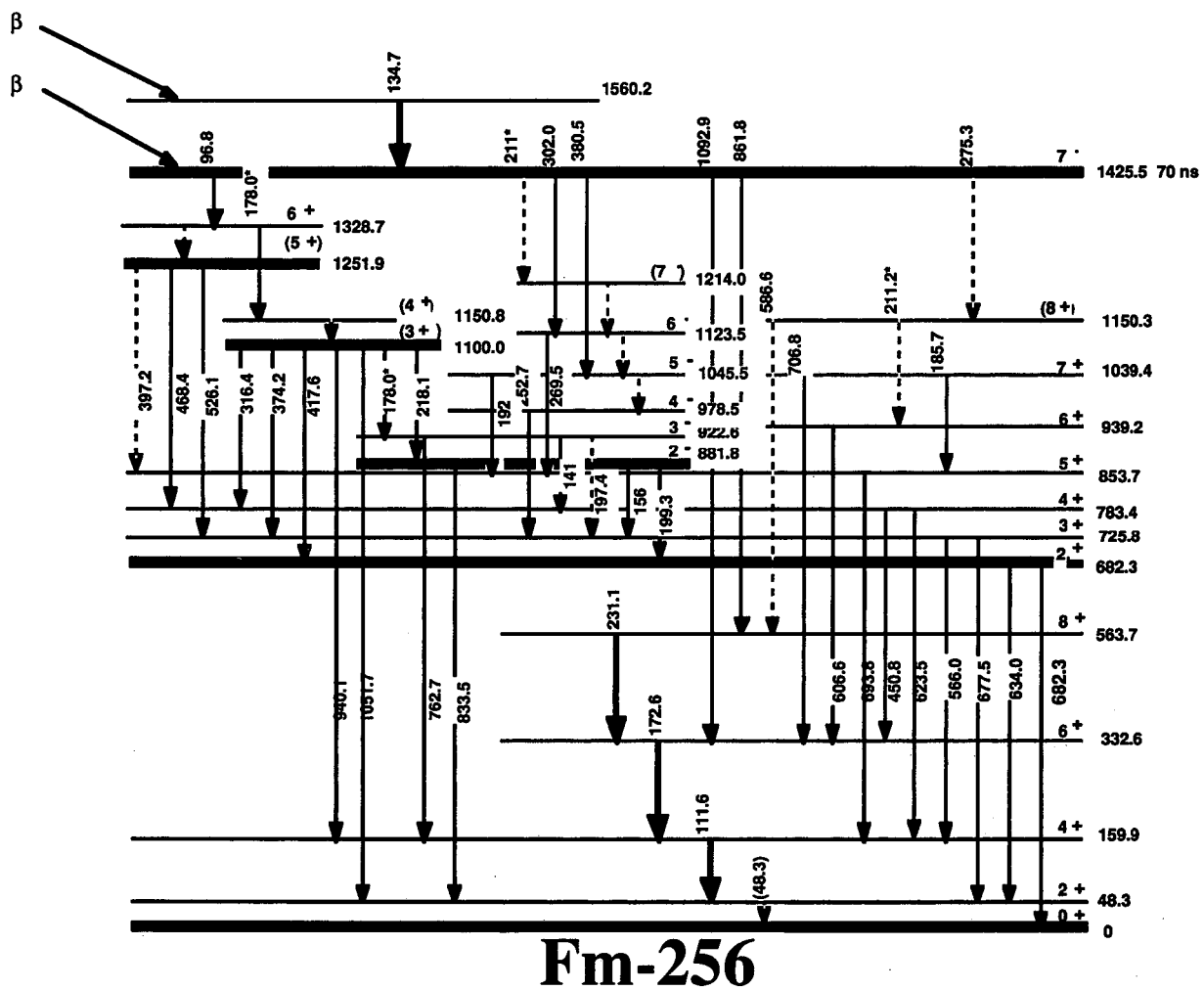

Fig. 1. Proposed level scheme for ^{256}Fm Transitions placed in the scheme more than once are marked with an asterisk. Bandhead levels are indicated by bold lines.

New Mode of Radioactive Decay: Si and Mg Emission from ^{238}Pu

Shicheng Wang,† D. Snowden-Ifft,† K.J. Moody,‡ E.K. Hulet,‡ and P.B. Price†

In addition to its two known hadronic decay modes – alpha decay (half- life 88 yr) and spontaneous fission (5×10^{10} yr) – we have found that ^{238}Pu also decays by emission of a Mg nucleus ($\sim 2 \times 10^{18}$ yr) and by emission of a Si nucleus ($\sim 6 \times 10^{17}$ yr). This extends to four (the other two being ^{14}C emission and Ne emission) the number of known modes of decay by emission of a fragment of mass between that of an alpha particle and that resulting from fission. The branching ratios relative to alpha decay are the lowest yet observed: $\sim 6 \times 10^{-17}$ for Mg emission and 1.4×10^{-16} for Si emission. Fig. 1 from the paper (see below) shows the identification of fragments emitted from ^{238}Pu as Mg, Si, and fissions (FF). Each symbol designates a specific event. The curves are based on calibrations obtained with ^{28}Si, ^{24}Mg, and ^{20}Ne ions at the SuperHilac.

Footnotes and References

*Condensed from Phys. Rev. C Rapid Communications.

†Physics Department, University of California at Berkeley

‡Nuclear Chemistry Division, University of California, Lawrence Livermore National Laboratory, Livermore, CA 94551

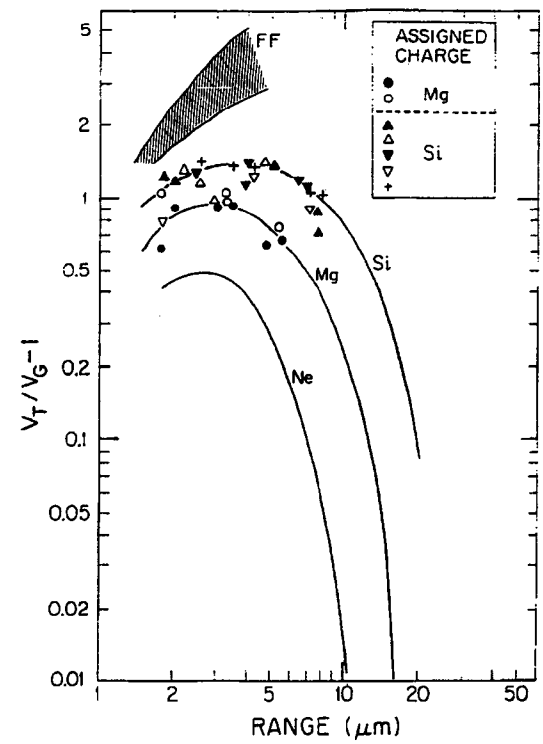

Fig. 1. Identification of fragments emitted from ^{238}Pu as Mg, Si, and fissions (FF). Each symbol designates a specific event. The curves are based on calibrations obtained with ^{28}Si, ^{24}Mg, and ^{20}Ne ions at the LBL SuperHilac.

Limits on Contribution of Cosmic Nuclearites to Galactic Dark Matter*

P.B. Price

Negative results of searches for tracks of magnetic monopoles in subsurface mica crystals and mountaintop arrays of plastic detectors, and of searches for tracks of ultraheavy cosmic rays in plastic detectors in the Skylab spacecraft, allow one to rule out nuclearites of strange matter, in the mass interval 10^{-16}g to 10^{2}g, as the source of the dark matter in our Galaxy.

Footnotes and References

*Condensed from Phys. Rev. D.

Further Analysis of Heavy Fragment Radioactivity of ^{234}U*

K.J. Moody,† E.K. Hulet,† Shicheng Wang,‡ and P.B. Price‡

In ref. 1, we reported the detection of three events in which ^{234}U decayed via Mg emission and 14 events in which it decayed via Ne emission. In a new experiment with nearly a factor ten greater collecting power we have detected 36 Mg fragments and 108 Ne fragments and have made a more accurate determination of the branching ratios relative to alpha decay, taking into account zenith-angle-dependent detection efficiency. The result is log B(Ne/α) = -12.36±0.05 and log B(Mg/α) = -12.86±0.08. Fig. 1 from ref. 1 shows the species distribution. Each event corresponds to the average of two data points made at two residual ranges.

Footnotes and References

*Condensed from Phys. Rev. C Brief Reports.

†Nuclear Chemistry Division, Lawrence Livermore National Laboratory Livermore, CA 94551

‡Physics Department, University of California at Berkeley

1. Phys. Rev. C Rapid Comm. **36**, 2717 (1987)

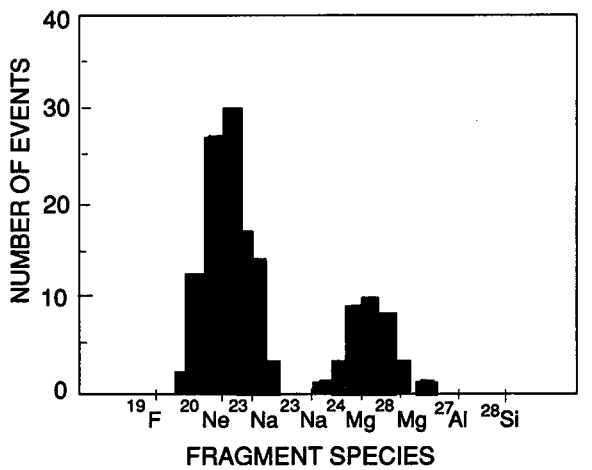

Fig. 1. Measured species distribution. Each event in this figure corresponds to the average of two data points made at two residual ranges.

Where Has All The Fusion Gone...?*

*E. Plagnol,† L. Vinet,‡ D.R. Bowman, Y.D. Chan, R.J. Charity,§ E. Chavez,** S.B. Gazes,†† H. Han,‡‡ W.L. Kehoe,§§ M.A. McMahan, L.G. Moretto, R.G. Stokstad, G.J. Wozniak, G. Auger****

At low excitation energies, the decay of compound nuclei proceeds mainly through a limited number of well defined channels: light particle evaporation, γ rays, and, for heavy nuclei, fission. This is well understood in terms of compound nucleus theory in which the dominant channels are those whose barriers are most comparable to the nuclear temperature. Nuclei can now be produced with much higher excitation energies, and compound nucleus theory indicates that a great variety of channels, ranging from symmetric fission to light fragment evaporation, should open up and compete effectively with the more traditional channels.[1,2] Consequently, at high enough excitation energies or angular momenta a significant amount of the fusion cross section should be associated with "complex fragments" produced in the decay of the compound nucleus or its products. This has been observed in experiments[3–7] for relatively heavy systems, where all the mass asymmetries ranging from light particle emission to symmetric splitting of the compound nucleus are represented.

In light systems the evaluation of fusion cross sections has been made traditionally by measuring the "evaporation residue cross section." A substantial onset of (statistical) binary decay in competition with the evaporation residue cross section may create an apparent disappearance of the fusion cross section with increasing bombarding energy. Conse-

quently, it seems important to determine systematically the cross sections for 1) evaporation residues; 2) isotropic (or compound nucleus-like) binary products; 3) non isotropic binary (quasi-elastic or deep inelastic) products. This separation of the cross section is a prerequisite to any attempt to interpret the reaction mechanism.

A series of experiments were performed at the 88-Inch Cyclotron on the ^{40}Ar + ^{12}C and the ^{40}Ar + ^{27}Al systems at 19.7 MeV/nucleon. In the case of complete fusion, the compound nuclei formed in these reactions are ^{52}Cr and ^{67}Ga with excitation energies of 200 and 340 MeV, respectively. Large differences in the excitation energy and angular momentum of the fusion products are expected and suggest possible dramatic differences in the role of binary decay in the two systems.

In order to have a "global" picture of these reactions, the experiments were designed to detect both the fusion residues resulting from the evaporation of light particles ($Z \leq 2$) alone, as well as the products associated with the statistical emission of heavier fragments ($Z \geq 5$) from the compound nucleus.

The quantitative results from the decomposition of the isotropic components are shown in Fig. 1. The shaded areas correspond to the binary components while the white areas correspond to the evaporation residues. For both targets, one observes that the yield of binary decay is quite important in the intermediate Z region (6–12). However, for the ^{40}Ar + ^{12}C system the evaporation residue yield appears to be dominant at large Z values, while for the ^{40}Ar + ^{27}Al system, binary decay seems to dominate at all Z values. This result is quite striking and indicates that, at the higher excitation energies and angular momenta associated with the latter system, even the fragments with $Z \geq 16$ (ordinarily believed to arise from light particle evaporation) are also strongly populated by binary decay. A corollary of this conclusion is that residues produced by the evaporation of particles with $Z \leq 2$ may represent but a limited fraction of the overall fusion cross section.

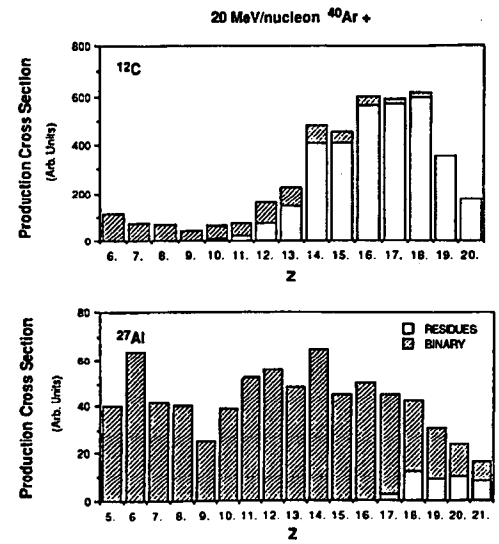

Fig. 1. Extracted yields of evaporation residues (white) and binary decay products (shaded) for the 20 MeV/nucleon ^{40}Ar + ^{12}C, ^{27}Al reactions. The excitation energies of the compound nuclei ^{52}Cr and ^{67}Ga are 200 and 340 MeV, respectively.

In conclusion, we have shown that both evaporation residues and binary decay products from fusion-like products are present in reactions of ^{40}Ar on ^{12}C and ^{27}Al at 19.7 MeV/nucleon. Evaporation residues dominate for the ^{40}Ar + ^{12}C system whereas binary products dominate for the ^{40}Ar + ^{27}Al system. For the latter system, the large excitation energy of the fusion-like products and higher angular momentum result in a very large probability for binary decay. Thus "standard" evaporation residues (produced by light particle emission ($Z \leq 2$) alone) are strongly depleted by the competing binary decay channels. This disappearance of evaporation residues should not be interpreted as the vanishing of fusion-like products. At even higher excitation energies, successive sequential binary decay of fusion-like products should lead to ternary and quaternary events.[2] Thus, the observation of three or four fragments at high energies may also be consistent with fusion-like processes.

Footnotes and References

*Condensed from LBL-25742.

†GANIL - B.P. 5027 - 14021 CAEN Cedex, France.

‡CERN, Division EP, Ch-1211, Geneva 23, Switzerland.

§Gesellschaft für Schwerionenforschung, 6100 Darmstadt, West Germany

**Instituto de Fisica UNAM, A.P. 20364, Mexico, 01000, D.F. Mexico

††Department of Physics, University of Rochester, Rochester, NY.

‡‡Institute of Atomic Energy, Beijing, China.

§§Department of Chemistry, University of Maryland, College Park, MD 20742

****Institut de Physique Nucléaire, B.P. No 1, 91406 Orsay, France.

1. L.G. Moretto, Nuclear Physics **A247**, 211 (1975)

2. L.G. Moretto and G.J. Wozniak, Prog. in Part. and Nucl. Phys. **21**, 401 (1988)

3. R.J. Charity *et al.*, Phys. Rev. Lett. **56**, 1354 (1986)

4. R.J. Charity *et al.*, Nucl. Phys. **A476** 516 (1988).

5. D.R. Bowman *et al.*, Phys. Lett. **189**, 282 (1987)

6. R.J. Charity *et al.*, Nucl. Phys. **A483**, 371 (1988)

7. F. Auger *et al.*, Phys. Rev. **35C**, 190 (1987).

Measurement of Interaction Cross Sections Using Isotope Beams of Be and B and Isospin Dependence of the Nuclear Radii

I. Tanihata, T. Kobayashi,† O. Yamakawa,† S. Shimoura,‡ K. Ekuni,‡ K. Sugimoto,§ N. Takahashi,** T. Shimoda,** and H. Sato††*

It was shown that nuclear radii can be determined from interaction cross sections of high-energy heavy-ion collisions.[1,2] In particular, the use of beams of radioactive nuclei provides a unique method for determining matter radii of unstable nuclei and enable us to make a direct comparison of radii between isobars. The isospin dependence of radii was difficult to study because, in most cases, only one stable isobar of the same mass number exists. In this report we present the isospin dependence of nuclear matter radii for isobars from mass numbers 6 to 12.

The secondary beams of radioactive isotopes ^{11}Be, ^{12}Be, ^{14}Be and ^{8}B, ^{12}B, ^{13}B, ^{14}B, and ^{15}B at 790 Mev/nucleon were produced through the projectile fragmentation of ^{20}Ne accelerated to 800 MeV/nucleon by the Bevalac. The interaction cross sections (σ_I) for these isotopes on Be, C, and Al targets were measured by a transmission experiment using a large acceptance spectrometer (HISS). The experimental procedures were the same as reported in the previous papers.[1,2]

Fig. 1 shows the effective RMS radii of nucleon distributions determined by assuming the harmonic oscillator model distribution as a function of neutron number (N). The radii of Li and Be isotopes depend similarly on N. It is seen that the majority of RMS radii of p-shell nuclei are almost constant(2.3–2.4 fm) except ones close to the neutron drip line. A large increase of the radii from ^{10}Be to ^{11}Be is observed, and a similar rate of increase is seen in ^{9}Li to ^{11}Li. The large size could be considered to be due to the large neutron halo in these nuclei (^{11}Be and ^{11}Li) because the separation energy of the last two neutrons is very small. In fact the model based on the neutron halo reproduces the relation between the separation energy of the last two neutrons and the observed radius in ^{11}Li4.

The effective RMS radii of nucleon distributions are plotted for isobars of mass number A= 6,7,8,9,11, and 12 in Fig. 2. A pair of nuclei with the same isospin (T) but different T_z, ^{7}Li-^{7}Be or ^{8}Li-^{8}Be, show equal radii. It suggests that the Coulomb effect on the radii is negligible for these light nuclei. On the other hand, a nucleus with large isospin shows a larger radius except for A=9 isobars. The isospin dependences of isobar radii thus obtained are compared with predictions of the droplet model and Hartree-Fock model calculations.

Comparisons of the data with Hartree-Fock calculations suggest that the density dependent force in

effective nuclear interactions is important to explain the isospin dependence of the nuclear radii.

Footnotes and References

*RIKEN, Wako, Saitama 351-01, Japan

†KEK, Tsukuba, Ibaraki 305, Japan

‡Faculty of Science, Kyoto University, Kyoto 606, Japan

§Faculty of Science, Osaka University, Toyonaka, Osaka 560, Japan

**College of General Education, Osaka University, Toyonaka, Osaka 560, Japan

††INS, University of Tokyo, Tanashi, Tokyo 188, Japan

1. I. Tanihata *et al.*, Phys. Lett. B160, 380 (1985)

2. I. Tanihata *et al*, Phys. Rev. Lett. 55, 2676 (1985)

3. R.B. Elton, Nuclear sizes (Oxford U.P., Oxford, 1961) pp. 21,22.

4. P.G. Hansen and B. Jonsen, Europhys. Lett. 4, 409 (1987)

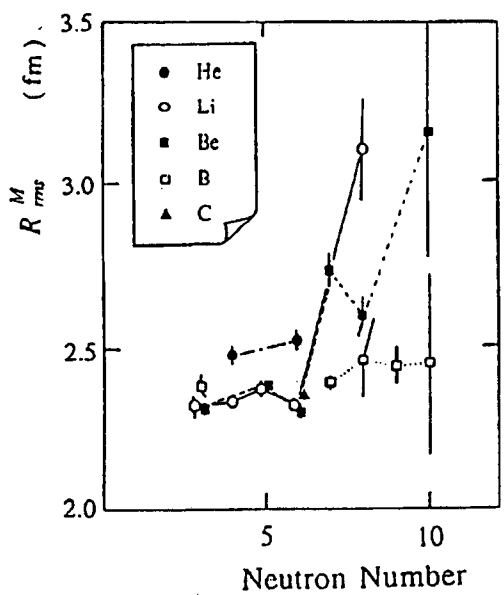

Fig. 1. The effective root-mean-square radii of nucleon distributions (RMRMS) determined by the interaction cross section measurements. Lines in the figure are only for guiding the eye. Considerable increase of radii are seen in nuclei far from the stability line.

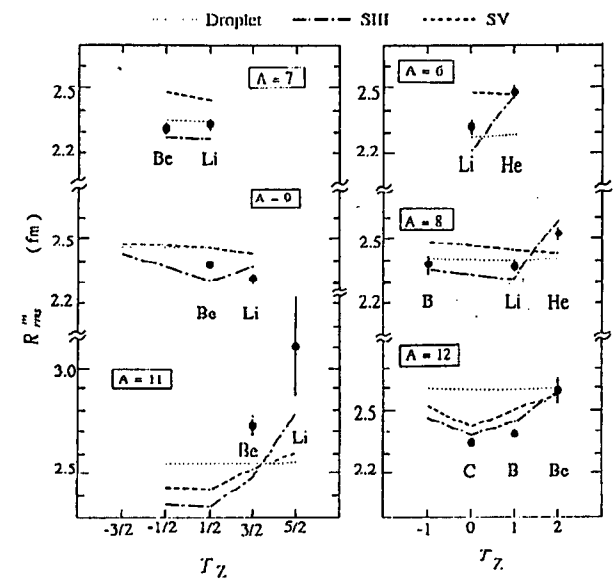

Fig. 2. Isospin dependence of the effective root-mean-square radii of nucleon distributions. Experimental values are shown by the solid circle. Dotted lines show RMS radii of nucleon distributions predicted by the droplet model calculations. Predictions of the Hartree-Fock calculations with Skyrme potentials are shown by the dash-dotted line (for the SIII potential) and by the dashed line (for SV).

Energy Dependence of Fragment Flow in High Energy Nuclear Collisions*

*H.Å. Gustafsson,† H.H. Gutbrod,‡,§ J. Harris, B.V. Jacak,** K.H. Kampert,††*
B. Kolb,‡ A.M. Poskanzer, H.G. Ritter, and H.R. Schmidt‡,§

Collective flow of light particles (Z = 1, 2) was measured as a function of multiplicity and beam energy for collisions of Ca+Ca, Nb+Nb and Au+Au with the Plastic Ball detector at the Bevalac. The multiplicity dependence shows the directed flow peaking at intermediate multiplicity events, i.e. between the third and fourth multiplicity bins. The mean value of the flow in these two multiplicity bins is shown in Fig. 1 as a function of the beam energy for all systems investigated. The flow increases monotonically with increasing beam energy; rather rapidly up to about 400 MeV per nucleon and leveling off at the highest bombarding energies. If in Fig. 1 the impact parameter averaged flow would have been plotted, then one would have found a slight fall-off at beam energies above 650 MeV per nucleon, as reported in ref. 1. This difference is mainly due to the dominant contribution of peripheral reactions which in fact show a weaker flow effect at bombarding energies higher than 650 MeV per nucleon. Thus the largest directed flow reached in semi-central collisions has been found to increase with bombarding energy, with projectile-target mass, and with fragment mass.

Footnotes and References

*Condensed from Mod. Phys. Letters **A3**, 1323 (1988).

†University of Lund, Lund, Sweden

‡Gesellschaft für Schwerionenforschung, D-6100 Darmstadt, West Germany

§Present address: CERN, EP-Division, CH-1211 Geneva 23, Switzerland

**Los Alamos National Laboratory, Los Alamos, New Mexico 87545

††Institut fur Kernphysik, D-4400 Munster, West Germany

1. Collective Flow Observed in Relativistic Nuclear Collisions H.Å. Gustafsson, H.H. Gutbrod, B. Kolb, H. Löhner, B. Ludewigt, A.M. Poskanzer, T. Renner, H. Riedesel, H.G. Ritter, A. Warwick, F. Weik, H. Wieman, Phys. Rev. Lett. 52, 1590 (1984).

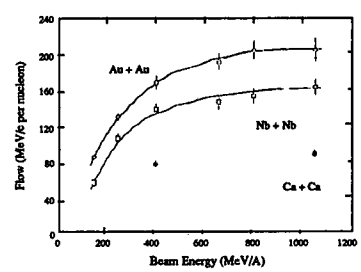

Fig. 1. Flow of semi-central collisions ($50\% \leq N_p/N_p^{max} < 100\%$) as a function of beam energy.

A New Component of the Collective Flow in Relativistic Heavy-Ion Collisions*

H.H.Gutbrod,† K.H.Kampert,‡ B.W.Kolb,† A.M.Poskanzer,
H.G.Ritter, and H.R.Schmidt†

The reaction Au+Au at 400 MeV/nucleon is analyzed in the coordinate system given by the principal axes of the kinetic energy flow ellipsoid. In addition to the previously observed side-splash and bounce-off we find a pronounced component perpendicular to the reaction plane at mid-rapidity both in position and momentum space.

This anisotropy in ϕ'' corresponds to an elliptical distribution of the particles in the x''-y'' plane. Fig. 1 shows the multiplicity dependence of the aspect ratio R''_y/R''_x (filled squares). First, the anisotropy in-

creases with multiplicity, reaches a maximum and then decreases with multiplicity. (In the limit of an impact parameter b = 0 symmetry requires that the ratios become equal to one.) In addition to the particle density, the same analysis can be done for the momenta per nucleon of the emitted particles. As can be seen from the second curve (open squares) in Fig. 1, we find that not only are there more particles in the squeeze-out region, but that they have more momentum per nucleon.

Footnotes and References

*Condensed from Phys. Lett. **B26**, 267 (1989).

†Gesellschaft für Schwerionenforschung, Darmstadt, West Germany

‡University of Munster, Munster, West Germany

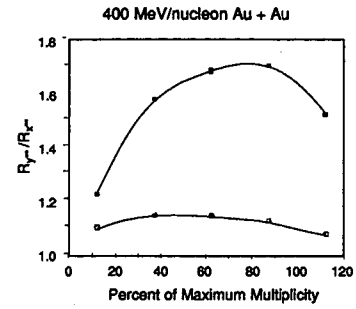

Fig. 1. Aspect ratio of an ellipsis describing the distribution of particles (filled squares) and the momentum per nucleon (open squares) in the x''-y'' plane as a function of multiplicity.

Bose-Einstein Correlations of Positive Pions in Collisions of Nb + Nb and Au + Au at 650 MeV/nucleon*

R. Bock, G. Claesson, K.G.R. Doss, H.Å. Gustafsson, H.H. Gutbrod, K.H. Kampert, B. Kolb, P. Kristiansson, H. Löhner, H.G. Ritter, H.R. Schmidt, T. Siemiarczuk, H. Wieman, and W. Wislicki

The Plastic Ball modules provided identification and energy measurements of π^+ in the kinetic energy range of 20 to 100 MeV. As the yield of the positive pions in the Bevalac energy region is only a few percent of the protons and heavier particles, in the simple ΔE-E identification the pions were overshadowed by the background of other particles. To make a clear identification of π^+, the delayed e^+ was recorded from the decay: $\pi^+ \rightarrow \mu^+ \rightarrow e^+$. The energy of the e^+ is up to 53 MeV and was easily detected in the plastic scintillator. The e^+, however, could penetrate the adjacent modules, accidentally coinciding with stable particles to simulate another π^+ signal. Therefore we applied a cut on the difference in time between pairs of π^+-e^+ signals measured in all tubes. A cut of $\leq$ 60 ns discarded the simulated π^+ and removed only about 2% of the real positive pion pairs. After the cut we were left with 102,000 Au+Au and 67,000 Nb+Nb events with at least two particles in the final state identified as positive pions.

Characteristics of the pion emitting region were extracted by assuming a Gaussian distribution of the pion point sources and fitting the expression:

$$C(q) = n(1 + \lambda exp(-q^2R^2/2))$$

to the experimental correlation function. In Fig. 1 we show the correlation function for Nb and Au. The curves represent the best fits of equation 1 giving R = 3.4 ± 0.4 fm for the Nb + Nb and 4.8 ± 0.6 fm for the Au + Au system.

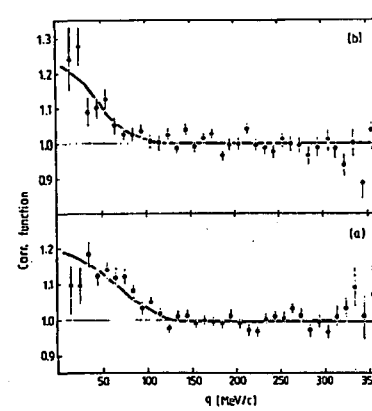

Fig. 1. The π^+-π^+ correlation function versus q for the Nb + Nb (a) and Au + Au (b) interactions at 650 MeV per nucleon.

Footnotes and References

*Condensed from Modern Phys. Letters.

Projectile Fragmentation of the Extremely Neutron Rich Nucleus ^{11}Li at 0.79 GeV/nucleon

T. Kobayashi, O. Yamakawa,* K. Omata,† K. Sugimoto,‡ T. Shimoda,§ N. Takahashi,§ and I. Tanihata***

A newly developed technique to produce a high-quality β-unstable nuclear beam[1] provides a new possibility to study the nucleon-density distribution and the momentum distribution of nucleons in unstable nuclei through the projectile fragmentation of those exotic nuclei. In this report we present the first measurements of fragments produced from the projectile fragmentation of extremely neutron-rich nuclei (^{11}Li, ^{8}He, and ^{6}He) at 0.79-GeV/nucleon incident energy, and then show evidence of the existence of a long tail in the neutron distribution of the ^{11}Li nucleus.

Projectile fragmentation was extensively studied using beams of stable nuclei.[2] An important finding is the regularity of a momentum distribution of the projectile fragments. It was found that the momentum distribution has a Gaussian shape in the projectile frame, and the width of the Gaussian σ is independent of target mass and beam energy but depend on the mass numbers of a projectile and a fragment in addition to a momentum fluctuation of nucleons inside the nucleus. In other words, internal momentum distribution can be determined from the measurement of projectile fragmentation.[3]

The transverse momentum distributions of fragments of ^{11}Li by the carbon target were measured at 0.79 GeV/nucleon. Fig. 1 presents a transverse momentum distribution of ^{9}Li, which shows two Gaussian structure in which a narrow peak lays on top of the other wider peak. A wider one has the width $\sigma_{\rm wide}$=95 12 MeV/c and the other has a narrow width $\sigma_{\rm narrow} = 23 \pm 5$ MeV/c. The two component structure had not been observed in fragmentation of stable nuclei and therefore is a new feature. The narrow peak indicates an existence of nucleons with extremely small momentum fluctuation. The $\sigma_{\rm wide}$ is consistent with the momentum fluctuations of usual nucleons. If we extend the method used for stripping reactions to many nucleon removal, the momentum width of the projectile fragment is related to the separation energy of last nucleons and then written as,

$$\sigma^2 = \mathrm{u} < \varepsilon > \mathrm{A_F}(\mathrm{A_B} - \mathrm{A_F})/\mathrm{A_B} \qquad (1)$$

where u is the atomic mass unit and $\langle\varepsilon\rangle$ is an average separation energy of the removed nucleons. The observed narrow width gives $\langle\varepsilon\rangle$ = 0.34±0.16 MeV which can be compared with separation energy of last neutrons; ΔE[(^{10}Li+n) - (^{11}Li)]= 0.96±0.1 MeV and ΔE[(^{9}Li+2n) - (^{11}Li)]= 0.19±0.10 MeV. The broad width, on the other hand, gives $\langle\varepsilon\rangle$ = 6.0±1.5 MeV which is roughly consistent with the normal nucleon separation energy. Therefore it is considered that the narrow component is produced by reactions in which weakly bound last two nucleons are removed from ^{11}Li. The small momentum fluctuation of last two neutron also indicates an existence of a long tail in the neutron density distribution because a decay constant of the wave function on nuclear surface is a Fourier transform of the momentum distribution.

Preliminary data on fragmentation of ^{14}Be also shows two Gaussian structure as shown in Fig. 1b. Therefore ^{14}Be shows same characteristics as ^{11}Li in both $\sigma_{\rm I}$ and the fragmentation spectrum.

In summary, projectile fragmentations of extremely neutron-rich nuclei, ^{11}Li, ^{8}He, and ^{6}He, were studied for the first time at 0.79- GeV/nucleon incident energy. (1) Momentum distributions of Li fragments from the fragmentation of ^{11}Li show two components. The narrow width was understood to be originating from the removal of the two weakly bound outer neutrons in the ^{11}Li nucleus. (2) Isotope production cross sections were measured and analyzed with the abrasion-ablation model. (3) Several observations in the ^{11}Li nucleus, (i) large root mean square radius, (ii) small momentum fluctuation in the projectile fragmentation, and (iii) small separation energy of the two outer neutrons, suggest the existence of a large neutron halo around the ^{11}Li

nucleus. (4) Momentum distributions and isotope production cross sections from a heavy target suggest that the electromagnetic dissociation process is also important in the fragmentation of neutron-rich nuclei from a heavy target.

Footnotes and References

*KEK, Tsukuba, Ibaraki 305, Japan

†INS, University of Tokyo, Tanashi, Tokyo 188, Japan

‡Faculty of Science, Osaka University, Toyonaka, Osaka 560, Japan

§College of General Education, Osaka University, Toyonaka, Osaka 560, Japan

**RIKEN, Wako, Saitama 351-01, Japan

1. I. Tanihata, Hyperfine Interact. 21, 251(1985); I. Tanihata *et al.*, Phys. Lett. 160B, 380(1985).

2. D.E. Greiner *et al.*, Phys. Rev. Lett. 35, 152(1975).

3. J. Hufner and M.C. Nemes, Phys. Rev. C23, 2538(1981).

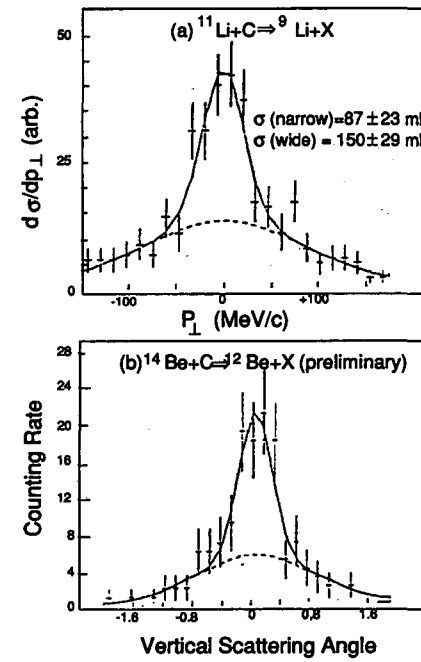

Fig. 1. Spectrum of fragments from ^{11}Li and ^{14}Be collisions.

Search for Free Quarks Produced at 800 GeV/c Using a New Concentration Technique*

*H.S. Matis, R.W. Bland,† D.H. Calloway,† S. Dickson,† A.A. Hahn,‡ C.L. Hodges,† D. Joyce,† M.A. Lindgren,† T.L. Palmer,† H.G. Pugh, M.L. Savage,† G.L. Shaw,‡ R. Slansky,§ A.B. Steiner,† and R. Tokarek***

A high sensitivity experiment was performed to detect free quarks produced in collisions of 800 GeV/c protons with a heavy target at Fermilab. Two quite different high concentration methods were used to obtain a small drop of Hg containing any produced quarks which stopped in a large amount of material. Using a new technique, secondaries were stopped in Hg tanks and the Hg was then distilled to small drops. In a second method, secondaries were stopped in liquid nitrogen tanks, and charged atoms were collected electrostatically on Au coated electrodes. The Au coatings were dissolved in Hg. The Hg drops from both techniques were then tested for quarks in the San Francisco State University automated Millikan apparatus. These results show that charged 1/3 quarks are produced below levels of 1.2×10^{-10} at 90% c.l. for both methods. Upper limits for charged 2/3 quarks are slightly more sensitive. The distillation technique should prove useful in performing high sensitivity quark searches in future beam dump experiments.

Footnotes and References

*Condensed from Phys. Rev. D

†Physics and Astronomy Department, San Francisco State University San Francisco, CA 94132

‡Physics Department, University of California, Irvine, CA 92717

§Los Alamos National Laboratory, Los Alamos, NM 87545

**Fermi National Accelerator Laboratory, Batavia, IL 60510

Di-Leptons at the Bevalac*

H.S. Matis

A program has been started to measure di-leptons at Bevalac energies. Before this program began, di-leptons had never been observed below 12 GeV. The production of di-electrons in proton-nucleus collisions with beams in the energy range 1.0 and 4.9 GeV and in calcium-calcium collisions at 1.0 and 2.0 GeV were studied. A signal was observed in all instances. From a very preliminary analysis, we find that the mass distribution is similar to that found at higher energies. However, the cross-section drops very fast for energies drops below 2.1 GeV.

Footnotes and References

*Condensed from a paper presented at the **Winter Workshop on Nuclear Dynamics V**, Sun Valley, ID, February 1988

Abnormally Large Momentum Loss in Charge Pickup by 900 MeV/N Au Nuclei*

G. Gerbier, Ren Guoxiao, and P.B. Price

Using a thin stack of glass detectors to measure Z/β of forward-projected fast fragments of interactions of 900 MeV/N ^{197}Au nuclei, we measure a cross section of 35±8 mb for charge pickup ($\Delta Z = +1$) from Au to Hg, and we infer a mean velocity downshift $\delta\beta \approx$-0.004 and a mean momentum downshift $\delta p_{\|} \approx$-6 GeV/c for Au to Hg, two orders of magnitude larger than observed for charge pickup by light nuclei. Implications of this result are discussed.

Footnotes and References

*Condensed from Phys. Rev. Lett. **60**, 2258 (1988).

Systematics of Charge-Pickup Reactions by GeV/nucleon Heavy Nuclei*

Ren Guoxiao, P.B. Price and W.T. Williams

We have measured cross sections for inclusive reactions in which 1.7 GeV/N ^{56}Fe, 1.46 GeV/N ^{84}Kr, 1.28 GeV/N ^{139}La, and 0.8 GeV/N ^{197}Au increased in charge by one unit. Combining these results with data on charge pickup by ^{12}C, ^{18}O and ^{20}Ne projectiles, we find that the cross section for charge pickup by ~GeV/nucleon projectiles is generally given to within a factor two by the expression $\sigma_{\Delta Z=+1} = 1.7 \times 10^{-4}\ \gamma_{PT}\ A_{P^2}$ (in mb), where $\gamma_{PT} = A_{P^{1/3}} + A_{T^{1/3}} - 1.0$. This expression, with roles of projectile and target interchanged, equally well fits cross sections for (p,xn) reactions at GeV energies when summed over x. The factor γ_{PT} implies peripheral collisions; the dependence on A_{P^2} is the steepest ever reported for a nuclear process. Fig. 1 from the paper (see below) shows the dependence of cross sections for charge pickup and single-charge-loss on projectile mass. Data are for 1.05 and 2.1 GeV/N ^{12}C in C, 0.95 GeV/N ^{20}Ne in Al, 0.9 GeV/N ^{12}C and ^{20}Ne in C, 1.7 GeV/N ^{18}O in Be, 0.8 GeV/N ^{197}Au in Al, and ^{56}Fe, ^{84}Kr, and ^{139}La in CR-39 (this work). Cross sections are summed over all isotopes of the product with nuclear charge Z_{P+1}. Solid lines are least squares fits to data.

Footnotes and References

*Condensed from Phys. Rev. C.

Observation of a Nonspherical Pion Source in Relativistic Heavy-Ion Collisions*

*A.D. Chacon, J.A. Bistirlich, R.R. Bossingham, H.R. Bowman, C.W. Clawson,† K.M. Crowe, O. Hashimoto,‡ T.J. Humanic,§ M.L. Justice, J.M. Kurck, W. McHarris,** C.A. Meyer,†† J.O. Rasmussen, J.P. Sullivan,‡‡ and W.A. Zajc§§*

The intensity interferometry method has been used to measure pion source parameters in the reaction 1.70 GeV/nucleon ^{56}Fe + Fe $\rightarrow 2\pi^- + X$ with the JANUS spectrometer. The high statistics available in this experiment allows for good determination of the parameters under the assumption of cylindrical symmetry about the beam axis (as opposed to the spherical symmetry usually assumed). The parameters show an oblate source ($R_\perp > R_\parallel$) in the center-of-mass frame for the spectrometer acceptance centered near 90° or 0° with respect to the beam axis for both systems studied. Intranuclear-cascade-model predictions, which show similar behavior, are compared to the experimental results.

The interferometry method is based on the Bose symmetry of the outgoing pionic wave function which results in intensity interference (the Hanbury-Brown/Twiss effect) in which the probability of detecting a pair of pions with similar momenta is enhanced to an extent determined by the source geometry. Experimentally, one measures the correlation function, defined as

$$C_2(p_1, p_2) = A \frac{\frac{d^6\sigma}{dp_1^3\, dp_2^3}}{\frac{d^3\sigma}{dp_1^3}\frac{d^3\sigma}{dp_2^3}} \qquad (1)$$

where A is a normalization constant. In practice, we measure only the two-pion inclusive cross-section and then determine the denominator of Eq.(1) from the two-pion data by "event-mixing," *i.e.*, pairing of pions from different events. We assume that the pion source can be described by a Gaussian space-time distribution, symmetric about the beam axis, and fit the correlation function to the functional form

$$C_2(q_\perp, q_\parallel, q_0) = 1 + \lambda exp\left[-\left(q_\parallel^2 R_\parallel^2 + q_0^2\tau^2\right)/2\right] \qquad (2)$$

where $q_\perp = |(\vec{p}_1 - \vec{p}_2)_\perp|$, $q_\parallel = |(\vec{p}_1 - \vec{p}_2)_\parallel|$, and $q_0 = |E_1 - E_2|$; $(\vec{p}_1, E_1)$ and $(\vec{p}_2, E_2)$ are the center-of-mass four-momenta of the two pions. $R_\perp$ and $R_\parallel$ are the transverse and longitudinal (with respect to the beam direction) radius parameters, and τ is the lifetime parameter. The λ parameter allows for correlations from effects other than Bose statistics and would be unity in their absence.

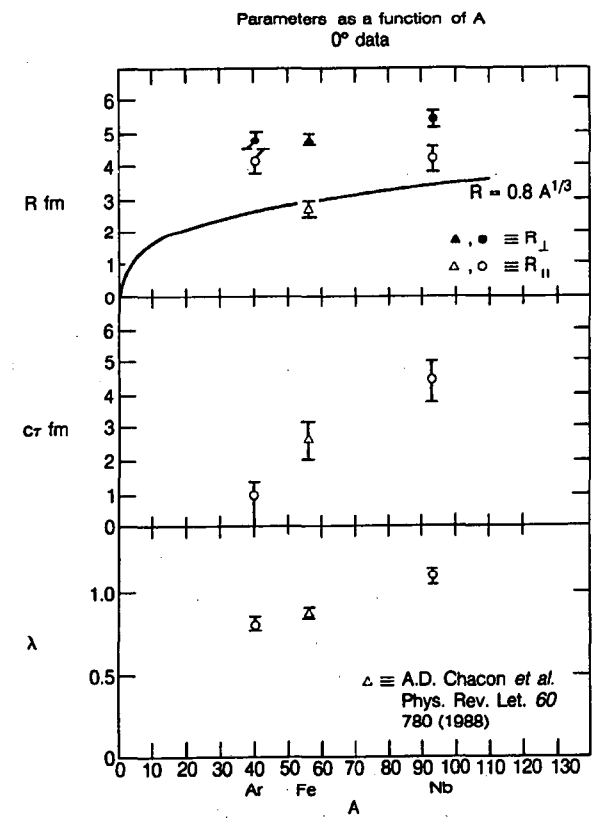

Fig. 1. Results as a function of nuclear mass number, A, for the Fe + Fe system, along with preliminary results for 1.80 A GeV Ar + KCl and 1.20 A GeV Nb + Nb; all for the 0° acceptance. The Fe results have been compared to an extended version of Cugnon's CASCADE code to which Bose correlations between pion pairs has been added.[1] Qualitatively, the CASCADE results agree with the experiment, although CASCADE tends to underpredict the oblateness and overpredict the overall source size.

Footnotes and References

*Condensed from Phys. Rev. Lett. **60**, 780 (1988)

†Current address: Tektronix, Mail Stop 50-324, P.O. Box 500, Beaverton, OR 97077.

‡Instititute for Nuclear Study, University of Tokyo, Tanashi, Tokyo, Japan

§Current address: Gesellschaft für Schwerionenforschung, 6100 Darmstadt 11, West Germany.

**Michigan State University, East Lansing, Michigan 48226

††Current address: Physik-Institut der Universität Zurich, CH-8001 Zurich, Switzerland.

‡‡Texas A & M University, College Station, Texas 77843

§§Current address: Columbia University, 538 W. 120 St., New York, NY 10027.

1. T.J. Humanic, Phys. Rev. C **34**, 191 (1986).

Study of the Energy Flow in Oxygen-Nucleus Collisions at 60 and 200 Gev/c per Nucleon*

NA35 Collaboration

*A. Bamberger,† J. Bartke,‡ H. Bialkowska,§ R. Bock,** R. Brockmann,** S.I. Chase, C. De Marzo,†† M. De Palma,†† I. Derado,‡‡ V. Eckardt,‡‡ C. Favuzzi,†† D. Ferenc,§§ H. Fessler,‡‡ P. Freund,‡‡ M. Gazdzicki,**** H.J. Gebauer,‡‡ C. Guerra,** J.W. Harris, W. Heck,††† T. Humanic,** K. Kadija,§§,‡‡ A. Karabarbounis,‡‡‡ R. Keidel,§§§ Kowalski,‡ M. M. Lahanas,††† S. Margetis,††† E. Nappi,†† G. Odyniec, G. Paic,§§ A.D. Panagiotou,‡‡‡ A. Petridis,‡‡‡ J. Pfennig,††† F. Posa,†† K.P. Pretzl,‡‡ H.G. Pugh, F. Pühlhofer,§§§ G. Rai, A. Ranieri,†† W. Rauch, R. Renfordt,††† D. Röhrich,††† K. Runge,† A. Sandoval,** N. Schmitz,‡‡ T. Schouten,‡‡ L.S. Schroeder, P. Seyboth,‡‡ J. Seyerlein,‡‡ E. Skrzypczak,**** P. Spinelli,†† R. Stock,†††,†††† H. Ströbele,††† A. Thomas,††† M. Tincknell, L. Teitelbaum, S. Tonse, G. Vesztergombi,‡‡ D. Vranic,§§ and S. Wenig†††*

Forward energy flow and transverse energy production in ultrarelativistic nucleus-nucleus interactions depend on the centrality of the collision and on the degree of stopping that takes place in each collision.

A systematic study of the forward energy flow and transverse energy production in the interactions induced by 60 and 200 GeV/nucleon ^{16}O projectiles with Al, Cu, Ag, and Au nuclei has been performed by the NA35 collaboration at the CERN SPS. We studied a range of trigger conditions from peripheral up to the most central collisions. First results have been published.[1]

The experimental set up consists of a streamer chamber in a superconducting vertex magnet followed by a set of calorimeters which covers the pseudorapidities forward of 2.0°.[2] The forward angles are covered by a set of four calorimeters to measure the energy flux of the emitted reaction products.The angular domain θ <0.3°, which corresponds to the projectile fragmentation region, is covered by a 4-segment "Veto" calorimeter. The subsequent interval, from 0.3°–2.2°, is seen by a single cell electromagnetic and hadronic Intermediate Calorimeter. The large angle domain is covered by the Photon Position Detector (PPD), an electromagnetic calorimeter of high granuality, which is backed up by the Ring Calorimeter.

The Veto Calorimeter energy spectra for ^{16}O + Au interactions at 60 and 200 GeV/c per nucleon are shown in Fig. 1a on a relative energy scale normalized to the beam energy. The probability for having almost no energy going forward is higher for 60 GeV/c then for 200 GeV/c. The E_{veto} spectra for different targets (Cu, Ag, Au) at 60 GeV/c are shown in Fig. 1b.

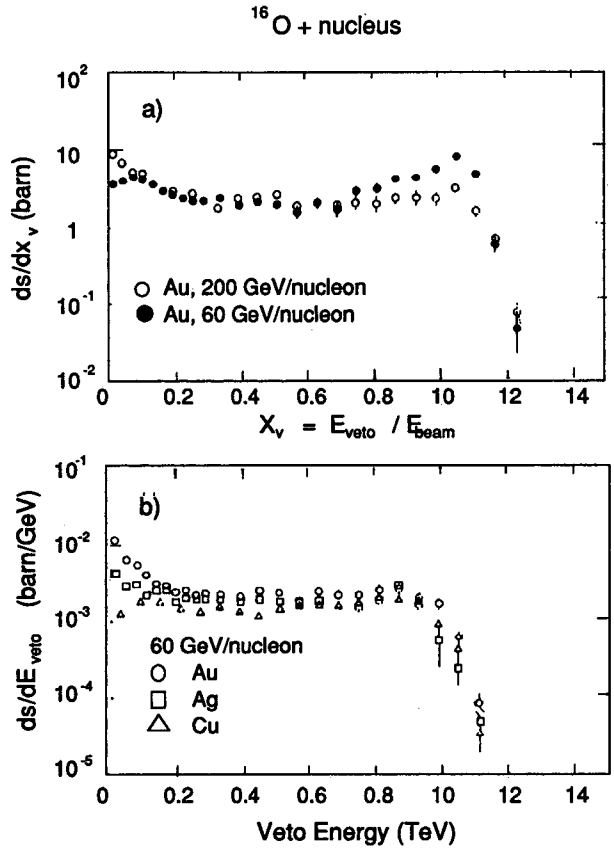

Fig. 1 a,b. Energy spectra in the Veto Calorimeter for an interaction trigger. In a) the veto energy is scaled by the beam energy to compare 60 and 200 GeV/nucleon ^{16}O + Au collisions (open and full circles respectively). The effect of the trigger onset is seen for $x_v > 0.9$. In b) spectra for three different targets are compared at 60 GeV/nucleon.

Controlled by the impact geometry of a collision, E_{veto} and transverse energy E_t are anticorrelated as can be seen from Fig. 2 for min. bias trigger O+Au collisions at 200 GeV/c – e.g., central collisions lead to low E_{veto} and high E_t.

Differential transverse energy distributions for ^{16}O at 200 GeV/c on Al, Cu, Ag and Au targets are shown in Fig. 3. Events corresponding to the hard E_t trigger (required minimum transverse energy of 39.5 GeV in PPD calorimeter) reach a maximum value of $dE_t/d\eta$ of 91 GeV for ^{16}O + Au at the low η edge of the calorimeter acceptance. The energy density of these events can be estimated using the Bjorken formula:[3]

$$\epsilon = \left(\frac{dE_t}{d\eta}\right)_{max} / (\pi R^2 \tau)$$

Taking R = 3 fm and τ = 1 fm one obtains an energy density of ϵ = 3.2 GeV/fm^3. WA80 and NA34 report similar results for the energy densities.[4,5]

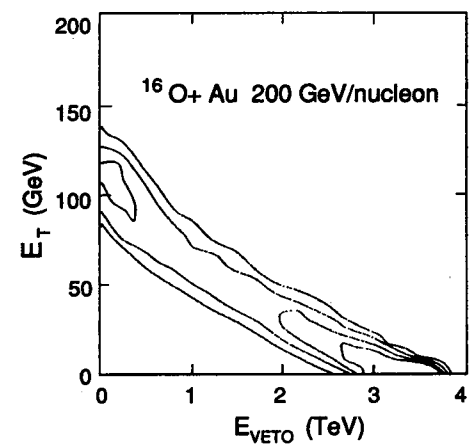

Fig. 2. Correlation between the transverse energy, E_t, observed in the NA35 acceptance and the forward energy flux, E_{veto}, in the projectile fragmentation cone for 200 GeV/nucleon ^{16}O + Au collisions for minimum bias trigger. Target out yield has been subtracted. The contour distances correspond to factors of 2.

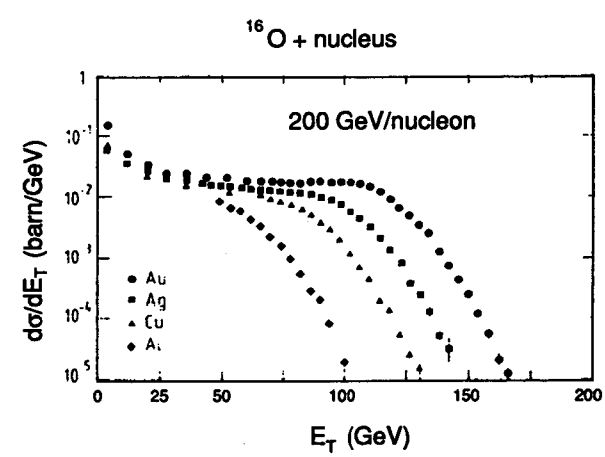

Fig. 3. Transverse energy spectra for ^{16}O on Au (●), Ag (■), Cu (▲), and Al (♦) at 200 GeV/nucleon as seen in the NA35 acceptance.

Footnotes and References

†Fakultät für Physik, Universität Freiburg, D-7800 Freiburg, Germany

‡Institute of Nuclear Physics, PL-30055 Cracow, Poland

§Institute of Nuclear Studies, PL-00681 Warszawa, Poland

**Gesellschaft für Schwerionenforschung, D-6100 Darmstadt 9, Germany

††Dipartimento di Fisica, Universita di Bari, and INFN, Bari Italy

‡‡Max-Planck-Institut für Physik und Astrophysik, D-8000 München, Germany

§§Rudjer Boskovic Institute, 41001 Zagreb, Yugoslavia

***Institut für Hochenergiephysik, Universität Heidelberg, D-6900 Heidelberg 1

†††Fachbereich Physik, Universität Frankfurt, D-6000 Frankfurt, Germany

‡‡‡Physics Department, University of Athens, 157-71 Athens, Greece

§§§Fachbereich Physik, Universität Marburg, D-3550 Marburg, Germany

****Institute of Experimental Physics, University of Warsaw, Warszawa, Poland

††††CERN, CH-129 Geneva 23, Switzerland

1. A. Bamberger *et al.*, Phys. Lett. B 184(1987)271.
2. A. Sandoval *et al.*, Nucl. Phys. A 461(1987)465.
3. J.D. Bjorken, Phys. Rev. D 27(1983)140.
4. R. Albrecht *et al.*, Phys. Lett. B 199(1987)297.
5. T. Akesson *et al.*, CERN-EP/87-176.

Strange Particle Production in the NA35 Experiment at CERN*

NA35 Collaboration

*A. Bamberger,† J. Bartke,‡ H. Bialkowska,§ R. Bock,** R. Brockmann,** S.I. Chase, C. De Marzo,†† M. De Palma,†† I. Derado,‡‡ V. Eckardt,‡‡ C. Favuzzi,†† D. Ferenc,§§ H. Fessler,‡‡ P. Freund,‡‡ M. Gazdzicki,**** H.J. Gebauer,‡‡ C. Guerra,** J.W. Harris, W. Heck,††† T. Humanic,** K. Kadija,§§,‡‡ A. Karabarbounis,‡‡‡ R. Keidel,§§§ Kowalski,‡ M. M. Lahanas,††† S. Margetis,††† E. Nappi,†† G. Odyniec, G. Paic,§§ A.D. Panagiotou,‡‡‡ A. Petridis,‡‡‡ J. Pfennig,††† F. Posa,†† K.P. Pretzl,‡‡ H.G. Pugh, F. Pühlhofer,§§§ G. Rai, A. Ranieri,†† W. Rauch, R. Renfordt,††† D. Röhrich,††† K. Runge,† A. Sandoval,** N. Schmitz,‡‡ T. Schouten,‡‡ L.S. Schroeder, P. Seyboth,‡‡ J. Seyerlein,‡‡ E. Skrzypczak,**** P. Spinelli,†† R. Stock,†††,†††† H. Ströbele,††† A. Thomas,††† M. Tincknell, L. Teitelbaum, S. Tonse, G. Vesztergombi,‡‡ D. Vranic,§§ and S. Wenig†††*

One of the main aims of the NA35 experiment is to determine the production rates for strange particles from heavy ion collisions. An enhancement of such a quantity relative to one from pp or p-nucleus collisions has been held as being a signature of a quark-gluon plasma.[1,2] The streamer chamber [3,4] is well suited for detecting the decays of neutral strange particles with lifetimes $\sim 10^{-10}$ sec, viz. Λ, K_s and $\overline{\Lambda}$. At LBL, streamer chamber pictures of O^{16}–Au collisions and p–Au collisions at 60 GeV/nucleon beam momentum were analysed, while a parallel effort was made on the corresponding 200 GeV data by our collaborators in Europe.

For the O^{16}–Au data set, the scanning team measured 1473 candidates from a sample of 997 events, and for the p–Au data 1753 candidates from 4678 events. Kinematical fits were performed to identify particles. [5] Besides Λ, K_s and $\overline{\Lambda}$ originating from primary interactions there is a background consisting of Λ and $\overline{\Lambda}$ produced from other hyperon decays, and of

photons converting in the chamber gas and the thin electrode grids. The particle identification was based on the kinematical fit probabilities calculated for the four hypotheses $(\pi^+\pi^-), (p\pi^-), (\pi^+\overline{p})$ and (e^+e^-). A candidate was assumed to be a photon if it originated in the grid position or if the kinematic fit probability for the $\gamma \rightarrow e^+e^-$ hypothesis was $\geq 1\%$. For Λ, K_s and $\overline{\Lambda}$ an additional constraint was imposed, requiring the momentum to project back to the target. The final particle yields were 341 Λ, 191 K_s and 23 $\overline{\Lambda}$ for the O^{16}–Au data and 558 Λ, 451 K_s and 32 $\overline{\Lambda}$ for the p–Au data.

In order to calculate production rates it was necessary to account for losses due to (a) decays outside the fiducial volume of the streamer chamber and (b) other causes such as low scanning efficiency in areas with a very dense population of tracks, or decay product tracks too short for a satisfactory momentum measurement. The losses from (a) can easily be corrected. To estimate the magnitude of the losses in (b), Bartlett's [6] method, of determining the mean lifetime of a data sample was used as an indicator to find those regions of phase space free from such losses, and only those areas were kept for subsequent analysis. The area in phase space (expressed in terms of transverse momentum p_T and rapidity y) for which we have both a good acceptance efficiency and sufficient statistics is roughly 0.25 GeV $< p_T <$ 2.0 GeV and $0.7 < y < 3.0$ for the O^{16}–Au data, and 0.1 GeV $< p_T <$ 2.0 GeV and $0.5 < y < 4.0$ for p–Au, although it varies slightly for the three particle types. In these areas of phase space we have calculated the mean strange particle multiplicity per event and also the ratio of strange particles to negative particles. Comparisons between data and the Lund FRITIOF model are also included.

The ratios of average mutltiplicities between O^{16}–Au and p–Au reactions for Λ, K_s, $\overline{\Lambda}$ and negative particles were calculated, imposing the O^{16}–Au phase space cuts mentioned above.

Within the phase space region accessible to the experiment we find that (1) The ratios of strange particle to negative particle production are the same in p–Au and central O^{16}–Au collisions and (2) Neutral strange particles are approximately 16 times more numerous in central O^{16}–Au than in p–Au reactions.

Footnotes and References

*Condensed from Zeitschrift für Physik C.

†Fakultät für Physik, Universität Freiburg, D-7800 Freiburg, Germany

‡Institute of Nuclear Physics, PL-30055 Cracow, Poland

§Institute of Nuclear Studies, PL-00681 Warszawa, Poland

**Gesellschaft für Schwerionenforschung, D-6100 Darmstadt 9, Germany

††Dipartimento di Fisica, Universita di Bari, and INFN, Bari Italy

‡‡Max-Planck-Institut für Physik und Astrophysik, D-8000 München, Germany

§§Rudjer Boskovic Institute, 41001 Zagreb, Yugoslavia

***Institut für Hochenergiephysik, Universität Heidelberg, D-6900 Heidelberg 1

†††Fachbereich Physik, Universität Frankfurt, D-6000 Frankfurt, Germany

‡‡‡Physics Department, University of Athens, 157-71 Athens, Greece

§§§Fachbereich Physik, Universität Marburg, D-3550 Marburg, Germany

****Institute of Experimental Physics, University of Warsaw, Warszawa, Poland

††††CERN, CH-129 Geneva 23, Switzerland

1. R. Anishetty, P. Koehler, L. McLerran, Phys. Rev. **D22**, 2793 (1980).

2. P. Koch, B. Müller, and J. Rafelski, Strangeness in Relativistic Heavy Ion Collisions, Phys. Rep. **142**, 167 (1986).

3. A. Sandoval *et al.*, Proc. **5** Quark Matter Conf., Asilomar (1986).

4. A. Bamberger *et al.*, Phys. Lett. **B205**, 583 (1988).

5. M. Anikina *et al.*, JINR, E1-83-524, Dubna (1983).

6. M. Bartlett, Phil. Mag. **44**, 249 (1953).

Table I: Average Multiplicities of produced strange particles and ratios with negatively charged particles. Predictions from Fritiof are also shown.

Observable	pAu, 60 GeV		OAu, 60 GeV/nucleon	
	Data	Fritiof	Data	Fritiof
$< K_s^0 >$	0.035 ± 0.012	0.021	0.473 ± 0.107	0.378
$< \Lambda >$	0.090 ± 0.017	0.025	1.407 ± 0.174	0.504
$< \overline{\Lambda} >$	0.003 ± 0.002	0.0014	0.037 ± 0.017	0.043
$< K_s^0 > / < h^- >$	0.254 ± 0.108	0.126	0.150 ± 0.039	0.145
$< \Lambda > / < h^- >$	0.267 ± 0.070	0.075	0.244 ± 0.038	0.100
$< \overline{\Lambda} > / < h^- >$	0.024 ± 0.016	0.015	0.014 ± 0.007	0.020

Table II: Ratios between O-Au and p-Au reactions of strange and negatively charged particle multiplicities at 60 GeV/c nucleon. Predictions from Fritiof are also shown.

	Data	Fritiof
$R(K_s^0)$	12.8 ± 4.8	18.8 ± 1.0
$R(\Lambda)$	14.6 ± 3.0	21.2 ± 1.0
$R(\overline{\Lambda})$	13.7 ± 7.0	19.6 ± 3.3
$R(h^-)$	23.0 ± 3.6	16.4 ± 0.2

Probing the Space-Time Geometry of Ultra-Relativistic Heavy-Ion Collisions*

NA35 Collaboration

A. Bamberger,[†] J. Bartke,[‡] H. Bialkowska,[§] R. Bock,[**] R. Brockmann,[**] S.I. Chase, C. De Marzo,[††] M. De Palma,[††] I. Derado,[‡‡] V. Eckardt,[‡‡] C. Favuzzi,[††] D. Ferenc,[§§] H. Fessler,[‡‡] P. Freund,[‡‡] M. Gazdzicki,[****] H.J. Gebauer,[‡‡] C. Guerra,[**] J.W. Harris, W. Heck,[†††] T. Humanic,[**] K. Kadija,[§§,‡‡] A. Karabarbounis,[‡‡‡] R. Keidel,[§§§] Kowalski,[‡] M. M. Lahanas,[†††] S. Margetis,[†††] E. Nappi,[††] G. Odyniec, G. Paic,[§§] A.D. Panagiotou,[‡‡‡] A. Petridis,[‡‡‡] J. Pfennig,[†††] F. Posa,[††] K.P. Pretzl,[‡‡] H.G. Pugh, F. Pühlhofer,[§§§] G. Rai, A. Ranieri,[††] W. Rauch, R. Renfordt,[†††] D. Röhrich,[†††] K. Runge,[†] A. Sandoval,[**] N. Schmitz,[‡‡] T. Schouten,[‡‡] L.S. Schroeder, P. Seyboth,[‡‡] J. Seyerlein,[‡‡] E. Skrzypczak,[****] P. Spinelli,[††] R. Stock,[†††,††††] H. Ströbele,[†††] A. Thomas,[†††] M. Tincknell, L. Teitelbaum, S. Tonse, G. Vesztergombi,[‡‡] D. Vranic,[§§] and S. Wenig[†††]

We report results from a pion interferometry analysis of 200 GeV/nucleon ^{16}O + Au collisions. Both a gaussian source model[1] and a model based on the inside-outside cascade[2] are used to fit the experimental correlation function, providing transverse (R_T) and longitudinal (R_L) shape parameters, a freezeout time parameter(τ_o) and a chaoticity parameter (λ) for the pion emitting source. The results from the

gaussian source fit are displayed in Fig. 1 for three rapidity bins of the pion pairs and for midrapidity pions from the Lund/Fritiof model. A transverse size is found that is consistent with the projectile radius except for pion pairs at the c.m. rapidity (Fig. 1c). There, significantly larger transverse and longitudinal sizes and a longer freezeout time, as displayed in Fig. 2 for the two models, are measured suggesting a thermalised source.

Footnotes and References

*Condensed from A. Bamberger, *et al.*, Phys. Lett. **203** (1988) 320

†Fakultät für Physik, Universität Freiburg, D-7800 Freiburg, Germany

‡Institute of Nuclear Physics, PL-30055 Cracow, Poland

§Institute of Nuclear Studies, PL-00681 Warszawa, Poland

**Gesellschaft für Schwerionenforschung, D-6100 Darmstadt 9, Germany

††Dipartimento di Fisica, Universita di Bari, and INFN, Bari Italy

‡‡Max-Planck-Institut für Physik und Astrophysik, D-8000 München, Germany

§§Rudjer Boskovic Institute, 41001 Zagreb, Yugoslavia

***Institut für Hochenergiephysik, Universität Heidelberg, D-6900 Heidelberg 1

†††Fachbereich Physik, Universität Frankfurt, D-6000 Frankfurt, Germany

‡‡‡Physics Department, University of Athens, 157-71 Athens, Greece

§§§Fachbereich Physik, Universität Marburg, D-3550 Marburg, Germany

****Institute of Experimental Physics, University of Warsaw, Warszawa, Poland

††††CERN, CH-129 Geneva 23, Switzerland

1. F.B. Yano and S.E. Koonin, Phys. Lett. B **78**, 556 (1978)

2. K. Kolehmainen and M. Gyulassy, Phys. Lett. B **180**, 203 (1986)

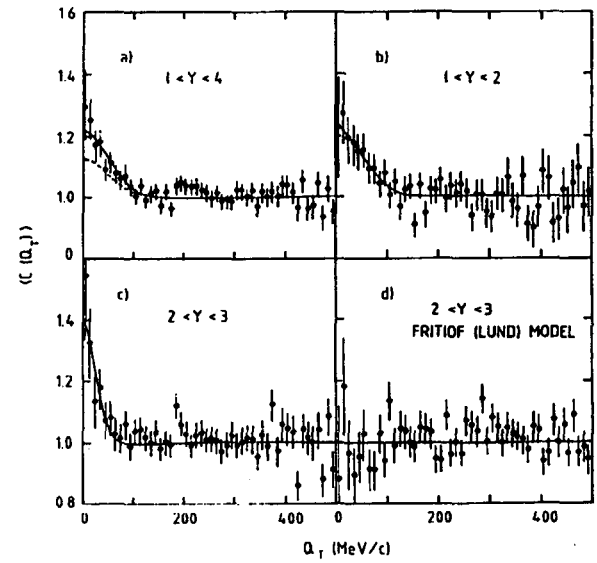

Fig. 1. Correlation function projected onto the Q_T axis (for pairs with $Q_L < 100$ MeV/c) for different rapidity intervals: a) $1 < y < 4$, b) $1 < y < 2$, and c) $2 < y < 3$, data; d) $2 < y < 3$, Fritiof calculation. The projected Gaussian fit is shown (solid curve) for each case, and in (a) the dashed curve shows the fit to the non-Gamow-corrected correlation function.

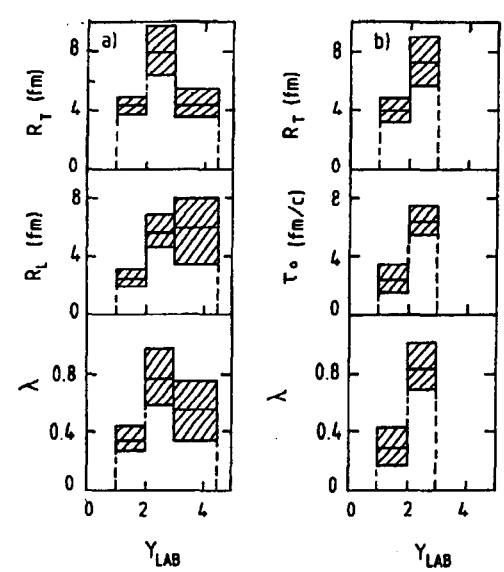

Fig. 2. Comparison of a) Gaussian and b) Kolehmainen-Gyulassy source parameters fitted to the data for different rapidity intervals.

Charged Particle Multiplicities and Inelastic Cross Sections in High Energy Nuclear Collisions*

NA35 Collaboration

A. Bamberger,[†] *J. Bartke,*[‡] *H. Bialkowska,*[§] *R. Bock,*[**] *R. Brockmann,*[**] *S.I. Chase, C. De Marzo,*[††] *M. De Palma,*[††] *I. Derado,*[‡‡] *V. Eckardt,*[‡‡] *C. Favuzzi,*[††] *D. Ferenc,*[§§] *H. Fessler,*[‡‡] *P. Freund,*[‡‡] *M. Gazdzicki,*[****] *H.J. Gebauer,*[‡‡] *C. Guerra,*[**] *J.W. Harris, W. Heck,*[†††] *T. Humanic,*[**] *K. Kadija,*[§§,‡‡] *A. Karabarbounis,*[‡‡‡] *R. Keidel,*[§§§] *Kowalski,*[‡] *M. M. Lahanas,*[†††] *S. Margetis,*[†††] *E. Nappi,*[††] *G. Odyniec, G. Paic,*[§§] *A.D. Panagiotou,*[‡‡‡] *A. Petridis,*[‡‡‡] *J. Pfennig,*[†††] *F. Posa,*[††] *K.P. Pretzl,*[‡‡] *H.G. Pugh, F. Pühlhofer,*[§§§] *G. Rai, A. Ranieri,*[††] *W. Rauch, R. Renfordt,*[†††] *D. Röhrich,*[†††] *K. Runge,*[†] *A. Sandoval,*[**] *N. Schmitz,*[‡‡] *T. Schouten,*[‡‡] *L.S. Schroeder, P. Seyboth,*[‡‡] *J. Seyerlein,*[‡‡] *E. Skrzypczak,*[****] *P. Spinelli,*[††] *R. Stock,*[†††,††††] *H. Ströbele,*[†††] *A. Thomas,*[†††] *M. Tincknell, L. Teitelbaum, S. Tonse, G. Vesztergombi,*[‡‡] *D. Vranic,*[§§] *and S. Wenig*[†††]

In this paper we present results of the CERN SPS experiment NA35 on inelastic cross sections and charged particle multiplicities in collisions of 60 and 200 GeV per nucleon ^{16}O beams with nuclear targets. First results from this experiment were published in ref. 1.

We observe that: (1) Oxygen-nucleus strong interaction cross sections are independent of the incident energy above 2 GeV/nucleon and follow a geometrical dependence of nuclear radii. (2) The average multiplicity of negative particles in minimum bias oxygen- nucleus collisions, normalized to that in p-p collisions, does not depend on the incident energy. It exhibits an approximate proportionality to $A_t^{1/3}$. (See Fig. 1.) (3) The multiplicity distribution of negative particles in minimum bias oxygen-nucleus collisions obeys KNO scaling as a function of energy, which is attributable to its dependence primarily on impact parameter. (See Fig. 2.) (4) The dispersion of negative particle multiplicitiy for minimum bias oxygen- nucleus collisions is roughly proportional to the multiplicity. The dispersion decreases drastically for central collisions. (5) The ^{16}O-Au multiplicity data are roughly consistent with a picture of superposition of independent nucleon-nucleus collisions, similar to our observation[1] that the transverse energy distribution of ^{16}O-nucleus collisions is well reproduced by a 16-fold convolution of p-nucleus E_T data at 200 GeV/nucleon.

Footnotes and References

*Condensed from Phys. Lett. B **205**, 583 (1988)

†Fakultät für Physik, Universität Freiburg, D-7800 Freiburg, Germany

‡Institute of Nuclear Physics, PL-30055 Cracow, Poland

§Institute of Nuclear Studies, PL-00681 Warszawa, Poland

**Gesellschaft für Schwerionenforschung, D-6100 Darmstadt 9, Germany

††Dipartimento di Fisica, Universita di Bari, and INFN, Bari Italy

‡‡Max-Planck-Institut für Physik und Astrophysik, D-8000 München, Germany

§§Rudjer Boskovic Institute, 41001 Zagreb, Yugoslavia

***Institut für Hochenergiephysik, Universität Heidelberg, D-6900 Heidelberg 1

†††Fachbereich Physik, Universität Frankfurt, D-6000 Frankfurt, Germany

‡‡‡Physics Department, University of Athens, 157-71 Athens, Greece

§§§Fachbereich Physik, Universität Marburg, D-3550 Marburg, Germany

****Institute of Experimental Physics, University of Warsaw, Warszawa, Poland

††††CERN, CH-129 Geneva 23, Switzerland

1. A. Bamberger, *et al.*, Phys Lett. B **184**, 271 (1987)

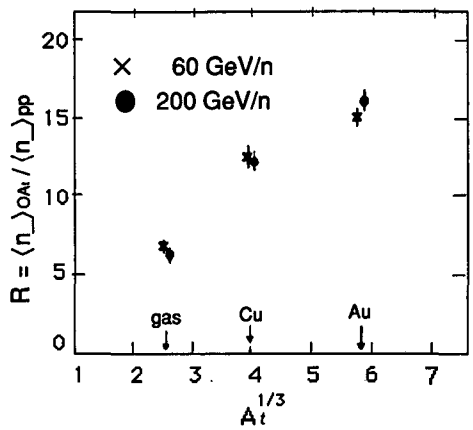

Fig. 1. The ratio R of the average multiplicity of negative particles observed in O-A_t interactions to that in p-p interactions at the same energy, plotted versus the target radius $A_t^{1/3}$.

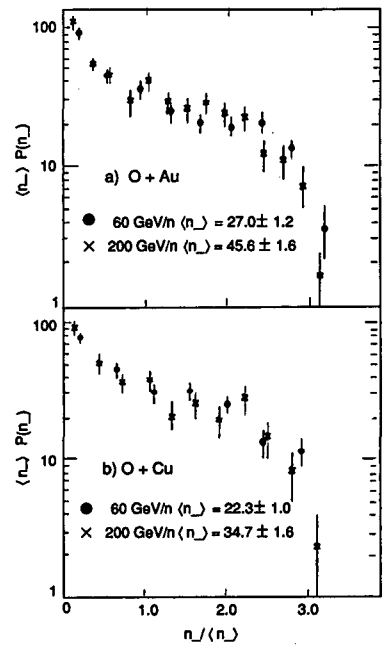

Fig. 2. Multiplicity distributions of negative particles for two energies of the ^{16}O projectile, presented in the KNO scaling variable, for Au(a) and Cu(b) targets.

Negative Particle Production in Nuclear Collisions at 60 and 200 GeV/c per Nucleon

NA35 Collaboration

A. Bamberger,[†] J. Bartke,[‡] H. Bialkowska,[§] R. Bock,[**] R. Brockmann,[**] S.I. Chase, C. De Marzo,[††] M. De Palma,[††] I. Derado,[‡‡] V. Eckardt,[‡‡] C. Favuzzi,[††] D. Ferenc,[§§] H. Fessler,[‡‡] P. Freund,[‡‡] M. Gazdzicki,[****] H.J. Gebauer,[‡‡] C. Guerra,[**] J.W. Harris, W. Heck,[†††] T. Humanic,[**] K. Kadija,[§§,‡‡] A. Karabarbounis,[‡‡‡] R. Keidel,[§§§] Kowalski,[‡] M. M. Lahanas,[†††] S. Margetis,[†††] E. Nappi,[††] G. Odyniec, G. Paic,[§§] A.D. Panagiotou,[‡‡‡] A. Petridis,[‡‡‡] J. Pfennig,[†††] F. Posa,[††] K.P. Pretzl,[‡‡] H.G. Pugh, F. Pühlhofer,[§§§] G. Rai, A. Ranieri,[††] W. Rauch, R. Renfordt,[†††] D. Röhrich,[†††] K. Runge,[†] A. Sandoval,[**] N. Schmitz,[‡‡] T. Schouten,[‡‡] L.S. Schroeder, P. Seyboth,[‡‡] J. Seyerlein,[‡‡] E. Skrzypczak,[****] P. Spinelli,[††] R. Stock,[†††,††††] H. Ströbele,[†††] A. Thomas,[†††] M. Tincknell, L. Teitelbaum, S. Tonse, G. Vesztergombi,[‡‡] D. Vranic,[§§] and S. Wenig[†††]

In the CERN SPS experiment NA35 we exposed a gold target to proton and ^{16}O beams at 60 and 200 GeV/c per nucleon. Negative particle spectra were obtained by stereoscopic reconstruction of particle tracks from three views recorded with a Streamer Chamber in a magnetic field under three trigger conditions: a minimum bias trigger (MBT) selecting all inelastic collisions, a forward energy trigger (FET) that accepted interactions with a total energy deposited in a forward calorimeter below a certain threshold, and a transverse energy trigger (TET) that required some minimum energy in a calorimeter covering mid-rapidity. The forward and transverse energy triggers selected central collisions. Details of

the detector set up can be found in refs. 1 and 2.

Fig. 1 shows the negative particle rapidity distributions in ^{16}O + Au. They are peaked well below the corresponding maxima in p-p collisions at the same beam energies which are $y_{\|}$=2.4 for 60 GeV/c and $y_{\|}$=3 for 200 GeV/c. We observed a slow increase of the width of the rapidity distributions when the trigger condition was changed from central to peripheral. Together with a decrease of the negative particle multiplicities and a shift of the maxima towards the $y_{\|}$ value, this shows the dependence of particle production on reaction geometry. When compared to minimum bias p-p reactions, the ^{16}O+Au rapidity distributions are narrower. On the other hand they are still wider than distributions from a thermal source at rest in the c.m. system, for which the width ($\Delta_{y_{FWHM}}$=1.8) is roughly temperature independent for T > 100 MeV.

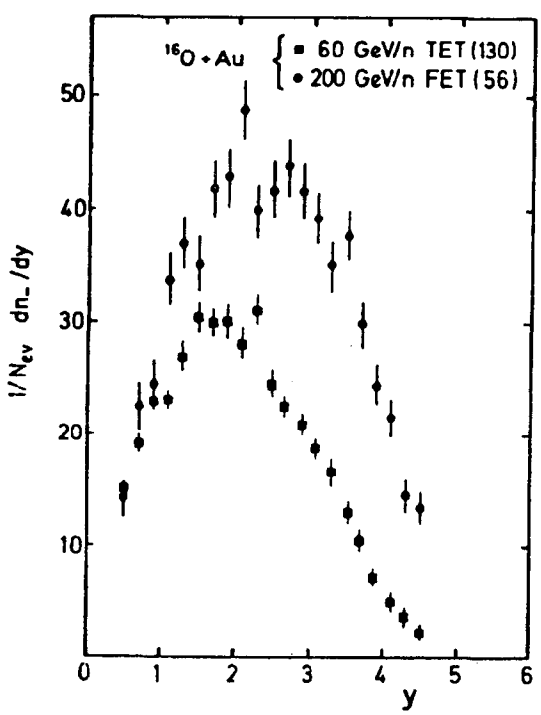

Fig. 1. Negative particle rapidity distributions for central ^{16}O+Au at 60 GeV/c and 200 GeV/c per nucleon.

Fig. 2 shows the transverse momentum spectra for central ^{16}O collisions at 200 GeV/c in the rapidity interval 2 < y < 3. The solid curve represents a fit of a model with a source of two temperatures at mid-rapidity to the data assuming all emitted particles are negative pions. The data are reproduced well for T_1 = 43±6 MeV, T_2 = 153±5 MeV, and the relative yield N_1/N_2 = 0.23±0.07 with χ^2/NDF = 1.8, whereas a fit with a single temperature (not shown in fig. 2) produces a χ^2 of 5.4/NDF. Comparing the ^{16}O+Au and p+Au negative particle $p_\perp$ distributions to minimum bias p-p data, the values for $<p_\perp>$ are close, but the shapes of the distributions differ significantly. Both show an excess at low ($p_\perp$ < 0.5 GeV/c) and high transverse momenta ($p_\perp$ > 1 GeV/c). For more discussions see ref. 3.

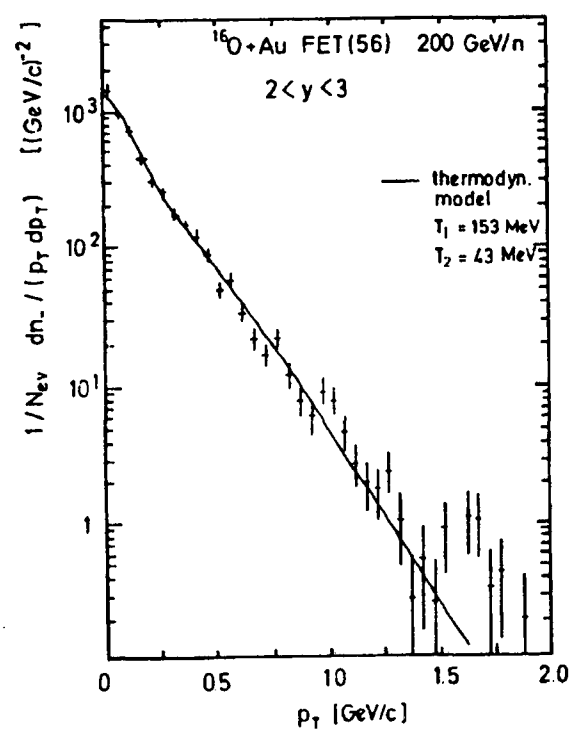

Fig. 2. Transverse momentum spectrum for central ^{16}O+Au collisions at 200 GeV/c per nucleon in the rapidity interval 2.0 < y < 3.

Footnotes and References

†Fakultät für Physik, Universität Freiburg, D-7800 Freiburg, Germany

‡Institute of Nuclear Physics, PL-30055 Cracow, Poland

§Institute of Nuclear Studies, PL-00681 Warszawa, Poland

**Gesellschaft für Schwerionenforschung, D-6100 Darmstadt 9, Germany

††Dipartimento di Fisica, Universita di Bari, and INFN, Bari Italy

‡‡Max-Planck-Institut für Physik und Astrophysik, D-8000 München, Germany

§§Rudjer Boskovic Institute, 41001 Zagreb, Yugoslavia

***Institut für Hochenergiephysik, Universität Heidelberg, D-6900 Heidelberg 1

†††Fachbereich Physik, Universität Frankfurt, D-6000 Frankfurt, Germany

‡‡‡Physics Department, University of Athens, 157-71 Athens, Greece

§§§Fachbereich Physik, Universität Marburg, D-3550 Marburg, Germany

****Institute of Experimental Physics, University of Warsaw, Warszawa, Poland

††††CERN, CH-129 Geneva 23, Switzerland

1. A. Sandoval *et al.*, Nucl. Phys. A461 (1987) 465c

2. W. Heck *et al.* NA 35 Collab.: Z. Phys. C38, 19 (1988)

3. H. Stroebele *et al.* NA 35 Collab.: Z. Phys. C38, 89 (1988)

Electromagnetic Spallation of 6.4 TeV ^{32}S Nuclei

P.B. Price, Ren Guoxiao, and W.T. Williams

We have studied the fragmentation of 6.4 TeV ^{32}S nuclei in Pb, Cu and Al targets. For Pb, the electromagnetic spallation (ES) cross sections are larger than the nuclear cross sections. For Pb and Cu the ES cross sections decrease with projectile charge loss ΔZ as $\sim\exp(-0.6\Delta Z)$ and show a dependence on target charge consistent with $Z_{T^{1.8}}$ as predicted by theory. Fig. 1 from the paper (see below) shows our measured cross sections for electromagnetic spallation in Pb and Cu and for nuclear spallation in Pb as a function of $\Delta Z \equiv Z_P - Z_F$. Straight lines are least-squares fits to exponentials. Dashed lines for Cu are for $Z_{T^{1.5}}$ and $Z_{T^{2.1}}$ dependence; solid line for Cu is for $Z_{T^{1.83}}$ dependence.

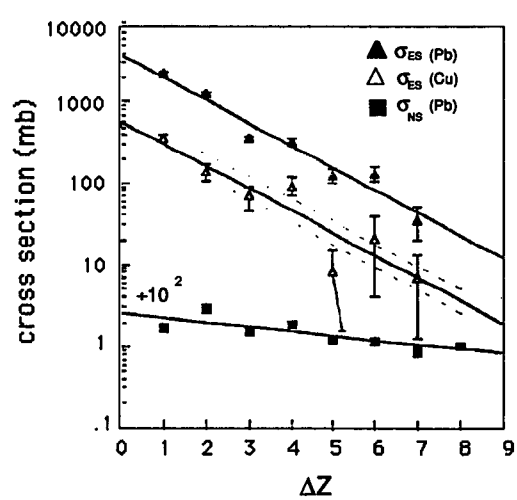

Fig. 1. Cross sections for electromagnetic spallation in Pb and Cu and for nuclear spallation in Pb as a function of $\Delta Z \equiv Z_P - Z_F$. Straight lines are least-squares fits to exponentials. Dashed lines for Cu are for $Z_{T^{1.5}}$ and $Z_{T^{2.1}}$ dependence; solid line for Cu is for $Z_{T^{1.83}}$ dependence.

PART III: THEORY

Nuclear Dissipation and the Order to Chaos Transition*

W.J. Świątecki

The transition from ordered to chaotic nucleonic motions in the nuclear mean-field potential is reflected in the disappearance of shell effects in nuclear masses and deformations, and in the transition from an elastic through an elastoplastic, to a dissipative behavior of the nucleus.

Footnotes and References

*Condensed from an invited talk at the Third International Conference on Nucleus-Nucleus Collisions, Saint-Malo, France, June 6–11, 1988; Nucl. Phys. **A488**, 375c (1988).

Structure Studies of Low-Lying 0^+ States in the Deformed Rare-Earth Region*

A.A. Shihab-Eldin,† M. Stoyer, and J.O. Rasmussen

To better understand the structure of the low-lying 0^+ states of even-even nuclides in the deformed rare-earth region, we have carried out calculations to generate the wavefunctions, energies and pair transfer rates from/to these states within a framework of exact diagonalization of the residual pairing and n-p forces. First we carried out exact diagonalization for the neutron and proton systems separately, using as a basis space the 126 vector space of four/five pairs within nine appropriate deformed Nilsson orbitals. For the pairing force we included both monopole and quadrupole terms. Next, we used the the lowest eight eigenfunctions from both the neutron and the proton systems to generate a new basis space composed of the 64 possible neutron-proton product vectors. The n-p force was approximated by a quadrupole-quadrupole force term which was then diagonalized within the new basis space. The resulting wave functions were used to calculate the neutron pair transfer strength from and to the various low 0^+ states.

Of the many possible parameters to vary we have constrained the calculations to only a few. First, we have constrained the Nilsson parameters and equilibrium deformation parameters ϵ_2, ϵ_4 and ϵ_6 to those values published by P. Möller and R. Nix.[1] We have adjusted the monopole pairing-force strength to reproduce generally the gap from ground to first-excited 0^+ states. For the rare earths we need $G_p \approx 0.23$ MeV and $G_n \approx 0.20$ MeV. These values are somewhat larger than those generally used, since our 9-orbital basis is much smaller than the basis set usually used in pairing calculations. The quadrupole pairing strength is a more uncertain parameter. Most pairing calculations have not included it, but the Surface Delta Interaction Model implies quadrupole pairing equal to monopole pairing. We have made most of our calculations here for these two extremes plus half strength, between the limits, as would be appropriate for a finite-range pairing interaction. To take into account the variation in the pair transfer amplitudes for individual Nilsson orbitals, we took the values calculated by Oothoudt and Hintz.[2]

At some reasonable values of the pairing and n-p strength, the calculation gave reasonable global agreement for the observed multiplicity of 0^+ states below 3 MeV in the even-even Gd, Dy and Er isotopes. Furthermore, for the cases where the deformation parameters do not change appreciably between the pair of nuclides involved in the pair transfer reaction, reasonable global agreement was obtained for the measured (t,p) and (p,t) pair transfer reaction strengths both to the ground and excited states 0^+ states accessible in these isotopes and also for ^{246}Pu and ^{248}Cm isotopes. The observed enhancement of (t,p) pair transfer strength to excited states in some of these isotopes was reproduced by the calculation. This enhancement is attributed to

the subshell gap and large relative transfer amplitude for an orbital near the Fermi surface. In Fig. 1 we show, as an example, the results of our calculations for ^{164}Dy. As for the ground-to-ground pair transfer strength, our model seems to reproduce more than just the qualitative enhancement, and the trends in the Gd (Fig. 2) and Dy isotopes compare well with experiment. Fig. 2 shows that at unphysically large neutron-proton coupling the pairing scheme begins to break down with a loss of ground pair transfer enhancement.

Finally our codes calculate E0 and E2 matrix elements among the bands, but we have just began to correlate these results with data.

Footnotes and References

*Condensed from LBL-26225, to appear in Proc. of Workshop on Microscopic Models in Nuclear Structure Physics, Oak Ridge (Oct. 3-6, 1988), World Scientific Press, Singapore

†On leave from Kuwait Institute for Scientific Research, Kuwait

1. P. Möller and J.R. Nix, Atomic Data and Nuclear Data Tables, **39**, 213 (1988), and Los Alamos Report LA-UR-86-3983, 1986.

2. M.A. Oothoudt and N.M. Hintz, Nucl. Phys. **A213**, 221 (1973).

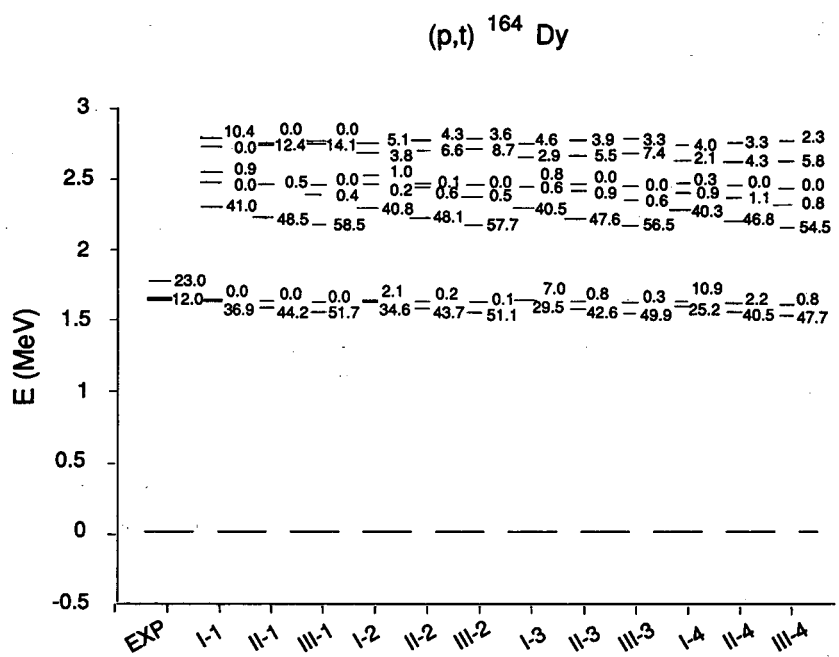

Fig. 1. For ^{164}Dy are shown experimental and calculated 0^+ level energies and (t,p) reaction strengths in percent of ground-to-ground strength. There are four clusters of calculations for increasing n-p coupling strengths (χ'_{np} = 0.0, 0.002, 0.003, 0.004, labeled 1, 2, 3 and 4, respectively). Within each cluster there are three pairing parameter sets, I, II, and III. In all cases G_{0p} = 0.23 MeV and G_{0n} = 0.2 MeV. Cases I, II, and III correspond to quadrupole pairing strength (G_Q) equal to the monopole pairing strength G_0, equal to half that value, and absent, respectively.

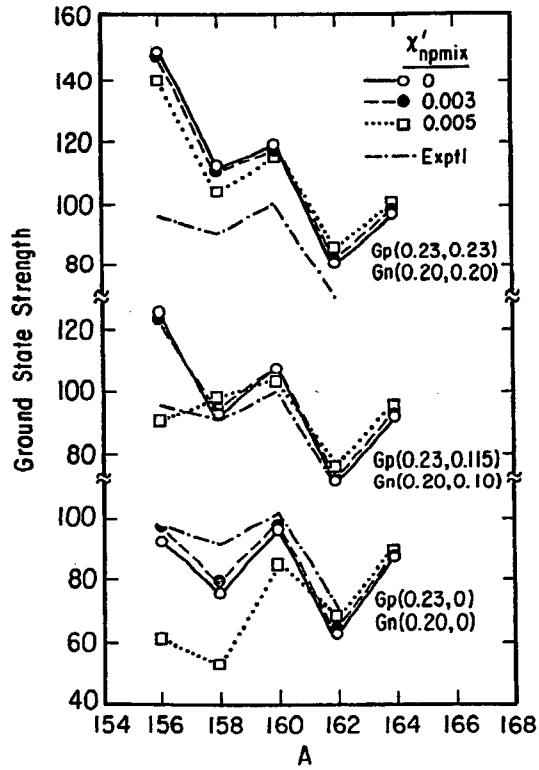

Fig. 2. For Gd isotopes we show experimental and calculated relative ground state (t,p) reaction strengths for various coupling strengths. The pairing strengths (MeV) are noted within parentheses (G_0,G_Q).

Classical Simulation of Nuclear Systems*

C. Dorso and J. Randrup

With a view towards nuclear collisions at intermediate energies, we have developed a novel quasi-classical model for nuclear systems. The model describes the nucleons as classical point particles subject to a momentum-dependent Pauli repulsion[1] and a modified Lennard-Jones nuclear interaction, in addition to a standard Coulomb repulsion between the protons.

The major advantanges of the model are as follows. First, as was already shown in ref. 1, the non-interacting Fermi gas is simulated rather well in terms of the Pauli potential, over an interesting range of temperatures and densities. For interacting nuclear matter, the behavior of the energy with density and temperature is also quite satisfactory. In particular, reasonable values result for both the saturation energy and the saturation density (although the latter value is around 10% too high). The effective compressibility, as indicated by the energy of cold matter at double density, is also close to that produced by standard nuclear models. For finite nuclei, a satisfactory global behavior is achieved for both binding energies and radii, with these quantitites being typically 10% and 20% too large, respectively.

Giving thus a reasonable reproduction of general thermostatic nuclear properties, the developed model presents a useful tool for theoretical studies of nuclear dynamical processes.

Footnotes and References

*Condensed from Phys. Lett. **B215**, 611 (1988)

1. C. Dorso, S. Duarte, and J. Randrup, Phys. Lett. **B188**, 287 (1987); J. Physique **48**, C2-143 (1987)

Deformation and Nilsson Configurations in A≈100 Nuclei*

K.-L. Kratz,[†] *B. Pfeiffer,*[†] *V. Harms,*[†] *E. Monnand,*[‡] *H. Gabelmann,*[†,§] *and P. Möller*[**,††]

Nuclear β-decay and deformation properties are studied experimentally and analysed with theoretical models based on Nilsson and folded-Yukawa single-particle models. The β-decay properties are studied in a quasi-particle RPA model[1] and the deformation properties are compared to a calculation based on the macroscopic-microscopic approach.[2] One observation is that in the Nilsson model it is difficult to find a parameter set that appropriately describes all nuclei in the $N = 56$ region. However, from comparing measured gross β-decay properties, such as $T_{1/2}$, P_n and S_β, to RPA calculations it is possible to tentatively assign Nilsson asymptotic quantum numbers to ground states, e. g., $\pi[431\frac{3}{2}]$ for ^{101}Rb, $\nu[411\frac{3}{2}]$ for ^{101}Sr and $\pi[422\frac{5}{2}]$ for ^{101}Y, respectively. As one moves away from $^{96}_{40}Zr_{56}$ one expects a gradual decrease in magnitude of the $N = 56$ subshell. However, for ^{92}Kr observations show an increase of $E(2^+)$ by about 60 KeV relative to ^{90}Kr, indicating a gap at $N = 56$ for $Z = 36$. The mechanism behind this change is not clear at present. Two possibilities that were suggested are that the effect is due either to an octupole instability at $\epsilon_2 = 0.0$ or to a *deformed* $N = 56$ subshell at $\epsilon_2 = 0.2$. From a comparison between experimental measurements of $T_{1/2}$, P_n and S_β and results of RPA calculations the latter possibility seems excluded.

Footnotes and References

*Condensed from: Z. Phys. A–Atomic Nuclei **330** (1988) 229 and Proc. Nuclei far from Stability, Fifth Int. Conf., Rosseau Lake, Ontario, Canada Sept. 14-19 1987, AIP Conference Proc. **164** (1988) 403 (New York 1988)

†Institut für Kernchemie, Universität Mainz, D-6500 Mainz, FRG

‡Department de Recherche Fondamentale, Centre d'Etudes Nucléaires, Grenoble, France

§CERN-ISOLDE, CH-1211 Geneva, Switzerland

**Idaho National Engineering Laboratory, EG&G Idaho Inc., Idaho Falls, ID 83415

††On leave from Department of Mathematical Physics, LTH, Box 118, S–221 00 Lund, Sweden

1. J. Krumlinde and P. Möller, Nucl. Phys. **A417**, 419 (1984).

2. P. Möller and J. R. Nix, At. Data Nucl. Data Tables **39**, 213 (1988).

New Features in the Calculation of Heavy-Element Fission Barriers*

P. Möller,[†,‡] *J.R. Nix,*[§] *and W.J. Świątecki*

We have calculated potential-energy surfaces and fission half-lives for heavy even and odd nuclei from $Z = 94$ to $Z = 110$. We base our study on the macroscopic-microscopic model. For the macroscopic part we use the Yukawa-plus-exponential (finite-range) model and for the microscopic part a folded-Yukawa (diffuse-surface) single-particle potential. To remove some deficiencies of the model that were associated with describing the transition from a single nuclear system to two different nuclear systems that occurs in the scission region, we have included three new features in the model. Shape dependences have been introduced for the Wigner and A^0 terms, a more appropriate smoothing range has been used in the Strutinsky shell-correction method, and the model has been extended to include odd-particle specialization energies for fissioning odd-particle nuclei.

We have also considered two additional effects in the calculations. The effect on saddle-point heights of mass-asymmetric shapes in the outer region of the new fission valley is included in a full three-

dimensional calculation of the potential-energy surface. The ϵ_6 shape-degree of freedom is included at the ground state. Because the effects of the new range in the Strutinsky method and the shape-dependent Wigner and A^0 terms approximately cancel we obtain results here that are very similar to those in our previous study.[1]

Our most important results may be summarized as follows. There are three paths in the calculated potential-energy surfaces, namely the old path, a new path to compact scission shapes and a switchback path from the new path to the old path. There is a much lower inertia associated with fission in the new valley than in the old valley. The new valley is present at least up to $Z = 110$ for neutron numbers close to $N = 2 \times 82$. Its existence lowers the fission half-lives of some of these elements relative to predictions that do not consider the new valley. Odd-particle specialization effects substantially increase the calculated fission half-lives also in the new valley. Because of the extreme sensitivity of the calculated fission half-lives to small changes in the ground-state potential energy, calculated and experimental half-lives agree with each other to within our expectations, despite the deviations seen in Fig. 1. The remaining deviations also suggest that fission along the switchback path should be be considered and that a microscopic model for how the inertia changes as one moves away from magic-fragment neutron and proton numbers should be developed.

Footnotes and References

*Condensed from Proc. Winter Workshop on Nuclear Dynamics V, Sun Valley, Idaho, 1988, (to appear) and P. Möller, J.R. Nix and W.J. Swiatecki Nucl. Phys. **A**

†Idaho National Engineering Laboratory, EG&G Idaho Inc., Idaho Falls, ID 83415, and Lawrence Livermore National Laboratory, Livermore, CA 94550, and Theoretical Division, Los Alamos National Laboratory, Los Alamos, NM 87545

‡On leave from Department of Mathematical Physics, LTH, Box 118, S–221 00 Lund, Sweden

§Theoretical Division, Los Alamos National Laboratory, Los Alamos, NM 87545

1. P. Möller, J.R. Nix, and W.J. Świątecki, Nucl. Phys. **A469** (1987)

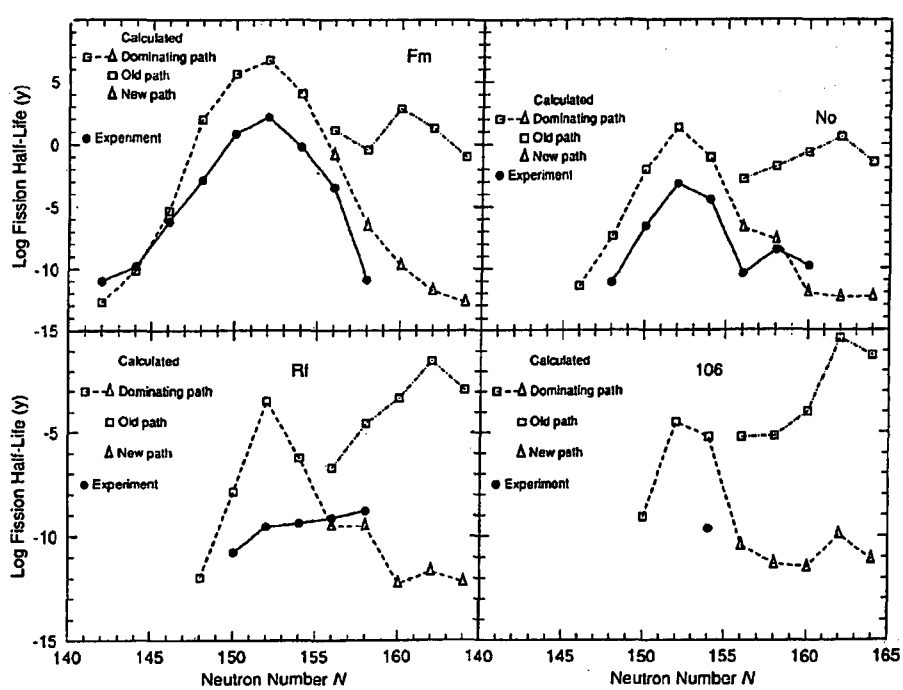

Fig. 1. Comparison between calculated and experimental fission half-lives. New path leads to the compact scission configuration of two touching spheres, old path to elongated scission shapes.

Astrophysical Implications of β-Strength and Shell Structure Properties far from Stability*

*K.-L. Kratz,† V. Harms,† A. Wöhr,† W. Hillebrandt,‡ W. Ziegert,†,‡ F.-K. Thielemann,‡,§ J. W. Truran,** and P. Möller††,‡‡*

Because of various uncertainties the theoretical predictions[1,2] of β-decay half-lives far from stability have been unable to provide substantial constraints on r-process scenarios. In our studies here we have used models[3–5] that account for nuclear structure effects on the β-strength function and on nuclear masses. Parameters of the single-particle models have been adjusted to reproduce properties of the waiting point nuclei ^{80}Zn and ^{130}Cd. With these parameters β-decay properties of astrophysical interest have been predicted for other waiting-point nuclei in the $N = 50$ and $N = 82$ regions. These calculations have yielded strong evidence that the solar r-abundances resulted from an (n-γ)-(γ-n) equilibrium and a β-flow equilibrium. This would exclude r-process scenarios that operate via a competition of neutron captures and β-decays like explosive He-burning. With these assumptions the single $T_{1/2}$ of ^{80}Zn implies a time scale longer than one second to build up the $A \approx 80$ r-abundance peak and pass the $N = 50$ waiting point. With the information that is becoming available from new nuclear structure calculations and experiments, further constraints may be put on different r-process models. Work in this direction is in progress.

Footnotes and References

*Condensed from Phys. Rev. C **38** (1988) 278 and J. Phys. G: Nucl. Phys. 14 Suppl. (1988) p. S331 and Proc. Nuclei far from Stability, Fifth Int. Conf., Rosseau Lake, Ontario, Canada Sept. 14-19 1987, AIP Conference Proc. **164** (1988) 558 (New York 1988)

† Institut für Kernchemie, Universität Mainz, D-6500 Mainz, FRG

‡Max-Planck Institut für Physik und Astrophysik, Garching, FRG

§Department of Astronomy, Harvard University, Cambridge, USA

**Department of Astronomy, University of Illinois, Urbana, USA

††Idaho National Engineering Laboratory, EG&G Idaho Inc., Idaho Falls, ID 83415

‡‡On leave from Department of Mathematical Physics, LTH, Box 118, S–221 00 Lund, Sweden

1. K. Takahashi, M. Yamada, and T. Kondoh, At. Data and Nucl. Data Tables, **12**, 101 (1973).

H.V. Klapdor, J. Metzinger and T. Oda, At. Data. Nucl. Data Tables **31**, 81 (1984).

J. Krumlinde and P. Möller, Nucl. Phys. **A417**, 419 (1984).

P. Möller and J. R. Nix, At. Data Nucl. Data Tables, **39**, 213 (1988).

P. Möller, W. D. Myers, W. J. Świątecki, and J. Treiner, At. Data Nucl. Data Tables, **39**, 225 (1988).

Comparison of Nuclear Transport Models on 800 AMeV La+La Data

J. Aichelin, J. Cugnon, K. Frankel, Z. Fraenkel, C. Gale, M. Gyulassy, D. Keane, C.M. Ko, J. Randrup, A. Rosenhauer, H. Stöcker, G. Welke, and J.Q. Wu

Since the discovery of collective nuclear flow phenomena in high energy nuclear collisions, there has been an intensified effort to develop microscopic nuclear transport models including effects due to nuclear mean fields. Before that time, intranuclear cascade models could reproduce most features of double

differential inclusive cross sections. However, when it became possible to measure triple differential inclusive cross sections for collisions of heavy nuclei with $A > 100$, it was found that the magnitude of the directed in-plane flow momenta was typically underestimated by a factor of two. To account for that discrepancy several groups developed transport models including effects of the repulsive nuclear mean field at high densities. While most of the new transport models can fit the observed in-plane flow momenta by adjusting the nuclear potential, $U(\rho, p)$, the best fit U differed substantially from one model to the next. At present, considerable controversy still surrounds the validity of particular model assumptions and the correct self-consistent formulation of high energy nuclear transport theory remains under active debate. The purpose of this work is to subject the models to a new test comparing calculated double differential p-like inclusive cross sections to recent data on La+La at 800 AMeV.[1,2]

The main result of this study is shown in Fig. 1. Part (a) compares Cugnon cascade model versions CG1 and CG2 with Fraenkel-Yariv cascade model FY. Part (b) compares momentum independent VUU and QMD with $K = 380$ MeV, to momentum dependent BUU with $K = 210$ MeV, and relativistic RVU. Part (c) shows effects at 20° and 60° of rescaling the free space NN cross sections in CG1 by a factor 0.5,1.0, and 3.0. The dotted curve shows results of the FREESCO fireball model FRS. Part (d) show the contributions to the 20° yield for QMD and CG2 from single collision ($N_c = 1$) and multiple collision ($N_c = 2 - 6$) components. We find that (1) the calculated p-like double differential cross sections are virtually identical in all models, i.e., these data are insensitive to the nuclear mean field effects, but (2) all calculations overpredict the 20 degree yield for momenta $p \gtrsim 1$ GeV/c. Therefore, either the systematic errors in the data have been underestimated and/or an important element of the reaction mechanism is still missing in all present models. We conclude that further tests of the nuclear collision term via double differential data on heavy nuclear collisions are urgently needed. More reliable constraints on the nuclear equation of state via detailed triple-differential differential cross sections will be possible only when the transport theories used in such analysis correctly reproduce first the basic double-differential cross sections.

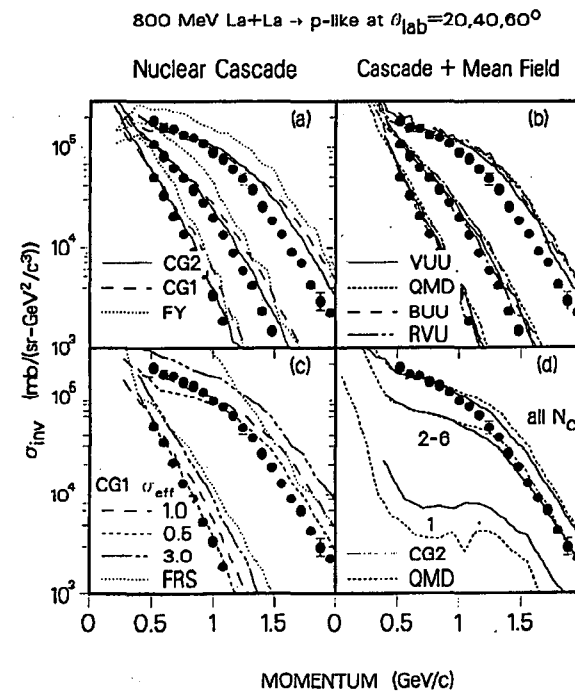

Fig. 1. Comparison of nuclear transport calculations to data.[1,2]

Footnotes and References

1. J. Aichelin *et al*, Phys. Rev. Lett. **62**, 1461 (1989).
2. S. Hayashi, *et al*, Phys. Rev. **C38**, 1229 (1988).

Implications of Pion Interferometry for O+Au at 200 GeV/nucleon*

M. Gyulassy and S.S. Padula

Correlations between identical pions provide unique information about the space-time dimensions of pion interaction region in hadronic processes. Recently, the NA35 collaboration[1] measured $\pi^-\pi^-$ correlations in O+Au at 200 GeV/nucleon and reported that the freeze-out distribution for pions in this reaction is characterized by a surprisingly large freeze-out proper time and transverse radius, $\tau_f \sim R_{\perp f} \sim 7$ fm. In addition, they reported an unusually high degree of coherence for pions away from the central rapidity region. These results are of interest because they may imply a breakdown of popular hadronic transport models like LUND and possibly provide evidence for novel dynamical effects associated with the formation of quark-gluon plasma in nuclear collisions. In this work, we show, however, that the above results are not conclusive and that the present data are in fact consistent with a wide range of pion source parameters when additional non-ideal dynamical and geometrical features are incorporated into the analysis. In particular, both the hadronic LUND transport model and a quark-gluon plasma hydrodynamic model[2] are found to be consistent with the present correlation data as shown in Fig. 1. We also study the sensitivity of "outward" and "sideward" transverse momentum interferometry and show that, in contrast to first expectations, much higher precision data will be required to differentiate between such competing dynamical models.

Footnotes and References

*Condensed from Phys. Lett. B **217**, 181 (1988).

1. A. Bamberger, *et al.* (**NA35** collab.) Phys. Lett. B203 (1988) 320.

2. G. Bertsch, M. Gong, M. Tohyama, Phys. Rev. **C37** (1988) 1896.

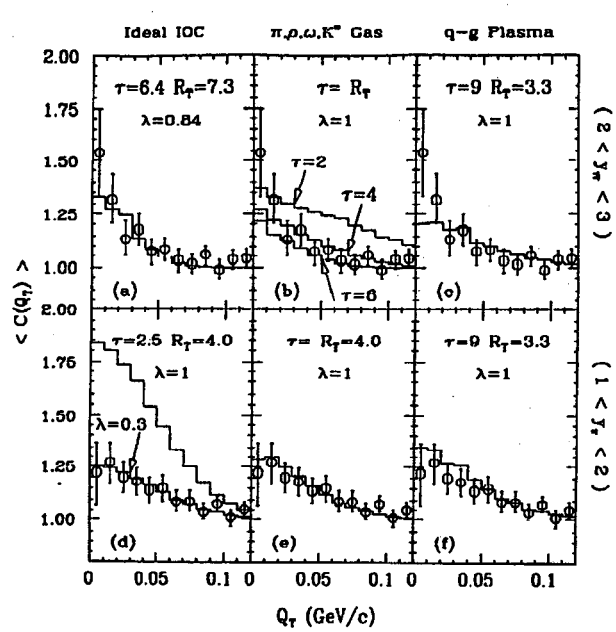

Fig. 1. Analysis of the transverse projected $\pi^-\pi^-$ correlation data of NA35[1]. The histograms in parts (a,d) are calculated assuming an ideal inside-outside cascade (IOC) source with parameters ($\tau \equiv \tau_f, R_T \equiv R_{\perp f}$) taken from [1]. In parts (b,e) a non-ideal resonance gas source is considered with parameters, $\tau \sim R_T \sim 4$ fm, as suggested by the ATTILA version of the LUND Fritiof model. Parts (c,f) correspond to the quark-gluon plasma model of [2]. Parts (a-c) refer to the central rapidity region, $2 < y_\pi < 3$, and parts (d-f) refer to the region $1 < y_\pi < 2$.

The Charge and Mass Dependence of Nuclear Interaction Cross Sections*

H.S. Chung† *and W.D. Myers*

The Thomas-Fermi model of Seyler and Blanchard[1] was employed for the purpose of calculating the interaction cross sections of nuclei as a function of charge and mass for comparison with the Bevalac experiments of Tanihata *et al.*[2] A set of force parameters was chosen for the model calculations that would give nuclear charge distributions in agreement with electron scattering and also be approximately correct for the nuclear binding energies. Then a simple Glauber Theory calculation was performed to determine the interaction radius R_I for comparison with the measured values. The agreement can be seen in Fig. 1. As expected the α particle is more compact than the statistical model prediction. It is also to be noted that the measured values for ^{11}Li and ^{14}Be both lie well above the model values.

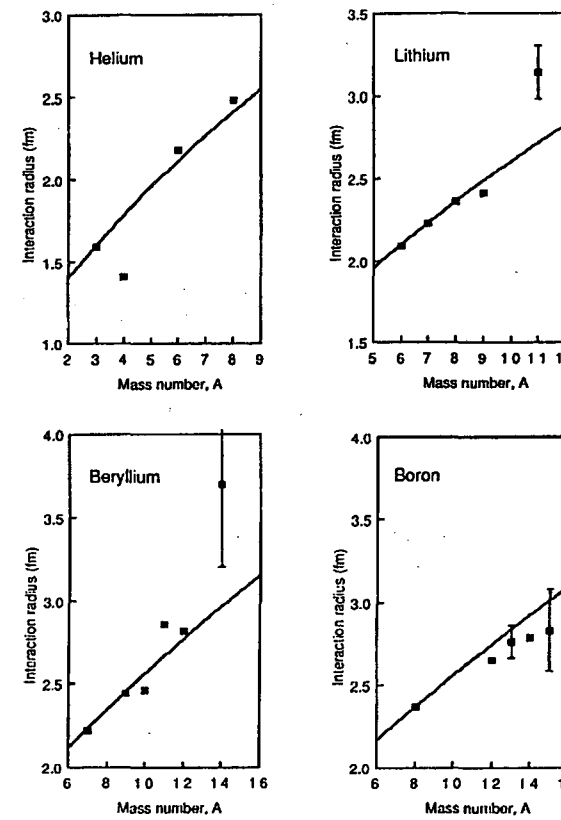

Fig. 1. The interaction radii R_I are plotted against the mass number A for different isotopic sequences. The solid squares represent the measured values for isotopes of helium, lithium, beryllium, and boron. The interaction radii calculated from the Thomas-Fermi density distributions are indicated by the lines in each figure.

Footnotes and References

*Condensed from LBL-26284

†1813 Windsong, Richardson, TX 75081

1. R.G. Seyler and C.H. Blanchard, Phys. Rev. 131 (1963) 355.

2. I. Tanihata *et al.*, Phys. Lett. ^{206}B (1988) 592.

On the Phase Equilibrium of Nuclear Matter*

C.-S. Wang† *and W.D. Myers*

The phase equilibrium of nuclear matter is studied at zero temperature. In the equation of state obtained from the Thomas- Fermi model of Seyler and Blanchard[1] two different phases of nuclear matter are possible: gas and liquid. Normal nuclear matter with equal numbers of neutrons and protons is a liquid, and pure neutron matter is always in the gas phase. For nuclear matter with two semi-infinite half spaces in contact at a plane boundary, we have studied the phase equilibrium in three cases determined by the value of the bulk nuclear matter asymmetry δ, defined in terms of the neutron and proton densi-

ties on the nuclear matter side of the boundary by the expression: $\delta = (\rho_N - \rho_Z)/(\rho_N + \rho_Z)$. The first case concerns nuclear matter from $\delta = 0$ up to the neutron drip point at $\delta_{ND} = 0.305$ where a neutron gas begins to appear in the previously empty half space on the other side of the boundary. The second case of interest is from the neutron drip point to the proton drip point at $\delta_{PD} = 0.678$, and the final case extends from the proton drip point up to a critical value of $\delta_C \approx 0.89$ where the difference between the two half spaces disappears and the system becomes homogeneous.

Footnotes and References

*Condensed from Comm. Theor. Phys. (Beijing, China) 8 (1987) 397

†Department of Technical Physics, Peking University, Beijing, China

1. R.G. Seyler and C.H. Blanchard, Phys. Rev. 131 (1963) 355.

The Effective Stiffness of Nuclei Near Magic Numbers*

W.D. Myers and P. Rozmej

In a recent study[1] of the isotope shifts for a long sequence of rubidium isotopes[2] (N = 39 to 61) we found that we were not able to explain the rapid increase in the apparent size of these nuclei around the magic number N = 50. Most workers in the field had assumed that the observed behavior was associated with collective zero-point motion, even though no calculations of this effect had been successful in establishing the connection. In order to further investigate the differences that remain between the measured values of the change in nuclear charge radius and the values that we calculated, we converted the width of the wave function in the collective coordinate to an effective stiffness against quadrupole distortions C. These values are shown as filled circles connected by a solid line in Fig. 1. The nuclei near the magic number are seen to be stiffer than the liquid drop model prediction (C $\approx$ 86 MeV) and the nuclei further away seem to be softer. The dashed line in the figure represents the behavior of the effective stiffness C_{eff} that would be required to correctly reproduce the observed size changes. The transition away from N = 50 is extremely abrupt, far in excess of any change that could be expected in the microscopic calculation of the potential energy surfaces.

Footnotes and References

*Condensed from a paper presented at the Winter Workshop on Nuclear Dynamics V, Sun Valley, ID, February 22-26,1988

†Department of Theoretical Physics, University of Lublin MCS, Lublin, Poland

1. W.D. Myers and P. Rozmej, Nucl. Phys. **A470** (1987) 107.

2. C. Thibaut, *et al.*, Phys. Rev. **C23** (1981) 2720.

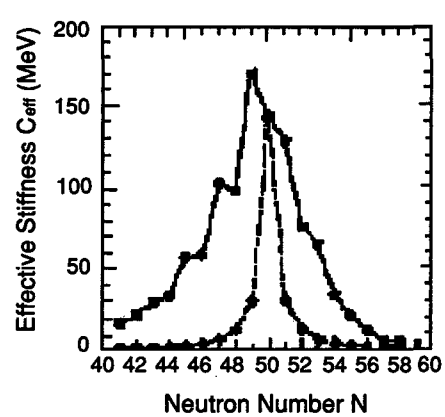

Fig. 1. The effective stiffness C_{eff} of a sequence of rubidium isotopes plotted against neutron number.

Dense Skyrmion Systems

L. Castillejo, P. S.J. Jones, A.D. Jackson, J. J.M. Verbaarschot, and A. Jackson

The Skyrme model,[1] is used to investigate dense baryonic matter. Solutions of static close packed skyrmions in arrays with fcc symmetry as well as bcc and intermediate symmetry are considered as a function of the density, and the phase transition into regular arrays of half skyrmions is investigated. There are several rather general conclusions to be drawn from these calculations. The salient feature is that there is a robust phase transition from a system of isolated skyrmions with no strongly preferred symmetry to a regular lattice of half skyrmions as the density is increased. The transition is in general second order and the condensed system has a lowest energy per baryon that is just 3.8% above the theoretical lower bound. This minimum occurs in the condensed half skyrmion phase corresponding to the fcc array. The phase transition and condensed phase look remarkably similar to the solution of Manton,[2] on a 3-sphere. The energy minimum occurs at a density of $0.217Fm^{-3}$ and the phase transition at $0.068Fm^{-3}$. These should not be compared directly to nuclear matter density $0.17Fm^{-3}$. Skyrmion matter contains both nucleons and Δ and the latter have not been projected out. At high density this may be a reasonable approximation but not at low densities. Furthermore the present calculations contain only potential terms and no kinetic energy contributions. The effects of including these to one loop order can be crudely estimated from the work of Zahed *et al.*,[3] for a single skyrmion on R_3 and Generalis and Williams[4] for S_3.

Footnotes and References

1. T.H.R. Skyrme, Nucl. Phys **31**, 556 (1962)

2. N.S. Manton, Commun. Math. Phys. **111**, 469 (1987)

3. I. Zahed, A. Wirzba and U.-G. Meissner, Phys. Rev. **D33**, 830 (1986)

4. S. Generalis and G. Williams, Nucl. Phys. **A484**, 620 (1988)

String-like Solutions in the Skyrme Model

A. Jackson

The equations of motion of the Skyrme model[1] with a mass term are studied, and we find a number of new solutions of the static equations of motion. These solutions are of the form that the gradients can be diagonalised in a suitably chosen orthonormal set of curvilinear coordinates. These properties have enabled us to solve the equations of motion with simple ansatze. In addition, we use these methods to demonstrate that the hedgehog (skyrmion) solves the equations.

The new solutions include a string-like solution having cylindrical symmetry, and a slab-like solution. The string-like solutions may be relevant to nuclear physics since one may speculate that these solutions are related to the QCD string. The string tension of the cylindrical solution is found to be approximately 0.85 GeV/fm. The size of the pion field in these solutions can be as large as $\sim f_\pi$. Nevertheless, due to the dimensional character of the solutions, they have baryon density zero everywhere. In consequence, all of the solutions presented here are classically unstable and can be expected to decay. Therefore, they require special physical circumstances (in which appropriate boundary conditions occur) to create them.

In the case of the string, the circumstances are similar to those where one normally uses Q.C.D. strings. For example, when the baryon density of a nucleon is separated into two pieces, unless baryon density is produced between these pieces one is forced (by continuity of the pion field) to have a tube of energy density between them. The character of this tubular field is similar to that of the string solution. The string solution is therefore expected to have a

wide variety of potential applications in nuclear and hadron physics.

For the solutions that cover a one-dimensional subspace of the internal space, the situation is more awkward. The typical form of the boundary values needed to produce these solutions are non trivial conditions imposed on the field on large surfaces or volumes. It is difficult to think of circumstances accessible to experiment in nuclear physics that fit the bill. Two possibilities come to mind. The first is in stopped collisions of ultra-relativistic heavy ions, where the stopped nucleons might be expected to throw off a large-amplitude pion field with a slab-like form. The second involves star-quakes on the surface of a neutron star. The position is more hopeful in solid-state physics, where the boundary conditions of the systems under investigation are more easily manipulated.

The instability that causes the string solution to decay has interesting properties in its own right. From continuity arguments, one can see that to produce the vacuum between the ends of the string one must produce (minimally) half a skyrmion and half an anti-skyrmion. The decay of the string is therefore accompanied by the production of baryon density, a feature reminiscent of the decay of a Q.C.D. string. These properties are investigated more fully elsewhere[2]

The Skyrme string and the Q.C.D. string occur in similar physical circumstances and have intriguing properties in common. However, there are several qualitative differences and problems that prevent one from making a firm identification between the two without modification of the Skyrme string. The most obvious of these is the absence of a chiral limit for the Skyrme string: we have shown that the width of the Skyrme string grows indefinitely as one takes the chiral limit. (Note though, that while the radius of the string dilates indefinitely as $m_\pi \to 0$, the string tension does not go to zero, due to the Bogomol'ny bound).[3]

Footnotes and References

1. T.H.R. Skyrme, Nucl. Phys. **31,** 556 (1962); T.H.R. Skyrme, Nucl. Phys. **31,** 550 (1962); T.H.R. Skyrme, Proc. Roy. Soc. London. **262,** 237 (1962); T.H.R. Skyrme, Proc. Roy. Soc. London. **260,** 127 (1961).

2. A. Jackson, "The decay of the string in the Skyrme model", LBL Preprint, LBL-25815 (1988).

3. A.A. Belavin and A.M. Polyakov, JEPT Lett. **22,** 245 (1975).

The Decay of the String in the Skyrme Model

A. Jackson

We discuss the decay of an unstable string-like solution in the Skyrme model.[1] Previously, we found this solution to have a string tension of approximately 0.85 GeV/fm.[2] String-like configurations in the Skyrme model arise naturally when objects with complimentary baryon number fractions are separated. These configurations are unstable, and we construct an homotopy that deforms the string-like solution to the vacuum while monotonically decreasing its energy. During the decay a baryon current flows along the string, producing half a baryon and half an anti-baryon. This production occurs wherever and whenever the string snaps, a feature startlingly reminiscent of the production of quark anti-quark pairs in Q.C.D. string models. We can restate these results in a particularly clear way using topological arguments. Topological charge is confined into integer lumps. When fractions of a baryon (say f and $(1-f)$) are separated from each other *without production of charge anti-charge density* then the energy of such a configuration will increase *at least* linearly with the separation. To circumvent this result, it is necessary to produce topological charge-anticharge density between the separated fractions. This charge anti-charge density *screens* the original topological charge density. This fits very nicely with the conjecture advanced by Witten.[3] Long strings can decay via many different decay modes, some pro-

ducing baryon anti-baryon pairs. Finally, we solve the equation of motion for the initial infinitesimal fluctuations that cause the decay, finding the form and growth rate of the unstable mode.

Several problems remain before one can hope to firmly associate the string-like configurations discussed here with Q.C.D. strings. However, if the connection of the Skyrme string to the Q.C.D. string can be made stronger, many applications suggest themselves. For example, in modeling the relativistic heavy ion collisions performed at CERN, frequent use is made of string models.[4] The density of strings arising from individual nucleon nucleon collisions in these models is on the order of $2/\mathrm{fm}^2$. It is therefore of urgent practical interest to understand the interactions that are possible between these strings. The interaction between Skyrme strings can be studied in the same way as the interactions between skyrmions and two-dimensional skyrmions, using the product ansatz[5] or lattice methods.[6,7] The latter suggests interesting possibilities. When the density of two-dimensional skyrmions gets large, a phase transition takes place restoring chiral symmetry and the skyrmions lose their individual identity.

Footnotes and References

1. T.H.R. Skyrme, Nucl. Phys. **31,** 556 (1962); Nucl. Phys. **31**, 550 (1962); Proc. Roy. Soc. London. **262,** 237 (1962); Proc. Roy. Soc. London. **260,** 127 (1961).

2. A. Jackson, "String-like solutions in the Skyrme model", LBL Preprint, LBL-25794 (1988) (accepted for publication in Nucl. Phys.

3. E. Witten, Nucl. Phys. **B223,** 433 (1983).

4. B. Andersson, G. Gustafson, and B. Nilsson-Almqvist, Nucl. Phys. **B281,** 289 (1987).

5. A. Jackson, A.D. Jackson and V. Pasquier, Nucl. Phys. **A432,** 567 (1985).

6. I. Klebanov, Nucl. Phys. **B262,** 133 (1985); E. Wust, G.E. Brown and A.D. Jackson, Nucl. Phys. **A467,** 450 (1987); N. Manton and A.S. Goldhaber, Phys. Lett. **198B,** 231 (1987).

7. "Solitons and superconductivity in two dimensions", A.D. Jackson, J.J.M. Verbaarschot, I. Zahed and L. Castillejo, Stony Brook Preprint (1988)

An Approach to General Covariance in String-Space of BRST String Field Theory*

J. Greensite† *and F.R. Klinkhamer*‡

We show that BRST quantized string field theory can be made invariant under string-dependent general coordinate transformations $x'^{\mu\sigma_1} = x'^{\mu\sigma_1}[x(\sigma)]$, where $\mu = 0,1,\ldots,D\text{-}1$ and $0 \leq \sigma \leq \pi$. This invariance is achieved by introducing a string-space metric tensor $g_{\mu\sigma_1,\nu\sigma_2}$ $[x(\sigma)]$, and following the usual steps of general relativity, with these differences: A constraint which we term "tangent contravariance," must be imposed on the coordinate transformations and metric tensor. This restriction emerges from requiring that $\partial_\sigma x^\mu$ transforms in string-space as a contravariant vector. Further stringent constraints on the metric tensor, including Ricci-flatness, arise from demanding nilpotence of the BRST charge.

Footnotes and References

*Condensed from Phys. Rev. **D39**, 2317 (1989)

†Physics and Astronomy Department, San Francisco State University, San Francisco, CA 94132

‡Physics Department L-413, Lawrence Livermore National Laboratory, University of California, CA 94550

Hard-Photon Production in the Nucleon-Exchange Transport Model*

J. Randrup and R. Vandenbosch†

We have extended a previously developed model[1] for pre-equilibrium nucleon emission following stochastic exchange of nucleons to include photon production as a perturbative process. The photons arise from bremsstrahlung radiation associated with p-n scattering of the transferred nucleons as they propagate through the receptor nucleus. No new parameters are introduced in this extension of our model to include photon emission.

The formalism for calculating photon emission from p-n collisions in nuclear matter was tested against the only relevant photon yield data for nucleon-nucleus reactions and the agreement is moderately good. We have also calculated inclusive energy spectra for all nucleus-nucleus collisions that have been studied at bombarding energies below 50 MeV/N. Again the agreement is generally good; for several studies with Ar and Kr projectiles the agreement is remarkably quantitative. With the exception of an early angular distribution measurement, our calculations of angular distributions are also in good agreement with experiment. The comparisons of the energy spectra and angular distributions with experiment suggest that bremsstrahlung production is the dominant mechanism for producing photons with energies in excess of approximately 30 MeV. We have also performed calculations to define impact parameter ranges for central and peripheral reactions. These calculations give a near-quantitative reproduction of a number of experimental results.

Furthermore, we have shown that the high-energy photons originate from collisions induced by nucleon exchange at an early stage of the nucleus-nucleus collision. First collisions are the dominant source of hard photons, particularly those with highest energy. The heating of the receptor nucleus due to prior collisions significantly increases the yield and also reduces the slope of the energy spectra, but is less important for photons than for pre-equilibrium neutrons in determining the spectra and angular distributions. We have found that simple scaling laws applicable to symmetric entrance channel reactions are not successful for asymmetric reactions.

Footnotes and References

*Condensed from Nucl. Phys. **A490**, 418 (1988)

†Nuclear Physics Laboratory, University of Washington, Seattle, Washington

1. J. Randrup and R. Vandenbosch, Nucl. Phys. **A474** (1987) 219

Further Studies of the Macroscopic Nuclear Surface Response*

V.I. Abrosimov† *and J. Randrup*

Recently, we studied the macroscopic response of the nuclear surface within the framework of Landau's kinetic equation.[1] In that work, the idealized limit of vanishing quasiparticle interaction was considered and a surface mode with a purely imaginary frequency was found. In the present work, we incorporate the quasi-particle interaction. By retaining the first *two* terms in the expansion of the normal surface stress in powers of the external frequency, we obtain an improved dispersion relation,

$$i\frac{3}{4}\rho_0 p_F\omega + \frac{1}{2}(\frac{3\pi}{8})^2\frac{F_0}{1+F_0}\frac{m\rho_0}{k_\perp}\omega^2 \;=\; \sigma k_\perp^2 \;,$$

which admits a truly complex eigenfrequency ω.

The above relation yields explicit expressions for the friction coefficient and the inertial mass for the damped surface motion. It is gratifying to note that the friction coefficient is identical to the that given by the standard wall formula.[2] On the other hand, the expression derived for the inertial mass is

directly proportional to the strength of the quasiparticle interaction, F_0, and is not expected to be as reliable as that obtained with the more realistic RPA calculations.[3]

The resulting response function has a finite integral and yields a good absolute reproduction of the gross behavior of the surface response observed via inelastic proton scattering.

Footnotes and References

*Condensed from Nucl. Phys. **A489**, 412 (1988)

†Institute for Nuclear Research, Prospect Nauki 119, 252028 Kiev, USSR

1. V.I. Abrosimov and J. Randrup, Nucl. Phys. **A449**, 446 (1986)

2. J. Błocki, Y. Boneh, J.R. Nix, J. Randrup, M. Robel, A.J. Sierk, and W.J. Swiatecki, Ann. Phys. **113**, 330 (1978)

3. G.F. Bertsch and H. Esbensen, Phys. Lett. **161B**, 248 (1985)

The Decay of Hot Nuclei*

L.G. Moretto and G.J. Wozniak

At low excitation energies, a dominant source of complex fragments is the binary decay of the compound nucleus (CN). If there is enough excitation energy available, the primary binary-decay products are also very excited and have a significant probability of decaying in turn into two fragments. In this very conventional way, one can foresee one possible explanation for several fragments in the exit channel (multifragmentation), namely several sequential binary decays. At high energies, these multifragment events may be responsible for a substantial background to other predicted multifragmentation mechanisms.

This process of sequential binary decay, controlled at each stage by the CN branching ratios, we call "nuclear comminution".[1] The limitations of this process are of two kinds: extrinsic and intrinsic.

The most obvious extrinsic limitation is the ability of the system to form a CN. In other words, the relaxation times associated with the CN formation may be too long when compared to the dynamical times leading the system to a different fate. Limitations of this sort are of course shared by all other multifragmentation modes involving an intermediate relaxed system.

The intrinsic limitations are associated with the aspect of sequentiality. Should two sequential binary decays occur too close in space-time, they would interact to an extent incompatible with the definition of sequentiality. In this case one may be lead to favor models in which fragments are formed simultaneously. Nonetheless, it may be possible to extend the sequential binary model to situations in which the interaction between two successive decays is only strong enough to perturb the angular distributions. The decay probabilities are overwhelmingly affected by the level densities of the corresponding final states. These level densities arise almost completely from the intrinsic degrees of freedom. The collective degrees of freedom on which the angular distributions depend hardly contribute to the level densities. Therefore, one can observe a multifragment pattern, whose branching ratios are still clearly binary, while the angular distributions may be substantially perturbed.

The lesson to be learned from these considerations is that the best way to establish the underlying mechanism of a multifragmentation process is to study the excitation functions of binary, ternary, quaternary events, which of course reflect the energy dependence of the branching ratios, and not to be troubled too much, should the angular distributions indicate multifragment interaction.

The calculations of the resulting mass distributions are trivial although tedious and time consuming. We have used the code GEMINI to generate

complete events on the basis of standard compound nucleus branching ratios. Examples of events with three and four complex fragments plus a multitude of lighter particles are illustrated in Figs. 1 and 2.

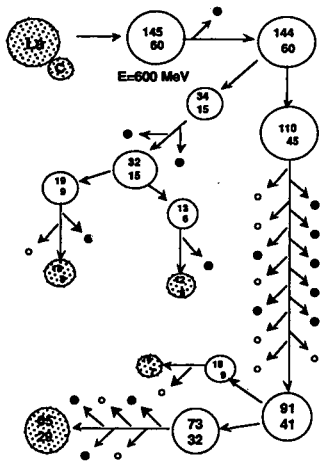

Fig. 1. An example of a sequential multifragment (4-body) event from the compound nucleus ^{145}Eu (ℓ_{max} = $60\hbar$, E_x = 600 MeV) as calculated by the statistical model code GEMINI. Evaporated neutrons and light charged particles (Z$\leq$22) are shown by the filled and open circles, respectively. Residue nuclei and complex fragments are labelled by their mass and charge numbers.

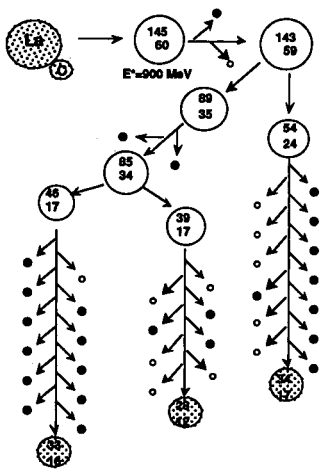

Fig. 2. An example of a sequential multifragment (3-body) event from the compound nucleus ^{145}Eu (ℓ_{max} = $60\hbar$, E_x = 900 MeV) as calculated by the statistical model code GEMINI.

Of course, the analysis of individual complete events does not reveal the "statistical" nature of the branching ratios. Little can be said concerning the fact that the first "binary" decay is in one case occuring at the beginning of the cascade and in another quite late in the cascade after the emission of a multitude of light particles. Nor is the selection of these "particular" events among a plethora of ordinary binary decays conducive to an appreciation of the underlying statistical processes. These can be appreciated more directly in the excitation functions for events with one, two, three, etc. fragments in the exit channel, like those plotted in Fig. 3. Here one can get, at a glance, a "qualitative" feeling of the statistical competition beside the direct quantitative predictions. In view of the uncertainies in the barriers used in the calculations, plus the fact that the temperature dependence of the barriers themselves has not been included, the qualitative dependence of the branching ratios upon energy may be the most important lesson to be derived from this exercise.

Footnotes and References

*Condensed from LBL-26207.

1. Prog. in Part. and Nucl. Phys. **21**, 401 (1988).

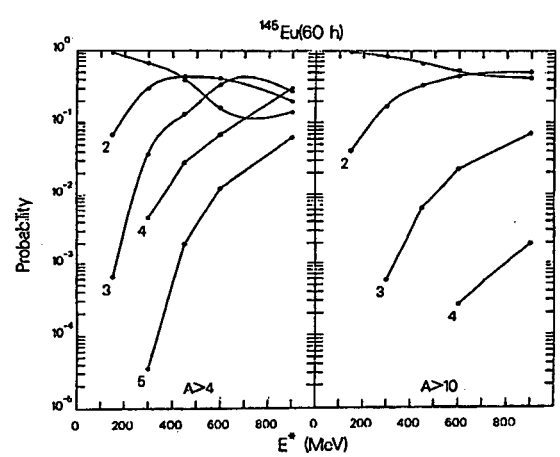

Fig. 3. Probability of producing exactly one, two, three, etc. fragments a) with A>4, b) A>10 as a function of excitation energy for the compound nucleus ^{145}Eu(ℓ_{max} = $60\hbar$).

Nuclear Spinodal Decomposition*

J.A. Lopez and G. Lubeck

We use computer simulations to study nuclear fragmentation as expected to occur in heavy ion reactions. Using a potential with an equation of state resembling that of hot and dense nuclear matter, we study the disassembly of two-dimensional classical drops. Along the lines of Cahn's theory of spinodal decomposition we calculate the structure factor of the system and extract information about the development of density fluctuations during the breakup. We observed a growth of these fluctuations after the expanding system enters the isothermal spinodal (see Fig. 1). We conclude that isothermal spinodal decomposition plays the dominant role in the breakup. Nucleation of bubbles in the two-phase region and adiabatic spinodal decomposition were found not to contribute to the fragment production. Strong density fluctuations were detected in disassemblies crossing the critical point.

Footnotes and References

*Condensed from LBL-26231

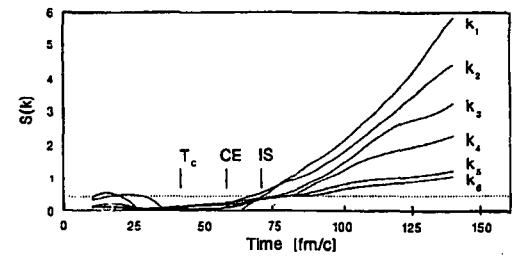

Fig. 1. Components of the structure factor S(k) as a function of time. Tc, CE and IS point to the times when the system crosses the critical temperature, coexistence curve and isothermal spinodal line, respectively. The wavenumbers correspond to the zeroes of the Bessel function Jo: 8.65, 11.79,... The dotted line represents the background fluctuations expected for thermal fluctuations in an infinite medium for the lowest wavenumber.

Hot Nuclei in a Nucleon Vapor*

G. Fai† *and J. Randrup*

We consider excited nuclear matter at densities somewhat below the saturation density, and at temperatures of the order of ten MeV, where the system can be described in terms of excitable nuclear fragments which interact with one another and are embedded in a nucleon vapor. We focus particularly on the description of a single such cluster, a *quasifragment*, embedded in a hot vapor of nucleons. Such a quasifragment can be regarded as a generalization of the concept of an ordinary atomic nucleus at low temperatures (where the coupling to the vapor is unimportant). The quantitative importance of incorporating unstable excited states into statistical models for nuclear disassembly is brought out by experimental evidence indicating that metastable composite fragments are formed abundantly in nuclear collisions at medium energies.

The partition function $\tilde{Z}_A$ for a quasi-fragment can be written in terms of its effective density of single-particle states,

$$\ln\tilde{Z}_A = \int \tilde{g}_A(\epsilon)\ln[1+e^{-\alpha-\beta\epsilon}]d\epsilon \quad . \qquad (1)$$

A 'parameter-free' definition of the effective single-particle level density $\tilde{g}_A(\epsilon)$ can be given in terms of the quantum-mechanical reflection coefficient for a nucleon in a given single-particle orbital, by demanding that the given orbital be considered as belonging to the fragment with a probability equal to its associated reflection coefficient $R_\ell(\epsilon)$. Thus, we advocate using $\tilde{g}_A(\epsilon) = \bar{R}_A(\epsilon)g_A^{FG}(\epsilon)$, where $g_A^{FG}(\epsilon)$ is the unmodulated Fermi-gas single-particle density of states and $\bar{R}(\epsilon)$ is the average reflection coefficient at the particular energy ϵ.

This prescription for defining a very excited com-

pound nucleus yields a mass-dependent limiting nuclear temperature, decreasing from 10–12 MeV for heavy nuclei to around 8 MeV for $A \approx 10$. Various other, commonly employed prescriptions for treating a single quasifragment have also been studied and compared.

Footnotes and References

*Condensed from Nucl. Phys. **A487**, 397 (1988)

†On leave of absence from Department of Physics, Kent State University, Kent, Ohio 44242

Hot Gluon Plasma at Large Distances*

R.F. Alvarez-Estrada and J.A. Lopez

We study some general features of the pure gluon plasma in equilibrium at high temperature and large distances, using both imaginary- and real-time formalisms. The plasma description in terms of a (confining) Yang-Mills theory in three spatial dimensions (YM-3) for magnetic gluons is outlined. Arguments are given that imply that, in such a regime, neither a direct quartic coupling of electric gluons nor a Higgs-like mechanism contribute. It is also shown that the only renormalization group equation valid in that regime is the trivial one, associated to the super-renormalizable YM-3 theory, and, on basis of this, it is argued that there are no free gluons at large distances. The real-time gluon Green function is given to one loop order and the instabilities it produces in the gluon plasma are displayed. These instabilities appear to reflect the long-range confining behavior of YM-3.

Footnotes and References

*Condensed from LBL-25866

Multifragmentation versus Sequential Fission: Observable Differences?*

J.A. Lopez and J. Randrup

To elucidate the observable distinctions between different reaction mechanisms for multifragment production in nuclear collisions at intermediate energies, we contrast two opposite extremes: sequential binary fission and simultaneous multifragment breakup (true multifragmentation). For identical multifragment channels produced by these two idealized mechanisms, we examine the kinetic-energy spectra and other quantities derived from the velocities of the observed fragments and find several noticeable differences. In particular the folding-angle distribution, which is rather simple (both conceptually and practically) and relates directly to the heavy fragments, appears to be a useful discriminator between the different disassembly mechanisms (see fig.1).

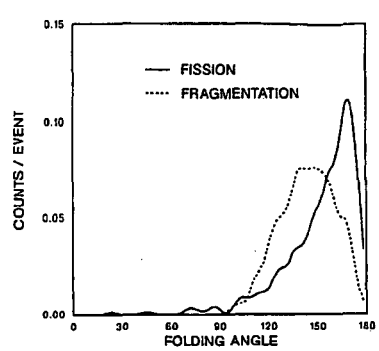

Fig. 1. Distribution of the asymptotic angles formed by the two heaviest fragments in each of 500 events of the decay of A=150, Z=62 at excitation energy per nucleon of 5 MeV/N. Sequential decay products appear to have been emitted nearly back-to-back, whereas the simultaneous breakup leads to folding angles peaked around 140 degrees.

Footnotes and References

*Condensed from LBL-25664

Nuclear and Astrophysical Evidence on the Equation of State

N.K. Glendenning

Evidence on the nuclear equation of state from a number of different sources, from nuclei, high energy nuclear collisions, supernova explosions and neutron stars is analyzed. From nuclear evidence, we examine the Landau sum rule and the droplet model of atomic masses as constraints on K. For relativistic nuclear collisions we employ nuclear field theory in a description of the hot dense matter to compute pion yields for differing coupling constants corresponding to soft and stiff equations of state. The current situation concerning supernova simulations is critically analyzed. It is shown that supernova explosions of the prompt kind have not yet been proven viable, since the equations of state employed were too soft to support known neutron stars against gravitational collapse. Consequently supernovae have not yet been demonstrated to provide a constraint on the nuclear equation of state, as has been claimed. In contrast to the prompt mechanism, the late-time neutrino reheating mechanism produces neutron stars of a wide spectrum of masses, depending on the progenitor. Consequently the data on neutron star masses should be taken literally as meaning that neutron stars *can* have any mass up to the black hole limit. Their masses are computed in relativistic field theory, and the reinterpretation of the data demanded by the above observation now implies a stiff equation of state. Additional evidence from the flow angle in relativistic nuclear collisions and new results on the Giant monopole resonance are reviewed. A summary of the current situation is shown in the figure.

Footnotes and References

*Condensed from Phys. Rev. C **37**, 2733 (1988)

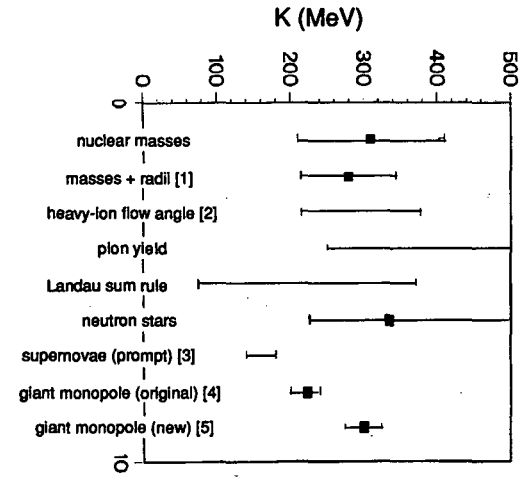

Fig. 1. See text.

Skyrme Topological Soliton Coupled to Gravity*

N.K. Glendenning, T. Kodama,† F.R. Klinkhamer,‡

In a recent series of papers, Friedberg, Lee and Pang[1] carried out an investigation of non-topological soliton stars and black holes. It was shown that, corresponding to a simple Lagrangian for a scalar field together with a meson or fermion field, a variety of interesting structures might exist, ranging from mini to massive soliton stars and black holes. Inspired by these results, we investigate the Skyrme topological soliton for large topological quantum number or large energy scale in general relativity for the purpose of learning whether stable or metastable stars consisting of a single topological soliton might exist. The Skyrme soliton[2] has attracted much interest in the last several years because of developments in QCD concerning the large N_c limit and because its properties resemble those of nucleons at the 30-40% level. We derive a variational technique for getting an approximate solution to Einstein's equations and the field equation of the matter field. The size of Skyrmions is independent of the topological quantum number, N, so that they must become black holes for sufficiently large N. Below the critical point, gravity contributes about 15% binding. However, loss of radial stability against collapse occurs before the

binding is great enough to provide single-particle stability. On the nucleon scale where $f_\pi \approx 70$ MeV, the critical topological number is $N_c \approx 10^{19}$ in contrast to neutron stars where the critical baryon number is $\approx 10^{57}$. The critical mass on the nucleon scale is $M_c \approx 0.5 \times 10^{-20} M_\odot$. We do not find stable or metastable Skyrmions between $N = 1$ and the black hole, at any energy scale, f_π. Such mini-black holes could have been created at the beginning of the Universe. It is unlikely that conditions favorable for their creation would occur at later times.

Footnotes and References

*Condensed from LBL-25129

†Permanent address: Centro Brasileiro de Pesquisas Fisicas, Rio de Janeiro - RJ - CEP **22920**, Brasil

‡Physics Department Lawrence Livermore National Laboratory University of California Livermore, California 94550

1. T.D. Lee, Phys. Rev. D **35**, 3637 (1987); R. Friedberg, T.D. Lee and Y. Pang, Phys. Rev. D **35**, 3640 (1987); ibid. 3658; T.D. Lee and Y. Pang, Phys. Rev. D **35**, 3678 (1987).

2. T.H.R. Skyrme, Proc. Roy. Soc. **A260**, 127 (1961).

Quark Matter '87: Concluding Remarks*

M. Gyulassy

In this report a summary of the Quark Matter 1987 Conference is presented. Possible implications of the preliminary findings of new CERN and AGS data for the search of the quark-gluon phase of matter are discussed. Problems needing further theoretical and experimental study are pointed out. Topics covered include estimates of initial conditions in nuclear consitions in the Landau stopping domain and the Bjorken scaling domain, extrapolation models from p+p to A+A collisions based on string models such as LUND, the space-time geometry of freeze-out, the unusual A dependence of the transverse momentum in hydrodynamic models, nuclear stopping power, the suppression of J/ψ and the enhancement of K^+/π^+, and the current status of QCD thermodynamics.

Footnotes and References

*Condensed from Z. Phys. **C38**, 361 (1988).

Comment on "Type-II Supernovae from Prompt Explosions"

N.K. Glendenning

The authors of a recent paper[1] seek to account for SN1987a, the supernova event of early 1987, with the prompt-bounce mechanism using a nuclear equation of state based on the parameterization known as BCK.[2]

It is characterized by the compression modulus $K(x)$ at the relevant proton fraction, $x = Z/A$ and by an index γ, whose value in ref. 1 is 2.5. The particular parameters used give $K(1/2) = 180$ MeV for nuclear matter. We have solved the Oppenheimer-Volkoff equations of star structure for the above parameters. Our results are shown in Fig. 1, for the value of $x = \frac{1}{3}$ employed in the supernova simulation, and for a somewhat smaller one, as might be claimed pertinent to a neutron star. The maximum mass is seen to be smaller than the masses of two known neutron stars. One is the very accurately measured mass of PSR1913+16,[3] and the other is the less well known mass of 4U0900-40.

Therefore an explosion energy large enough to eject the mantle promptly is bought, in the simulation, at the price of an equation of state that is too soft to support several neutron stars of known mass.

We have also tested those equations of state employed in ref. 2 that are cited to produce successful first bounce supernovae. Of the five successful cases, four are incompatible with neutron star masses and the remaining one, ($K(1/2) = 180$ MeV $\gamma = 3$), yields a low explosion energy.

In summary, it has not yet been demonstrated that supernovae can explode on the prompt bounce, and the now much quoted claim that supernovae events provide evidence of a soft equation of state , is therefore premature, especially since there exists an alternative mechanism[4] that works without the restriction on the equation of state .

Footnotes and References

*Condensed from LBL-24172

1. E. Baron, H.A. Bethe, G.E. Brown, J. Cooperstein and S. Kahana, Phys. Rev. Lett. **59** (1987) 736.

2. E. Baron, J. Cooperstein and S. Kahana, Phys. Rev. Lett. **55** (1985) 126.

3. J. M. Weisenberg and J. H. Taylor, Phys. Rev. Lett. **52** (1984) 1348; J. H. Taylor (private communication, April 1987).

4. J. R. Wilson, R. Mayle, S. E. Woosley and T. Weaver, Ann. New York Acadamy of Sciences **470** (1986) 267.

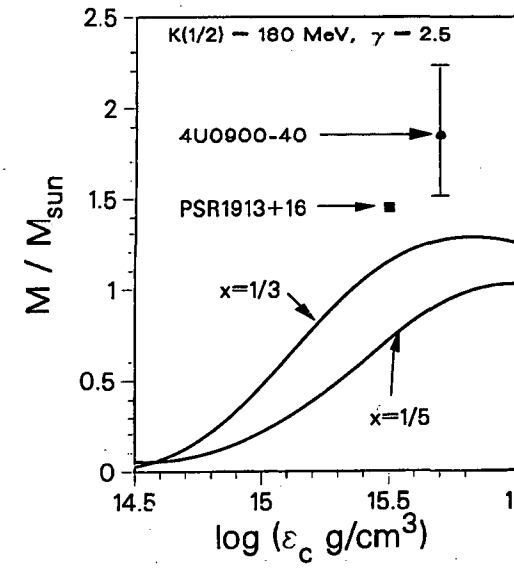

Fig. 1. Neutron star gravitational mass as a function of central density for the BCK equation used in ref. 1. Only the y-coordinate of the data points has meaning, since the central density of the stars is unmeasured.

Pion Interferometry of Ultrarelativistic Nuclear Collisions with Final State Cascading*

S.S. Padula, M. Gyulassy, and S. Gavin

We derive a semi-classical expression for the m-pion correlation function for the case that the spatial and momentum variables are correlated dynamically due to final state cascading using the Wigner density formalism. We find a remarkable cancelation of the contributions from intermediate scattering times and only the final collision phase space coordinates are relevant. The formula is generalized to a covariant form and compared to the analogous one in the current ensemble formalism and the Yano-Koonin prescription. Special cases including the uncorrelated Gaussian source and the highly correlated inside-ouside cascade source are compared in detail. The intermixing of dynamical and geometrical effects in the later case is clearly revealed analytically.

Footnotes and References

*Condensed from LBL-24674 (1988) submitted to PRC.

Heavy Ion Physics Challenges at Bevalac/SIS Energies*

M. Gyulassy

In this summary report of the 8th High Energy Heavy Ion Study, the main new theoretical and experimental developments and the near future promise of the field of nuclear collisions at energies of ~ 1 GeV/nucleon are discussed. The primary goal of this field is to establish experimental constraints on the *thermodynamic* (P, S, W) and *transport* (η, κ, ξ) properties of nuclear matter at high densities and temperatures. While the new data reported significantly extended the nuclear collective flow data base from which those properties could be extracted, no clear consensus on the form of the nuclear equation of state has yet been reached. At present, the effective compressibility of dense matter remains uncertain to a factor of two ($K = 200 - 400$ MeV). It is easy to identify several obstacles that hinder the convergence rate toward narrower constraints on the nuclear equation of state.

1. The momentum dependence of the mean field.
2. The uncertainties associated with 4π experimental filters.
3. The uncertain density and temperature dependence of effective transport cross sections.
4. The absence of self-consistent calculations of the equation of state with present nuclear transport models.
5. The uncertain Δ_{33} dynamics and pion absorption mechanisms at high densities.

I emphasize that the experimental obstacle is severe but that it may be overcome with new generation detectors and experiments. Theoretically, the main focus at present is on the third obstacle. I also emphasized that a major problem today is the uncontrolled proliferation of poorly documented nuclear transport codes and urged the establishment of a computed library for such codes. New promising directions for experimentation in the future include exploiting dilepton and photon probes and using subtreshold K^+ production as a novel probe of dense matter.

Footnotes and References

*Condensed from LBL-24398

Vacuum Polarization Effects in the Non-Linear σ, ω-Model

Norman K. Glendenning

We evaluated the vacuum polarization effects on the equation of state in the non-linear relativistic nuclear field theory (σ, ω -theory). It was found that the energy shifts are not small, but when the coupling constants are chosen so as to reproduce the four saturation properties of nuclear matter, B/A, ρ_0 , K, $m^\star$, then whether or not vacuum corrections are included, the equation of state is virtually identical over a wide density range. However when only the saturation density and binding are controlled as in ref. 1, the equation of state in the two cases diverge at higher density. It is therefore important that all four of the above properties be controlled, so as not to intermix the effects of different saturation properties with those of vacuum polarization. This can be done only in the non-linear version of the model.

Footnotes and References

*Condensed from LBL-24947

1. B.D. Serot and H. Uechi, Ann. Phys. (N. Y.) **179**, 272 (1987).

Vacuum Polarization Effects on Nuclear Matter and Neutron Stars

Norman K. Glendenning

Vacuum polarization effects on the equation of state and neutron stars in the σ, ω, ρ theory are not negligible, although they are considerably smaller than found for the chiral sigma model.[1] However it was found that when the coupling constants are renormalized so as to reproduce the five saturation properties of nuclear matter in each case, whether or not renormalization is carried out, the equation of state and neutron star properties are virtually identical in the two approximations. On the other hand, when only the saturation density and binding are controlled as in ref. 2, the equation of state and neutron star properties, computed with and without vacuum polarization diverge at higher density. Failure to adequately constrain the equation of state at saturation can therefore lead to spurious conclusions in applications to dense matter as in neutron stars, and as well, perhaps, in applications to nuclear structure, especially for properties that depend on K or $m^\star$. We studied the sensitivity of neutron star masses to the saturation properties of the corresponding nuclear matter. First, as discussed above, whether the σ, ω, ρ theory yields the same or different are incorporated, depends on how tightly the saturation properties are controlled. So within this theory, which is the only known relativistically covariant field theory of matter that can account for both nuclear matter and finite nuclei, the saturation properties and the higher density behavior are intimately connected. In fact this has to be true of any comprehensive theory of matter, since the coupling constants everywhere specify the equation of state. It need not be true of parameterizations of the equation of state, for which there is no underlying theory. Second, we explicitly demonstrated, that although the density of matter at the center of a neutron star is fairly high, $\rho_c \approx 7\rho_0$, the mass of a star, even at the limiting mass, is not dominated by dense matter. Instead, fully one half is contributed by matter at densities less than three times nuclear density. This also establishes a dependence of the limiting star mass on the equation of state near saturation. We calculated a number of additional neutron star properties, that may become tests of the theory as more data on neutron stars becomes available. We reemphasized the role of equilibrium in neutron star structure and the equation of state. The fraction of baryons that are hyperons in the limiting mass star is about 20 percent, and hyperons are the dominant baryons in the central core.

Footnotes and References

*Condensed from LBL-25032

1. N.K. Glendenning, Nucl. Phys. **A480**, 597 (1988); T.L. Ainsworth, E. Baron, G.E. Brown, J. Cooperstein, M. Prakash, Nucl. Phys. **A464**, 740 (1987).

2. B.D. Serot and H. Uechi, Ann. Phys. (N. Y.) **179**, 272 (1987).

PART IV: INSTRUMENTATION AND METHODS

New Developments for OASIS

R.M. Chasteler, J.M. Nitschke, L.F. Archambault, A.A. Wydler

During the 1987-1988 running period, the first heavy-ion beams in the new E42 beamline were delivered into Cave N at the LBL SuperHILAC . This beamline, which replaces the E89 beamline, allows full-rigidity (8.5 MeV/nucleon) beams up to ^{238}U to be used in the OASIS mass-separation facility[1] for the first time. These heavy beams provided the capability to use Deep Inelastic Collisions to produce neutron-rich rare-earth and actinide nuclei. These experiments required modifications to the normal surface ionization sources used successfully in OASIS for compound nucleus reactions[2] and shown in Fig. 1. The compound nucleus ion source places the target upstream of tantalum capillaries which isolate the target from the extremely hot end of the source and prevent the products, which recoil out the target and are stopped in a Ta anode endplate, from migrating back towards the cooler regions of the ion source. However, the capillaries impose severe entrance angle limitations on the recoiling products. Since DIC products can recoil with large angles in the lab frame, the target must be moved closer to the high temperature region of the source. Due to the extreme temperature(~3000 C) in this region, only refractory metals like Ta or W can be used. The best design so far has been to replace the Ta anode endpiece with a W endpiece and use it as the target(W showed the best cross sections for these DIC reactions). Capillaries are still used to stop diffusion of the ions into the SuperHILAC's vacuum. Further tests are in progress to determine the efficency of sources using thin W targets (2-12mg/cm^2) located at the end of the capillaries, to compare sources with and without the capillaries, and to determine how Ta or W anode endpieces affect diffusion times and ionization efficiencies.

The narrow acceptance angle of the capillaries require that the SuperHILAC beams be perfectly parallel to the capillaries or the beam (or products from compund nucleus reactions) will hit the walls of the capillaries. The new E42 beamline presented problems in determining if this criterion was being met. Two beam scanners have been installed about 1 meter apart and 1/3 meter upsteam of the OASIS ion source. These scanners consist of a helical wire perpendicular to the beamline, that when rotated about the helix axis, would cause the wire to scan across the beam first horizontally and then vertically. By measuring the current on the wires and using a digital storage oscilloscope for display, both horizontal and vertical beam profiles can be obtained from both scanner positions without interrupting the beam. Since all the ion optics for the E42 beamline are upstream of the scanners, the ion beams becomes parrallel to the capillaries if the beam is centered on both scanners.

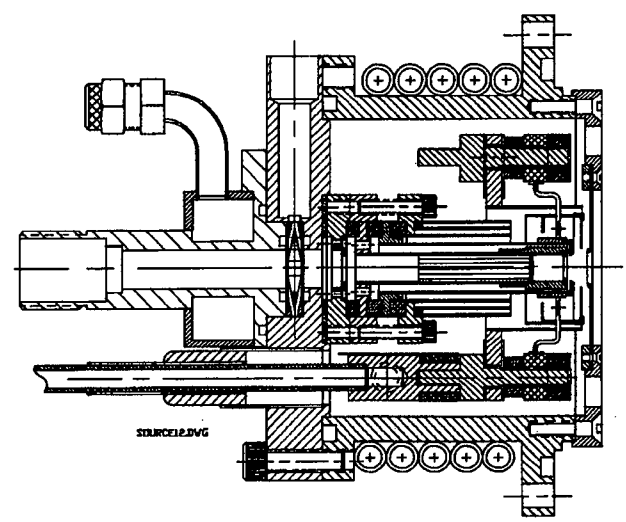

Fig. 1. Diagram of the OASIS surface ionization source.

Footnotes and References

1. J.M. Nitschke, Nucl. Instr. & Meth. **206**, 341 (1983).

2. P. Wilmarth, *et al.*, Nuclear Science Division Annual Report1986-1987,**LBL-25295**, 141 (1988).

Initial Evaluation of a Large NaI(Tl) Spectrometer

J.M. Nitschke and K.S. Vierinen

A large NaI(Tl) (14" long × 14" diameter) well detector was obtained commercially; together with an 8" long x 2" diameter "plug" detector. The NaI(Tl) crystal is intended as the main component of a total absorption γ-ray spectrometer, to be used in conjunction with the OASIS facility at the SuperHILAC. The crystal is viewed by eleven 3" diameter photomultiplier tubes (PMTs) with active bases. The tubes are gain matched using the 2.734 MeV sum peak of ^{88}Y. The gain matching is carried out by an IBM-AT computer that determines the peak position and adjusts the high voltage of the PMT's *via* CAMAC controlled power supplies. During the actual operation, the signals of all PMT's are summed, and stabilized by the computer with respect to a stabilized light pulser. Spectra of standard sources like ^{22}Na, ^{24}Na, ^{88}Y, and ^{60}Co have been obtained with good resolution and close to 100% efficiency. Monte Carlo simulations of the spectrometer response to γ radiation were carried out using the EGS4[1] code. A comparison between a simulated *vs.* experimental ^{88}Y spectrum is shown in Fig. 1. Minor discrepancies between the two spectra can probably be corrected by paying closer attention to the exact geometries and material compositions in the simulation, and by including the – thus far neglected – β-particle component of the ^{88}Y decay. The ultimate goal of these calculations is to obtain the complete response matrix of the spectrometer in order to unfold γ spectra of arbitrary complexity.

Footnotes and References

1. The EGS4 Code System: Computer Programs for the Monte Carlo Simulation of Electromagnetic Cascade Showers, R.W. Nelson, H. Hirayama, and D.W.O. Rogers, SLAC Report No. **265** (1985).

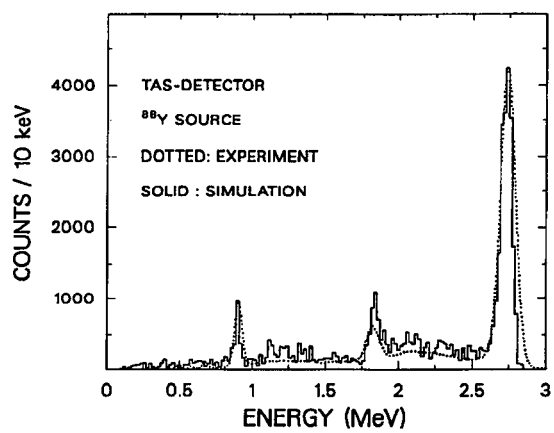

Fig. 1. Simulated (histogram) *vs.* experimental (dotted line) ^{88}Y γ-ray spectra of the 14" x 14" NaI(Tl) well crystal.

Monte-Carlo Simulation of Gamma-ray Cascades in a Ge Detector

K.S. Vierinen, J.L. Feng, P.A. Wilmarth, and J.M. Nitschke*

The EGS4 Monte-Carlo (MC) simulation code[1] was used to simulate the response of a 52.3% coaxial Ge detector to radioactive standard sources, since large efficiency Ge detectors and small source to detector distances gives rise to strong summing effects that influence the structure of measured γ-ray spectra. The effects of geometrical parameters such as source to detector distance and the size of the source, as well as various nuclear structure contributions such as γ-ray energies, γ-ray angular correlations and multiplicities of γ-ray cascades, were studied.

Fortran subroutines were written for the experimental geometries and to create simulated γ-ray cascades corresponding to different radioactive sources. These subroutines were combined with the EGS4 MC code for the detector response simulations. Simulations of the Ge crystal were performed with a simple cylindrical geometry and also with the actual well-shaped geometry (as taken from the detector specifications). The volume of the inactive hole in the

well-shape was only ~1.8% of the Ge crystal volume. At 250 mm distance, using 1.332 MeV (^{60}Co) γ-rays a 10% reduction in the efficiency in the Ge detector was obtained when the hole of the well-shaped geometry was taken into account. This effect was found to be much smaller at closer distances (only 2.5% at a distance of 15 mm).

The simulated/calculated efficiency for the 1.332 MeV γ ray (^{60}Co) in the Ge detector was compared to the efficiency of a standard 3"×3" NaI(Tl) crystal (250 mm source to detector distances were used in both cases) and found to be in good agreement with the experimental result of 52.3%. In Fig. 1 the simulated spectra of ^{60}Co γ-ray cascade with 250 mm and with 11 mm (prominent sum peak at 2.5 MeV) distances are shown.

Footnotes and References

*Summer student, present address Trinity College, Cambridge, England.

1. W.R. Nelson, H. Hirayama, D.W.O. Rogers, **The EGS4 Code System,** SLAC Report No. **265**, 26–50 (1985).

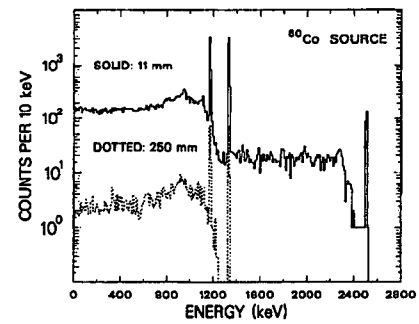

Fig. 1. Simulated γ-ray spectra measured with 250 and 11 mm source to detector distances using ^{60}Co γ-ray cascades. In both cases 100,000 decays of ^{60}Co were simulated.

PERALS – Photon-Electron Rejecting Alpha Liquid Scintillation Spectrometer

R.B. Chadwick, M.J. Nurmia, D.M. Lee, and D.C. Hoffman

The efficient detection of alpha and fission activity is necessary to extend knowledge of the chemistry of the heaviest elements. Our group has acquired and installed a liquid scintillation alpha and fission spectrometer that allows detection of alpha activity with an efficiency of 99.7% while rejecting unwanted pulses from beta and gamma activity with 99.95% efficiency. The PERALS spectrometer developed by W.J. McDowell of Oak Ridge National Laboratory is based on the differences of interaction of radiation with liquid scintillators.[1] The light pulses produced by alpha and fission radiation are longer in duration and different in shape from those produced by beta and gamma activity. This allows discrimination between these types of radiation through the use of a pulse-shape discriminator and coincidence gate.

To operate the PERALS, an aqueous phase containing the activity of interest is equilibrated with an aromatic organic phase containing an extractive agent such as HDEHP, TOPO or TBP, a fluor such as BPPO (2-(4-biphenylyl)-6-phenylbenzoxazole), and an energy transfer agent such as naphthalene. After equilibration, the organic phase containing the activity of interest is sparged with argon gas to remove dissolved oxygen and counted.

We anticipate that the PERALS spectrometer will be a useful tool in our chemical studies of the heaviest elements. The 4π geometry and rapid sample preparation will allow the detection of many more alpha and fission events than was previously possible.

Footnotes and References

1. W.J. McDowell, "Alpha Counting and Spectrometry Using Liquid Scintillation Methods," Nuclear Science Series, NAS-NS-3116, NTIS, Technical Information Center, Office of Scientific and Technical Information, United States Department of Energy (1986).

Gas Phase Isothermal Chromatography of Hahnium Bromide Complexes

K.E. Gregorich, W. Brüchle, U. Baltensperger,† H. Gäggeler,† J. Kratz,‡ D.M. Lee, C. Lienert,§ D. Jost,† M.J. Nurmia, Y. Nai-Qi,† R.A. Henderson, H.L. Hall, C.M. Gannett, R.B. Chadwick, J.D. Leyba, K.R. Czerwinski, D.C. Hoffman, M. Schädel,* U. Scherer,‡ A. Türler,§ P. Zimmermann,‡*

Early studies of the gas phase thermochromatography of bromide complexes of element 105 (hahnium), performed by Zvara *et al.* at Dubna, showed that Ha forms bromide complexes which are volatile at about 300°C. This result is questionable, though because of the non-specificity of the method used for the identification of the hahnium decays. In September and October of 1988, we hosted a collaboration to study the chemical properties of hahnium. One of the goals of this collaboration was to measure the isothermal chromatographic properties of these volatile bromide complexes of hahnium.

For these studies, the 34-s isotope, ^{262}Ha, was produced at the 88-Inch Cyclotron by the ^{249}Bk(^{18}O,5n) reaction. The recoiling activities were transported to the isothermal chromatography apparatus on KCl aerosol particles by the He-jet technique. Here, the activity bearing KCl particles were trapped in a quartz wool plug which was kept at 1000°C. At this point, a flow of HBr gas and BBr_3 vapors was added as a brominating agent. Under these conditions, elements of groups 4 and 5 of the periodic table were found to form volatile bromide complexes which moved with the gas flow past the quartz wool plug and down the isothermal part of the column which was kept at temperatures between 200°C and 800°C. At the end of the column, the activities were reattached to KCl aerosol particles and transported, via the He jet technique, to our MG rotating wheel system for the detection of alpha and fission activities (the lighter members of groups 4 and 5 were detected by capturing these aerosol particles on a filter and monitoring the gamma rays emitted in their decay).

The retention time of these complexes in the isothermal part of the column was measured as a function of the temperature by monitoring the yield of short-lived isotopes. If the retention time was significantly longer than the half-life, the isotope would decay in the column, and be unavailable for detection at the end of the column. If the retention time was shorter than the half-life, the nuclide would be available for detection at the end of the column after only a small fraction decayed in the column.

^{262}Ha was detected in yields significantly smaller than expected, indicating that either: a) bromide complexes of hahnium are not formed, or are broken up in the thermochromatography column, b) bromide complexes of hahnium are not volatile or they stick to the quartz column at temperatures below about 500°C, or c) Bromide complexes of hahnium are so volatile that they were pumped off the sources collected in the MG vacuum chamber. Further analysis is necessary to determine the exact yields of ^{262}Ha in these experiments.

Footnotes and References

*Gesellschaft für Schwerionenforschung, Darmstadt, West Germany

‡Universität Mainz, FRG

†Paul Scherrer Institute, Würenlingen, Switzerland

§Universität Bern, Switzerland

Development of a Low Energy Proton Detector Array

D.M. Moltz, J.D. Robertson, N.W. Madden, D.A. Landis,* J.E. Reiff, T.F. Lang, and J.C. Cerny*

We have been interested in measuring the decay properties of exotic nuclei far from beta stability for some time. Unfortunately, attempts to measure these decays are hampered by low production cross sections and very short half-lives. This latter problem has been addressed by the development of a fast rotating wheel for nuclides with half-lives in the 200 ms – 50 ms range.[1] The first problem can only be aided by utilizing very high geometry detectors in close proximity to the production point (which is the beam in the case of an accelerator experiment).

We have proposed several experiments to search for light ground state proton emitters and for the heretofore undiscovered ground state two-proton radioactive decay mode. Both of these searches necessarily require the detection of very low-energy protons. To accomplish this, we developed detectors capable of observing protons with energies down to 250 keV.[2] This represented a first capability for one to observe particle identified protons of this energy on an event-by-event basis. Although these original single telescope detectors worked extremely well, an extended array suitable for use with the fast rotating wheel was needed. Additionally, the very strong radiation background due to the close proximity of an intense accelerator beam required the development of electronics capable of detecting a few very small signals in a copious sea of large signals. For instance, it was desirable to be able to generate a fast timing signal from a 50 mV pulse on top of 100 mV of noise.

These detector telescopes are very similar to the single telescope version.[2] The silicon detectors have been manufactured on a single wafer by Micron Semiconductor, Ltd. (England). More details concerning the operating characteristics of these detectors will be given in a forthcoming publication.[3] The most important changes for operating these telescopes in a high radiation field occurred in the counting electronics. These new modules were all designed by the LBL Electronics Engineering Group. The "slow" electronics required a much higher gain amplifier with both fast and slow outputs. The redesigned Dual Shaping Amplifier (21X5881P-3) has $\sim \times 10$ in gain over any comparable unit for both outputs. Even with this higher fast amplifier gain, the only discriminator capable of obtaining the required low threshold is the LeCroy 623B. The input to this amplifier comes from a custom redesigned preamp with special low noise FETs (the gas version has an additional high voltage protective network). The fast output of these preamps has also required the development of X5 fast amplifers on both the preamp and processing ends, each with $\sim$15 ns of integration, resulting in an overall gain of $\times 15$ which is then used to drive a standard CFD. This network can indeed obtain <50 ns timing for 50 mV signals on 100 mV of noise (Si counters only; gas counters have unique problems which will be addressed elsewhere[3]–normal timing between the gas and silicon detectors is $\sim$20 ns.

This detector array has been strenuously tested in a high radiation field. Although the telescopes are capable of observing low-energy protons in a sea of betas only when the beam is turned off, this mode of operation is quite satisfactory to proceed with our searches for ground state two-proton radioactivity and new ground state proton emitters.

Footnotes and References

*Electronics Engineering Group, LBL.

1. J.E. Reiff *et al.*, Nucl. Instrum. Meth. **A276**, 228–232 (1989).

2. J.D. Robertson *et al.*, NSD Annual Report LBL-25295, p. 137.

3. D.M. Moltz *et al.*, to be submitted to Nucl. Instr. Meth.

A Multiple Target Gas-Jet System for Light-Ion Bombardments of Heavy Targets*

H.L. Hall, M.J. Nurmia, and D.C. Hoffman

A target system has been designed which allows exploitation of all of the advantages of light-ion reactions while minimizing the effect of the disadvantages. Since light ions lose very little energy while passing through reasonably thin targets and target backings, multiple targets can be bombarded concurrently with only a small spread in incident beam energy. A system using up to three light-heavy atom targets (e.g., magnesium) has been reported,[1] but this has never been done with a large number of heavy targets where the recoil range becomes very small. If an incident energy spread of a few MeV was acceptable, ten or more actinide oxide targets on 0.025-mm beryllium backings could be bombarded with the same beam. This multiplication of the targets compensates for the low recoil range of the compound nucleus, yielding effectively a thick target.

The low recoil range of the compound nucleus could also be exploited to suppress the collection efficiency of fission products. For example, the recoil range in helium of ^{241}Am* produced by the bombardment of ^{237}Np with 100-MeV alpha particles can be estimated[2] to be about 4 mm at atmospheric pressure. A typical fission fragment, with an energy of about 1 MeV/nucleon, has a recoil range[2] in helium of about 2500 μg/cm^2, or about 140 mm. Hence, by arranging the spacing between the targets to be greater than the recoil range of the compound nucleus but much less than that of fission fragments, most of the fission fragments will embed in the next target backing rather than attach to aerosols. This severely decreases the gas-jet extraction yield of the fission products, and hence greatly reduces the β-γ background resulting from fission products.

The use of high beam fluxes was also desirable, so the target system design had to incorporate two primary safety features. First, the system had to accept the high fluxes without suffering design failures due to the large amount of heat generated by high fluxes. Secondly, the amount of induced radioactivity, primarily in the beam stop, had to be minimized to reduce the hazards of handling the system following a bombardment. These criteria led to the use of a thick beryllium plug in a water-cooled copper heat sink as a beam stop. A large diameter collimator allowed large diameter targets (12.7 mm) to be used, hence reducing the risk of target failure due to localized heating. Fortunately, the energy deposition in the targets can be kept low enough by using suitably thin target backings so that the flow of helium in the KCl/He-jet provides adequate cooling.

The Light Ion Multiple Target System (LIM target system) we designed is shown schematically in Fig. 1. The target material is electrodeposited onto 25.4-μm beryllium foils by a standard technique.[4–7] The number of targets, their composition, and their spacing can be varied in the target system. The beam, after passing through all the targets and the volume limiting foil after the last target, impinges on a 25-mm thick beryllium plug. This plug is press-fitted into a water-cooled copper jacket to dissipate the heat generated in a high-flux bombardment.

The transport efficiency of the gas jet through the target system was measured with an ^{225}Ac ($t_{1/2}$ = 10.0 days) recoil source by measuring the 4.8-minute daughter ^{221}Fr. The yield was measured as the ratio of ^{221}Fr collected per unit time passing through the system to the amount of ^{221}Fr collected per unit time without going through the target system. This ratio was consistently 90% or better. Of course, the overall gas-jet yield is the product of the attachment efficiency, the transport efficiency, and the collection efficiency. In an on-line measurement using 100-MeV ^{4}He^{2+} to bombard ^{237}Np, we measured a ten-fold increase in the ^{232}Am activity collected when switching from a single target with a large recoil volume (~100 cm^3) to a ten target arrangement in the LIM target system with the targets spaced 8.6 mm apart. This

implies that the attachment efficiency in the LIM target system is as least as good as that of the traditional one-target, one-capillary system. The collection efficiency should remain constant since the same apparatus was used to collect the aerosols in each case. Comparison of our measured cross section for this isotope with the published cross section[3] gives an overall gas-transport yield of 70-95%.

In conclusion, we have constructed a target system capable of accepting up to 25 targets at one time. The system is specifically designed to allow the use of high beam fluxes safely. Nuclei produced in reactions can be selected according to their recoil ranges by the appropriate spacing of the targets to suppress long-range activities. Range-selected products are transported away from the system via a KCl/He-jet with high efficiency. The helium also serves to cool the targets. The LIM target system has already been used in several nuclear physics experiments, and greatly enhances the effective yield in light ion bombardments with heavy targets.

Footnotes and References

*Condensed from Nucl. Instr. Meth. A **276**, 649 (1989).

1. D.M. Moltz, J.M. Wouters, J. Äystö, M.D. Cable, R.F. Parry, R. D. von Dincklage and J. Cerny, Nucl. Inst. Meth. **172**, 519 (1980).

2. L.C. Northcliffe and R.F. Schilling, Nucl. Data Tables **A7**, 233 (1970).

3. D. Habs, H. Klewe-Nebenius, V. Metag, B. Neumann and H.J. Sprecht, Z. Physik A **285**, 53 (1978).

4. V.B. Bedov and V.N. Kosyakov, Proc. Int'l Conf. Peaceful Uses of Atomic Energy **7**, 369 (1956).

5. J.E. Evans, R.W. Lougheed, M.S. Coops, R.W. Hoff and E.K. Hulet, Nucl. Inst. Meth. **102**, 389 (1972).

6. D.C. Aumann and G. Müllen, Nucl. Inst. Meth. **115**, 75 (1974).

7. G. Müllen and D.C. Aumann, Nucl. Inst. Meth. **128**, 425 (1975).

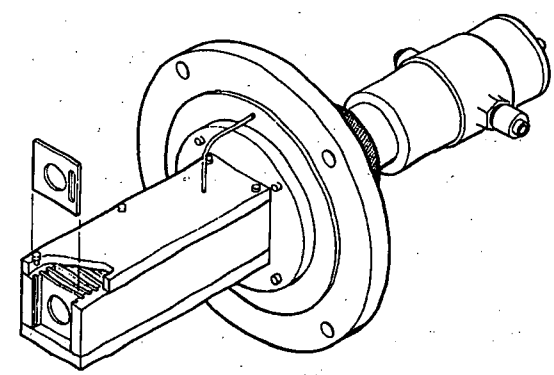

Fig. 1. Light Ion Multiple (LIM) Target System

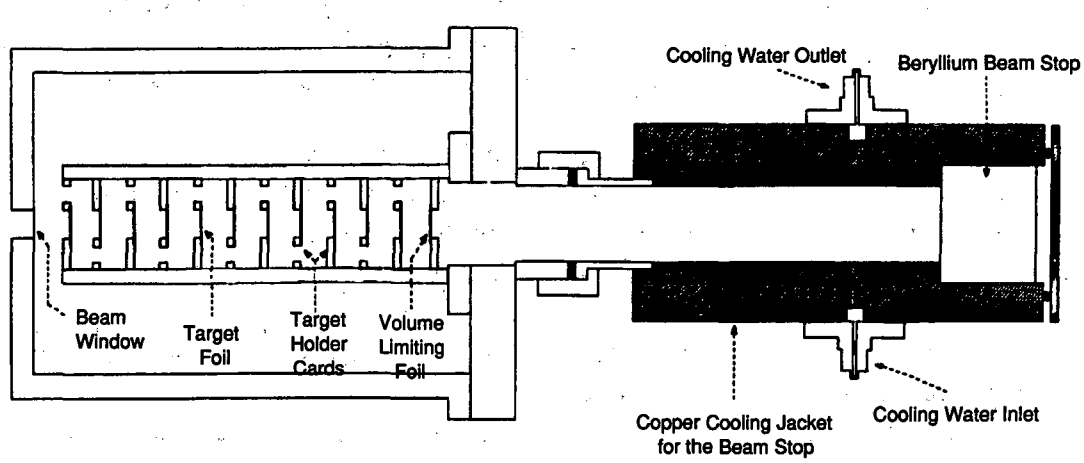

Fig. 2. Horizontal cross-sectional view of the LIM target system. Note the alternating arrangement of the open gas vents, forcing the gas jet to sweep out the volume behind each target. The gas jet is extracted after the last target position by a single 1.4-mm i.d. capillary.

Completion of SASSY2

A. Ghiorso

After four years of construction and development SASSY2[1] is finally ready for sub-nanobarn experiments in the heavy element region. The final modification, installation of new pole tips in the quadrupole, has been accomplished along with the necessary realignment. Several months were spent in the debugging of the new multiplex electronic system[2] for the 50-detector focal plane unit and new silicon detector wafers were tested successfully.

Using satellite beam time, a number of heavy ion beams with different magnetic rigidities were tuned through SASSY[2]. The variation of this quantity with magnetic field was found to be quite linear, as expected. It was very gratifying to find that the pole-tip modification now allowed the instrument to tune to a magnetic rigidity of 20.6 Kg-m, the predicted value for element-110 recoils made in the Co-59 reaction on Bi-209, without saturation of the qudrupole pole tips.

Unfortunately, only a little beam time was available to check the overall efficiency, and that, only indirectly. Fe-56 reactions with rare earth targets were found to give a focal plane image that was almost entirely contained within the vertical confines of the detector crystals. Simultaneously, the horizontal width of this image occupied less than 30 crystals (each crystal is 3 mm wide). Since the dead area is only a few percent of the active area it can be deduced that the transmission of fusion recoils through SASSY[2] must be very high. An absolute value for the yield can best be obtained by the reaction of Ca-48 on Pb-208 to form 1-min No-254.

Experiments aimed at identifying heavy elements made with picobarn cross sections require very low backgrounds. A simple experiment with Co-59 on Bi-209 run at a level of 50 particle nanoamperes on a fixed target showed that the gross in-beam background was only a few hundred counts per minute when extrapolated to the 500 pna beam level desired for serious long runs. This is orders of magnitude less than that observed in the GSI experiments with SHIP to produce element 109. The out-of-beam background with SASSY[2] was very small in the high energy regions of interest.

Footnotes and References

1. S. Yashita and A. Ghiorso, LBL-21570, NSD Annual Report 1984-1985, p. 204.

2. C.H. Lee and A. Wydler, LBL-21570, NSD Annual Report 1984-1985, p. 205.

Phosphate Glass Detectors with High Sensitivity to Nuclear Particles*

Shicheng Wang,† S.W. Barwick,† D.E. Day,‡ D. Snowden-Ifft,† P.B. Price,† A. Westphal†

Until now, the most sensitive glass for recording and identifying nuclear particle tracks has been VG-13, a phosphate glass that is not produced in the U.S. because it contains uranium. In a search for a replacement for VG-13, we have studied about 150 phosphate glasses, as well as a few other types. We summarize here the results of that study. We have developed a new glass, BP-1, composed of 65 P_2O_5, 25 BaO, 5 Na_2O, and 5 SiO_2 (wt%), which has several advantages over VG-13: it contains no uranium; it is colorless and transparent; and it is more sensitive to ionizing particles.

Footnotes and References

*Condensed from Nucl. Instr. Meth. **B35**, 43 (1988).

†Physics Department, University of California at Berkeley

‡Graduate Center for Materials Research, University of Missouri, Rolla 65401

A Non-aqueous Method for Separating 1+ and 3+ Cations

R.A. Henderson, H.L. Hall, C.E.A. Palmer, P.A. Baisden,* and D.C. Hoffman*

Our group is involved in studying the chemical properties of the heaviest elements at the limits of the periodic table. The large nuclear charge of elements at the bottom of the periodic table leads to the relativistic contraction and stabilization of electronic orbitals with lower angular momentum, particularly s orbitals. Relativistic effects are used to explain the normal oxidation states of Tl^{1+} and Pb^{2+} as compared to their homologous elements, In^{3+} and Sn^{4+} respectively.[1] At the end of the actinide series, relativistic effects in Lr may be strong enough to stabilize the 7s electron pair and allow the existence of a 1+ oxidation state, which does not exist in its homologous lanthanide element, Lu. In previous experiments[2] we have attempted to reduce Lr with relatively weak reducing agents, Cr^{2+} and V^{2+}, and set a limit on the reduction potential for the proposed Lr (III-I) couple of -0.44V. The use of very strong reducing agents in these chemical studies requires that the medium chosen as the solvent for these elements be able to withstand the presence of a powerful reducing agent without itself being reduced. Non-complexing aqueous systems are limited by the reduction of water by this half-reaction:

$$2H_2O + 2e^- \leftrightarrow H_2 + 2OH^- \quad E^o = -0.8277 \text{ V}$$

Organic solvents are in general capable of withstanding reducing potentials of about -3 V. However, most organic solvents do not have the solvation power of water, and it is difficult to find one that will adequately solvate inorganic salts. During the preparation for a reduction experiment of the heaviest actinide elements, a non-aqueous separation scheme has been developed to separate 1+ reduced ions from 3+ non-reduced ions. A reverse-phase chromatography column consisting of an inert support with HDEHP (Di-2-ethylhexylorthophosphoric acid) sorbed onto it provides the stationary phase. A solution of propylene carbonate with 10 vol. % THF (tetrahydrofuran) dissolved in it provides the mobile phase. With this system, 3+ cations, e.g. the lanthanide and heavy actinide ions, are adsorbed onto the column, while 1+ ions, e.g. Cs, Fr, and reduced actinide ions, are not retained by the column. This procedure has been automated using our ACCESS (Automated Chromatographic Chemical Separation System) system, and thus provides a quick method for separating 1+ and 3+ charge state ions. The system has been tested with Cs^{1+}, Tm^{3+}, and Eu^{3+} tracers. The separation between the 1+ and 3+ tracers was found to be quite satisfactory.

Footnotes and References

*Lawrence Livermore National Laboratory, Livermore, Ca

1. U.W. Scherer, J.V. Kratz, M. Schädel, W. Brüchle, K.E. Gregorich, R.A. Henderson, D. Lee, M. Nurmia, and D.C. Hoffman, Inorganica Chimica Acta **146**, 249-254 (1988)
2. K.S. Pitzer, Acc. Chem. Res. **12**, 271-276 (1979)

The Response of Scintillators to Heavy Ions - I. Plastics*

M.A. McMahan

The response of various scintillator detectors to ions of A = 1 – 84 and energies E/A = 5 – 30 MeV has been measured, and is found to be linear above an energy of 100 MeV. Results are presented for a typical organic plastic scintillator including parametrizations of the data as a function of Z, A and energy. These results are useful to anyone employing scintillators as heavy ion detectors, with one calibration point giving a normalization that allows use of the whole set of curves. The response functions are compared to previous parameterizations at lower energies and discussed in terms of the theory of δ-ray formation in the scintillator.

Footnotes and References

*Condensed from IEEE Transitions of Nucl. Sci. **25** No. 1, 42 (1988).

Comparison of Two Programs for Prediction of Neutron Evaporation Cross Sections for Actinide and Light Projectile Reactions

G.R. Haynes, J.D. Leyba, D.M. Lee, and D.C. Hoffman*

Two FORTRAN programs, SPIT and JORPLE, which predict neutron evaporation cross sections for actinides and light to medium mass projectile reactions, were compared. The predictions of these two codes were compared to experimental data for target/projectile combinations of $^{233,238}U + ^{12}C$, ^{16}O, ^{18}O and $^{244,248}Cm + ^{12}C$. Both programs evolved from the same original code but predict different excitation functions due to the use of diferent internuclear and Coulomb potentials. The two programs predict the excitation function peak energy and cross section equally well. SPIT was found to predict the excitation function shape better than JORPLE.

Footnotes and References

*Student Research Semester Participant, Center for Science and Engineering Education

A Novel Approach to the Measurement of the Neutron Multiplicity Associated with Reverse Kinematics Heavy Ion Reactions*

A. Pantaleo,† L. Fiore,† G. Guarino,† V. Paticchio,† G. D'Erasmo,‡ E.M. Fiore,‡ N. Colonna,‡ R.J. Charity,§ G.J. Wozniak and L.G. Moretto

A new fast neutron high multiplicity detector is proposed based on the measurement of the total light yielded by the neutrons in a plastic scintillator. Its performance is simulated by Monte Carlo methods and compared to existing neutron multiplicity detectors. A cost-effective design for reverse kinematics heavy ion reactions is presented and connected problems are discussed.

Footnotes and References

*Condensed from Nucl. Instr. and Methods **A269**, 580 (1988).

†Istituto Nazionale di Fisica Nucleare, Sezione di Bari, 70126 Bari, Italy.

‡Dipartimento di Fisica dell'Università di Bari, Via Amendola, 173, 70126 Bari, Italy.

§Gesellschaft für Schwerionenforschung, 6100 Darmstadt, West Germany.

NMR on β-Emitter ^{37}Ca Produced through Projectile Fragmentation in High-Energy Heavy-Ion Collisions*

M. Izumi,† A. Kitagawa,† K. Takeyama,† Y. Nojiri,† T. Minamisono,†
*K. Sugimoto,† S. Shimoura,‡ K. Ekuni,‡ I. Tanihata,§ T. Kobayashi,***
K. Omata,†† Y. Shida,†† K. Matsuta, J.R. Alonso, G.F. Krebs, and T.J.M. Symons

Experimental NMR studies on mirror magnetic moments in the $f_{7/2}$ shell have been continued using a new ISOL[1] built in B44 of the Bevalac. A test run on ^{37}Ca($I^{\pi} = 3/2^{+}$, $T_{1/2}$=173 msec) was undertaken as a first example of the NMR measurements on unknown moments of the same mass 40 region.

The ^{37}Ca nuclei were produced through projectile fragmentations of ^{40}Ca primary beams of 24 MeV/nucleon and separated through rigidity and range analyses. After compressed in the momentum distributions of ^{37}Ca and retarded with a suitable degrader, the nuclei were polarized as passing through ten tilted thin foils made of mylar (0.5 mm thick), on each surface of which a thin Au layer is evaporated (the tilted foil technique[2]). To maintain their polarization, ^{37}Ca were finally implanted in a thin CaF_2 single crystal. Beta rays emitted from ^{37}Ca in the crystal were detected with two sets of counter telescopes located above and below the crystal. A time spectrum of the β rays from ^{37}Ca was obtained as shown in the figure. Half life of the main decaying component was determined to be 169.9±9.4 msec, which is in good agreement with the previous known value for ^{37}Ca.[3]

To perform NMR measurements4 on ^{37}Ca in CaF_2, an oscillating rf magnetic field (1800±55 kHz) was applied perpendicularly to an external static field (4.826 kOe). Searches for the NMR effect of unknown ^{37}Ca g-factor were undertaken by changing frequencies of the rf-field under the constant static field. These measurements are still continuing.

Footnotes and References

*Condensed from Proc. of Symp. on Heavy Ion Phys. and Nucl. Astrophys. Problems, Tokyo, 1988.

†Faculty of Science, Osaka University, Toyonaka, Osaka 560, Japan

‡Faculty of Science, Kyoto University, Kyoto 606, Japan

§RIKEN, Wako, Saitama 351-01, Japan

**KEK, Tsukuba, Ibaraki 305, Japan

††INS, University of Tokyo, Tanashi, Tokyo 188, Japan

1. Y. Nojiri *et al.*, Nucl. Instr. and Meth. in Phys. Res. **B33**, 193 (1988)

2. Y. Nojiri *et al.*, J. Phys. Soc. Japan **55 suppl.**, 391 (1986).

3. J.C. Hardy *et al.*, Phys. Rev. Lett. **13**, 764 (1964)

4. T. Minamisono, J. Phys. Soc. Japan **34 Suppl.**, 324 (1973).

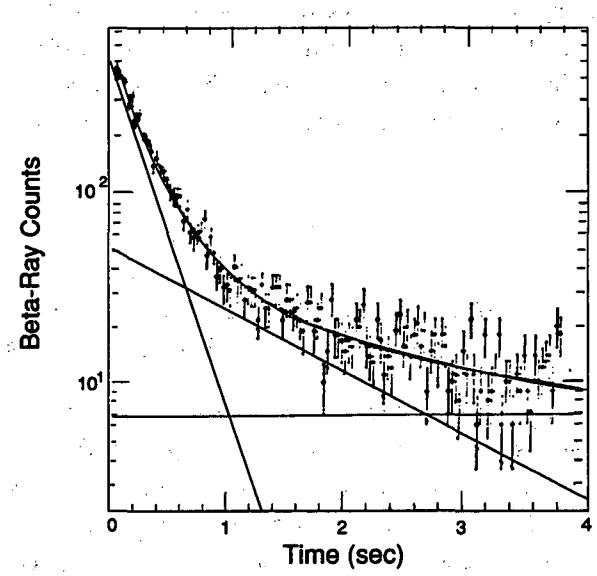

Fig. 1. Time spectrum of β rays.

Sampling Calorimeters for the Relativistic Heavy-Ion Experiment WA80 at CERN*

T.C. Awes[†], *C. Baktash,*[†] *R.P. Cumby,*[†] *R.L. Ferguson,*[†] *A. Franz, T.A. Gabriel,*[†] *H.A. Gustafsson,*[‡] *H.H. Gutbrod,*[§] *J.W. Johnson,*[†] *B.W. Kolb,*[§] *I.Y. Lee,*[†] *F.E. Obenshain,*[†] *A. Oskarsson,*[**] *I. Otterlund,*[**] *S. Persson,*[**] *F. Plasil,*[†] *A.M. Poskanzer, H.G. Ritter, H.R. Schmidt,*[§] *S.P. Sorensen,*[†,††] *and G.R. Young*[†]

Samping calorimeters designed for use in the relativistic heavy-ion experiment WA80 at CERN are described. Calibration and performance results are presented for a calorimeter used at midrapidity and for a calorimeter used at zero degrees. Over the energy range of 2 to 50 GeV, the response of the midrapidity calorimeter (MIRAC) was linear, and its energy resolution σ/E was found to be given by $0.014 + 0.11/\sqrt{E}$ and $0.034 + 0.34/\sqrt{E}$ for electromagnetic and hadronic showers, respectively. Signal ratios of 1.20 and 1.4 were obtained for the e/h ratio of the lead-scintillator electromagnetic section and the iron-scintillator hadronic section, respectively. The MIRAC provided an accurate transverse energy trigger with a response and resolution for high-energy heavy ions which was somewhat better than anticipated on the basis of the low-energy calibrations. The uranium-scintillator zero-degree calorimeter (ZDC) was found to have a linear response to heavy ions and an in-beam hadronic resolution ranging from $\sigma/E = 0.013 + 0.33/\sqrt{E}$ at low intensities to $\sigma/E = 0.02 + 0.67/\sqrt{E}$ at higher intensities. The e/h ratio of the electromagnetic section was measured to be 1.12 at 135 GeV. The ZDC operated reliably with incident beams of 3.2-TeV oxygen and 6.4-TeV sulfur at intensities of over 10^6 nuclei per spill. It provided a trigger both for minimum bias events and for violent central collisions.

Footnotes and References

*Submitted to Nucl. Instr. and Meth. in Phys. Res.

†Oak Ridge National Laboratory, Oak Ridge, TN 37381

‡University of Lund, S-223 62 Lund, Sweden and European Laboratory for Particle Physics, CH-1211 Geneva, Switzerland

§Gesellschaft für Schwerionenforschung, D-6100 Darmstadt, West Germany

**University of Lund, S-223 62 Lund, Sweden

††University of Tennessee, Knoxville, TN 37996

Quad Time-to-Amplitude Converter (LBL #21x9191 P-1)*

R.J. McDonald, D.A. Landis and G.J. Wozniak

Four Time-to-Amplitude Converters (TACs) have been designed and packaged in a single-width NIM module. These moderate-resolution units (~0.1% full scale) are ideal for applications where large numbers of TACs are required because of the high packing density provided by the quad configuration. Full-scale ranges of 100 ns, 300 ns, 1 μs and 3 μs are switch selectable. Readout of each unit may be either internally or externally controlled. All units may be read out at the same time via a common "group readout". The readout time is adjustable between 2 and 20 μs. An LED indicates a valid event.

Footnotes and References

*Condensed from LBL-24220.

PART V: APPENDICES

Appendix I: Seminars

Nuclear Science Division Seminars

October 20, 1987	Dr. Amos Breskin Weizmann Institute	New Ideas on UV-Detectors for Ring Imaging Čerenkovs
October 26, 1987	Dr. W. Świątecki LBL	Introduction to order of Chaos Series
November 9, 1987	Dr. N. K. Glendenning LBL	Equation of State from Nuclear and Astrophysical Evidence
November 23, 1987	Dr. P. Cvitanovic Niels Bohr Institute	Universality In Chaos
December 7, 1987	Dr. Janos Polonyi MIT	Quantum Mechanics on a Circle and Physics of Deconfinement
December 14, 1987	Dr. K. Danzmann Stanford University	Heavy-Ions Collisions: A source of New Light Bosons?
January 4, 1988	Dr.C. Lyneis LBL	ECR ION SOURCES: Applications in Nuclear and Relativistic Heavy Ion Physics
January 11, 1988	J. Leyba, GSRA Winthrop Williams, GSRA	Heavy Actinide Production from The Interaction of 44Ca with 248Cm Precision Measurements using Plastic Track Detectors
January 19, 1988	Dr. J. M. Nitschke LBL	The Study of Neutron - and Proton-Rich Nuclei with OASIS: Latest Results
January 25, 1988	Dr. David Campbell Los Alamos National Laboratory	Nonlinear Science: Paradigms to Practicalities
February 1, 1988	Robert Chasteler GSRA Krysta Wyatt, GSRA	New Neutron-Rich Studies with OASIS A Search for Bound States of Neutrons and Negative Pions
February 8, 1988	Dr. Feingold The James Franck Institute, Univ. of Chicago	Implications of Chaos for Nuclear and Atomic Systems
February 22, 1988	Dr. Hans-Georg Ritter LBL	Nucleus-Nucleus Collisions at 60 and 200 GeV per Nucleon (WA80)

March 7, 1988	Scott Chase, GSRA Walter L. Kehoe, GSRA	Charge Coupled Devices (CCDS for Streamer Chamber events at the Bevalac and NA35. Complex Fragment Emission from La Induced Reactions at 47 MeV/n
March 14, 1988	Dr. S. Sanders Argonne National Laboratory	Asymmetric Fission In Light Nuclear Systems
April 4, 1988	Robert Chadwick, GSRA Dan Ifft, GSRA	The Synergistic Solvent Extraction of Cf, Am and Eu Measuring Iron Isotopes in Cosmic Rays
April 25, 1988	Professor Wick Haxton University of Washington	The Neutral Current Production of ^{19}F and Other Supernova Neutrino Stories
May 3, 1988	Mr. Bert Yost LeCroy	Pattern Recognition and Triggers with Programmable Logic
May 16, 1988	Dr. Robert Arvieu Institut des Sciences Nucléaires, Grenoble	Order and Chaos in the Phase Space of a Rotating Potential
June 20, 1988	Dr. Ray Arnold SLAC	The SLAC/NPAS Program
June 27, 1988	Dr. Karl Van Bibber Stanford	PEGASYS - A Proposed Nuclear Physics Facility for the PEP Storage Ring.
August 1, 1988	Professor Walter Greiner University of Frankfurt	Strong Fields and the e^+e^- Puzzle
September 12, 1988	Dr. Wolfgang Stoeffl LLNL	Neutrino Mass Experiment
September 19, 1988	Dr. Reinhard Stock University of Frankfurt	Ultrarelativistic Nucleus-Nucleus Collisions
September 20, 1988	Dr. John Durell University of Manchester	Fission Fragment Gamma-Ray Spectroscopy
September 23	Dr. Wolfgram von Oertzen, Hahn-Meitner Institute	Nucleon Transfer Between Very Heavy Nuclei at the Coulomb Barrier
September 28	Dr. Peter M. Endt, University of Utrecht	"26A1: A Complete Nucleus"
September 30	Dr. John Sharpey-Schafer, University of Liverpool	Super Deformation, Shape Coexistence, and the Decline and Fall of Pairing all between N=86 and N=92

Nuclear Theory Seminars

October 5, 1987	Per Arve MSU	The Delta Resonance in Nuclei
October 6, 1987	Larry Wilets Seattle	Is the Proton a Dirac Particle
October 20, 1987	Sean Gavin LBL	Pion Dynamics in Ultrarelativistic Nuclear Collisions
October 26, 1987	Andrew Jackson LBL	The psi at Finite Temperature
November 3, 1987	Jorge A. Lopez LBL	Nuclear Multifragmentation
November 6, 1987	Friedrich Beck Darmstadt	Quasielastic Response in Relativistic Mean Field Theory
December 7, 1987	Janos Polonyi MIT	Quantum Mechanics on a Circle and Physics of Deconfinement
December 11, 1987	Sandra Padula LBL	Bose-Einstein Correlations in Landau's Hydrodynamical Model
December 11, 1987	Takeshi Kodama CBPF, Rio de Janeiro	Relativistic Effects in Coulomb Excitation - Breakdown of the Semiclassical Approximation
January 29, 1988	Sean Gavin LBL	Hadronic J/psi Suppression in Ultrarelativistic Nuclear Collisions
Feb 19, 1988	Walter Geist LBL	A New Signature of Deconfinement
March 10, 1988	Cheng-Li Wu Jilin Univ. and Univ. Tennessee	Recent Developments in the Fermion Dynamical Symmetry Model
March 16, 1988	Andrew D. Jackson SUNY	Skyrmions and High-Tc Superconductivity
March 18, 1988	Karen E. Tang LBL	Formation of H-particles at the AGS
March 21, 1988	Michael Plhmer Marburg	Gluon-Interaction Description of Energy-Momentum Loss in pp, pA, and AA Collisions
May 3, 1988	Special Lounge Discussion (Karl Van Bibber et al.)	Quark Hadronization in the Nuclear Medium - Implications for the Target Spectator
May 19, 1988	Che-ming Ko Texas A&M	Dilepton Production as a Probe of Pion Dynamics
Jun 14, 1988	Sean Gavin LBL	Mechanisms of J/psi Suppression
Jun 15, 1988	Hans Hansson SUNY	Linear Response of Hot Gluons

Jun 28, 1988	Jadunath De Calcutta	Limiting Temperatures in Finite Nuclei
July 13, 1988	Wolfgang Cassing Giessen	Covariant Transport Theories
July 18, 1988	Henning Heiselberg NORDITA	Instabilities in Hot Nuclear Matter: A Mechanism For Nuclear Fragmentation
July 19, 1988	Qui, Xi-jun Shanghai	Quark and Meson Model for NN Interaction and Phase Shifts
July 21, 1988	Bernhard Blattel Giessen	Observables within a Covariant Transport Approach
July 25, 1988	Bernard Remaud Nantes	Semi-Classical Kinetic Theory of Heavy-ion Collisions
July 26, 1988	Bernhard Blattel Giessen	Results with a Covariant Transport Approach
July 27, 1988	Georg Peilert Frankfurt	Multifragmentation and Fragment Flow in Heavy-Ion Collisions
July 29, 1988	Carsten Greiner Frankfurt	Quark Droplets as a Signal for the Phase Transition From Guark-Gluon Plasma To Hadron Matter
August 1, 1988	Wolfgang Bauer Cal Tech	Some Remarks on Energy Spectra Intermediate Mass Fragments
August 1, 1988	Walter Greiner Frankfurt, (NSD Seminar)	Strong Fields and the e+e- Puzzle
August 3, 1988	Lene Hau Aarhus, Denmark	Phonon Assisted Lamb Shift In Channelling Radiation
August 3, 1988	Raimund Heuer Frankfurt	Coherent and Incoherent Aspects of Photon Production in Heavy-Ion Collisions
August 9, 1988	Sakir Ayik Tennessee Tech	Incorporating Fluctuations into the BUU Equation
August 10, 1988	Arnold R. Bodmer Chicago	Comments on Nonlinear Relativistic Mean Field Theories
August 22, 1988	Ramon F. Alvarez-Estrada Madrid, Spain	QCD at High Temperatures And Large Distances
August 23, 1988	Intro. by Jim Carroll U.C. Riverside	Di-Lepton Discussion: Present Capabilities And Future Needs
August 24, 1988	Philip J. Siemens Corvallis, Oregon	Mesons in Nuclei: Implications For Collision Dynamics
August 31, 1988	Philip J. Siemens Corvallis, Oregon	The Bevalac beyond Boltzmann: Transport Theory of Fluctuating Fields
October 26, 1987	Władysław J. Swiatecki LBL	Introduction to the Program Order, Chaos, and the Atomic Nucleus

November 1987	Władysław J. Świątecki LBL	Nonlinearese: A Crash Course in the Terminology of Nonlinear Dynamics, a Series of Four Lectures
November 23, 1987	Predrag Cvitanovic Niels Bohr Institute	Universality in Chaos
December 8, 1987	Allen J. Lichtenberg UCB	Phase Space Structure and Diffusion
January 25, 1988	David K. Campbell LANL	Nonlinear Science: Paradigms to Practicalities
March 1, 1988	Oriol Bohigas Orsay	Aspects of Quantum Chaos
March 1, 1988	Robert Littlejohn UCB	Semi-Classical Methods
March 10, 1988	Erick Heller Univ. of Washington	The Correspondence Principle, Classical Chaos and Quantum Mechanics
May 15, 1988	Martin Kruskal Princeton University	Asymptotics Beyond All Orders
May 16, 1988	Robert Arvieu Grenoble	Order and Chaos in the Phase of a Rotating Potential
July 1, 1988	January P. Blocki Swierk, Poland	Continuation of an Ongoing Project with W.J. Świąteckion the Subject of Order, Chaos and Nuclear Dynamics
August 2, 1988	Peter Ring Munich	Berry's Phase in Rotating Nuclei
August 4, 1988	Michael Wilkinson Glasgow	A Model for Dissipation
August 16, 1988	Jerrold E. Marsden Mathematics, UCB	On Berry's Phase
August 16, 1988	Gottfried Mayer-Kress LANL	Quantification of Chaos
August 17, 1988	Wladyslaw J. Świątecki LBL, NSD	Nuclear Studies
August 17, 1988	Oriol Bohigas Orsay	Quantum Spectral Fluctuations and Classical Motion
August 18, 1988	Jonathan Robbins Physic, UCB	Complex Periodic Orbits in Rotational Spectra
August 18, 1988	Michael Nauenberg Physics, UCSC	Wave Packets and Chaos
August 19, 1988	Robert Littlejohn Physics, UCB	Stadium Calculations
September 22, 1988	John D. Gibbon Imperial College London	Finite-Dimensional Attractors and Inertial Manifolds in Partial Differential Equations

Appendix II: Author Index

A

Abriola, D. 16
Abrosimov, V.I. 100
Aichelin, J. 92
Akovali, Y.A. 27 35
Aleklett, K. 51 52
Alonso, J.R. 121
Alvarez-Estrada, R.F. 104
Archambault, L.F. 111
Ashworth, M. 55
Auger, G. 66
Avignone, F.T. III 37
Awes, T.C. 122

B

Bacelar, J.C. 22 24 30
Baisden, P.A. 61 119
Baktash, C. 122
Baltensperger, U. 49 114
Bamberger, A. 76 78 80 82 83
Bartke, J. 76 78 80 82 83
Barwick, S.W. 118
Batchelder, J.C. 15
Beausang, C. 24 26 29
Beck, E.M. 22 24 30
Bennett, D.A. 41 48
Bialkowska, H. 76 78 80 82 83
Bistirlich, J.A. 75
Bland, R.W. 73
Bock, R. 63 71 76 78 80 82 83
Bossingham, R.R. 75
Bowman, D.R. 55 57 58 66 75
Brüchle, W. 49 114
Bradley, S. 57
Brandt, R. 51
Braun-Munzinger, P. 63
Brockmann, R. 76 78 80 82 83
Browne, E. 21 33

Burde, J. 24 26 29

C

Calloway, D.H. 73
Carlini, R.D. 20
Casey, C. 52
Castillejo, L. 97
Cerny, J.C. 13 15 115
Chacon, A.D. 75
Chadwick, R.B. 43 45 48 49 113 114
Chan, Y. 19 17 18 66
Charity, R.J. 55 57 58 59 66 120
Chase, S.I. 76 78 80 82 83
Chasteler, R.M. 27 34 35 37 39 48 111
Chavez, E. 19 66
Chen, K.B. 45 47
Choi, W.C. 20
Chung, H.S. 95
Claesson, G. 71
Clawson, C.W. 75
Cline, D. 28
Colonna, N. 120
Crema, E. 16
Crowe, K.M. 75
Cugnon, J. 92
Cumby, R.P. 122
Czerwinski, K.R. 45 49 61 114

D

diTada, M. 16
D'Erasmo, G. 120
Dacal, A. 18
Day, D.E. 118
DeMarzo, C. 76 78 80 82 83
DePalma, M. 76 78 80 82 83
Deleplanque, M.A. 23 24 26 28 29 30
Derado, I. 76 78 80 82 83
Dersch, G. 51
DiGregorio, D.E. 16 17 18
Diamond, R.M. 23 24 26 28 29 30

Dickson, S. 73
Donahue, J.B. 20
Dorso, C. 89
Doss, K.G.R. 71
Dougan, R.J. 46
Dracoulis, G.D. 29
Draper, J.E. 23 24 26 30
Durkin, L.S. 20
Duyar, C. 26

E

Eckardt, V. 76 78 80 82 83
Eichler, B. 44
Ekuni, K. 68 121
Elgue, M. 16
Emling, H. 63
Etchegoyen, A. 16
Etchegoyen, M.C. 16

F

Fai, G. 103
Favuzzi, C. 76 78 80 82 83
Fazely, A. 20
Feige, G. 51
Feng, J.L. 112
Ferenc, D. 76 78 80 82 83
Ferguson, R.L. 122
Fernández Niello, J.O. 16
Ferrero, A.M.J. 16
Fessler, H. 76 78 80 82 83
Fiore, E.M. 120
Fiore, L. 59 120
Firestone, R.B. 27 31 32 34 35 37 40
Fraenkel, Z. 92
Frankel, K. 92
Franz, A. 122
Freedman, S.J. 20
Freifelder, R. 63
Freund, P. 76 78 80 82 83
Friedlander, E.M. 51

Fujikawa, B.K. 20

G

Gäggeler, H. 49 44 114
Gabelmann, H. 90
Gabriel, T.A. 122
Gale, C. 92
Gannett, C.M. 45 46 48 49 61 114
Ganssauge, E. 51
Garvey, G.T. 20
Gavin, S. 107
Gazdzicki, M. 76 78 80 82 83
Gazes, S.B. 19 66
Gebauer, H.J. 76 78 80 82 83
Gerbier, G. 74
Ghiorso, A. 50 118
Gilat, J. 31 32 40
Glendenning, N.K. 105 106 108 109
Gnirs, M. 63
Gobbi, A. 59 63
Goodman, A.L. 35
Greensite, J. 99
Gregorich, E.K. 44 45 47 48 49 61 64 114
Grosse, E. 63
Guarino, G. 59 120
Guerra, C. 76 78 80 82 83
Gustafsson, H.A. 70 71 122
Gutbrod, H.H. 70 71 122
Gyulassy, M. 92 94 106 107 108

H

Hübel, H. 24
Hahn, A.A. 73
Hall, H.L. 33 45 45 48 49 61 64 114 116 119
Han, H. 66 55
Harmon, B.A. 17 18
Harms, V. 90 92
Harper, R.W. 20
Harris, J. 70 76 78 80 82 83
Hashimoto, O. 75

Hasse, G. 51
Haynes, G.R. 45 120
Heck, W. 76 78 80 82 83
Helmer, K. 28
Henderson, R.A. 33 45 45 46 48 49 61 64 114 119
Herrmann, J. 51
Herrmann, N. 63
Hildenbrand, K.D. 59 63
Hillebrandt, W. 92
Hodges, C.L. 73
Hoffman, D.C. 33 41 43 44 45 46 47 48 49 51 61 64
. . . . . 113 114 116 119 120
Hulet, E.K. 46 65 66
Humanic, T. 76 78 80 82 83 75
Hyde, E.K. 49

I

Imlay, R.L. 20
Izumi, M. 121

J

J. Truran, W. 92
Jäger, E. 44
Jacak, B.V. 70
Jackson, A. 97 98
Jackson, A.D. 97
Jarvine, G.D. 43
Jing, K.X. 55
Johnson, J.W. 122
Jones, P.S.J. 97
Jost, D. 49 44 114
Joyce, D. 73
Judek, B. 51
Justice, M.L. 75

K

K.S.Vierinen 37
Kühn, W. 63
Kadija, K. 76 78 80 82 83

Kamermans, R. 19
Kampert, K.H. 70 71
Karabarbounis, A. 76 78 80 82 83
Kavka, A. 28
Keane, D. 92
Kehoe, W.L. 57 66
Keidel, R. 76 78 80 82 83
Keller, O.L., Jr. 49
Kernan, W. 28
Kitagawa, A. 121
Klinkhamer, F.R. 99 105
Kluge, H. 24
Knop, R. 18
Ko, C.M. 92
Kobayashi, T. 68 72 121
Kodama, T. 105
Kolb, B. 70 71 122
Kortelahti, M.O. 34 37 38
Kowalski 76 78 80 82 83
Kratz, J. 49 114
Kratz, K.-L. 90 92
Krebs, G.F. 121
Kristiansson, P. 71
Kuhnert, A. 24
Kulessa, R. 63
Kurck, J.M. 75

L

Löhner, H. 71
Lahanas, M.M. 76 80 82 83 78
Landis, D.A. 115 122
Lang, T.F. 13 13 15 115
Larimer, R.-M. 22 21 33
Lee, D. 52 45 46 48 49 61 64 113 114 120
Lee, I.Y. 122
Lesko, K.T. 17 20 21 22 33
Leyba, J.D. 45 48 49 61 114 120
Lienert, C. 49 114
Liguori Neto, R. Neto 16
Liljenzin, J.D. 52
Lindgren, M.A. 73
Ling, T.Y. 20

Liu, X.T. 28
Liu, Z.H. 57 58
Lopez, J.A. 103 104
Lougheed, R.W. 46
Loveland, W. 51 52
Lubeck, G. 103

M

Möller, P. 40 90 92
Macchiavelli, A. 16 23 24 26 28 29
Madden, N.W. 115
Maier, K.H. 24
Margetis, S. 76 78 80 82 83
Matis, H.S. 73 74
Matsuta, K. 121
Matulewicz, T. 63
Maurenzig, P.R. 63
McDonald, R. 24 26 28 57 58 59 122
McGaughey, P.L. 51
McHarris, W. 75
McKeown, R. 20
McMahan, M.A. 57 58 59 66 120
Metag, V. 63
Metcalf, W.J. 20
Meyer, C.A. 75
Mignerey, A.C. 57
Minamisono, T. 121
Mitchell, J.W. 20
Moisan, C. 18
Moltz, D.M. 13 15 35 115
Monnand, E. 90
Moody, K.J. 46 65 66
Moretto, L.G. 52 54 55 57 58 59 63 66 101 120
Murzel, M. 24
Myers, W.D. 95 96

N

Nai, Y.-Qi 49 114
Napolitano, J. 20
Nappi, E. 76 78 80 82 83

Nitsche, H. 41
Nitschke, J.M. 27 31 32 34 35 36 37 38 40 41 111 112
Nix, J.R. 90
Nojiri, Y. 121
Norman, E.B. 17 21 22 33
Novotny, R. 63
Nurmia, M.J. 45 48 49 61 113 114 116

O

Obenshain, F.E. 122
Odyniec, G. 76 78 80 82 83
Olmi, A. 63
Omata, K. 72 121
Ortiz, M.E. 18
Oskarsson, A. 122
Otterlund, I. 122

P

Pühlhofer, F. 76 78 80 82 83
Pacheco, A.J. 16
Padula, S.S. 94 107
Paic, G. 76 78 80 82 83
Palmer, C.E.A. 61 119
Palmer, T.L. 73
Panagiotou, A.D. 76 78 80 82 83
Pantaleo, A. 59 120
Paticchio, V. 120
Pelte, D. 63
Persson, S. 122
Petridis, A. 76 78 80 82 83
Pfeiffer, B. 90
Pfennig, J. 76 78 80 82 83
Plagnol, E. 18 55 66
Plasil, F. 122
Porile, N.T. 51
Posa, F. 76 78 80 82 83
Poskanzer, A.M. 70 70 122
Potvin, L. 18
Pouliot, J. 17 18
Pretzl, K.P. 76 78 80 82 83

Price, P.B. 65 66 74 85 118
Pugh, H.G. 73 76 78 80 82 83

R

Roy, R. 18
Röhrich, D. 76 78 80 82 83
Rai, G. 76 78 80 82 83
Rami, R. 63
Randrup, J. 89 92 100 100 103 104
Ranieri, A. 76 78 80 82 83
Rao, M.N. 35
Rasmussen, J.O. 28 75 87
Rauch, W. 76 78 80 82 83
Reiff, J.E. 13 15 115
Ren, Guoxiao 74 85
Renfordt, R. 76 78 80 82 83
Rioux, C. 18
Ritter, H.G. 70 71 122
Robertson, J.D. 13 15 115
Romanowski, T.A. 20
Rosenhauer, A. 92
Rozmej, P. 96
Runge, K. 76 78 80 82 83

S

Sandberg, V.D. 20
Sandoval, A. 76 78 80 82 83
Sarantites, D.G. 59
Sarantities, D.G. 58
Sato, H. 68
Savage, M.L. 73
Schädel, M. 44 49 114
Scherer, U. 49 114
Schmidt, H.R. 19 70 71 122
Schmitz, N. 76 78 80 82 83
Schouten, T. 76 78 80 82 83
Schroeder, L.S. 76 78 80 82 83
Seaborg, G.T. 47 51 52
Seyboth, P. 76 78 80 82 83
Seyerlein, J. 76 78 80 82 83

Shaw, G.L. 73
Shida, Y. 121
Shihab-Eldin, A.A. 27 34 35 37 87
Shimoda, T. 68 72
Shimoura, S. 68 121
Shulz, W. 51
Siemiarczuk, T. 71
Silva, R.J. 41
Silveira Gomes, P.R. 16
Simon, R.S. 63
Skrzypczak, E. 76 78 80 82 83
Slansky, R. 73
Smith, B.F. 43
Smith, E.S. 20
Snowden-Ifft, D. 65 118
Sobotka, L.G. 59
Somerville, L.P. 50
Sorensen, S.P. 122
Sousa, D.C. 35
Spinelli, P. 76 78 80 82 83
Stöcker, H. 92
Stefanini, A.A. 63
Steiner, A.B. 73
Stelzer, H. 63
Stephens, F.S. 23 24 26 28 29 30
Stock, R. 76 78 80 82 83
Stokstad, R.G. 16 17 18 19 66
Stoyer, M. 28 87
Ströbele, H. 76 78 80 82 83
Stuchbery, A.E. 29
Sugimoto, K. 68 72 121
Sullivan, J.P. 75
Sur, B. 21 21 21 33
Świątecki, W.J. 87 90
Symons, T.J.M. 121

T

Türler, A. 48 49 114
Takahashi, N. 68 72
Takeyama, K. 121
Tanihata, I. 68 72 121
Teitelbaum, L. 76 78 80 82 83

Testoni, J.E. 16
Thielemann, F.-K. 92
Thomas, A. 76 78 80 82 83
Timko, M. 20
Tincknell, M. 76 78 80 82 83
Tokarek, R. 73
Tonse, S. 76 78 80 82 83
Toth, K.S. 27 34 35 36 37 38 40

V

von Gunten, H.R. 48
Vandenbosch, R. 100
Vanin, V.R. 16
Verbaarschot, J.J.M. 97
Vesztergombi, G. 76 78 80 82 83
Vierinen, K.S. 27 31 32 34 35 37 38 112
Vinet, L. 55 66
Vogel, Ch. 44
Vogel, K.R. 21
Vogt, E. 28
Vranic, D. 76 78 80 82 83

W

Wöhr, A. 92
Wang, C.-S. 95
Wang, Shicheng 65 66 118
Welke, G. 92
Wenig, S. 76 78 80 82 83
Wessels, J. 63
Westphal, A. 118
Wieman, H. 71
Wild, J.F. 46
Williams, W.T. 74 85
Wilmarth, P.A. 27 31 32 34 35 36 37 38 40 41 112
Wislicki, W. 71
Wozniak, G.J. 52 54 55 57 58 59 66 101 120 122
Wu, C.Y. 28
Wu, J.Q. 92
Wydler, A.A. 111

X

Xu, Z. 52

Y

Yamakawa, O. 68 72
Yashita, S. 50
Young, G.R. 122
Yu, Y.W. 47

Z

Zajc, W.A. 75
Zieger, W. 92
Zimmermann, P. 49 114

☆U.S. GOVERNMENT PRINTING OFFICE; 1989 785-130 - 1008

LAWRENCE BERKELEY LABORATORY
TECHNICAL INFORMATION DEPARTMENT
1 CYCLOTRON ROAD
BERKELEY, CALIFORNIA 94720